Vol. 287, No. 3, March 21, 1994
Completing Volume 287

ISSN 0003-2670

ANALYTICA CHIMICA ACTA

An international journal devoted to all branches of analytical chemistry

ELSEVIER

ANALYTICA CHIMICA ACTA

Scope. *Analytica Chimica Acta* publishes original papers, rapid publication letters and reviews dealing with every aspect of modern analytical chemistry. Reviews are normally written by invitation of the editors, who welcome suggestions for subjects. Letters can be published within **four months** of submission. For information on the Letters section, see inside back cover.

Submission of Papers

Americas

Prof. Harry L. Pardue
Department of Chemistry
1393 BRWN Bldg, Purdue University
West Lafayette, IN 47907–1393
USA

Tel:(+1-317) 494 5320
Fax:(+1-317) 496 1200

Computer Techniques

Prof. J.T. Clerc
Universität Bern
Pharmazeutisches Institut
Baltzerstrasse 5, CH-3012 Bern
Switzerland

Tel:(+41-31) 6314191
Fax:(+41-31) 6314198

Prof. Sarah C. Rutan
Department of Chemistry
Virginia Commonwealth University
P.O. Box 2006
Richmond, VA 23284-2006
USA
Tel:(+1-804) 367 1298
Fax:(+1-804) 367 7517

Other Papers

Prof. Alan Townshend
Department of Chemistry
The University
Hull HU6 7RX
Great Britain

Tel:(+44-482) 465027
Fax:(+44-482) 466410

Prof. Willem E. van der Linden
Laboratory for Chemical Analysis
Department of Chemical Technology
Twente University of Technology
P.O. Box 217, 7500 AE Enschede
The Netherlands
Tel:(+31-53) 892629
Fax:(+31-53) 356024

Prof. Paul Worsfold
Dept. of Environmental Sciences
University of Plymouth
Plymouth PL4 8AA
Great Britain

Tel:(+44-752) 233006
Fax:(+44-752) 233009

Submission of an article is understood to imply that the article is original and unpublished and is not being considered for publication elsewhere. *Anal. Chim. Acta* accepts papers in English only. There are no page charges. Manuscripts should conform in layout and style to the papers published in this issue. See inside back cover for "Information for Authors".

Publication. *Analytica Chimica Acta* appears in 16 volumes in 1994 (Vols. 281–296). *Vibrational Spectroscopy* appears in 2 volumes in 1994 (Vols. 6 and 7). Subscriptions are accepted on a prepaid basis only, unless different terms have been previously agreed upon. It is possible to order a combined subscription (*Anal. Chim. Acta* **and** *Vib. Spectrosc.*).
Our p.p.h. (postage, packing and handling) charge includes surface delivery of all issues, except to subscribers in the U.S.A., Canada, Australia, New Zealand, China, India, Israel, South Africa, Malaysia, Thailand, Singapore, South Korea, Taiwan, Pakistan, Hong Kong, Brazil, Argentina and Mexico, who receive all issues by air delivery (S.A.L.–Surface Air Lifted) at no extra cost. For Japan, air delivery requires 25% additional charge of the normal postage and handling charge; for all other countries airmail and S.A.L. charges are available upon request.

Subscription orders. Subscription prices are available upon request from the publisher. Subscription orders can be entered only by calendar year and should be sent to: Elsevier Science B.V., Journals Department, P.O. Box 211, 1000 AE Amsterdam, The Netherlands. Tel: (+31-20) 5803 642, Telex: 18582, Telefax: (+31-20) 5803598, to which requests for sample copies can also be sent. Claims for issues not received should be made within six months of publication of the issues. If not they cannot be honoured free of charge. Readers in the U.S.A. and Canada can contact the following address: Elsevier Science Inc., Journal Information Center, 655 Avenue of the Americas, New York, NY 10010, U.S.A. Tel: (+1-212) 6333750, Telefax: (+1-212) 6333990, for further information, or a free sample copy of this or any other Elsevier Science journal.
Advertisements. Advertisement rates are available from the publisher on request.

US mailing notice – Analytica Chimica Acta (ISSN 0003-2670) is published 3 times a month (total 48 issues) by Elsevier Science B.V. (Molenwerf 1, Postbus 211, 1000 AE Amsterdam). Annual subscription price in the USA US$ 3035.75 (valid in North, Central and South America), including air speed delivery. Second class postage paid at Jamaica, NY 11431. *USA Postmasters*: Send address changes to Anal. Chim. Acta, Publications Expediting, Inc , 200 Meacham Av., Elmont, NY 11003. Airfreight and mailing in the USA by Publication Expediting.

ANALYTICA CHIMICA ACTA

An international journal devoted to all branches of analytical chemistry

(Full texts are incorporated in CJELSEVIER, a file in the Chemical Journals Online database available on STN International; Abstracted, indexed in: Aluminum Abstracts; Anal. Abstr.; Biol. Abstr.; BIOSIS; Chem. Abstr.; Curr. Contents Phys. Chem. Earth Sci.; Engineered Materials Abstracts; Excerpta Medica; Index Med.; Life Sci.; Mass Spectrom. Bull.; Material Business Alerts; Metals Abstracts; Sci. Citation Index)

VOL. 287 NO. 3 CONTENTS MARCH 21, 1994

(Continued overleaf)

Analytica Chimica Acta, 287 (1994) 147–190
Elsevier Science B.V., Amsterdam

Review

Determination of carbon, phosphorus, nitrogen and silicon species in waters

Kevin Robards

School of Science and Technology, Charles Sturt University-Riverina, P.O. Box 588, Wagga Wagga 2678 (Australia)

Ian D. McKelvie and Richard L. Benson

Water Studies Centre, Monash University, P.O. Box 197, Caulfield East 3145 (Australia)

Paul J. Worsfold and Nick J. Blundell

Department of Environmental Sciences, University of Plymouth, Drake Circus, Plymouth PL4 8AA (UK)

Harry Casey

Institute of Freshwater Ecology, River Laboratory, East Stoke, Wareham, Dorset BH20 6BB (UK)

(Received 31st August 1993)

Abstract

This review examines the analytical chemistry of the nutrient elements carbon, phosphorus, nitrogen and silicon in environmental waters. The speciation of these elements is discussed and the terminology used for classification is described. The analytical approach is considered in general terms, with particular regard to sample collection and preservation, sample treatment and methods of analysis. A critical appraisal of the analytical methods available for each of the elements (and their speciation) is provided together with the relevant analytical figures of merit.

Keywords: Carbon; Nitrogen; Nutrients; Phosphorus; Review; Silicon; Waters

Water quality is widely used as if a single concept of water quality were universally recognizable. In fact, the quality of a water depends on the criteria against which it is judged. Traditionally these criteria have been use-related whereas current interest is focused on setting wider criteria, for instance, to assess how well water bodies are able to support appropriate ecosystems. There are two broad approaches to water monitoring which provide complementary information. The first involves examining physical and chemical characteristics of water samples and the other, biological monitoring, involves examining the flora or fauna of waterbodies. Chemical monitoring provides data on the chemical status at the time of sampling and can be performed on an extremely large number of determinands. A simple catalogue of groups of such substances in waters includes: the major ions, sodium, potassium, magnesium, calcium, sulphate, chloride and hydrogencarbonate which are generally dissolved in quantities of at least mg l^{-1}, atmospheric gases; key nutrient ions (with typical concentrations in the range μg l^{-1}–mg l^{-1}), which include phos-

Correspondence to: K. Robards, School of Science and Technology, Charles Sturt University-Riverina, P.O. Box 588, Wagga Wagga 2678 (Australia).

SSDI 0003-2670(93)E0542-F

phates, nitrate, ammonium, sometimes silicate and occasionally iron, manganese, and molybdenum; trace nutrients (ng l^{-1}–$\mu g\ l^{-1}$), including copper, zinc, boron, cobalt, vanadium, fluorine, bromine; other trace ions (ng l^{-1} or less) such as cadmium, mercury, lead, silver, arsenic, antimony and tin; refractory (i.e., not decomposed by high intensity ultraviolet radiation) organic substances such as hydrocarbons, phenolic substances, carboxylic acids, tannins, humic and fulvic substances, pesticides; and labile organic substances (e.g., amino acids, sugars, alcohols). The order of this list largely reflects the progressive difficulty of analysis of individual substances in the groups and, consequent on that, the historical order in which the groups have been investigated [1]. It does not reflect any particular order of importance of the groups to aquatic systems. In some waters, the availability of one of the key nutrient ions may be paramount, in others a toxic trace metal may be of greatest significance. Hence the needs of the particular monitoring program should always be considered. In some situations it may be more appropriate to measure causal factors (e.g., nutrient concentrations) whereas in others a consequential factor (algal biomass or chlorophyll *a*) may be more appropriate.

Algae and higher plants are the primary food source in the complex food webs in freshwater environments. These species require nutrients for growth. For example, diatoms and green algae require 18 nutritional elements and, of these, eight (hydrogen, carbon, oxygen, potassium, sodium, magnesium, calcium and sulphur) are usually adequately abundant in surface waters. Of the remaining ten elements, nitrogen and phosphorus are crucial as they are not always readily available in sufficient amounts. Thus, the availability of nutrients in general and in particular of phosphorus and nitrogen determines the rate of plant and algal growth and the biomass that they can achieve, on which the rest of the biological community in turn depends [2]. The term eutrophication is used to describe the enrichment of water by plant nutrients.

There are many sources of nutrients which may contribute to the total nutrient load of a river (vide infra). Rivers are the main arteries of nutrient transport from land regions to freshwater lakes and the sea. Other forms of transport include glacial scour and continental dust fallout over the oceans. An understanding of the chemical composition of a water body requires knowledge of the sources and mechanisms of nutrient transport. Climate, nature of the vegetation and land use also impact significantly on the quality of a water body [3]. Rock weathering and sea spray still dominate the major ion composition of the world's fresh waters, whilst farming and settlement probably have greatest impact on nutrient concentrations and industry and atmospheric pollutants influence those of trace elements [1]. A detailed study of elemental budgets has been conducted on the subcatchments of streams draining into the Hubbard Brook in New Hampshire, USA [4]. Input sources were snow and rain, dry deposition (as gas), fixation and rock weathering. Most of the calcium, magnesium, sodium, potassium and phosphorus was supplied by weathering whereas significant amounts of sodium, nitrogen and sulphur were supplied by rain and snow. Fixation accounted for most of the nitrogen input and dry deposition of SO_2 was also a significant source of sulphur [5]. The fate of these elements was incorporation into the biomass, litter or soil, or loss to the stream in a dissolved or suspended state. Potassium, nitrogen and sulphur were selectively retained by the ecosystem whereas most of the calcium, magnesium, sodium and sulphur was lost to the stream largely in dissolved form. Biological components of the water body also influenced the daily, seasonal and long-term cycles of the elements. In terms of the net gain or loss of each element to the land ecosystem, the elements fell into two categories: those for which there was a net loss from the soil-biomass system (sodium, potassium, magnesium, calcium) and those for which there was a net gain (nitrogen, phosphorus and sulphur). The latter group is particularly important in determining the productivity of fresh waters. Other elements which play major biogeochemical roles in aquatic environments include carbon and silicon.

Phytoplankton, particularly cyanobacteria (blue–green algae) are the main bloom-causing

algal group in fresh waters. Common management practice is to limit the concentrations and loads of phosphorus and nitrogen entering a waterbody on the assumption that there is a direct causal relationship between these nutrients and phytoplankton mass. Considerable confusion exists, however, as to whether nutrients limit the biomass or rate of growth of phytoplankton or both. Furthermore, consideration needs to be given to the other factors that can influence the growth of aquatic plants [6–8]. These include light, temperature, current velocity and substrate stability. Nevertheless, the ability to measure the concentrations and fluxes, both spatial and temporal (daily, seasonal and long-term) variations of these species in aquatic systems is desirable in many areas including environmental chemistry and geochemistry and for rationalisation of related industrial chemical processes. A knowledge of their levels is useful to environmental chemists, biologists, geochemists and physical oceanographers. For example, physical oceanographers use the silicon content of water masses as a tracer for studying movements of water masses and marine mixing processes [9].

This review examines the analytical chemistry of the nutrients carbon, phosphorus, nitrogen and silicon in river, lake and estuarine waters, groundwaters, rain water, sea water and soil waters. Related material is contained in a number of sources (for example Refs. 1, 10–12). SCOPE 42 [13] and the Report of the Royal Commission on Environmental Pollution [2] are particularly notable. SCOPE 42 assesses the mass of data which has been gathered worldwide on the discharge by rivers of organic matter, nutrients and minerals into world oceans. Scientific analyses include spatial variability, remote sensing and chemical analysis. Much useful data on phosphorus are also contained in the regional workshops

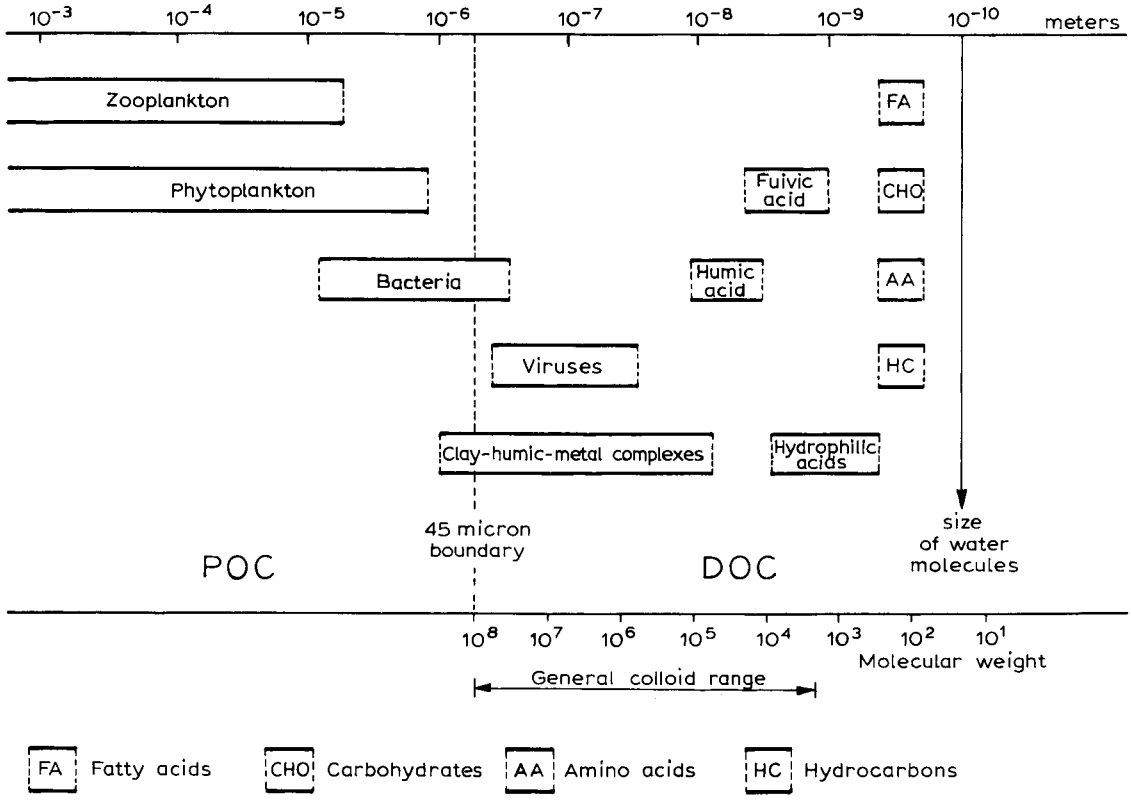

Fig. 1. Continuum of organic matter in natural waters [18].

[14–16] arranged by the Scientific Committee on Problems of the Environment (SCOPE) and the United Nations Environmental Programme (UNEP). A special issue of *Marine Chemistry* [17] was devoted to various aspects of the measurement of carbon and nitrogen in waters and represents an excellent source of information on recent developments and problems associated with the analytical chemistry of these elements in waters.

SPECIATION AND TERMINOLOGY

Carbon, phosphorus, nitrogen and silicon occur in numerous physico-chemical forms in waters. Speciation is a broad term which describes the occurrence and determination of the various physico-chemical forms of a particular element in a system. Thus, simplistically, if there are n distinct chemical forms in each of m physical states in a system, the total number of possible species is $n \times m$. However, speciation is often defined by the aims of particular work using operational classifications based on the experimental technique. Speciation in aquatic systems has become increasingly important due to the realisation that the environmental behaviour of an element (i.e., bioavailability, bioaccumulation and biogeochemical transport) is often critically dependent on its physico-chemical form. Unfortunately, operationally defined measurements suffer from the limitation that they may involve some modification of the analyte. For example, in the measurement of dissolved reactive phosphorus, the hydrolytic action of some of the chromogenic reagents may mean that in addition to orthophosphate some easily hydrolysed organic and condensed phosphates may be included in this fraction.

Carbon

The organic matter in natural waters consists of a continuum of compounds as represented in Fig. 1. Organic matter plays a central role in the biogeochemistry of aquatic ecosystems. Bulk analysis of organic matter is essential to an understanding of the overall state of the production–decomposition cycle and its spatial and temporal variability [18]. More detailed chemical studies such as analysis of individual chemical constituents or measurement of complexing ability can be normalised by analysis of organic matter. High concentrations of organic matter in surface waters can result in depletion of dissolved oxygen with subsequent adverse effects upon aquatic life. Much attention has been devoted to the energy flow through ecosystems. Energy, however, cannot be measured directly at all trophic levels and first order approximations are used to relate the organic matter or, more commonly, the organic carbon to the energy of a trophic level.

The nutrient carbon is present in all fresh and marine waters and plays a major role in many processes: biological (productivity), geological (sedimentation) and chemical (flocculation, metal complexation and adsorption phenomena). The total carbon (TC) can be fractionated [19] into total inorganic carbon (TIC) and total organic carbon (TOC). In almost all waters the concentration of inorganic carbon far exceeds that of organic carbon. For example, sea water represents one extreme where the amount of inorganic matter is typically several orders of magnitude greater than organic matter. Groundwaters have approximately 100 times more inorganic matter while lakes and rivers have about ten times more inorganic matter. Swamps, marshes and bogs represent the opposite extreme where organic matter predominates [20]. Inorganic carbon is a potential nutrient source and is the major source of buffering capacity of the water. The concentrations of carbonate and hydrogencarbonate also determine the corrosive, scale-forming and coagulation/flocculation properties of water [21]. Whereas dissolved inorganic carbon is chemically well defined, until recently little has been known about organic carbon species despite the identification of more than 1300 carbon compounds in natural waters [22]. While the complete identification and characterisation of all carbon compounds is clearly desirable, it is neither technically nor economically feasible as a routine procedure. Accordingly, various group parameters have been defined and measured. Thus, TIC consists of carbonate including colloidal and particulate

forms, hydrogencarbonate and dissolved carbon dioxide whereas the literature contains at least nine common terms for organic matter in water (see Table 1). The more important of these for most waters are TOC, particulate organic carbon (POC) and dissolved organic carbon (DOC) which together give the total amount of organic carbon in water. Almost all waters have a DOC concentration much greater than the POC concentration. For example, in sea water DOC predominates over POC by a factor of 50–100 with average DOC concentrations of the order of 1.0 mg l^{-1} [23].

TABLE 1

Acronyms of commonly used terms for organic matter in water [a]

Acronym	Meaning
BOD	Biological oxygen demand
COD	Chemical oxygen demand
TOC	Total organic carbon
DOC	Dissolved organic carbon
POC	Particulate organic carbon
VOC	Volatile organic carbon (purgeable organic carbon)
DOM	Dissolved organic matter
POM	Particulate organic matter
TOM	Total organic matter
COM	Colloidal organic matter

[a] BOD: A measure of oxygen consumption during decomposition of both organic and inorganic substances. (Humic substances will not decompose in 5-day test and therefore their influence is not included.) COD: A measure of biological oxygen demand and the oxygen demand of decomposable organic and inorganic substances by a chemical oxidant (e.g., dichromate). A qualitative estimate of organic water quality. TOC: The sum of DOC+POC (or SOC). DOC: Organic carbon passing through a 0.45-μm silver or glass fibre filter. POC: Organic carbon retained by a 0.45-μm membrane filter. VOC: Amount of volatile organic compounds in water that are measured by purging them from the sample and trapping them on an adsorbent. DOM, POM, TOM: Analogous to DOC, POC and TOC; organic matter refers to the entire organic molecule and includes other elements such as oxygen and hydrogen. Difficult to quantify and measurements of organic carbon are preferred. Generally, DOM, POM and TOM are equal to 2x the DOC, POC and TOC, respectively. And COM: Organic matter in the range 1 nm–0.45 μm (or > 5000–10000 molecular mass). Difficult to quantify: < 10% of organic carbon in natural waters; more important in swamp and marsh waters.

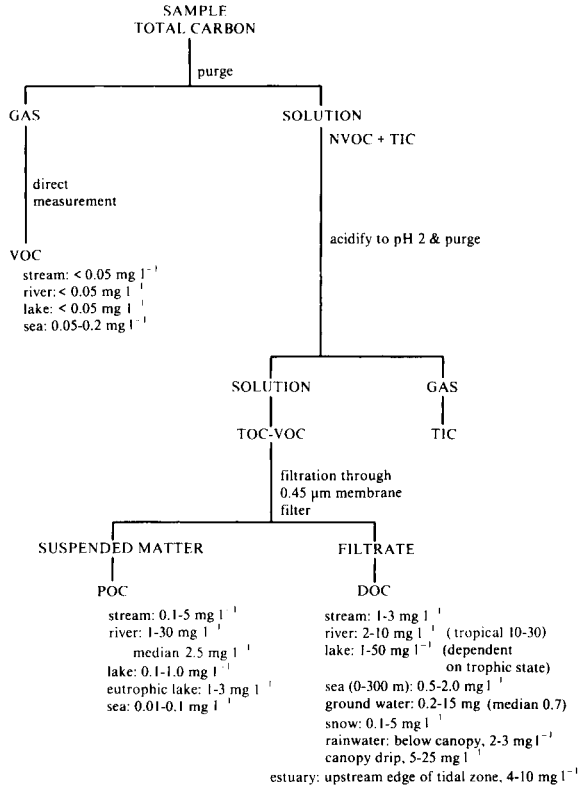

Fig. 2. Operational classification and typical values of aquatic carbon species.

POC refers to the organic carbon fraction retained on a 0.45-μm filter (see Fig. 2). From Fig. 1, POC is comprised of zooplankton, algae, bacteria and detrital organic matter from soil and plants together with some suspended organic matter associated with clay particles.

DOC is operationally defined as the organic carbon fraction passing through a 0.45-μm filter. It quantifies the fraction of organic carbon dissolved in the water and provides a useful indicator of the level of biological activity (from degradation products of plant or animal life) or of the extent of pollution by sewage or industrial effluents. Furthermore, the quantity of DOC in the oceans has been estimated [24] at about 10^{18} g and constitutes one of the major reservoirs of organic carbon. In productive ocean surface waters, as much as a third to a half of the DOC may be present as labile material, degraded biologi-

cally in hours to days [25]. The DOC fraction consists of a range of organic substances plus variable amounts of colloidal material together with viruses and some ultra-small bacteria. The organic matter may occur naturally or may be introduced from industrial effluents or runoff as in the case of pesticides. It ranges from relatively simple compounds of short life time, for example glucose, to stable high molecular mass (500–5000) polymeric organic acids known as humic substances. Aquatic humic substances may be defined operationally as coloured, polyelectrolytic, organic acids with carboxylic, hydroxyl and phenolic functional groups, isolated from waters on ion-exchange resins. The pK_a values of the humic substances result in their being anionic at pH values typical of natural waters (i.e., pH 6–8). This anionic character gives buffer capacity to the organic matter and provides binding sites for metal ions. Humic substances are the major class of organic compounds in waters comprising 50–75% of the DOC. Within aquatic humic substances there are two fractions, humic and fulvic acids. Humic acid is that fraction precipitated at pH 2.0 or less and fulvic acid is that fraction remaining in solution at pH 2.0 or less. The precise molecular nature of at least 90% of this material [26] is unknown. The colloidal organic matter is approximately 10% of the DOC in most natural waters. It comprises large aggregates of humic acids which are commonly associated with clay minerals or oxides of aluminum and iron. Recent trends in DOC levels in small streams and the effects of land use on these have been reported [27].

Phosphorus

Phosphorus occurs in waters in various concentrations, either in dissolved or particulate forms and, as inorganic or organically bound species. Total phosphorus concentrations in waters can vary from less than 0.01 mg l^{-1} in small near pristine mountain streams [28] to over 1 mg l^{-1} in heavily polluted rivers. Estimated background levels of phosphorus in United Kingdom river waters unaffected by sewage or other human activities are 0.005–0.01 mg l^{-1} [2]. In many situations inorganic phosphate is the major com-

TABLE 2

Nitrogen and phosphorus concentrations of various natural waters. Concentrations expressed as mg l^{-1}, elemental N or P

Location	Nitrate	Nitrite	Ammonia	Orthophosphate	N/P	Ref.
UK						
Estuary	1.6	0.009	< 0.001			29
Sea	0.23	0.03	0.005			30
River Dee, Iron Bridge	1.34	0.04	0.075	0.287		2
River Don, Doncaster	4.86	0.20	5.07	1.91		2
River Teith upper	0.2			0.01	20	2
lower	0.3			0.02	15	2
River Tyne upper	3.5			0.02	175	2
lower	4.5			0.3	15	2
River Tay, Perth	0.65			0.01	65	2
River Cuckmere, Sussex						
upper	2.0			0.02	100	2
lower	3.4			0.21	16	2
River Stour, Wye	6.0			1.20	5	2
River Great Eau, Lincolnshire	8.5			0.083	102	2
Australia						
Marine waters	0.016–0.056		< 0.003	0.001–0.016		31
Cockburn Sound, Western Australia	0.005–0.011		0.002–0.024	0.001–0.007		31

TABLE 3

Total phosphorus concentrations and levels of lake productivity, after Vollenweider, modified by Wetzel [45]

General level of lake productivity	Total phosphorus ($\mu g\ l^{-1}$)
Ultra-oligotrophic	< 5
Oligo-mesotrophic	5– 10
Meso-eutrophic	10– 30
Eutrophic	30–100
Hyper-eutrophic	> 100

ponent of the total phosphorus and the values given in Table 2 provide an indication of phosphate levels typically encountered.

Nitrogen may be a limiting nutrient in some situations [32] but phosphorus is generally regarded as the limiting nutrient for primary production. Excessive loading of phosphorus in its various physico-chemical forms is known to be a causal factor in the eutrophication of both lotic and lentic waters [33–40]. Furthermore, classification of the trophic status of standing water bodies is still largely based on the total phosphorus concentrations suggested by Vollenweider in 1968 [33,37] (Table 3) rather than concentrations of dissolved phosphorus. The traditional view has been that algae utilise dissolved phosphate, while bacteria mineralise organically-bound phosphorus, but it is now generally accepted that both algae and bacteria compete for available orthophosphate. Bacteria are known to utilise low concentrations of orthophosphate more efficiently than algae, and it is postulated that algal production is controlled by the rate of bacterial orthophosphate release. Algae, on the other hand, may control heterotrophic bacterial production by limiting the rate at which organic matter is supplied [42]. Under conditions of orthophosphate abundance, many algae exhibit "luxury-uptake" which involves intracellular storage of phosphorus in polyphosphate vesicles [43,44]. This stored phosphorus may be hydrolyzed by intracellular acid phosphatase when free orthophosphate is in short supply. While this storage process is not observed in bacteria, both algae and bacteria can produce extracellular alkaline phosphatases to enable utilization of dissolved organic phosphorus compounds through hydrolytic degradation [45] in orthophosphate-deficient waters.

In closed systems such as batch culture work there is a relatively simple relationship between nutrient concentration and the rate of algal growth. However, in real systems a universal relationship has not been established between either total phosphorus concentration or that of various species and the rate of phytoplankton growth. Here, the rate at which phosphorus cycles between the various storage compartments including the sediment pool [46–52] and secondary effects such as food web manipulations [53] must be considered. Processes occurring in the aquatic system may either consume phosphorus (e.g., sedimentation, sorption onto suspended solids or sediment, algal uptake) or produce phosphorus (e.g., desorption, biological degradation, resuspension). As a result of these exchange processes phosphorus is distributed between three major compartments in the water column:

(1) a biological compartment in association with aquatic organisms including algae;

(2) a dissolved compartment comprising the various forms of orthophosphate; and

(3) a particulate compartment involving phosphorus species which are sorbed on the surface of the particles or retained in the particle matrix [54,55]. Surface adsorption reactions are rapid involving time scales of minutes to days whereas the solid state diffusion reactions into and out of the matrix have time scales of months to years.

The relative kinetics associated with exchange of phosphorus between the various compartments determines the concentration and bioavailabilty of phosphorus. In the case of stream and lake ecosystems cycling is reported to be very rapid [56,57]. The Vollenweider approach to predicting annual algal biomass from the annual total-P and total-N loadings [38,58] is successful in limited situations such as deep, relatively clear lakes and reservoirs. Smalls and Cannon [59] identified a total-P concentration of 10 $\mu g\ l^{-1}$ as the critical value above which algal problems occurred, substantiating the data in Table 3 for distinguishing oligotrophic from mesotrophic waters. In other situations, relationships between total phosphorus concentrations and algal biomass either do

not occur or are variable in time. For example, considerably higher concentrations than 10 $\mu g\ l^{-1}$ of total phosphorus occur in Mount Bold Reservoir, South Australia, without any resulting algal problems [60,61]. Once again this highlights the need to consider other factors influencing algal growth as Mount Bold Reservoir is relatively turbid and therefore potentially light-limited. Alternatively, the distinction between the behaviour of turbid and clear waters may result from the decrease in the bioavailability of phosphate due to its rapid adsorption onto the surfaces of suspended particles [62,63].

Phosphorus species. The inorganic forms of phosphorus comprise orthophosphate (largely PO_4^{3-}) and pyrophosphate ($P_2O_7^{4-}$), as well as their cyclic polymers (metaphosphates) and linear polymers (polyphosphates), which together are referred to as condensed phosphates. Condensed phosphates, both dissolved and particulate, are generally resistant to hydrolysis in natural waters [64], or when subjected to mild hydrolytic conditions for the purpose of analysis [65]. They are however, converted by mild acid hydrolysis at about 100°C to dissolved orthophosphate. The hydrolysis of organic phosphate during this procedure may be minimised by correct selection of acid concentration and hydrolysis time and temperature. The fraction of phosphorus determined following mild acid hydrolysis is termed the "acid hydrolysable phosphorus" and this may be either dissolved (DAHP) or particulate (PAHP). Generally, it includes condensed phosphates such as pyrophosphate, tripolyphosphate and higher molecular mass species such as hexametaphosphate, but it is fairly arbitrarily defined, and it is questionable whether this operational separation of condensed and organic phosphorus species is sufficiently selective.

Organic phosphorus compounds are typically phosphate esters although phosphonates in which carbon is bonded directly to phosphorus are also of interest because of their occurrence in marine invertebrates, bacteria and phytoplankton. Specific compound groups include [40] nucleic acids, phospholipids, inositol phosphates, phosphoamides, phosphoproteins, sugar phosphates, aminophosphonic acids, phosphorus-containing

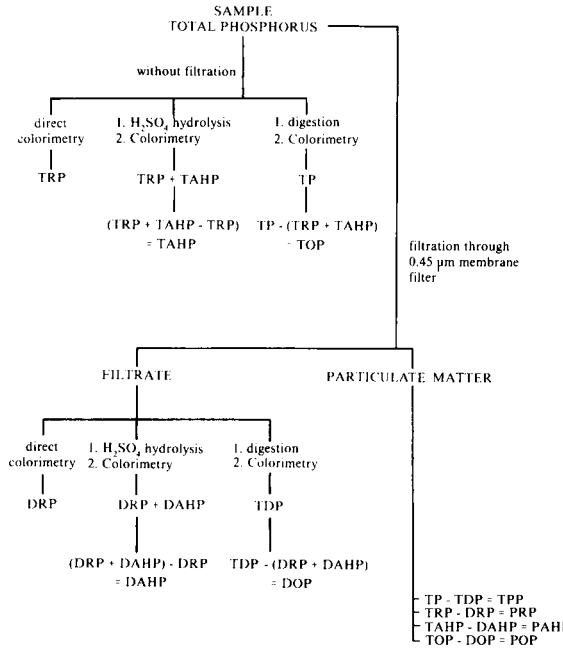

Fig. 3. Operational classification of aquatic phosphorus species.

pesticides and organic condensed phosphates. Analytically, organic phosphorus is considered as the fraction that is converted to orthophosphate after oxidative destruction of organic matter. The severity of the oxidation procedure depends on the nature and, to a lesser extent, the amount of the organic phosphorus-containing compounds. Like other phosphorus fractions, organic phosphorus occurs in both dissolved (DOP) and particulate (POP) fractions which are largely operationally defined by currently used methods.

An operational classification for phosphorus (summarised in Fig. 3) depends on filtration through a 0.45-μm membrane filter for the separation of phosphorus into dissolved (DP) and particulate (PP) fractions. This procedure does not effect a strict separation [18,66] of dissolved and particulate forms but it is convenient and, in general, reproducible. Problems which have been identified [67] include clogging, contamination and variation in pore size of the filter, and destabilization of colloids and other charge related artifacts. Furthermore, transmission of particles

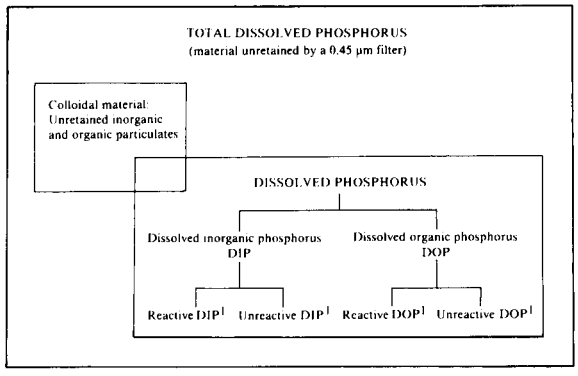

Fig. 4. Schematic representation of the operationally defined components of total dissolved phosphorus. Adapted from Broberg and Persson [67]. [1] Operationally defined by the DRP-detection according to Murphy and Riley [70].

far in excess of the nominal filter pore size has been reported [68]. In general, total phosphorus fractions are determined on the unfiltered sample, dissolved fractions are determined on the filtrate following membrane filtration and the particulate fractions are determined by difference as indicated in Fig. 3.

The nomenclature of the various species and several equivalents is discussed further by Olsen [69]. The total dissolved phosphorus (TDP) fraction contains soluble species such as orthophosphate, condensed phosphates and organic phosphates as well as colloidal-sized phosphorus species [66], including those associated with humic substances [18]. A possible fractionation of TDP has been proposed by Broberg and Persson [67] (see Fig. 4). The dissolved inorganic phosphorus, DIP, fraction which comprises orthophosphate (principally HPO_4^{2-} and PO_4^{3-}) [71], and condensed phosphate, has usually been measured colorimetrically on the assumption that it represents readily available or biologically utilizable phosphorus. The fraction of phosphorus determined by direct colorimetry is termed "reactive phosphorus" and this occurs in both particulate (PRP, also called suspended reactive phosphorus) and dissolved (DRP) forms. DRP is largely a measure of orthophosphate but also includes a fraction of any labile condensed and organic phosphate which is hydrolysed during the analytical measurement. This is corroborated by a number of studies which report that measurement of DRP tends to overestimate the concentration of orthophosphate. Elevated results for DRP can be attributed to hydrolysis of labile phosphorus-containing species, dissolution of colloid-associated phosphorus and metal–humic substance–phosphate complexes and interference from arsenate [72,73].

Broberg and Persson [67] have identified the three main sources of particulate phosphorus-containing species as:

(1) cellular material of plant, bacterial and animal origin;

(2) weathering products such as primary or secondary minerals; and

(3) direct precipitation of inorganic phosphorus (authigenic mineral formation) or sorption to other precipitates. Additional components are formed by degradation and fragmentation of cells providing organic detritus and the flocculation of phosphorus-containing macromolecules results in larger-sized aggregates. Finally, another components of particulate phosphorus may arise from formation of organic/inorganic coprecipitates or the inclusion of phosphorus by metal–phosphorus binding (Ca, Al, Fe, Mn).

It is impossible to draw any general conclusions about the occurrence of particular fractions in different water bodies because of the variation in the relative contribution of phosphorus fractions in a particular catchment. As an illustration, the Redon River entering Lake Geneva [74] had 5% PP, 85% DRP during low flow conditions and 78% PP, 15% DRP during high flow conditions. Australian rivers are generally more turbid than European systems. Under these circumstances the spatial distribution of total phosphorus concentrations frequently reflects that of turbidity, consistent with the fact that most instream phosphorus is generally bound to particulate matter [75]. The study of the dynamics of phosphorus in aquatic systems [14,46,76–83] is an important consideration and suitable field-based instruments which can continuously monitor phosphorus and ultimately measure the different species in real-time are needed if ecosystem function is

to be understood and water resources properly managed.

Sources of phosphorus. The growing utilization of synthetic detergents and phosphate fertilisers [84] has resulted in increased concentrations of inorganic phosphorus in aquatic systems. Similarly, increasing organic phosphorus is largely due to anthropogenic sources such as domestic sewage, plant and animal wastes [85] and industrial effluents.

The concentration of nutrients in a flowing water is determined both by the amount of nutrient entering the system and by the flow. Nutrient load measurements form the basis of the OECD work on eutrophication [86]. Unfortunately, nutrient load measurements are more difficult to obtain than concentration measurements, needing flow gauging. Nevertheless, their value is being increasingly recognised and load data are used for both water resource management and sewage treatment management. Although the load can be evaluated from measurements of the mean flow and nutrient concentration, the most effective studies of nutrients in flowing waters have used a simple mass balance approach on either a whole catchment or individual rivers [14]. The total phosphorus load of a river may arise from many sources. These include phosphorus from:

(a) the leaching and weathering of igneous and sedimentary rocks such as calcium hydroxyapatite, fluorapatite, strengite, whitlochite and berlinite;

(b) the decomposition of organic matter containing phosphorus compounds either weakly associated with the organic material or chemically bound to it;

(c) effluents of domestic or industrial origin including of more recent importance the loads from fish farms;

(d) diffuse inputs from agricultural land due to inorganic fertilizer use and organic manure application; and

(e) atmospheric deposition [87] and soil/river bank erosion during storm events.

The entry of phosphorus into a river may be classified as either point sources, surface runoff, subsurface runoff, groundwater runoff or as direct wet and dry deposition [14]. Point source inputs such as sewage treatment plants are of greater significance during periods of low flow and in dry years. In wetter years and during storm events diffuse inputs are the dominant nutrient source. The in-stream concentration of nutrients rises during storm events and even in situations where this increase is marginal the effect on nutrient load is significant because of the combination of higher concentration and more significantly higher flow. Allowance must be made for this variation in the design stage of a monitoring programme. As a minimum requirement data should be collected for wet, normal and dry periods. One study in Australia showed that 40% of the flow and 60% of the phosphorus ran off the catchment in 1% of the time [88]. Many studies are limited by logistic and financial constraints to

TABLE 4

Effect of land use on nutrient yields

Type of land use	Total P ($kg\ ha^{-1}\ yr^{-1}$)	Total N ($kg\ ha^{-1}\ yr^{-1}$)	Concentration in stream water ($mg\ l^{-1}$)
Urban, South Eastern Australia [89]	0.6 – 0.9	4 –8	
Pasture, South Eastern Australia [89]	0.1 – 0.3	0.6–1	
Forest, South Eastern Australia [89]	0.009– 0.03	1 –5	
Urban [90]	0.92 – 3.4		0.081–1.18
Cereal field plots [90]	0.1 –67		
Agriculture [90]	0.08 – 6.3		
Forest [90]	0.02 – 0.68		0.006–0.071

continuous measurement of streamflow but only manual grab sampling of water quality parameters. In some instances, manual grab sampling has been combined with rising stage samplers designed to collect water samples as the water level rises during or following a storm event.

The significance of diffuse sources in any given situation depends on the nutrient load or yield (expressed in kilograms per hectare per annum) generated by the particular land-use activity. The highest loads are generally from urban lands with successively lower loads from agricultural and forested catchments (Table 4) [14,91]. Urban loads are conveniently calculated per head of population with daily estimates between 1.9 and 4.0 g of phosphorus per person entering rivers [14]. The phosphorus concentration of a typical treated sewage effluent is about 10 mg l^{-1}. In order to remain below the background phosphorus levels, a dilution factor of between 100:1 and 1000:1 is necessary on discharge. In many situations this dilution will be exceeded but in heavily populated areas particularly at times of low flow it may not be achieved. The European Communities directive on urban wastewater treatment (as reported in Ref. 2) requires sewage works discharging into "sensitive areas" and serving populations of between 10 000 and 100 000 to achieve annual average phosphorus concentrations below 2 mg l^{-1} in their effluents.

Variability in the nutrient yield from agricultural catchments is dependent on the soil structure, crop type and the relative importance of surface and sub-surface run-off. Although phosphorus is generally retained by most soils, subsurface runoff by field drains may contain relatively high concentrations of DRP because of the diminished contact between the subsoil and percolating water [14].

Nitrogen

Nitrogen levels in aquatic systems, as with phosphorus, are intimately linked with excessive algal growth [92]. Total nitrogen levels in waters can vary from as low as 0.1 mg l^{-1} to in excess of 10 mg l^{-1} in heavily polluted rivers. The forms of nitrogen of greatest interest in waters [93] are nitrate, nitrite, ammonia and organic nitrogen.

TABLE 5

Maximum admissible concentrations and guide levels (expressed as elemental concentrations) for various species in water to be used for human consumption

Species	MAC (mg l^{-1}) [101]	GL (mg l^{-1}) [101]	GL (mg l^{-1}) [31]
Nitrate	11.3	5.65	10
Ammonia (total)	0.38	0.038	0.1
Nitrite	0.03	–	1.0
Kjeldahl nitrogen	1	1	–
Phosphate	1.091	0.087	

These forms are all interconvertible with each other and with molecular nitrogen. Levels of the various species vary widely depending on geographical location, local geology and land use but nitrate is usually the most important in waters. The values given in Table 2 provide an indication of the levels typically encountered. Ammonia-N and nitrite-N concentrations in river waters are usually much lower than nitrate-N values and rarely exceed 0.5 mg l^{-1}. Higher values are normally the result of industrial pollution and can reach levels as high as 2 mg l^{-1}.

Elevated nitrate levels warrant some clinical concern [94,95] because of links with methaemoglobinaemia (blue baby syndrome) [96] and gastric and stomach cancers [97,98]. Such reports have led to legislation by the World Health Oganisation [99] and the EC [100] stipulating guidelines for nitrate and ammonia levels in water to be abstracted for public consumption. These maximum admissible concentration (MAC) and guide levels (GLs) are summarised in Table 5. A number of criteria documents [102,103] specify a limit of 20–30 μg l^{-1} of non-ionised ammonia based largely on the toxicity of ammonia to sensitive cold-water fish. However, the concentration of non-ionised ammonia is controlled by pH and temperature. The total ammonia concentration corresponding to these limit values at selected pH and temperatures is given in Table 6. Data are insufficient to provide detailed no-effect levels for nitrate and nitrite in drinking water for different animal species. Meanwhile, recommended maximum concentrations [31] for drink-

TABLE 6

Selected total (ammonia + ammonium ion) concentrations corresponding to a concentration of non-ionised NH_3 of 0.02–0.03 mg l^{-1} (Source: USEPA 1985)

pH	Total (ammonia + ammonium) concentration (mg l^{-1}) at temperature (°C)			
	0	10	20	30
6.5	2.5	2.2	1.49	0.73
7.5	2.5	2.2	1.5	0.74
8.5	0.49	0.45	0.32	0.17
9.0	0.16	0.16	0.13	0.08

ing water for livestock are 30 mg l^{-1} NO_3-N and 10 mg l^{-1} NO_2-N. Various bodies have proposed guideline values for nutrients in rivers and streams. More recently, there has been a recognition of the fact that the blanket imposition of a single numerical criterion is inappropriate because individual systems differ in their response and ability to cope with elevated nutrient levels. Site specific studies are necessary to determine the potential for nuisance plant growth following which guidelines can be set for the particular water bodies. Meanwhile, levels of phosphorus and nitrogen species which have given rise to algal problems in various water bodies are summarised as indicative concentrations in Table 7.

Nitrogen species. Inorganic nitrogen species are chemically well characterised whilst organic nitrogen [104] includes a number of naturally occurring compounds such as urea, proteins, peptides and nucleic acids in addition to numerous synthetic organic substances. Functionally, organic nitrogen is defined as organically bound nitrogen in the −3 oxidation state and thus, does not include all organic nitrogen compounds. From an analytical viewpoint, organic nitrogen and ammonia have been referred to as "total Kjeldahl nitrogen" reflecting the technique by which they are determined. Other operationally defined nitrogen fractions (Fig. 5) include total dissolved nitrogen (TDN), dissolved organic nitrogen (DON) and dissolved inorganic nitrogen (DIN = nitrate + nitrite + ammonia). DON dominates the flux of total nitrogen from land to sea, generally making up to 60% of total export [105]. It is usually measured as the difference between TDN and DIN (i.e., DON = TDN − DIN).

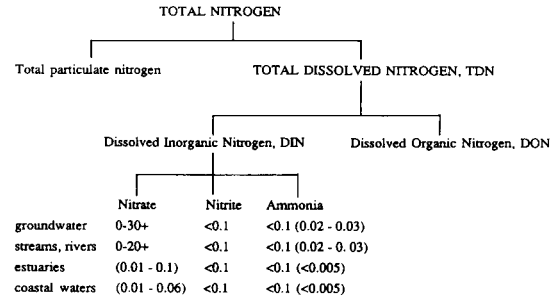

Fig. 5. Nitrogen speciation in natural waters. Concentrations are expressed as mg nitrogen per litre. Values are quoted as ranges typically encountered in a variety of waters. The values in brackets represent indicative values [31] at or above which problems have been known to occur, depending on a range of other factors. TON is usually used to refer to total oxidized nitrogen (i.e., NO_3-N + NO_2-N) and less commonly to total organic nitrogen with which it must not be confused.

Sources of nitrogen. Nitrogen-containing species arise [78,106,107] from both normal processes (e.g., hydrolysis of urea) and from anthropogenic sources (e.g., nitrite used as a corrosion inhibitor in industrial process waters). Ammonia is a product of microbiological decay of plant and animal protein and is applied directly to land as

TABLE 7

Indicative levels of various species at or above which problems have been known to occur in Australian waters [31]

Parameter	Concentration (mg l^{-1})			
	Rivers/streams	Lakes/reservoirs	Estuaries/embayments	Coastal waters
Total-P	0.01–0.1	0.005–0.05		
Total-N	0.1 –0.75	0.1 –0.5		
PO_4-P			0.005–0.015	0.001–0.01
NO_3-N			0.01 –0.1	0.01 –0.06
NH_3-N			< 0.005	< 0.005

fertilizers. The presence of NH_3-N in surface waters usually reflects domestic pollution whereas its presence in groundwaters is normal and a result of microbiological processes. Nitrite-N occurs as an intermediate stage in the microbiological decomposition of nitrogen-containing compounds. Nitrite-forming bacteria convert ammonia to nitrite under aerobic conditions. Bacterial reduction of nitrates to nitrites can also occur under anaerobic conditions. The most oxidised form of nitrogen (oxidation state +5) commonly found in waters is nitrate. Nitrate-forming bacteria convert nitrites into nitrate under aerobic conditions. Large amounts of nitrate are also formed by direct conversion of atmospheric nitrogen by lightning.

Apart from the natural input of nitrogen from rainfall [5,108], the main inputs of nitrogenous matter into freshwater come from farm slurry and sewage and, most significantly, from leaching of fertiliser from agricultural land [11,109] via wastewater point discharges or diffuse runoff. Over the last few decades nitrate levels have increased steadily in many freshwaters due predominantly to increasingly intensive agricultural practices [110–114]. Available evidence supports the conclusions of the Royal Commission on Environmental Pollution [115] that changes in agricultural practice [84], including fertiliser use, are a major contributor to the rising trends in nitrate levels in both rivers and groundwaters.

Although the link between fertiliser usage and nitrate concentrations in rivers and groundwater is not a simple one, it has been estimated that the addition of nitrogen-based fertilisers (mainly ammonium nitrate and urea) has increased over tenfold in the UK in the last 50 years [116] and is predicted to increase by 4–5% annually [110]. On average only 50% of available nitrate in the soil is recovered in the crops [117]. Most of the particles in the soil are negatively charged so that nitrate is not adsorbed and is carried by rainfall and soil solution into underground aquifers and drainage water. The nitrogen cycle in the soil is extremely complex and the amount of nitrate leached depends on many factors, including the crop, chemical and physical conditions in the soil, soil moisture and rainfall. Moderate environmental disturbances such as floods causing minor changes in the vegetation of the drainage basin usually result in increased nitrate in streams. More severe land disturbance which accelerates erosion mobilises

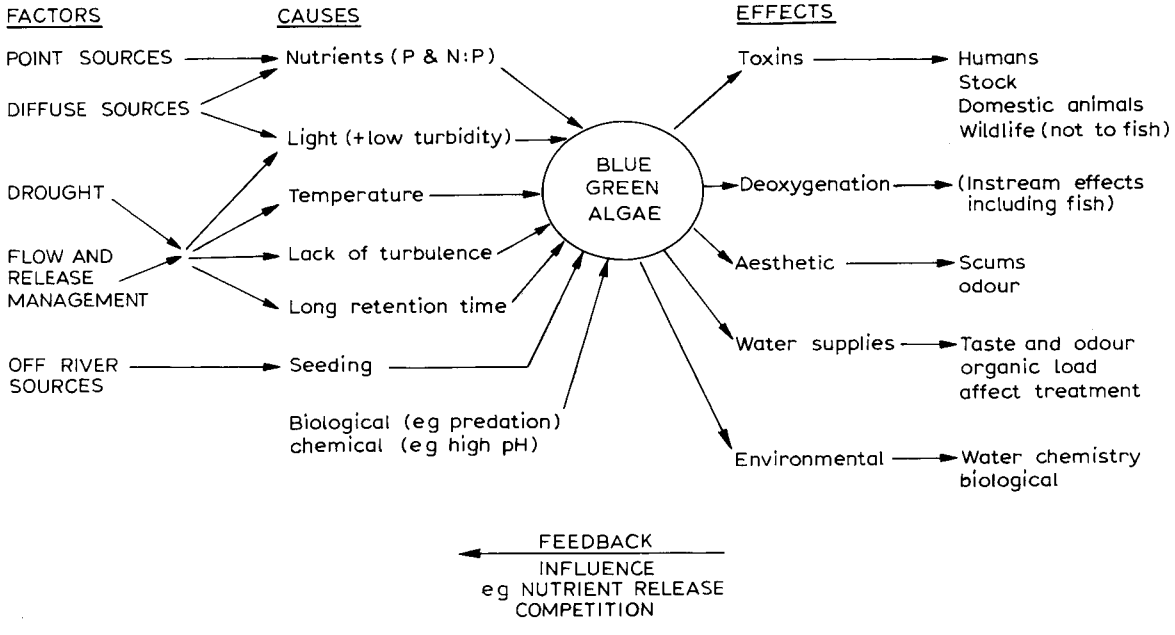

Fig. 6. A conceptual model of algal dynamics showing major causes and effects of blue-green algal blooms.

nitrate in solution and large quantities of phosphate bound to sediment particles.

The N to P ratio [118,119] (Table 2) has found increasing use as a tool in the control of nuisance algal blooms. However, there are many situations where this management tool is inappropriate for a variety of reasons, including the uncertainty over what measures of N and P should be used in calculating the N to P ratio.

Models. Various models have been developed for algal dynamics which demonstrate the key role of nutrients. These models generally belong to one of three main groups as: mechanistic, empirical, or conceptual, although most models assume aspects of more than one approach. Moreover, it is possible and usual to start with one model type and progress to or utilise the others. Mechanistic models are mathematical descriptions of systems based on theoretical principles. The present state of knowledge is insufficient to allow the development of a comprehensive mathematical model but there is adequate information to represent the various interactions between the factors affecting algal growth. Moreover, recent work has been strongly influenced by the largely empirical eutrophication studies of the OECD [120]. Conceptual models have been widely used as display and management tools or as frameworks on which to build models of other types. The conceptual model developed by the New South Wales Blue-Green Algae Task Force (Fig. 6) illustrates the interactions between causes, consequences and effects in relation to algal blooms.

Silicon

Diatoms require large quantities of silica for their cell walls [121,122] and, where diatoms are the predominant algae, silicon can therefore be a limiting element for phytoplankton growth. Both geochemical and biochemical processes affect the silicon content of natural waters; the annual input of soluble silicon from glacial weathering of rocks in the Antarctic exceeds 400 million tonnes. Silicon occurs in natural waters predominantly as reactive silica, i.e., soluble SiO_4^{2-} and its short chain polymers but also as longer polymers and inorganic and organic fractions of suspended material. Dissolved silica shows a considerable range of concentrations (Table 8) [127], from values exceeding 20 mg l^{-1} in hot springs down to trace levels in the surface waters of the sea at the time of the spring diatom bloom. Reactive silica is probably the only form that is readily available for diatom growth. Other forms such as clays and colloidal silica play an important physico-chemical role by providing sorption sites for phosphate and ammonium. Seasonal changes in silicon concentration due to biological production have been demonstrated for many rivers [128–130]. The behaviour of silica in estuaries has been studied by Burton and Liss [131]. House [124] has reviewed aspects of the reaction of silica with water and the study of silica in experimental microcosms and also its chemical speciation.

TABLE 8

Silicate concentration in waters [123–126]

Water type	Concentration (mg l^{-1})
Stream	5
River	1–15
Lake	< 0.5–60
Sea, surface	Trace
deep ocean	4
Brine	Up to 1000

Other elements

Many other elements are of interest as either micronutrients or because of their toxicity. Ecological interpretation of the role of elements such as manganese, zinc, copper, molybdenum, cobalt, vanadium and boron is complicated by incomplete data on their speciation and biotic availability. Daily, seasonal and annual variations in temperature, dissolved oxygen, pH, and chelating capacity of the water may rapidly change both the total and biologically available quantities of these elements. Various aspects of the speciation of these elements are treated in a number of reviews [132–139] and a critical comparison of methods for the determination of this group of elements has been presented [140].

ANALYTICAL APPROACHES

General considerations

Trace analysis is at the forefront of analytical chemistry. The meaning of the term "trace analysis" inevitably shifts with developments in instrumentation and the background or interest of the analyst. Nevertheless, current usage implies an upper limit for a trace determination of the order of 5 mg l^{-1} with the lower limit being set by the detection limit for the method. This range encompasses the concentration of nutrients in many waters and the problems which beset trace analysis, in general, (and their solutions) are relevant to the current discussion. The trend in trace analysis has been to extend the lower limit of this range by reducing detection limits. However, each improvement in analytical technology has simultaneously created the desire to know more about a sample by characterising more components or by determining target compounds at ever decreasing limits of detection. Progress in fields as diverse as optics, solid state electronics and computer technology combined with demands for increasingly detailed chemical knowledge, have stimulated this need. Unfortunately, the ability to measure low levels of analytes has, in many instances, exceeded the ability to understand and interpret the data and this has contributed to the problems of poor precision and low accuracy which are highlighted in various collaborative surveys [141].

Topping [142] has identified the three factors which contribute to the quality of environmental data as the design and conduct of a representative (and contamination-free) sampling programme, the selection and use of suitable storage procedures to minimise changes in analyte concentrations and speciation prior to analysis, and the adoption of analytical procedures of appropriate accuracy and precision. The increasing use of robotics, chemometrics, standard reference materials and collaborative surveys [141], all of which involve a cost, can contribute to establishing the reliability of the sampling and storage procedures and the analytical measurement programme. Standard reference materials have an obvious role in ensuring that the analytical measurement programme is performed reliably [143]. The Sagami Chemical Research Centre produces a reference material for nitrate and phosphate. However, these standards are prepared in either fresh water or in 30.5 g l^{-1} sodium chloride solution. The use of autoclaved sea water as a reference material for nitrate and phosphate has also been described [144]. This highlights a common problem; that reference materials of suitable concentration and matrix are unavailable for many of the analytes covered by this review. In contrast, standard methods for the analysis of waters are provided by groups such as the American Public Health Association (APHA) [145] and various regulatory bodies including the Environmental Protection Agencies of Japan and the USA and DIN in Germany and in the so-called "Blue Book" methods in the United Kingdom [146]. Standard methods such as USEPA Methods 350.1 for ammonia, 353.2 for nitrate + nitrite, 365.1 for orthophosphate, 365.4 for total phosphorus and 370.1 for silica offer many advantages, not least of which is that they are well validated. On the other hand, standard methods can be very time consuming and frequently do not use state-of-the-art technology. In all cases, methods of expressing concentrations must be unambiguous. Concentrations of nitrate, nitrite or ammonia, for example, should be expressed as elemental nitrogen. Hence nitrate is expressed as NO_3-N in milligrams per litre (mg l^{-1}) or micrograms per litre (μg l^{-1}) or as millimolar (mM) or micromolar (μM) using nitrogen = 14. The reader may be uncertain of the method of expression especially in some older literature.

The ever-increasing numbers of samples collected during oceanographic and limnological investigations and the current trend towards legislation relating to water quality, e.g., the environmental quality objectives stipulated by the EC [101,147–152] are likely to increase the burden on resources available for water monitoring. In these circumstances, the introduction of automated methods of nutrient analysis is essential. Methods based on immobilised enzyme technology [153,154], conductive electroactive polymers [155] and fiber optic (bio)sensors [156–159] when incorporated in flow-injection manifolds will un-

doubtedly increase in popularity. Disposable sensor devices [160] will also have an important role when developed and tested for a broader range of analytes.

Sample collection and preservation

Details of sampling, field treatment and storage of samples are specific to individual analytes and techniques. Nevertheless, some generalisations can be made. The problems associated with the taking, filtration and storage of water samples have been discussed [141,161–164]. Sampling programme design must recognise and enable measurement of the different components of variability in data. Variability of environmental data has three major sources. There is the environmental (temporal and spatial) variability itself. Secondly, the sampling techniques may introduce error and thirdly, analytical methods may also introduce error. The overall variability ultimately determines the sampling design and frequency. However, compromise is usually necessary between statistically correct design and practicality in order to match the needs of monitoring programmes with available resources. This compromise must be acknowledged when decisions are made using the results of the programmme. In the case of non-point sources temporal variations are especially important as much of the total annual mass transport or load occurs during a short period of high flow during flood events. Flow measurements are subject to significant error which must be accounted for in calculating loads. Indeed, of the total variability in load data, the effect of sampling and measurement is probably small in comparison with the variability in flow.

Polyethylene, other plastic or hard rubber bottles are suitable collection and storage vessels in most situations although phosphorus-containing species may be adsorbed onto the walls of plastic containers. Borosilicate glass is generally a less desirable choice, particularly when silica is to be determined in waters of pH > 8 or with sea water, where a significant amount of silica in the glass can dissolve. However, for measurement of organic carbon fractions glass is the preferred storage container [163]. Sampling, preconcentration, extraction and separation of organic compounds have been reviewed by McCarthy et al. [165]. Where measurement of dissolved gases such as carbon dioxide and ammonia is necessary, sampling requirements are more exacting than general sampling needs for water analysis because of problems of contamination and degassing [166].

The use of automatic samplers which can be programmed to take samples at specific time intervals or when a flow related event takes place has increased dramatically; however, there can be problems associated with these samplers [164]. Most reliable data are obtained on fresh samples and immediate analysis is always preferable. Where speciation into dissolved and particulate fractions is required, the filtration should be performed immediately after sampling. If an immediate analysis is not possible, storage at a low temperature (4°C) immediately after collection may be suitable in some instances. On the other hand, storage $\leqslant -10$°C is recommended for samples requiring determination of phosphorus species [145]. Freezing may lower soluble silica values, however, by as much as 20–40%. Changes in phosphorus fractions during storage of lake water [167] and the effect of frozen storage on the concentration of dissolved phosphate and nitrate in open-ocean sea water samples [168] have been reported. In light of these recent data re-evaluation of recommended storage conditions for waters may be in order. Chemical preservatives should only be used where they have been shown not to interfere in the analysis required. For example, addition of mercury(II) chloride and chloroform to the filtrate from alumina treated water reportedly stabilises nitrite and nitrate for several months [169]. However, no single method of sample preservation is entirely satisfactory [170] and all methods of preservation are probably inadequate when applied to samples containing a high concentration of particulate matter. This is illustrated by the determination of organic nitrogen where samples may be preserved by acidification to pH 1.5 to 2.0 and storage at 4°C. In this case, mercury(II) chloride cannot be used as it interferes with removal of ammonia in the analytical method. In contrast, addition of

acid must be avoided where phosphorus speciation is required [145]. Here, addition of mercury(II) chloride (40 mg l^{-1}) and storage at −10°C is the recommended method [145] of preservation for samples that cannot be analysed immediately. Nevertheless, the use of mercury salts as a preservative should be discouraged on environmental grounds.

The reliability of quantitative data for phosphorus is a notable problem [171] in many laboratories. Poor reproducibility and interference effects are common. As an instance, membrane filters may contribute a significant phosphorus blank and should be pre-washed before use by soaking in distilled water [172]. Commercial detergents containing phosphate should never be used for cleaning glassware used in phosphate analyses.

Techniques

The continuing use of analytical techniques based on operational definitions is likely to persist at least for the present. Such procedures are convenient but require considerable care in use and interpretation of data. As an illustration, methods for particulate or dissolved species are dominated by techniques involving separation, isolation and characterisation of fractions whose exact chemical identity is unknown. In such procedures, reproducibility of the particle size cut-off between fractions is an important consideration which depends on the quality of commercial filters. Moreover, the possible introduction of contaminants from the filter membrane is always present. Both glass and silver fiber membranes contain variable amounts of organic carbon that must be removed by combustion at around 400°C before use. This combustion effectively removes the carbon but it also alters the effective pore size of the filters [25]. The filtration step certainly warrants close examination if accurate data are to be obtained [173]. When considered in relation to Fig. 1, the choice of a 0.45 μm cutoff appears inappropriate and can only be justified by convenience.

The conventional approach to water quality monitoring is to combine periodic manual sampling with batch analysis in the laboratory. Many problems are associated with this approach which is labour intensive and time-consuming. The benefits of automating nutrient analysis in waters [174] and wastewater treatment plants [175] have been recognised and utilised for several decades. Continuous flow analysis (CFA), both segmented (AutoAnalyzer) and unsegmented (Flow-injection analysis, FIA) has been widely used for this purpose. The analysis of all major nutrients in sea water, for example, has been automated by segmented CFA, including the determination of nitrate and nitrite, silicate, phosphate and ammonia. FIA is also capable of automated analysis [176]. The two techniques are complementary and the choice between them depends on a number of factors [177]. With proper plumbing of the manifold, sample cleanup and preconcentration, zone sampling and reagent injection [178] can be utilised in both segmented and flow-injection methods. These techniques are particularly useful for difficult samples such as sea water which contain very low levels of analyte and are of varying salinity. As a result of this variable matrix, refractive index effects are observed with photometric detectors. Automation eliminates many of the problems associated with batch analysis, but sample contamination and stability problems are still encountered. The most serious difficulty is that the data are neither continuous nor immediate. Nevertheless, both manual and automated batch analysis continue to exist.

There is a growing interest in automated on-site monitoring devices for measurement of water quality parameters and in the control of treatment plants [179]. Such devices must meet several criteria in addition to those of accuracy, precision, sensitivity and selectivity which are required of laboratory-based methods. These criteria include low power consumption, a facility for periodic recalibration, long term stability, compact and robust design and a data logging or direct data transmission facility. All automatic monitors rely upon having a good pumping and filtration system in order that the sampling line does not run dry, become blocked by suspended solids or fouled by biofilms. If possible, the system should be gravity fed which eliminates the problems of power interruption resulting in failure of water

supply pumps. If possible it is advisable to have a battery backup in case of power failures.

Most of the commercial instruments currently available for on-site use are based on electrochemical detection, are subject to physical and chemical interferences, and are restricted to a limited number of chemical parameters such as conductivity, pH and dissolved oxygen. On the other hand, well documented spectrophotometric methods are available for a wide range of analytes which are readily adapted to flow-injection techniques. When coupled with in situ sampling for field monitoring, FIA has the potential for frequent and immediate acquisition of quantitative data on the different physico-chemical forms of nutrients. Field monitoring also eliminates many of the problems associated with sampling and sample storage.

In one programme aimed at providing information on water quality in rivers of the UK a network of water quality stations was established and measurements made at some 245 stations [180]. Frequency of sampling ranged from once every few days to once a month, the aim being to determine the annual mean concentrations of discharged pollutants to an accuracy of $\pm 20\%$ or better. Obviously a more intense sampling programme is needed to detect changes in concentration occurring over a shorter time period as in the case of nitrate in rivers which shows not only large seasonal variations [112,181] but also short term changes [182,183]. Automatic samplers have been used [181,182] to detect these changes, sampling times varying between hourly and six hourly. A number of automatic water quality monitoring stations have been set up with varying degrees of success [184,185] and these provide the best estimates of short term changes in water quality.

SPECIFIC ELEMENTS

Carbon

The carbon pool in fresh and marine waters represents a major component in the global organic budget and yet, its accurate determination presents considerable analytical difficulties. Inorganic carbon is more easily measured than organic carbon because it is better characterised and generally present at higher levels in waters. Numerous analytical procedures have been developed for determining total inorganic carbon (TIC) reflecting the fundamental importance of this parameter in water resource management and treatment. The distribution of TIC among the various components (carbonate, hydrogencarbonate, dissolved CO_2 and suspended carbonate) is largely a function of pH. The analysis procedure must therefore be performed in a way that provides the information required. Total carbon dioxide, for example, can be obtained by acidifying the unfiltered water prior to purging with or without heating. On the other hand, free available carbon dioxide may be determined by a purging operation without acidification provided there is no volatile organic carbon. Gas dialysis has also been used in a number of instances as a highly selective means of isolating carbon dioxide [186,187].

Methods for measuring TIC. Direct methods for TIC include spectrophotometric titrations [188], chromatographic separations [189] such as gas chromatography [166] or indirect ion chromatography with UV detection at 250 nm [190–192], nondispersive IR absorption measurements of evolved CO_2 gas [193,194] and, more recently, flame IR emission (FIRE) detection [195]. The FIRE-TIC system consists of two commercially available purge devices coupled to a FIRE detector. Water samples are acidified in the purge device to convert carbonate and hydrogencarbonate to carbon dioxide which is then purged from the sample with helium and introduced into a hydrogen/air flame where the CO_2 is vibrationally excited. Measurement of TIC is accomplished by monitoring the 2264 cm^{-1} infrared emission intensity from the excited CO_2 molecule using a lead selenide photoconductive detector. The detection limit with this system corresponds to 0.03 mM Na_2CO_3 and although elevated levels of volatile organic carbon interfere, results for (T)IC in natural waters agreed with values obtained by alkalinity titrations. Other direct procedures for (T)IC involve FIA with either IR [196] or colorimetric detection [197] following isolation of the gaseous CO_2 by gas diffusion, the use of a fiber optic chemical sensor [198] and the en-

hancement of luminol chemiluminescence caused by CO_2 [199]. Interference by ions which also enhance the chemiluminescence was eliminated with a continuous flow membrane. However, many of these procedures are tedious and/or expensive. Hence, the most common measure of (T)IC is indirect and involves the measurement of the total alkalinity of a water which is defined as the quantitative capacity of the water to neutralise strong acid [200].

In many natural waters, carbonate, hydrogencarbonate and hydroxide are the only Brønsted bases and the total alkalinity can be determined by measuring the specific conductance of the water or, more commonly, by titration [201] to a pre-selected end point with a strong acid. End point detection can be achieved with either an indicator or potentiometer. The pre-selected end point for natural waters may vary between pH 5.1 and 4.5 [145] depending on a number of factors including the expected concentration of CO_2. However, alkalinity measurements are subject to many interferences [202] and require prior knowledge of the water composition for proper selection of the end point pH. Computer calculated coefficients are available [201] to correct for the influence of pH and calcium ion concentration on the inorganic carbon. However, even in the area of inorganic carbon, which is relatively well characterised, there exists an unfilled need for a reliable method suitable for field monitoring [203].

Methods for measuring organic carbon. In contrast to inorganic carbon, the organic carbon is extremely diverse and present at much lower concentrations. Physical measurements of the organic carbon such as absorbance [204] and turbidity are attractive in that they are simple and readily automated to provide real time data. In general, the correlation between absorbance at 330 nm and DOC is relatively poor ($r^2 = 0.710$) [205] although the predictive power of absorbance measurements increases when samples are split into groups of origin [204]. However, such methods are non-specific, suffering from interference by particulate matter and coloured species. Allowance for the 1,10-phenanthroline-reactive iron, for example, improved the correlation ($r^2 = 0.962$) between absorbance at 330 nm and the DOC in peat water. Furthermore, absorption at 250 nm and fluorescence at 470 nm (using 365 nm excitation) of humic waters varied with the molecular size of the dissolved organic matter [206], limiting the value of such measurements. On the other hand, traditional methods of obtaining information on the bulk organic matter of water such as chemical oxygen demand (COD) and biological oxygen demand (BOD) are time consuming and suffer various limitations. The BOD test is the oldest and measures the amount of oxygen consumed via biological degradation of organic carbon (and inorganic matter such as iron(II) and sulphides) in a sample during a specified time period. BOD may also measure the oxygen consumption by reduced forms of nitrogen unless their oxidation is prevented by an inhibitor. BOD determination is time consuming, all compounds are not readily biologically degradable or degrade at varying rates, is often not reproducible [207] and is not sufficiently sensitive to detect small changes. The BOD test has its widest application in measuring waste loadings to treatment plants and in evaluating the efficiency of such systems. COD determination measures the ultimate oxygen consumption of a sample. The COD test requires less time and the results are more reproducible but requires expensive and toxic reagents, includes inorganic compounds and does not adequately measure contaminants stable and resistant to biological degradation [208]. As a consequence, it has been necessary to resort to chemical methods. Procedures for measuring individual carbon compounds or groups are relatively well documented. However, complete characterisation is not feasible on a routine basis and experimental procedures for measuring organic matter [209] generally exploit the common feature that all organic compounds contain oxidizable carbon. Thus, methods for the determination of organic carbon (whether DOC, POC or TOC) in natural waters usually comprise an oxidation step followed by separation and measurement of the resultant carbon dioxide. Variations on this basic approach differ both in the means of oxidation and of measurement. The total organic carbon (TOC) test was developed as an alternative to the BOD and COD tests. It

TABLE 9

Selected procedures for the determination of carbon in waters

Sample	Fraction	Procedure	Detection	Ref.
Natural water	IC; VOC, NVOC	Isotope ratio	Mass spectrometry	20
Surface water	IC	Acidification and gas dialysis	Colorimetry	186
Natural water	Total alkalinity	Titration	Potentiometry	200
Fresh water	TIC	Segmented flow analysis of acidifed, heated sample. diffusion membrane	Indirect colorimetry	187
Sea water	IC; DOC	FIA using photo-oxidation	IR spectrometry	196
Pond water	Dissolved IC	Continuous flow	CO_2 electrode	210
Natural water	Free CO_2	Gas exchange		211
Natural water	TIC	Acidification and purging	Flame IR emission detector	195
Sea water	TIC	Continuous flow	Coulometric titration	203
Lake water	TIC; VOC	Acidification and purging	IR gas analyser	194
Natural water	TIC	Titration	Visual indicator	202
Natural water	TOC	Continuous flow system on purged sample	ICP-AES	212
Natural water	TOC	Peroxydisulphate digestion	Electroconducto-metric titration	213
Natural water	TC; ?	Heat sample at high temper-ature in air in presence of nickel catalyst	Flame ionisation detection of methane	214
Potable water	TOC	Segmented flow analysis of stripped and peroxydisulphate oxidized sample	IR gas analyser	215
Natural water	POC	Glass fiber filtration and high temperature combustion	TCD	216
Lake water	POC	Glass fiber filtration		217
Sea water	DOC	Continuous flow analysis based on photo-chemical oxidation of purged sample	Colorimetry	218
Sea water; estuarine water	DOC	Continuous flow analysis based on photo-chemical oxidation of purged sample	FID	219
Sea water	DOC	Comparison of methods	Various	24
Lake water	DOC	Wet chemical or UV oxidation of purged sample	IR gas analyzer	220
Fresh water	DOC	Segmented flow analysis of acidified, purged sample. Phot-chemical oxidation	Photochemical oxidation	208
Stream water	DOM, DOC	Oxygen consumption during dichromate oxidation	Absorbance at 360 nm	221
River water	DOC	Comparison of sensitizing agents for photo-chemical oxidation		222
Water	biodegradable DOC	Bioassays to measure biologically available DOC	TOC analyser	223–226
Water	DOC	Modified ampoule sealing procedure for perioxydisulphate oxidation of purged sample	TCD or IR gas analyser	227
Peat water	DOC	Not available	Absorbance at 330 nm	205
Natural water	DOC	High temperature combustion	ICP-AES	228

TABLE 9 (continued)

Sample	Fraction	Procedure	Detection	Ref.
Sea water	DOC	High temperature oxidation of purged sample; membrane filtration of fresh sample	IR gas analyzer	229
River water	DOC fractions	LC	UV at 254 nm; DOC IR gas analyser	230
River water	DOC fractions	Not available		231
Natural water	DOC fraction	Chromatographic fractionation	DOC detector	232
Treated water	DOC fractions	Fractionation using ultra-filtration		233
Natural water	DOC fractions	Chromatographic fractionation	IR gas analyzer	234
Lysimeter water	DOC fractions	Fractionation using chromatography and ultra-filtration	UV at 254 nm	235

measures the concentration of organic carbon in a sample regardless of its degradability. The TOC value can aid in the assessment of pollution and biological degradation in natural waters and the adverse effects of a high concentration of organic compounds, via oxygen depletion, on the aquatic ecosystem.

Measurement of the various operationally defined carbon fractions (Table 9) may involve preliminary processing of water samples. In the determination of TOC, for example, interference by the inorganic carbon fraction can be eliminated by acidifying samples to pH 2 or less and subsequently purging the sample with purified gas to remove the CO_2. However, VOC is also removed by purging [236] and so the fraction determined in this manner is strictly the NVOC. In many waters the VOC contribution to TOC is negligible and, in practice, determination of NVOC is substituted for TOC. The validity of this procedure must be established for each sample type as the volatile purgeable fraction of TOC is dependent on analytical conditions of sample temperature, volume and salinity, purging gas flow-rate and time, and dimensions of the purging vessel. Alternatively, TC and TIC may be measured independently and the TOC obtained as the difference between the two results. Although TOC may be measured directly, in itself it is not the most useful term as the contribution of the individual components, DOC and POC, is variable. For example, POC increases dramatically in river water with increasing discharge while there is less variation in DOC.

Four principal approaches used for the oxidation of organic matter to carbon dioxide are wet chemical oxidation, dry combustion, high temperature catalytic combustion and UV photo-oxidation [25]. The most widely accepted method has been wet chemical oxidation using a variety of oxidants [25] which vary in strength. The standard procedure has become the peroxodisulphate technique involving reaction of sample with peroxodisulphuric acid in a heated sealed ampoule [227]. Photo-oxidation with high intensity UV radiation is now well established as a technique for the decomposition of organic matter. It may be used with a chemical oxidant [218,219,237–239] or alone [196]. Potassium peroxodisulphate is more effective than other compounds such as mercury(II) chloride for accelerating photochemical oxidation [222] of organic matter in waters. Photo-oxidation methods also differ in the intensity of the source and the time of exposure. Photo-oxidation has several advantages relative to chemical oxidation, the most important being that the oxidant is generated continuously and therefore is not subject to exhaustion. There are also disadvantages of photo-oxidation; the failure to oxidise particulate matter efficiently is notable. Combustion methods are conveniently divided into dry combustion methods in which the sample is dehydrated prior to high temperature combustion and direct injection, high temperature cat-

alytic combustion [25,240]. A knowledge of the catalyst structure and function [241] is required in order to avoid the application of the high temperature catalytic oxidation methods in an entirely "black box" manner.

Discrepancies between results from the four approaches have been identified by several workers for a number of sample types [25,242] and have been attributed [218] to analytical bias and the low oxidation efficiency of chemical oxidation procedures for high molecular mass organic substances. Complete oxidation of organic matter has generally been assumed during high temperature combustion and such techniques have been considered the reference methods [243] for DOC. The high temperature combustion method gave a result for DOC in sea water [24] which was 5% higher than that obtained by photo-oxidation procedures. Although this variation was not significant at the 95% level there was a significant difference between the value as determined by high temperature combustion and peroxodisulphate oxidation with the latter giving the lower result. Sugimura and Suzuki [229] highlighted the problems of DOC measurement in a key paper published in 1988. Although elevated DON concentrations were reported as early as 1985 [244], it was the report of elevated DOC levels in 1988 that aroused most interest [245] because of the ramifications for global carbon cycles and budgets. The results for DOC suggested the existence of a previously overlooked pool of DOC [246] that is probably biologically labile. The approach used in this paper has now been refuted and Suzuki himself has admitted [247] to errors in his earlier approach. Analytical blanks account for much but not all of the poor precision in measurement of DOC [248,249]. Blank values can be significant [250] and must be measured carefully to obtain reliable data for DOC. Although the results of this study have now been refuted it in no way diminishes the problems of DOC measurement which have been identified subsequent to the initial report. Unfortunately, there is still no reliable method for the measurement of DOC. This can be attributed [251] to "an incomplete understanding of the structural characteristics of dissolved organic matter (DOM) in natural waters, and the general unavailability of representative reference samples and clean water for blank determinations". Moreover, "the difficulty of separating the effects of instrument blanks from variations in the completeness of oxidation have made both high and low values suspect, with no guarantee of truth in between". Theoretically, complete oxidation of essentially all organic compounds is feasible with both UV- and peroxodisulphate-based oxidation procedures. The key to the failure in achieving this goal is the kinetics of the oxidations because the free radical reactions [252] involved have a wide variety of pathways and rates. Moreover, the efficiency of chemical oxidation and photo-oxidation [253] also varies between different classes of simpler low molecular mass compounds [254] and this must be considered when choosing standards for calibration purposes. Reaction conditions may affect oxidation efficiency as evidenced by the adverse effects of excessive sample acidification on DOC recoveries [254]. The question of the completeness of oxidation cannot be answered without an absolute reference method for DOC.

Potential problems in the sampling and processing of waters for DOC measurement should not be overlooked. Primary among these is the need for minimizing biological activity without changing the DOC content. There is substantial evidence [25] to suggest that bacterial decomposition of DOC is rapid over the first hour after sampling. Moreover, the possibility of sorptive losses of DOM to container walls has not been addressed.

Once oxidized to carbon dioxide, the quantification step is relatively non-problematic and can be achieved by a variety of procedures including gas chromatography, manometry and non-dispersive IR spectrometry [194,213,255] to yield precise results. Various chromatographic detectors [256] are suitable for measuring the CO_2 directly or indirectly after reduction to methane. Procedures using flame ionisation [219,257] or thermal conductivity detection [216] are extremely sensitive but require relatively sophisticated instrumentation. Typical detection limits of 1–5 mg l^{-1} may be decreased to 0.3 mg l^{-1} with the use of inductively coupled or d.c. plasma atomic emis-

sion spectrometry [212,228,258] to measure the quantity of CO_2 produced. Colorimetric measurement [218] is simple and compatible with continuous flow analysers. The usual procedure involves diffusion into a weakly buffered indicator solution and measurement of the loss in colour

TABLE 10

Selected procedures for the determination of phosphorus as DRP in waters

Sample	Technique and mode of detection	Species detected	Calibration range ($\mu g\ l^{-1}$)	Ref.
Water effluent	Batch, spectrophotometry	Orthophosphate–alizarin red sulphonate complex	30–600	260
Waste water	FIA, spectrophotometry	Orthophosphate–Crystal Violet ion pair	0–5000	261
Natural water	FIA, spectrophotometry	[a] MP-malachite green ion pair	10–800	262
Sea water, natural water	FIA, spectrophotometry (reagent injection, field system)	MP blue	3.1–31; 0–2000	174, 176
Natural water	FIA, spectrophotometry (ion exchange preconcentration)	MP blue	0.2–5.0	263
Natural water	FIA, spectrophotometry (long capillary cell)	MP blue	0.03–15	264
Potable water	FIA, spectrophotometry (simultaneous detection)	MP and Rhodamine B	50–2500	265, 266
Sea water	FIA, spectrophotometry (reagent injection)	MP blue	2–130	267
Surface water	FIA, spectrophotometry	MP blue	50–500	268
Potable and mineral water	FIA, spectrofluorimetry	Differential kinetic measurement of thiochrome produced by oxidation of thiamine by molybdosilicophosphate	20–1000	269
Natural water	FIA, spectrofluorimetry	Quenching of Rhodamine 6G fluorescence by MP	5–100	270
Natural water	FIA, spectrophotometry	MP blue	0–4000	271
Water	Batch, FIA, gel-phase absorptiometry	MP-malachite green ion pair	various	272
Surface water	Batch, FIA, spectrophotometry	MP blue	50–5000 in 3 ranges	273
Water	Batch, spectrophotometry	MP blue	100–6000	171
Natural water	Indirect AAS and flotation spectrophotometry	MP-malachite green ion pair		274
Natural water	Solvent extraction/ICP-AES	not available		275
Marine and natural water	Coprecipitation with brucite	MP blue	0.5–5	276
Water	Capillary-fill device; amperometry	MP	150–60 000	160
Water	Ion chromatography; spectrophotometry, post column reactor	MP blue	100–2000	277

[a] MP = 12-Molybdophosphate.

[186,187]. A number of colorimetric procedures have been adapted for automated [209,219] and field use [203].

FIA [196,239,259] is suitable for field applications subject to appropriate sample conditioning. A variety of flow-injection systems have been described for measuring organic matter. One system combines [239] in-line UV photo-oxidation in a PTFE reactor with indirect spectrophotometric monitoring of the generated CO_2. The detection limit was less than 0.1 mg C l^{-1} and the technique can be applied to a broad range of sample concentrations. However, chloride interferes giving elevated organic carbon concentrations and further investigation is required before the technique is applied to samples of elevated salinity.

The use of a UV thin film reactor equipped with an active stirring mechanism for the film to promote efficient oxidation combined with IR detection has been thoroughly investigated for FIA of organic and inorganic carbon [196] in the low μg l^{-1} range. The results of this systematic study suggest that airborne contamination and sorption processes on glassware are potential problems in the measurement of organic carbon.

Aqueous suspensions of titanium dioxide illuminated with near-UV light can be used to photocatalyse organic matter. For application to FIA there are advantages in using immobilised titanium dioxide on a stationary support as the sample may be passed continuously over the illuminated photo-catalyst to an appropriate detector. A system incorporating a titanium dioxide-coated PTFE tubing reactor has been described [259], and a commercial instrument (ANATOC) based on this process has recently been released. The detector response can be increased by increasing any one of several physical parameters of the reactor.

Phosphorus

The most commonly measured forms of phosphorus in aquatic ecosystems are dissolved phosphorus (DRP) (Table 10), total dissolved phosphorus (TDP) and particulate phosphorus (TPP). These fractions were originally chosen as a compromise between ease of measurement and predictive power with regard to biological and environmental effects, e.g., bioavailability estimates and nutrient budget calculations. Different aspects of phosphorus determination have been summarised in a number of reviews [67,278]. Methods based on reaction of orthophosphate ions with molybdate ions totally dominate the literature on phosphorus analyses.

Methods for measuring orthophosphate. Full details of earlier methods are given by Strickland and Parsons [279] and by Golterman and Clymo [280]. Standard methods [145] are based on reaction of orthophosphates with acidic molybdate, to form 12-molybdophosphate, which when reduced forms a strongly coloured molybdophosphate blue species. This reaction was first reported by Osmond in 1887 [281] and has been the subject of considerable empirical scrutiny. The absorbance of the coloured species has been examined as a function of known interferences, volumes of sample and reagent, acidity, molybdate and reductant concentrations, time, reagent temperature and the stoichiometry of the molybdophosphate [171]. Formation of 12-molybdophosphate is still the basis for many methods of phosphate determination and several modifications of this method have been reported, usually involving use of different reductants and acid strength in attempts to improve selectivity and stability of the blue chromophore produced [282,283]. The methods now most widely used for batch and some automated analyses are based on the work of Murphy and Riley [70], and utilise ascorbic acid as a reductant with a catalyst of potassium antimonyl tartrate. This method is preferred because it is less salt and temperature sensitive, and has a more stable chromophore than the tin(II) chloride reduction method [284]. Detection is achieved at either 660–690 nm or 880 nm depending on the nature of the molybdophosphate blue species being measured [171]. Using ascorbic acid as reductant with detection at 880 nm and a 5-cm cell, phosphorus concentrations as low as 0.01 mg l^{-1} are detectable. Positive interference may arise from arsenates whereas hexavalent chromium and nitrite interfere to give results about 3% low at concentrations of 1 mg l^{-1} and 10–15% low at 10 mg l^{-1} [145, p. 4-177]. In natural waters, silicate is the most likely interfering anion. However, the pro-

portion of acid and molybdate in the test solution can be adjusted [278] to minimise silicate interference. Condensed phosphates do not form molybdophosphate; they must be subjected to prior hydrolysis. A preliminary hydrolysis step is included, therefore, where total phosphorus fractions are required. Further details of hydrolysis procedures are discussed below.

Methods based on spectrophotometric measurement as molybdophosphate suffer two main disadvantages, low sensitivity and interference from several anions. In order to be suitable for measurement of phosphate in natural waters a method with a detection limit of 1 μg P l^{-1} or less is desirable. Apart from reduction to molybdophosphate blue, various techniques have been used to enhance sensitivity and specificity. Solvent extraction using solvents such as amyl alcohol, isobutanol, butyl acetate and benzene [278] either before or after the reduction step is an obvious procedure. Extraction with isobutanol is relatively efficient in eliminating silicate interference [278] whilst enhancing sensitivity about tenfold compared with methods not incorporating an extraction step [69]. Unfortunately liquid–liquid extraction procedures are tedious and time consuming and are not widely used. The molybdophosphate species interacts with a number of basic dye compounds (e.g., malachite green, crystal violet and Rhodamine 6G) in acidic solution to form extractable ion association complexes. The extracted complexes may be quantified by either spectrophometry or spectrofluorimetry. For example, a spectrophotometric method for sea water analysis has been described [285,286] based on extraction of a molybdophosphate–malachite green complex. Similarly, the ion association complex of vanadomolybdophosphate and malachite green has been used [287] to determine phosphate in river water. Ions commonly found in river water did not interfere and, in the case of silicate, interference was less than that found in the corresponding malachite green molybdophosphate procedure. The detection limit for both malachite green procedures is about 0.1 μg P l^{-1}. Stability of the ion association complex is a problem unless stabilised by addition of a surfactant. The difficulty here relates to the availability of a suitable phosphate-free surfactant although poly(vinyl alcohol) appears to be satisfactory. Although the malachite green methods are very sensitive and interference by co-existing ions is minimal, they are tedious in routine operation due to the need for extraction.

Future developments with cells of very long path length (ca. 1 m) [264] and thermal lensing may result in considerably improved detection limits for molybdophosphate methods.

At least two enzymatic methods for the determination of orthophosphate have been reported. In one approach [288], the inhibitory effect of orthophosphate on alkaline phosphatase was utilised as a means of determining as little as 0.1 μg P l^{-1} in natural waters. This method showed no interference from trace metals or oxoanions such as arsenate or silicate; however, interference from some phosphomonoesters and organic esters was noted. In the second approach, orthophosphate was determined [289] in natural waters following reaction with glyceraldehyde-3-phosphate to form 1,3-diglycerophosphate in the presence of glyceraldehyde-3-phosphate dehydrogenase and oxidised nicotinamide adenine dinucleotide. The reduced nicotinamide adenine dinucleotide produced by this reaction was determined spectrophotometrically and used as a measure of orthophosphate. When applied to natural waters, both enzymatic methods for orthophosphate gave consistently lower results than DRP.

Other analytical techniques available for phosphorus determination include CFA, atomic absorption spectrometry, ion chromatography, voltammetry, inductively coupled plasma atomic emission spectrometry [275] and inductively coupled plasma mass spectrometry (ICP-MS) and gas chromatographic measurement of phosphine [264] generated from total dissolved phosphorus. For various reasons none of these procedures, with the exception of CFA, have been widely applied to water analyses. For example, the high cost of ICP-MS is prohibitive whereas detection limits for ion chromatographic methods currently offer no advantages relative to established procedures.

One of the earliest applications of FIA, reported in 1975, was for the determination of phosphorus [290–292] and flow injection has since

been widely adopted for determination of DRP in natural, marine and waste waters, using a variety of detection techniques. Some of the advantages of using FIA for determination of dissolved phosphorus species include the ability to measure DRP at high sample throughput rates and at low concentrations. In addition, detection chemistries which would be so involved as to be unworkable, or susceptible to unacceptable interferences in batch mode, can be used to advantage in flow-injection mode. Simplex optimization or factorial design [293] may be used to optimise the configuration of the flow-injection manifold.

Procedures for DRP based on formation of 12-molybdophosphate dominate FIA. While for batch DRP analysis, antimony-catalysed ascorbic acid reduction is preferred, a number of workers have opted for the use of the tin(II) chloride reduction method [273] for low level DRP measurements by FIA. The higher sensitivity of this method has been attributed [268,293] to faster reaction kinetics. The deficiencies of the tin(II) chloride reduction method under batch analysis conditions (i.e., temperature and salt effects) are scarcely problematic when the same chemistry is employed in a flow-injection system, and this particular method is now widely used for DRP analysis [294]. The conventional approach has involved injection of sample into a flowing reagent or inert carrier stream. In some instances, however injection of reagents into a flowing sample stream has been adopted [295]. This approach has obvious advantages in terms of minimising reagent consumption which is crucial with on-site field monitors. Less obvious however is the enhanced sensitivity claimed for this reverse or reagent-injection FIA [267]. In this mode, the acidity of the carrier stream is critical [271] to ensure successful formation of molybdophosphate blue.

The selectivity and sensitivity of FIA can be enhanced by incorporating a sorbent microcolumn in the flow-injection manifold. Both reversed-phase C_{18} and ion-exchange packings are suitable for this purpose. Optosensing spectrophotometric measurements of the coloured derivative (e.g., molybdenum blue) may be made [178,272] directly on the sorbent column. The ion association complexes used in batch analysis to enhance sensitivity are also suitable for FIA [262]. Using the green molybdophosphate–malachite green ion pair phosphorus has been measured in river waters at the $\mu g\ l^{-1}$ level with a sample rate of 40 h^{-1}. In a slightly different approach phosphate has been measured indirectly [270] by the quenching effect of phosphomolybdate on the fluorescence of Rhodamine 6G. The detection limit is similar to that of the malachite green procedure, while the sampling rate is much higher at 120 h^{-1}.

The principles which have been discussed have been employed [263] in developing an FIA procedure for DRP in pristine waters. The tin(II) chloride–molybdate method was optimised using a modified simplex optimization method. Silicate interference up to 5 mg l^{-1} Si was removed by addition of tartaric acid to the reagent stream and an in-line preconcentration anion-exchange column was employed to enhance sensitivity. Under these conditions a detection limit of 0.1 μg P l^{-1} was achieved. An inexpensive detector consisting of a flow cell and a simple photometer that incorporates a super-bright light emitting diode as the source and a photodiode as the detector was used. The low cost of this system makes it suitable for field-based application. Further enhancement of detection limit may be achieved by use of a longer preconcentration period.

Methods for measuring particulate, organic and total phosphorus. Acid hydrolysable phosphorus is defined operationally as the difference between reactive phosphorus as measured in the untreated sample and phosphorus found after mild acid hydrolysis, and provides an approximate measure of the concentration of condensed phosphates. Acid hydrolysable phosphorus may be determined on the original sample (TAHP) or the filtrate (DAHP) and/or residue (PAHP) following filtration through a 0.45-μm filter. On the other hand, the total particulate phosphorus (or TPP) fraction is mostly quantified as the difference between total phosphorus (TP) and total dissolved phosphorus (TDP) [296]. Alternatively, particulate phosphorus may be determined directly on the retained particles following filtration

of the sample through a 0.45-μm filter. The use of adequate methods for the hydrolysis of phosphorus-containing organic substances and condensed phosphates is essential in both cases. Treatment procedures include wet chemical digestion, high temperature digestion, UV photo-oxidation and microwave digestion. The peroxodisulphate method either with acid [297,298] or without acid [299] gives reproducible results which generally compare favourably with other methods [300]. It has been used for simultaneous determination of total phosphorus and total nitrogen in freshwater samples [301]. Nonetheless, poor recoveries of phosphorus have been reported in some situations [302] and, in general, recoveries are significantly lower than with stronger oxidation procedures [303,304]. In general, the more vigorous digestion procedures (e.g., digestion with a mixture of perchloric, nitric and sulphuric acids at reflux temperature, 220°C) are to be preferred in order to obtain the total phosphorus. In some situations, e.g., estimates of bioavailability, the refractory materials not digested by peroxodisulphate may be of little interest [67]. Moreover, high temperature magnesium nitrate oxidation of the organic phosphorus compounds in sea water has proven superior [305] to either perchlorate oxidation or high-intensity UV-irradiation methods for quantitative P recovery from phosphonates and polyphosphates.

UV photo-oxidation has been used to mineralise dissolved organic phosphorus [306]. Solorzano and Strickland [307] have noted that UV photoxidation alone is insufficient to convert condensed phosphates to orthophosphate, and have suggested that use of UV photo-oxidation provides a basis for discrimination between the DOP and condensed phosphorus fractions. However, in most batch UV photo-oxidation methods reported to date, acidic peroxodisulphate or peroxide were used. These conditions, and the higher temperatures reached during UV exposure of up to 8 h with high wattage lamps will cause both oxidation of DOP and hydrolysis of the condensed phosphates, behavior which has been noted [308]. Under these conditions TDP will be reported rather than DOP. An FIA method involving short time (< 60 s) UV exposure under alkaline peroxodisulphate conditions gave complete recoveries for organic phosphorus species, but negligible values for condensed phosphates [309]. These results emphasise the need for digestion procedures to be thoroughly investigated using a range of organic and condensed phosphorus standards at varying reactivities.

Progress in the automated determination of total phosphorus fractions (e.g., TP, TDP) and DOP fractions is dependent on developments in sample handling techniques. In many instances FIA determination of these fractions has followed manual digestion of samples outside the flow-injection system. Alternatively, for a continuous determination, the digestion procedure must be incorporated on-line in the flow-injection manifold. The latter approach is easily automated and applicable to in-field monitors [310]. A number of procedures have been used in other areas and are now being extended to nutrient analysis in natural waters. In essence these systems involve the introduction of sample into a carrier stream containing an oxidizing reagent which is then passed through a heated coil. The temperature, flow and composition of the carrier can be controlled to allow complete digestion. A coiled PTFE capillary digestor (10 m $\times$ 1 mm i.d.) containing a platinum wire as catalyst for peroxodisulphate oxidation of condensed and organic phosphorus species at 160°C has been used [311] to determine total phosphorus in sea water with a detection limit of 2 μg l^{-1}. The use of microwave ovens for batch sample digestion has become widespread. Their application in FIA for on-line TDP and TP digestion has also been described [312] and when coupled with peroxodisulphate oxidation gave recoveries ranging from 91 to 100% for organic phosphorus compounds and with perchloric acid oxidation recoveries ranging from 60 to 70% for inorganic polyphosphates. TP analyses obtained using a similar system [313] were in excellent agreement with those from batch nitric–sulphuric acid digestions. Williams et al. [314] however, used only dilute nitric acid for TDP digestion and found it necessary to pretreat samples with pyrophosphatase in order to hydrolyze condensed phosphates.

Inductively coupled plasma atomic emission

spectrometry presents an alternative approach for the determination of TDP and TP. While use of high temperature plasma systems obviates the need for pre-digestion and provides rapid sample throughput, the technique is relatively insensitive for phosphorus, and the equipment is expensive to purchase and operate, and is inherently unsuitable for field use.

Less rigorous, non-oxidative sample treatment is necessary where determination of inorganic polyphosphates or acid hydrolysable phosphorus is required. In this case, hydrolysis can be effected with a strongly acidic solution at an elevated temperature. A procedure has been described [315] in which the hydrolysis and colour-producing reaction are combined by using a strongly acidic carrier containing both molybdenum(V) and molybdenum(VI). Since the reaction coil is maintained at 140°C, a back pressure coil is necessary to eliminate the noise caused by gas bubbles. An in-line photo-oxidation flow-injection system has been described [309] for the rapid determination of DOP in natural waters. This system, which involved the use of a low wattage UV source and a PTFE photoreactor, was capable of 45–60 analyses per hour. Debubbling of the digestate stream was achieved by the use of microporous tubular polypropylene membranes. No significant difference between the measurement of DOP + DRP and TDP of a series of natural waters was noted.

Characterisation of various fractions. Isolated phosphorus fractions such as particulate phosphorus may be characterised in a number of ways by, for example, origin, physical properties or chemical structure. Detailed procedures may be devised [67] to estimate the amount of phosphorus in isolated particulate components, e.g., cells, organic detritus or mineral components. Extraction should only be applied, however to samples where the dominance of the components concerned is demonstrated as in the case of particulate phosphorus derived from cells and minerals in lakes and rivers, respectively. An advanced extraction scheme [316] may include the determination of phosphorus according to many classes of cell constituents. Similar well-defined procedures exist for particulate phosphorus in minerals [317–320]. Differences in solubility in acids and bases of varying strength and temperature, lipophilic extractants, selective precipitation and chromatography are exploited in fractionations of this type. For example, Stevens and Stewart [318,321] separated soluble phosphorus by precipitation with lanthanum, fractionation by acid and base treatment followed by gel chromatography. Nonetheless, it is unrealistic to expect such schemes to be both completely selective and accomplish a quantitative extraction.

Measurement of bioavailable phosphorus. While the bioavailability of various phosphorus species in natural waters is still poorly understood, it is generally agreed that the most available form is dissolved orthophosphate [322]. Some dissolved organic phosphates are also utilised, but others exhibit refractory behaviour [323]. Consequently, the two forms of dissolved phosphorus that are most frequently analysed are DRP and TDP, which are used to estimate amounts of *immediately* or *readily*-bioavailable phosphorus (i.e., orthophosphate) and *potentially*-bioavailable dissolved phosphorus. However, as noted earlier, DRP may overestimate [73] the true orthophosphate concentration. The validity of DRP as a predictor of bioavailable phosphorus is therefore open to question. Furthermore, various bioassays [324] for bioavailability of phosphorus compounds may still give poor estimates of phosphorus availability in freshwater ecosystems and results from different assays may not be interchangeable [62]. Consequently, considerable emphasis has been given to investigation of techniques which could potentially provide a true value of orthophosphate, or better still, the bioavailable phosphorus (BAP) fraction [325–327].

A number of approaches have been reported, including some studies aimed at preventing, or minimizing the hydrolytic breakdown of DOP during determination of orthophosphate. Chamberlain and Shapiro [72], for example, reported a "six-second" technique in which the molybdophosphate forming reaction was stopped by adjustment of acid strength prior to formation of molybdophosphate blue. Tarapchak [328] found that hydrolysis of DOP occurred very rapidly, in both acidic and acid-free molybdate, and Dick

and Tabatai [329] claim to have overcome this problem by complexing surplus molybdate with a citrate–arsenate reagent.

Gel filtration has also been used in attempts to separate lower molecular mass phosphorus (LMMP), which includes orthophosphate, and higher molecular mass phosphorus (HMMP) in studies of the cycling of phosphorus in aquatic ecosystems [73,321,330]. Some HMMP was found to be reactive to molybdate (i.e., RHMMP) [331], and this RHMMP was thought to consist of orthophosphate adsorbed to colloidal material, and hence was included in the measurement of DRP. In uptake studies using *Chlorella*, RHMMP was utilised less rapidly than PO_4-P, and this behaviour was confirmed by bioassay studies. Similar studies [321,332] have shown that RHMMP is less bioavailable than orthophosphate to algae and bacteria. Sephadex gel filtration has been used by a number of workers, often in conjunction with ^{32}P isotope studies, to separate and quantify LMMP and HMMP [321]. Unfortunately, gel filtration studies are generally slow, and are subject to problems associated with solute–gel interactions. A gel filtration–FIA system used for rapid separation of PO_4^{3-} and higher molecular mass phosphorus has recently been reported [333].

Ultrafiltration using a 500-dalton membrane has been proposed [67] as an alternative to the traditional TDP/DRP analysis. However, like gel filtration, this approach is slow and also suffers from solute interactive effects with the ultrafiltration membrane.

Algal bioassay or growth potential techniques have also been used widely to estimate bioavailable phosphorus. A high correlation ($r^2 > 0.97$) was reported [334] for total reactive phosphorus (TRP) with biologically active phosphorus in lake waters with a total phosphorus concentration exceeding 30 $\mu g\ l^{-1}$. Similar agreement has been reported [335] between algal growth rates and TRP. While algal bioassay procedures may provide better indications of phosphorus utilization in real ecosystems, issues such as the most appropriate measure of growth (growth rate, algal mass, algal numbers, intracellular phosphorus concentration) and the choice of algae must be addressed. Bioassay tests are time consuming to set-up and perform, usually non-specific and may not provide adequate estimates of phosphorus bioavailability [62].

While it may be possible to measure true orthophosphate using some of the approaches described, this may not necessarily provide a better measure of biologically active phosphorus. DOP can form a significant proportion of the TDP, and it is likely that within this fraction some constituents will range from readily bioavailable to refractory [67]. Olsson and Jansson [336], for example, have shown that a residual fraction of DOP, consisting of DNA, RNA and phosphodiesters, was not amenable to enzymatic attack by alkaline phosphatase. It would therefore be informative to determine either the fraction which is available, or alternatively refractory to hydrolysis by phosphomonoesterase. One recently reported technique [337,338] involves the use of immobilised phosphohydrolytic enzymes and flow-injection analysis in an attempt to determine the fraction of DOP which is potentially bioavailable through hydrolysis by microbial exocellular enzymes. A group of compounds included in this latter category are the inositol phosphates. These compounds, especially myoinositolhexakisphosphate (phytic acid), are known to occur in sediments and soils [339,340], either as salts or associated with humic substances [341], and it would be surprising if they were not to be found in natural waters either through runoff or groundwater input. Largely inferential evidence from a number of studies suggests that inositol phosphates may comprise a significant proportion of DOP [342–344], but only a few studies [345,346] have actually demonstrated their existence in natural waters.

If the behaviour and bioavailability of the various phosphorus species in aquatic ecosystems is to be properly understood, there is a need for rapid, sensitive methods of analysis of fractions such as DOP, DRP, biologically active phosphorus, and other measures of bioavailable and unavailable phosphorus.

Nitrogen

Traditional methods for the determination of nitrate, nitrite, ammonia and organic nitrogen [279,347] continue to exist alongside newer tech-

niques such as ion selective electrode methods for inorganic nitrogen species at levels between about 10^{-5} and 10^{-1} M. Standard methods described by the APHA [145] for ammonia use colorimetry, titrimetry or an ammonia selective electrode. The factors that influence the selection of the particular method are ammonia concentration and presence of interferences. In the case of nitrate and nitrite, colorimetric, ion chromatographic and ion selective electrode methods are prescribed whilst organic nitrogen traditionally has been measured by either macro or semi-micro Kjeldahl involving acid digestion of the sample in the presence of a catalyst. The procedure determines amino-nitrogen of most organic compounds in addition to free ammonia and ammonium-nitrogen but fails to account for nitrogen in the form of azide, azine, azo, hydrazone, nitrate,

TABLE 11

Selected procedures for the determination of nitrate and nitrite in waters

Species	Sample	Method [a]	Detection	Range (mg l^{-1})	Ref.
Nitrate	Water	Nitrate selective electrode	Amperometry	1–1000	359
Nitrate	Natural water	Reduction to nitrite then reaction with 3-aminonaphthalene-1,5-disulphonic acid	Fluorimetry	10^{-4}–3	360
Nitrate	Drinking and river water	Reaction between nitrate and the uranyl ion	Polarography	10^{-2}–0.1	361
Nitrate	Hydroponic fluids	Nitration of organics	Amperometry	10^{-1}–70	362
Nitrite	Fresh and saline water	Diazotisation then cathodic stripping voltammetry	Amperometry	5×10^{-6}–2×10^{-3}	363
Nitrite	Drinking water	Ion exclusion chromatography	Electrochemistry	10^{-4}–1	364
Nitrite	Natural water	Kinetic effect of nitrite on the oxidation of thionine by potassium bromate	Photometry	10^{-4}–2×10^{-2}	365
Nitrite	Wastewater	Kinetics of the reaction between iodine and EDTA	Amperometry	3×10^{-3}–1×10^{-1}	366, 367
Nitrite	Water	Kinetics of the oxidation of phenosafranine by bromate	Fluorimetry	9×10^{-3}–1×10^{-1}	368
Nitrite	Drinking and river water	Voltammetry at a stationary mercury dropping electrode	Amperometry	1×10^{-3}–1	369
Nitrite, TON	Sea water	FIA; diazotisation using sulphanilamide and NED	Photometry (LED/phototransistor)	8×10^{-2}–8×10^{-1}	370
Nitrite, nitrate	Sea water	CFA; diazotisation using sulphanilamide and NED	Photometry	7×10^{-4}–7×10^{-2}	371
Nitrate	Sea water	CFA; diazotisation using sulphanilamide and NED	Photometry	3×10^{-5}–1×10^{-3}	372
Nitrate	River water	Automated FIA; diazotisation using sulphanilamide and NED	Photometry (LED/photodiodes)	0.03–12	373
Nitrite	River water	Diazotisation using 3-nitroaniline and NED	Photometry	10^{-2}–0.8	374
Nitrite	Polluted water	Diazotisation using 3-nitroaniline and 1-aminonaphthalene-2-sulphonic acid	Photometry	0.08–0.68	375

[a] FIA, flow-injection analysis; CFA, continuous flow analysis; NED, *N*-(1-naphthyl)ethylenediammonium chloride.

nitrite, nitrile, nitro, nitroso, oxime or semicarbazone. If ammonia is not removed in the initial stages of the procedure and prior to sample digestion then the result of a Kjeldahl determination is referred to as "total Kjeldahl nitrogen" (TKN) rather than "organic nitrogen". Interferences in the Kjeldahl method are well documented [145] and arise from nitrate-induced oxidation of ammonia released from the digested organic nitrogen or by pyrolytic decomposition of nitrogen if the digestion temperature rises above 400°C due to a high solids content in the digestion mixture. Furthermore, the fraction determined by the Kjeldahl method is largely undefined and there is an increasing trend towards replacing Kjeldahl determinations by measurement of total organic nitrogen.

A variety of procedures has been described [348] for ammonia. Classical colorimetric methods (both manual and automated) using Nessler's reagent [349] or species related to indophenol blue [145,350–352] which is formed by reaction of ammonia, phenol and hypochlorite are well established. In particular, the indophenol reaction is the standard method recommended, for example, by the Environmental Protection Agency. Alternative methods include titration, potentiometry, ion selective electrode potentiometry [353,354] and spectrofluorimetric detection at 430 nm following derivatization with *o*-phthalaldehyde [355]. The latter has been particularly successful when combined with ion chromatography [356] for the determination of ammonia. In another chromatographic application, dansylamide formed by reaction of ammonia with dansyl chloride [357] was determined by liquid chromatography (LC) with UV detection at concentrations of as low as 25 μg NH_3-N l^{-1}. However, for routine in-field monitoring the indophenol reaction with photometric detection has many advantages including the use of relatively unsophisticated and inexpensive instrumentation. This system has been investigated thoroughly and detection limits have been improved using laser photothermal detection [358] due to the low background signal. In addition, ammonia can be measured in water samples with low turbidity without interference.

Reports of new techniques and methodologies for the determination of nitrate and nitrite (Table 11) have occurred steadily over the past 6 years. These reports can be split into two broad sections depending on the detection method used. The first of these sections, based on electrochemical detection [362,363,369,376–382], contains the majority of work in this area with spectrophotometric (colorimetric) detection [374,375,383,384] occupying a secondary, but significant place. The majority of papers reporting electrochemical procedures have been reports of new electrode coatings such as $[Os(bipy)_2(pvp)_{10}Cl]Cl$ modified glassy carbon electrode [385], a ruthenium-containing polymer modified electrode system [386], or are methods based around single sweep polarography [378,380,387,388]. Many of the reports published have involved chromatographic methods coupled to the detection system or are standard analytical methods adapted to either new matrices (natural waters, soil extracts, etc.) or to automated systems.

Relatively few direct analytical methods have been published for nitrate or nitrite, but amongst those reported is a method for the capillary gas chromatographic determination of nitrate [389] based, for example, on the measurement of nitrobenzene formed by reaction of nitrate with benzene in acidic medium [390]. Using this procedure nitrate can be measured with a sensitivity exceeding that of conventional methods. The disadvantage of such methods is the need for derivatisation and relatively expensive equipment. On the other hand, nitrate has been determined directly using ion selective electrodes [391], other electrochemical measurements, spectrophotometric measurement after reaction with reagents including brucine (10,11-dimethoxystrychnine), chromotropic acid [392], methylene blue [393], 2,4-xylenol [392,394] and by UV spectrophotometry [395–397]. Interference in the UV method due to chloride and organic matter is reduced by using a detection wavelength of 210 nm and by controlling the ionic strength of the solution. Derivative UV spectrophotometry has also been reported for the determination of nitrite and nitrate in waters [398–404]. The typical detection limit for nitrate is 0.01 mg l^{-1} of N. Both first order and second order [399,402] derivative spec-

tra have been used although it has been claimed [400,401] that the first order spectra at 205–210 nm are superior.

Indirect spectrophotometric methods for nitrate are based largely on reduction to nitrite. These methods utilise either a homogeneous reduction with, e.g., hydrazine [405] or titanium(III) [406] or heterogeneous reduction with zinc, amalgamated zinc [407,408], cadmium or cadmium admixtures [409–413] or sodium borohydride [414]. The nitrite produced by reduction can be measured directly or linked to a diazotization/coupling reaction to permit measurement at 545 nm. The cadmium reduction procedure is widely used in automated systems as a Cu–Cd column or, more recently, a Cu–Cd reactor coil. Apart from any health considerations associated with the use of cadmium, practical difficulties preparing the columns/coils, concerns over column efficiency and several potential interferences in the reduction step [409], Cu–Cd remains the most widely used reductant for nitrate analysis. Moreover, salinity does not affect the response which is useful in marine studies. Miscellaneous methods for nitrate include an indirect spectrophotometric method based on measurement of the iron(III)-thiocyanate complex formed by displacement of thiocyanate from an ion exchange column [415] and a chemiluminescence procedure using luminol [416].

Procedures for nitrite are equally diverse and include liquid chromatography [417–419], coulometry [420], voltammetry [378,382,421] and the use of modified electrodes [422] and chemiluminescence measurements [423,424]. Methods based on catalytic reactions offer significant advantages [425] which have been exploited in kinetic methods [365,367,368,426,427] for nitrite determination. The most notable amongst these involves spectrophotometric analysis based on the catalytic effect of nitrite on the oxidation of 2,2′-azinobis(3-ethylbenzothiazoline-6-sulphonic acid) [428], or iron(II) in the presence of oxygen [429], the oxidation of thionine by potassium bromate [365] and the determination of nitrite in drinking water by fluorometry [430]. A kinetic method based on the inhibitory effect of nitrite on the photochemical reaction between iodine and EDTA has also been reported [367]. Spectrophotometric methods for nitrite have been based on reaction with various reagents including salbutamol sulphate in acidic medium [431] followed by measurement at 410 nm. However, the most popular spectrophotometric method for nitrite still involves diazotization and coupling to form an intensely coloured dye [432–434] with subsequent colorimetric determination [375,435–437]. An example of the latter is the diazotization of *p*-aminobenzophenone followed by coupling with *N*-(1-naphthyl)ethylenediamine [436] to form a product absorbing at 555 nm. This procedure has been applied successfully to the analysis of river, estuarine and sea water samples with nitrite concentrations in the range 0.04–1.0 mg NO_2-N l^{-1}. In addition, this method is ideally suited, after conversion from a batch to a flow-injection sampling scheme, for laboratory automation [438,439] and field-based analysers [114,174,373]. In the latter connection it has been applied to the determination of nitrate and phosphate using photodiodes instead of a spectrophotometer [440]. Nitrate reduction followed by diazotization and coupling is the standard laboratory method for the routine determination of total oxidised nitrogen (nitrate + nitrite) in environmental samples either as a segmented continuous flow or flow-injection procedure.

FIA has been applied to the determination of nitrate, nitrite [360,361,406,441–450] and ammonia [451–455] by several authors. These reports can be split into three broad sections depending on whether spectrophotometric (colorimetric) detection [406,441,447,449,452], luminescence detection [360,442,451] or electrochemical detection [444,445,453,454] was used. More detailed information on the wealth of published FIA methods is covered extensively in comprehensive reviews by Chen et al. [456] and earlier by Van Staden [457]. A spectrophotometric flow-injection method for ammonia based on diffusion through a PTFE gas diffusion membrane [458,459] into alkaline bromothymol blue solution has been adapted for in-field use over the range 0–400 μg NH_3-N l^{-1}. In another method based on diffusion all three inorganic nitrogen species were measured [460]. Nitrate and nitrite were reduced

to ammonia using a zinc column and the ammonia measured by conductivity after passing through a diffusion cell.

Several papers have been published on the determination of nitrate and nitrite by chromatography [418,461–472]. The various techniques used for this purpose include ion chromatography [473], ion-exclusion [364] and ion-interaction chromatography [474]. Nitrate and nitrite analysis in sea water or other samples containing high concentrations of chloride [472] can be difficult because of near co-elution of the three ions. This problem is overcome by using reversed-phase ion-interaction chromatography [474]. The major advantage of chromatographic techniques is the ability to simultaneously determine a range of ions including nitrate, chloride and sulphate, nitrate and nitrite [475–477]. Typical detection limits are 1 μg NO_3-N l^{-1} and 10 μg NO_2-N l^{-1} with UV detection. A comparison of ion chromatography, segmented flow analysis and FIA for nitrate determination [478] favours ion chromatography and segmented flow analysis for lower detection limits but the sampling rate for FIA at 30–60 samples per hour greatly exceeds that of ion chromatography at 10 samples per hour.

Reviews covering related aspects include the design and operation of automatic monitors for the determination of nitrate and ammonium in ultrapure water [479], ion-selective electrode methods for ammonium and nitrate in waters [480] and electrochemical analyzers for ammonium, nitrate and nitrite [481]. The use of different commercial instruments [482] for automated determination of nitrate and the merits of four spectrophotometric methods [483] for nitrate determination have been compared. The brucine method and a derivative spectrophotometric method were suitable only after elimination of interference by naturally occurring substances. In contrast, the phenoldisulphonic acid and indigo carmine methods gave reproducible and reliable results for nitrate. Comparison of the phenoldisulphonic acid method and Cu–Cd reduction to nitrite showed [373] the reduction method gave results approximately 0.12 mg l^{-1} higher.

Procedures for total nitrogen, total organic nitrogen and DON involve preliminary oxidation to various nitrogen oxides followed by luminescent or spectrophotometric measurement. In most instances, DON has been obtained by difference after subtracting independently measured concentrations of DIN from TDN. Digestion procedures [484] parallel those used for organic carbon and include high temperature (greater than 680°C) catalytic oxidation, extremely high temperature (e.g., 1100°C) oxidation without catalyst, UV photo-oxidation [485] and various wet oxidation procedures, of which potassium peroxodisulphate oxidation in alkaline conditions is the most common [486,487]. Comparative analyses of DON and DOC [25,488] clearly demonstrate the need for improved measurements of both parameters. The variability in the case of DON apparently results from the fundamental disadvantage that this parameter is usually determined as a small difference between two large values.

The nitrate resulting from oxidation can be reduced to nitrite or can be measured directly, for example, by UV spectrophotometry at 200–210 nm [489] or at 220 and 275 nm [490] with a detection limit of 0.05 mg l^{-1}. With background correction for bromide ion [491], results for total nitrogen in sea water agree with those obtained by Cu–Cd column reduction as used in some commercial autoanalysers for nitrate determination. Alternatively, bromide and bromate interference can be eliminated [492] by boiling the peroxodisulphate digest with potassium permanganate–sulphuric acid at pH 3 followed by removal of excess potassium permanganate and manganese dioxide with sodium thiosulfate. Evaluations of various procedures for the determination of total nitrogen in waters can be found in a number of references [493]. Alkaline peroxodisulphate digestion for total nitrogen [494] is easier, more accurate and more suited to routine analysis than the Kjeldahl procedure. Photo-oxidation [495] and wet chemical oxidation procedures for total dissolved nitrogen are easily automated by FIA.

Silicon

Classical procedures for dissolved silicon were based on formation of a yellow molybdosilicate

acid complex which exists in two forms depending on pH [496]. The α-isomer is formed at pH 3.5–4.5 and is very stable once formed [497,498] whereas the β-isomer is formed rapidly in the pH range 0.8–2.5 but is much less stable [499]. Most analytical procedures are based on formation of the β-isomer although a variety of reaction conditions have been used reflecting the complex chemistry of the reaction [500]. The formation of intensely coloured blue heteropoly acid species by reduction of the molybdosilicate acid greatly enhances sensitivity. Several reducing agents including tin(II) chloride, ascorbic acid, ascorbic acid–antimony [501] and iron(II)–fluoride [502] have been examined but the most common is a mixture of *p*-methylaminophenol sulphate (metol) and sulphite [503]. The reduction reaction is slow and the time required for colour development depends on the amount of silicon present [127]. Interference of phosphate is eliminated [504] by the addition of oxalic acid which decomposes molybdophosphoric acid. Alternatively, phosphate can be measured as the difference between two determinations performed with and without addition of oxalic acid [505]. The oxalic acid serves a second purpose to prevent reduction of excess molybdate reagent.

Many of the classical procedures based on formation of molybdosilicate have been adapted to FIA. Detection has involved voltammetry [506], spectrophotometry [507] or spectrofluorimetry [508]. Sensitivity can be enhanced by monitoring the molybdenum blue species formed by reduction of the molybdosilicate [509,510]. The correct choice of analytical conditions for the reduction reaction eliminates interference by phosphorus, iron, calcium and magnesium. Fluorimetric detection is based on measurement [508] of thiochrome produced by oxidation of thiamine with molybdosilicate. Alternatively, molybdosilicate can be monitored [511] by reduction at a glassy carbon electrode using a flow electrolysis cell.

Polymeric silicon species are relatively labile and can be depolymerised by addition of 0.05 M sodium hydroxide solution [512] prior to measurement. Furthermore, colloidal silicic acid is rapidly altered from its colloidal form in the acid conditions used for colorimetric determinations and is included in the silicon fraction determined colorimetrically. The concentration of suspended silicon in natural waters is usually very small but when total silicon is required treating the sample with an alkaline peroxodisulphate solution will break down these species. Carbonate fusion is necessary only when large amounts of clay material are present.

Simultaneous measurement

The ability to measure several parameters simultaneously is an attractive proposition. Atomic absorption spectrometry [513] can provide multielement analyses but is more commonly applied to the measurement of single species. For example, silicon was measured at trace levels in waters with a standard deviation of 2–6%. On the other hand, atomic emission spectrometry is better suited to multi-element analyses and has been used, for example, to measure arsenic, boron, carbon, phosphorus, selenium and silicon in natural waters [258,514]. Spectrometric methods are generally restricted to providing data on total concentrations without regard to speciation unless there is some on-line treatment.

Ion chromatography has obvious applications to simultaneous determination of a number of ions [475] where the advantages of high resolution and sensitivity are used. Moreover, chromatography is undoubtedly the premier technique for speciation studies such as the simultaneous determination of phosphate and phosphonate [515], nitrate and nitrite [419,474,516]. The oxoanions of arsenic, germanium, silicon and phosphorus have been determined [277] after separation on an anion-exchange column. Detection was based on formation of molybdenum blue in a post-column reactor. Various procedures have also been described [238,256] for measuring both dissolved phosphorus and DOC. Recent advances may see capillary electrophoresis supplant ion chromatography as a fast method for separation [517] and determination of anions in waters; the sensitivity of this approach, however, is generally limited by the detection techniques employed.

Oxoanions such as phosphate, silicate, arsenate and germanate react with molybdate in acid

media to form the corresponding heteropolymolybdate. Depending on relative concentrations mutual interference can pose a serious problem in spectrophotometric determinations although in most natural waters the effects of arsenate and germanate can usually be ignored. The determination of the individual species has been addressed by use of preliminary separation (e.g., by precipitation or selective extraction), masking agents [269] and differential kinetics arising from the acidity of the reaction medium used [518]. These methods are generally insensitive and those involving separation are slow and laborious. Reversed flow-injection manifolds using reagent injection [519] or FIA coupled with on-line anion-exchange separation [520] offer an alternative which is both sensitive and rapid. In one approach, preliminary separation of phosphate, silicate and arsenate on a TSK-gel SAX anion exchange column [521] is followed by formation and detection of the heteropoly blue formed with ascorbic acid as reducing agent. Detection limits are suitable for measurement of phosphate and silicate in natural waters. As an alternative to on-line separation the flow-injection manifold can be configured to allow two or more measurements at different times on each sample injected [269] to account for the different rates of formation of the heteropolymolybdic acids. Detection was achieved by monitoring thiochrome fluorescence produced by oxidation of thiamine by the heteropolyacids of phosphate and silicate. Measurement [265] has also been based on the differential rate of formation of the heteropolymolybdic acids of phosphate and silicate and the subsequent formation of ion association complexes of the heteropolymolybdic acids and Rhodamine B.

CONCLUDING REMARKS

This review considers carbon, phosphorus, nitrogen and silicon species in waters with particular emphasis on the relative merits of various approaches to their analysis. There is a significant amount of literature on classical approaches (predominantly spectrophotometric) for the analysis of particular species, e.g., cadmium reduction and diazotization for total oxidised nitrogen (NO_2-N + NO_3-N) and the molybdenum blue reaction for orthophosphate. The difficulties involved in performing reliable analyses, or measurements which are biologically significant, are illustrated by the current level of publications relating to these techniques.

Speciation is clearly an important aspect of the environmental chemistry of the four elements and there is a definite, and as yet unrealised need for reliable methods that characterise, e.g., the organic fraction of the total for each element. Given the difficulty of fractionation and the challenge presented by the ultra-trace concentrations of many fractions, this is an area that requires considerably more attention from the environmental analytical community.

Another area of increasing importance is the gathering of in situ information on both total element and individual species concentrations. This is due to problems associated with sample stability after sampling and the need to record changes in concentration over short time scales, e.g., minutes to hours, that result from rapid changes in environmental conditions caused by, e.g., storm events.

A third area of importance is the quality assurance of the various methods. This includes the availability of suitable certified reference materials and greater participation in inter-laboratory comparisons [25,105,250]. Repeatability and reproducibility are both essential for monitoring the environment but are not sufficient. Accuracy is essential to the application of results to modelling and ecological theory development and comparisons of data from different parts of the world. The use of standardised procedures does not guarantee accuracy. The use of methods with an accuracy demonstrated by certified reference materials is a preferable and more effective approach [522].

Three of us (N.J.B., P.J.W. and H.C.) would like to thank NERC/AFRC for support under grant number GST/02/587 relating to Pollutant Transport in Soils and Rocks.

REFERENCES

1 B. Moss, Ecology of Freshwaters: Man and Medium, Blackwell, Oxford, 2 edn., 1988, p. 37.

2 Royal Commission on Environmental Pollution, Sixteenth Report, Freshwater Quality, HMSO, London, 1992.
3 A.L. Heathwaite and T.P. Burt, in N.E. Peters and D.E. Walling (Eds.), Sediment and Stream Water Quality in a Changing Environment: Trends and Explanation, International Association of Hydrological Sciences, Wallingford, 1991, pp. 209–218.
4 G.E. Likens, F.H. Bormann, R.S. Pierce, J.S. Eaton and N.M. Johnson, Biogeochemistry of a Forested Ecosystem, Springer Verlag, New York, 1977.
5 M. Hornung, B. Reynolds, P.A. Stevens and S. Hughes, in R.W. Edwards, A.S. Gee and J.H. Stoner (Eds.), Acid Waters in Wales, Kluwer, London, 1990, pp. 223–241.
6 C.S. Reynolds, The Ecology of Freshwater Phytoplankton, Cambridge University Press, Cambridge, 1984.
7 G.P. Harris, Phytoplankton Ecology: Structure, Function and Fluctuation, Chapman and Hall, New York, 1986.
8 J.M. Quinn, Guidelines for the control of undesirable biological growths in water, Consultancy report No. 6213/2. Water Quality Centre, Hamilton, New Zealand, 1991.
9 F.A.J. Armstrong, in J.P. Riley and G. Skirrow (Eds.), Chemical Oceanography, Academic Press, New York, 1965, pp. 409–430.
10 N.E. Peters and D.E. Walling (Eds.), Sediment and Stream Water Quality in a Changing Environment: Trends and Explanation, International Association of Hydrological Sciences, Wallingford, 1991.
11 M.L. Richardson (Ed.), Chemistry, Agriculture and the Environment, Royal Society of Chemistry, Cambridge, 1991.
12 W.A. House, Research in Chemical Kinetics, Vol. 1, Elsevier, Amsterdam, 1993.
13 E.T. Degens, S. Kempe and J.E. Richey, Editors, Biogeochemistry of Major World Rivers, SCOPE 42, Wiley, New York, 1991.
14 H. Tiessen (Ed), Phosphorus Cycles in Terrestrial and Aquatic Ecosystems, Regional Workshop 1: Europe, Czerniejewo, Poland, May 1–6, 1988, Saskatchewan Institute of Pedology, Canada, 1989.
15 H. Tiessen, D. Lopez-Hernandez and I.H. Salcedo (Eds.), Phosphorus Cycles in Terrestrial and Aquatic Ecosystems, Regional Workshop 3, Maracay, Venezuela, Nov. 28–Dec. 6., 1989.
16 H. Tiessen and E. Frossard (Eds.), Phosphorus Cycles in Terrestrial and Aquatic Ecosystems, Regional Workshop 4, Nairobi, Kenya, March 18–22, 1991.
17 Various authors, Mar. Chem., 41 (1993).
18 P.J. Statham and P.J. le B. Williams, in K. Grasshoff, M. Ehrhardt and K. Kremling (Eds.), Methods of Seawater Analysis, Verlag Chemie, Weinheim, 2 edn., 1983.
19 L.M. Games and J.M. Hayes, Anal. Chem., 48 (1976) 130.
20 E.M. Thurman, Organic Geochemistry of Natural Waters, Martinus Nijhoff/Dr. W. Junk Publishers, Dordrecht, 1985.
21 AWWA, Introduction to Water Treatment: Principles and Practices of Water Supply Operations, American Water Works Association, Denver, CO, Vol. 4, 1984.
22 R.B. Baird, C.A. Jacks, R.L. Jenkins, J.P. Gute, L. Neisess and B. Scheybeler, in W.J. Cooper (Ed.), Chemistry in Water Reuse, Vol. 2, Ann Arbor Science, Ann Arbor, MI, 1981, p. 145.
23 J. Hedges and J. Farrington, Mar. Chem., 41 (1993) 5.
24 R.M. Gershey, M.D. Mackinnon, P.J. le B. Williams and R.M. Moore, Mar. Chem., 7 (1979) 289.
25 P.J. Wangersky, Mar. Chem., 41 (1993) 61.
26 J. Namiesnik, J. Gorecki, M. Biziuk and L. Torres, Anal. Chim. Acta, 237 (1990) 1.
27 I.C. Grieve, in N.E. Peters and D.E. Walling (Eds.), Sediment and Stream Water Quality in a Changing Environment: Trends and Explanation, International Association of Hydrological Sciences, Wallingford, 1991, pp. 201–208.
28 B.T. Hart, P. Freeman and I.D. McKelvie, Hydrobiologia, 235/236 (1992) 573.
29 R.A. Herbert, in D.B. Nedwell and C.M. Brown (Eds.), Sediment Microbiology, Academic Press, London, 1982, pp. 53–71.
30 P.G.W. Jones, Aquat. Environ. Monit. Rep., M.A.F.F. Direct Fish. Res. Lowestoft, 7 (1982) 22.
31 Australian Water Quality Guidelines for Fresh and Marine Waters, Australian and New Zealand Environment and Conservation Council, 1992.
32 C.R. Goldman and A.J. Horne, Limnology, McGraw Hill, New York, 1983, p. 19.
33 M. Jansson, Hydrobiologia, 170 (1988) 177.
34 A.D. Cembella, N.J. Antia and P.J. Harrison, CRC Crit. Rev. Microbiol., 11 (1985) 13.
35 M. Ladle, H. Casey, A.F.H. Marker and J.S. Welton, The use of large experimental channels for ecological research, Proc. World Symp. on Aquaculture in Heated Effluents and Recirculation Systems, Stavanger, 28–30 May 1980, EIFAC 80, Berlin, Vol. 1, 1981, pp. 279–287.
36 A.D. Cembella, N.J. Antia and P.J. Harrison, CRC Crit. Rev. Microbiol., 10 (1984) 317.
37 R.A. Vollenweider, Scientific fundamentals of the eutrophication of lakes and flowing waters, with particular reference to nitrogen and phosphorus as factors in eutrophication, OECD Report No. DAS/CSI/68.27, Organisation for Economic Cooperation and Development, Paris, 1968.
38 B. Moss, Limnol. Oceanogr., 14 (1969) 591.
39 J.M. Melack, P. Kilham and T.R. Fisher, Oecologia, 52 (1982) 321.
40 W.F. Vincent, W. Wurtsbaugh, C.L. Vincent and P.J. Richerson, Limnol. Oceanogr., 29 (1984) 540.
41 D.W. Schindler, Science, 184 (1974) 897.
42 R.A. Vollenweider, Mem. Ist. Ital. Idrobiol., 33 (1976) 53.
43 D.W. Schindler, Science, 195 (1977) 260.
44 W. Stumm and J.J. Morgan, Aquatic Chemistry, Wiley, New York, 1981.
45 R.G. Wetzel, Limnology, Saunders College Publishing, Philadelphia, 1983.

46 R.L. Klotz, Can. J. Fish. Aquat. Sci., 48 (1991) 84.
47 R.L. Klotz, Can. J. Fish. Aquat. Sci., 45 (1988) 2026.
48 P.C.M. Boers, Water Res., 25 (1991) 309.
49 L.A. Kelly, Hydrobiologia, 235 (1992) 569.
50 M.L. Ostrofsky and G.G. McGee, Can. J. Fish. Aquat. Sci., 48 (1991) 233.
51 D.T. Van der Molen, Water Res., 25 (1991) 737.
52 L.M. Svendsen, A. Rebsdorf and P. Nomberg, Water Res., 27 (1993) 77.
53 P. Boers, L. Van Ballegooijen and J. Uunk, Freshwater Biol., 25 (1991) 9.
54 P.N. Froelich, Limnol. Oceanogr., 33 (1988) 649.
55 N.J. Barrow, J. Soil Sci., 34 (1983) 733.
56 P.J. Mulholland, J.W. Elwood, J.D. Newbold, L.A. Ferren and J.R. Webster, Ecology, 66 (1985) 1012.
57 B.T. Hart, P.R. Freeman, I.D. McKelvie, S. Pearse and D.G. Ross, Verh. Int. Verein. Limnol., 24 (1991) 2065.
58 R.A. Vollenweider, Schweiz. Z. Hydrol., 37 (1975) 53.
59 I.C. Smalls and D. Cannon, Growth response of phytoplankton to environmental factors, AWRC Conference Series No. 7, Australian Government Publishing Service, Canberra, 1983.
60 G.G. Ganf, Factors controlling the growth of phytoplankton in Mount Bold Reservoir, South Australia, AWRC Technical Paper No. 48, Australian Government Publishing Service, Canberra, 1980.
61 G.G. Ganf, Aust. J. Mar. Freshwater Res., 33 (1982) 475.
62 B. Bostrom, G. Persson and B. Broberg, Hydrobiologia, 170 (1988) 133.
63 K.F. Walker and T.J. Hillman, Aust. J. Mar. Freshwater Res., 33 (1982) 223.
64 J.E. Shannon and G.F. Lee, Int. J. Air Water Poll., 9 (1966) 735.
65 E.J. Griffith, Pure Appl. Chem., 44 (1975) 1173.
66 H. De Haan, T. De Boer, H.A. Kramer and J.R. Moed, Verh. Int. Verein. Limnol., 22 (1984) 876.
67 O. Broberg and G. Persson, Hydrobiologia, 170 (1988) 61.
68 J.G. Stockner, M.E. Klut and W.P. Cochlan, Can. J. Fish. Aquat. Sci., 47 (1990) 16.
69 S. Olsen, in H.L. Golterman and R.S. Clymo (Eds.), Chemical Environment in the Aquatic Habitat, North Holland, Amsterdam, 1967 pp. 63–105.
70 J. Murphy and J.P. Riley, Anal. Chim. Acta, 27 (1962) 31.
71 P.C. Head (Ed.), Practical Estuarine Chemistry, Cambridge University Press, Cambridge, 1985.
72 W. Chamberlain and J. Shapiro, Limnol. Oceanogr., 14 (1969) 921.
73 M.P. Stainton, Can. J. Fish. Aquat. Sci., 37 (1980) 472.
74 E. Pilleboue and J.M. Dorioz, in P.G. Sly (Ed.), Sediments and Water Interactions, Springer-Verlag, New York, 1986, Chap. 9.
75 B.T. Hart and I.D. McKelvie, in P. DeDecker and W.D. Williams (Eds.), Limnology in Australia, CSIRO Australia, Melbourne and Dr. W. Junk Publishers, Dordrecht, 1986.
76 L.E. Fox, Geochim. Cosmochim. Acta, 55 (1991) 1529.
77 R.H. Foy and R. Rosell, Aquaculture, 96 (1991) 31.
78 S.W. Hager and L.E. Schemel, Estuaries, 15 (1992) 40.
79 L.L. Janus, D.M. Soballe and B.L. Jones, Verh. Int. Verein. Theor. Angew. Limnol., 24 (1990) 538.
80 N.A. Jaworski, P.M. Groffman, A.A. Keller and J.C. Prager, Estuaries, 15 (1992) 83.
81 M.E. Lebo, Limnol. Oceanogr., 35 (1990) 1279.
82 L. Lijklema, Hydrobiol. Bull., 24 (1991) 165.
83 A. Spacie and S.L. Loeb, Verh. Int. Verein. Theor. Angew. Limnol., 24 (1990) 464.
84 K. Iserman, Fertilizer Res., 26 (1990) 253.
85 S.E.A. Van der Zee, F. Leus and M.J.P. Louer, Neth. J. Agric. Sci., 37 (1989) 387.
86 J. Clasen, OECD Co-operative Program for Inland Water (Eutrophication Control). Shallow Lakes and Reservoirs, Water Resource Centre, Medmenham, 1980.
87 J.J. Cole, N.F. Caraco and G.E. Likens, Limnol. Oceanogr., 35 (1990) 1230.
88 P. Cullen, Phosphorus Cycling in Aquatic Systems, Proc. National Workshop on Phosphorus in Aust. Freshwaters, Wagga Wagga, June 10–11, 1993, Land and Water Resources Research and Development Corporation, Occasional Paper 03/93, 1993, p. 7.
89 R.S. Rosich and P. Cullen, in B.T. Hart (Ed.), Water Quality Management Monitoring Programs and Diffuse Runoff, Australian Society for Limnology and Water Studies Centre, Chisolm Institute of Technology, 1982, pp. 103–119.
90 J.C. Ryden, J.K. Syers and R.F. Harris, Adv. Agron., 25 (1973) 1.
91 I.C. Campbell and T.J. Doeg, Aust. J. Mar. Freshwater Res., 40 (1989) 519.
92 K.L. Seip, Can. J. Fish. Aquat. Sci., 48 (1991) 2551.
93 P.J. Johnes and T.P. Burt, in N.E. Peters and D.E. Walling (Eds.), Sediment and Stream Water Quality in a Changing Environment: Trends and Explanation, International Association of Hydrological Sciences, Wallingford, 1991, pp. 349–358.
94 A.P.S. Terblanche, Water SA, 17 (1991) 77.
95 O.C. Bockman and T. Granli, in M.L. Richardson (Ed.), Chemistry, Agriculture and the Environment, Royal Society of Chemistry, Cambridge, 1991, pp. 373–388.
96 P.N. Magee, Philos. Trans. R. Soc. London, B296 (1982) 363.
97 P.N. Magee, Ambio, 6 (1977) 123.
98 J.J. Rademacher, T.B. Young and M.S. Kanarek, Arch. Environ. Health, 47 (1992) 292.
99 European Standards for Drinking Water, World Health Organisation, Copenhagen, 2 edn., 1970.
100 European Economic Community, 1980, Council directive on the quality of water for human consumption, Official Journal, 23, No. 80/778, EEC L 229, 11–29.
101 J. Gardiner and G. Mance, United Kingdom Water Quality Standards Arising from European Community Directives, Technical Report TR 204, Water Research Centre, Marlow, 1984.
102 Ambient water quality criteria for ammonia-1984, EPA-440/5-85-001, Criteria and Standard Division, US Environmental Protection Agency, Washington, DC.
103 Canadian Water Quality Guidelines, Canadian Council

of Resource and Environment Ministers, Inland Water Directorate, Environment Canada, Ottawa, 1991.
104 N.J. Antai, P.J. Harrison and L. Oliveira, Phycologia, 30 (1991) 1.
105 C. Hopkinson, Mar. Chem., 41 (1993) 23.
106 K.R. Hinga, A.A. Keller and C.A. Oviatt, Ambio, 20 (1991) 256
107 C.J. Barnes, G. Jacobson and G.D. Smith, J. Hydrol., 137 (1992) 181.
108 D.A. Farley and A. Werrity, J. Hydrol., 109 (1989) 351.
109 S.C. Rose, G.L. Harris, A.C. Armstrong, J.R. Williams, K.R. Howse and N. Tranter, in N.E. Peters and D.E. Walling (Eds.), Sediment and Stream Water Quality in a Changing Environment: Trends and Explanation, International Association of Hydrological Sciences, Wallingford, 1991, pp. 249–258.
110 Royal Society Report, The nitrogen cycle of the U.K., A study group report, London, 1983, p. 61.
111 C. Betton, B.W. Webb and D.E. Walling, in N.E. Peters and D.E. Walling (Eds.), Sediment and Stream Water Quality in a Changing Environment: Trends and Explanation, International Association of Hydrological Sciences, Wallingford, 1991, pp. 169–180.
112 H. Casey and R.T. Clarke, Freshwater Biol., 9 (1979) 91.
113 H. Casey, S.M. Smith and R.T. Clarke, Chemistry Ecology, 4 (1990) 85.
114 H. Casey, R.T. Clarke, J.R. Clinch, S. Smith and P.J. Worsfold, Anal. Chim. Acta, 227 (1989) 379.
115 Royal Commission on Environmental Pollution, Seventh Report, Agriculture on Pollution, HMSO, London, 1979.
116 H. Casey, R.T. Clarke and S.M. Smith, Chemistry Ecology, 8 (1993) 105.
117 G.W. Cooke, A review of the effects of agriculture on the chemical composition and quality of surface and underground waters, M.A.F.F. Technical Bulletin No. 32, HMSO, London, 1974.
118 A. Molot and P.J. Dillon, Can. J. Fish. Aquat. Sci., 48 (1991) 140.
119 R.E. Hecky and P. Kilham, Limnol. Oceanogr., 33 (1988) 796.
120 R.A. Vollenweider and J. Kerekes, Prog. Water Technol., 12(2) (1980) 5.
121 R.W. Gensemmer, Verh. Int. Verein. Theor. Angew. Limnol., 24 (1991) 2635.
122 H. Horn and W. Horn. Int. Rev. Ges. Hydrobiol., 75 (1990) 461.
123 J.D. Hern, Study and Interpretation of the Chemical Characteristics of Natural Water, United States Government Printing Office, Washington, DC, 2nd edn., 1970, pp. 108, 109.
124 W.A. House, Research in Chemical Kinetics, Vol. 1, Elsevier, Amsterdam, p. 52.
125 M.H. Brymner, Water Quality of the River Murray – The Influence of Albury-Wodonga, Albury Wodonga Development Co., 1982.
126 Gippsland Regional Environmental Study Input Streams Assessment, Vol. 1, State Rivers and Water Supply Commission, Victoria, Australia, 1978.
127 P.G. Brewer and J.P. Riley, Anal. Chim. Acta, 35 (1966) 514.
128 H. Casey, R.T. Clarke and A.F.H. Marker, Freshwater Biol., 11 (1981) 335.
129 A.M.C. Edwards, Freshwater Biol., 4 (1974) 267.
130 T.J. Lock, Freshwater Biol., 1 (1971) 213.
131 J.D. Burton and P.S. Liss, Geochim. Cosmochim. Acta, 37 (1973) 1761.
132 D. Behne, Analyst, 117 (1992) 555.
133 M. Betti and P. Papoff, CRC Crit. Rev. Anal. Chem. 19 (1988) 271.
134 M.P. Shibu, A.N. Balchand and P.N.K. Nambisan, Sci. Total Environ., 97/98 (1990) 267.
135 G.E. Batley, in G.E. Batley (Ed.), Trace Element Speciation: Analytical Methods and Problems, CRC Press, Boca Raton, Fl, 1989, pp. 1–24.
136 H.V. Leland, S.N. Luoma, J.F. Elder and D.J. Wilkes, J. Water Pollut. Control Fed., 50 (1978) 1469.
137 S.N. Luoma and G. Bryan, in E.A. Jenne (Ed.), Chemical Modelling in Aquatic Systems, ACS Symposium Series 93, American Chemical Society, Washington, DC, 1979.
138 G. Mance, Pollution Threat of Heavy Metals in Aquatic Environments, Elsevier, London, 1987.
139 G. Mance and J. Yates, Proposed environment quality standards for List II substances in water, zinc. Technical Report TR 209, Marlow, Water Research Centre, 1984.
140 G. Tölg, Analyst, 112 (1987) 365.
141 D. Kirkwood, A. Aminot and M. Perttila, Report on the Results of the ICES Fourth Intercomparison Exercise for Nutrients in Sea Water, Cooperative Research Report No. 174, International Council for the Exploration of the Sea, Copenhagen, 1991.
142 G. Topping, Sci. Total Environ., 49 (1986) 9.
143 A.R. Byrne, Analyst, 117 (1992) 251.
144 A. Aminot and R. Kerouel, Anal. Chim. Acta, 248 (1991) 277.
145 Standard Methods for the Examination of Water and Wastewater, American Public Health Association, Washington, DC, 17th edn., 1989.
146 Methods for the Examination of Waters and Associated Materials, HMSO, London; Silicon in Waters and Effluents 1980; Phosphorus in Waters, Effluents and Sewages, 1980; The Instrumental Determination of Total Organic Carbon, Total Oxygen Demand and Related Determinands 1979; Oxidised Nitrogen in Waters 1981.
147 N. Haigh, European Community Environmental Policy in Practice, Vol. 6, Comparative Report: Water and Waste in Four Countries, Trotman, London, 1986.
148 N. Haigh, EEC Environmental Policy in Britain, Longman, Harlow, 2nd edn., 1989.
149 W. Howarth, Water Pollution Law, Shaw and Son, London, 1988.
150 International organization for Standardization, ISO 5667,

Water Quality – Sampling, Parts 1–12, International Organization for Standardization, Geneva.
151 G. Premazzi, G. Chiaudani and G. Ziglio, Scientific Assessment of EC Standards for Drinking Water Quality. Environment and Quality of Life, CEC Joint Research Centre, EUR 12427 EN.
152 R. Macrory, Water Law, Principles and Practice, Longman, London, 1985.
153 L. Gorton, E. Csoregi, E. Dominguez, J. Emneus, G. Jonsson-Pettersson, G. Marko-Varga and B. Persson, Anal. Chim. Acta, 250 (1991) 203.
154 L.D. Bowers, Anal. Chem., 58 (1986) 513A.
155 G. Wallace, University of Wollongong, New South Wales, Australia, personal communication.
156 F. Scheller and F. Schubert, Biosensors, Techniques and Instrumentation in Analytical Chemistry, Vol. 11, Elsevier, Amsterdam 1992.
157 R. Niessner, Trends Anal. Chem., 10 (1991) 310.
158 O.S. Wolfbeis, Anal. Chim. Acta, 250 (1991) 181.
159 M. Izawa, Anal. Chim. Acta, 250 (1991) 249.
160 A.G. Fogg, S.P. Scullion, T.E. Edmonds and B.J. Birch, Analyst, 115 (1990) 1277.
161 H. Casey and S.M. Walker, Int. Environ. Safety, Oct. (1981) 16.
162 Encyclopedia of Analytical Science (Water Analysis), Academic Press, in press.
163 J.H. Sharp, Mar. Chem., 41 (1993) 37.
164 H. Casey, Anal. Proc., 29 (1992) 401.
165 P. McCarthy, R.W. Klusman and S.W. Cowling, Anal. Chem., 63 (1991) 301R.
166 K. Robards, V.R. Kelly and E. Patsalides, in J.C. Giddings, E. Grushka and P.R. Brown (Eds.) Advances in Chromatography, Marcel Dekker, New York, Vol. 32, 1992, pp. 53–86.
167 D. Lambert and W. Maher, Water Res., 26 (1992) 645.
168 L.A. Clementson and S.E. Wayte, Water Res., 26 (1992) 1171.
169 J. Luo and R. Sun, Lihua Jianyan, Huaxue Fenxi, 25 (1989) 127. C.A., 112 (1990) 104469g.
170 M. Roman, R. Dovi, R. Yoder, F. Dias and B. Warden, J. Chromatogr., 546 (1991) 341.
171 T.G. Towns, Anal. Chem., 58 (1986) 223.
172 H. Casey and S.M. Walker, Arch. Hydrobiol., 96 (1983) 515.
173 B. Norman, Mar. Chem., 41 (1993) 239.
174 P.J. Worsfold, J.R. Clinch and H. Casey, Anal. Chim. Acta, 197 (1987) 43.
175 K.M. Pedersen, M. Kummel and H. Soeberg, Anal. Chim. Acta, 238 (1990) 191.
176 K.S. Johnson, R.L. Petty and J. Thomsen, in A. Zirino (Ed), Mapping Strategies in Chemical Oceanography, American Chemical Society, Washington, DC, 1985, Chap. 2.
177 R.F. Berman, C.N. Renn and S.F. Arment, Am. Lab., 23 (18) (1991) 23.
178 N. Lacy, G.D. Christian and J. Ruzicka, Anal. Chem., 62 (1990) 1482.
179 N.J. Blundell, H. Casey, A. Hopkins and P.J. Worsfold, J. Auto. Chem., in press.
180 T.J. Marsh, Water Services, (1980) 601.
181 J.M. Hill, Nitrates in surface waters: observations from some rivers in the Lee drainage basin, WRC Report, 598M, Medmenham, 1983.
182 H. Casey, Prog. Water Technol., 8 (1977) 225.
183 R.J. Stevens and R.V. Smith, Water Res., 12 (1978) 823.
184 G.A. Best, Effluent and Water Treatment J., July (1974) 357.
185 D.C. Hinge, Inst. Water Eng., 6 (1980) 546.
186 J. Crowther and W.B. Moody, Anal. Chim. Acta, 120 (1980) 305.
187 L.S. Gravelet-Blondin, H.R. Van Vliet and B.W.H. Schoones, Water SA, 6 (1980) 135.
188 A. Granelli and T. Anfalt, Anal. Chim. Acta, 91 (1977) 175.
189 G. Brandt, G. Matuschek and A. Kettrup, Fresenius' Z. Anal. Chem., 321 (1985) 653.
190 K. Hayakawa, S. Kitamoto, N. Okubo, S. Nakamura and M. Miyazaki, J. Chromatogr., 481 (1989) 323.
191 T. Small and T.E. Miller, Anal. Chem., 54 (1982) 462.
192 T. Hironaka, M. Oshima and S. Motomizu, Bunseki Kagaku, 36 (1987) 503.
193 P.D. Goulden, Water Res., 10 (1976) 487.
194 K. Salonen, Water Res., 15 (1981) 403.
195 S.W. Kubala, D.C. Tilotta, M.A. Busch and K.W. Busch, Anal. Chem., 61 (1989) 1841.
196 S.A. Huber and F.H. Frimmel, Anal. Chem., 63 (1991) 2122.
197 S. Motomizu, K. Toei, T. Kuwaki and M. Oshima, Anal. Chem., 59 (1987) 2930.
198 P. MacCarthy, R.W. Klusman and S.W. Cowling, Anal. Chem., 63 (1991) 301R.
199 T. Aoki, K. Ito and M. Munemori, Anal. Lett., 21 (1988) 1881.
200 A.G. Dickson, Deep-Sea Res., Part A, 28 (1981) 609.
201 J. Gelbrecht, G. Henrion and R. Henrion, Acta Hydrochim. Hydrobiol., 15 (1987) 19.
202 D.E. Wilson, Arch. Hydrobiol., 87 (1979) 379.
203 C. Robinson and P.J. le B. Williams, Mar. Chem., 34 (1991) 157.
204 T.R. Moore, N.Z. J. Mar. Freshwater Res., 21 (1987) 585.
205 T.R. Moore, Soil Sci. Soc. Am. J., 49 (1985) 1590.
206 H. de Haan and T. De Boer, Water Res., 21 (1987) 731.
207 A. Jirka and M.J. Carter, Advances in Automated Analysis, 7th Technicon International Conference, 1976, pp. 27–31.
208 L.R. Gravelet-Blondin, H.R. Van Vliet and P.A. Mynhardt, Water SA, 6 (1980) 138.
209 L. Fitzgerald, J.R. Montgomery and J.K. Holt, J. Aut. Chem., 6 (1984) 80.
210 T. Kawai, K. Miyamoto and Y. Umezawa, Bunseki Kagaku, 39 (1990) 649.
211 J. Kegel, Fresenius' Z. Anal. Chem., 276 (1975) 45.
212 O. Emteryd, B. Andersson and H. Wallmark, Microchem. J., 43 (1991) 87.

213 J. Pempkowiak, Stud. Mater. Oceanol., 34 (1981) 33.
214 B.V. Stolyarov and E. Galev, Soviet J. Water Chem. Tech., 10 (1988) 57.
215 R.A. van Steenderen, W.D. Basson and F.A. Van Duuren, Water Res., 13 (1979) 539.
216 J. Hilton, J.P. Lishman, S. Mackness and S.I. Heaney, Hydrobiologia, 141 (1986) 269.
217 K. Salonen, Hydrobiologia, 67 (1979) 29.
218 A. Aminot and R. Kerouel, Analusis, 18 (1990) 289.
219 G. Cauwet, Mar. Chem., 14 (1984) 297.
220 P.D. Goulden and P. Brooksbank, Anal. Chem., 47 (1975) 1943.
221 I.C. Grieve, Earth Surf. Processes Landforms., 10 (1985) 75.
222 G.K. Korolev, A.A. Nazarova and V.B. Stradomskii, Gidrokhim. Mater., 84 (1983) 91.
223 F. Lucena, J. Frias and F. Ribas, Environ. Technol., 12 (1991) 343.
224 F. Ribas, J. Frias and F. Lucena, J. Appl. Bacteriol., 71 (1991) 371.
225 P. Servais, G. Billen and M.C. Hascoet, Water Res., 21 (1987) 445.
226 P. Servais, A. Anzil and C. Ventresque, Applied Environ. Microbiol., 55 (1989) 2732.
227 W.H. McDowell, J.J. Cole and C.T. Driscoll, Can. J. Fish. Aquat. Sci., 44 (1987) 214.
228 R. Roehl and H.J. Hoffman, Fresenius' Z. Anal. Chem., 322 (1985) 439.
229 Y. Sugimura and Y. Suzuki, Mar. Chem., 24 (1988) 105.
230 J.K. Schneider, R. Gloor, W. Giger and R.P. Schwarzenbach, Water Res., 18 (1984) 1515.
231 S.H. Eberle, K.P. Knobel and S. Von Hodenberg, Wasser, 53 (1979) 53.
232 R. Gloor, H. Leidner, K. Wuhrmann and T. Fleischmann, Water Res., 15 (1981) 457.
233 M. Jarret and C. Ducauze, Rev. Fr. Sci. Eau, 4 (1985) 163.
234 J.A. Leenheer, Environ. Sci. Technol., 15 (1981) 578.
235 M. Spiteller, Sci. Total Environ., 62 (1987) 47.
236 I. Gacs and K. Payer, Anal. Chim. Acta, 220 (1989) 1.
237 A.N. Shkil, I.T. Gavrilov and A.V. Krasnushkin, Zh. Anal. Khim., 44 (1989) 143.
238 A.N. Shkil, A.V. Krasnushkin and I.T. Gavrilov, Zh. Anal. Khim., 45 (1990) 1615.
239 R.T. Edwards, I.D. McKelvie, P.C. Ferrett, B.T. Hart, J.B. Bapat and K. Koshy, Anal. Chim. Acta, 261 (1992) 287.
240 H.J.W. de Baar, C. Brussaard, J. Hegeman, J. Schijf and M.H.C. Stoll. Mar. Chem., 41 (1993) 145.
241 J.E. Bauer, M.L. Occelli, P.M. Williams and P.C. McCaslin, Mar. Chem., 41 (1993) 75.
242 A.E.J. Miller, R.F.C. Mantoura, Y. Suzuki and M.R. Preston, Mar. Chem., 41 (1993) 223.
243 R. Benner and J.I. Hedges, Mar. Chem., 41 (1993) 161.
244 Y. Suzuki, Y. Sugimura and T. Itoh, Mar. Chem., 16 (1985) 83.
245 E.T. Peltzer and P.G. Brewer, Mar. Chem., 41 (1993) 243.
246 C. Lee and S.M. Henrichs, Mar. Chem., 41 (1993) 105.
247 Y. Suzuki, Mar. Chem., 41 (1993) 287.
248 R. Benner and M. Strom, Mar. Chem., 41 (1993) 153.
249 J. Hedges and J. Farrington, Mar. Chem., 41 (1993) 5.
250 P.J. le B. Williams, Mar. Chem., 41 (1993) 11.
251 J. Hedges, C. Lee and P. Wangersky, Mar. Chem., 41 (1993) 289.
252 G.R. Peyton, Mar. Chem., 41 (1993) 91.
253 P. Blazka and L. Prochazkova, Water Res., 17 (1983) 355.
254 R.A. van Steenderen and J.-S. Lin, Anal. Chem., 53 (1981) 2157.
255 T. Aoki, K. Ito and K. Munemori, Bunseki Kagaku, 37 (1988) 133.
256 K. Nakajima, Water Res., 18 (1984) 555.
257 B.V. Stolyarov and E.E. Galev, Soviet J. Water Chem., Technical., 10 (1988) 234.
258 I.T. Urasa, Anal. Chem., 56 (1984) 904.
259 G.K.-C. Low and R.W. Matthews, Anal. Chim. Acta, 231 (1990) 13.
260 A.M. Abdallah, M.E. Khalifa and M.A. Aki, Anal. Chim. Acta, 251 (1991) 207.
261 D.T. Burns, D. Chimpalee, N. Chimpalee and S. Ittipornkul, Anal. Chim. Acta, 254 (1991) 197.
262 S. Motomizu, T. Wakimoto and K. Toei, Talanta, 30 (1983) 333.
263 P.R. Freeman, I.D. McKelvie, B.T. Hart and T.J. Cardwell, Anal. Chim. Acta, 234 (1990) 409.
264 F.I. Ormaza-Gonzalez and P.J. Statham, Anal. Chim. Acta, 244 (1991) 63.
265 F. Mas, J.M. Estela and V. Cerda, Int. J. Environ. Anal. Chem., 43 (1991) 71.
266 F. Mas, J.M. Estela and V. Cerda, Water, Air Soil Pollut., 52 (1990) 359.
267 K.S. Johnson and R.L. Petty, Anal. Chem., 54 (1982) 1185.
268 J.J. Pauer, H.R. van Vliet and J.F. van Staden, Water SA, 14 (1988) 125.
269 P. Linares, M.D. Luque de Castro and M. Valcarcel, Talanta, 33 (1986) 889; and references cited therein.
270 Wei Fusheng, Wu Zhongxiang and Ten Enjiang, Anal. Lett., 22 (1989) 3081.
271 D.J. Malcolme-Lawes and K.H. Wong, Analyst, 115 (1990) 65.
272 K. Yoshimura, S. Nawata and G. Kura, Analyst, 115 (1990) 843.
273 G. Schulze and A. Thiele, Fresenius' Z. Anal. Chem., 329 (1988) 711.
274 T. Nasu and M. Kant, Analyst, 113 (1988) 1683.
275 O. Fujino, Y. Koga and K. Hiraki, Bunseki Kagaku, 40 (1991) 19.
276 D.M. Karl and G. Tien, Limnol. Oceanogr., 37 (1992) 105.
277 P. Jones, R. Stanley and N. Barnett, Anal. Chim. Acta, 249 (1991) 539.

278 O. Broberg and K. Pettersson, Hydrobiologia, 170 (1988) 45.
279 J.D.H. Strickland and T.R. Parsons, A Practical Handbook of Seawater Analysis, Fish. Res. Board Can. Bull., 167, Ottawa, 2 edn., 1972.
280 H.L. Golterman and R.S. Clymo (Eds.), Chemical Environment in the Aquatic Habitat, Amsterdam, 1967.
281 F. Osmond, Bull. Soc. Chem. Paris, 47 (1887) 745.
282 D.E. Armstrong, in M. Halmann (Ed.), Analysis of Phosphorus Compounds in Natural Waters, Analytical Chemistry of Phosphorus Compounds, Wiley Interscience, New York, 1972, pp. 744–769.
283 J.E. Going and S.J. Eisenreich, Anal. Chim. Acta, 70 (1974) 95.
284 J.E. Harwood and W.H.J. Hattingh, in E.J. Griffith, A.M. Beeton, J.M. Spencer and D.T. Mitchell (Eds.), Colorimetric Methods of Analysis of Phosphorus at Low Concentrations in Water, Environmental Phosphorus Handbook, Wiley, New York, 1973, pp. 289–302.
285 S. Motomizu, T. Wakimoto and K. Toei, Talanta, 31 (1984) 235.
286 S. Motomizu, T. Wakimoto and K. Toei, Analyst, 108 (1983) 361.
287 S. Motomizu, M. Oshima and A. Hirashima, Anal. Chim. Acta, 211 (1988) 119.
288 K. Pettersson, Int. Rev. Ges. Hydrobiol., 64 (1979) 585.
289 R.J. Stevens, Water Res., 13 (1979) 763.
290 J. Ruzicka and E.H. Hansen, Anal. Chim. Acta, 78 (1975) 145.
291 J. Ruzicka and J.W.B. Stewart, Anal. Chim. Acta, 79 (1975) 79.
292 J.W.B. Stewart and J. Ruzicka, Anal. Chim. Acta, 82 (1976) 137
293 T.A.H.M. Janse, P.F.A. van der Wiel and G. Kateman, Anal. Chim. Acta, 155 (1983) 89.
294 B. Karlberg and G.E. Pacey, Flow Injection Analysis – A Practical Guide, Elsevier, Amsterdam, 1989.
295 H. Casey and S. Smith, Trends Anal. Chem., 4 (1985) 256.
296 R. Gachter, A. Tessier, E. Szabo and R. Carignan, Aquat. Sci., 54 (1992) 1.
297 M.E. Gales, E.C. Julian and R.C. Kroner, J. Am. Water Works Assoc., 58 (1966) 1363.
298 L.J. Lennox, Water Res., 13 (1979) 1329.
299 D.W. Menzel and N. Corwin, Limnol. Oceanogr., 10 (1965) 280.
300 J.E. Harwood, R.E. van Stenderen and A.L. Kuhn, Water Res., (1969) 425.
301 P.J. Johnes and A.L. Heathwaite, Water Res., 26 (1992) 1281.
302 D.S. Jeffries, F.P. Dieken and D.E. Jones, Water Res., 13 (1979) 275.
303 T.J. Logan, T.O. Oloya and S.M. Yaksich, J. Great Lakes Res., 5 (1979) 112.
304 D. Ziegler and M. Readnour, Trans. Missouri Acad. Sci., 9 (1975) 144.
305 A.D. Cembella, N.J. Antia and F.J.R. Taylor, Water Res., 20 (1986) 1197.
306 A. Henriksen, Analyst, 95 (1970) 601.
307 L. Solorzano and J.D. Strickland, Limnol. Oceanogr., 13 (1968) 515.
308 J.T. Goossen and J.G. Kloosterboer, Anal. Chem., 50 (1978) 707.
309 I.D. McKelvie, B.T. Hart, T.J. Cardwell and R.W. Cattrall, Analyst, 114 (1989) 1459.
310 T. Korenaga and K. Okada, Bunseki Kagaku, 33 (1984) 686.
311 M. Aoyagi, Y. Yasumasa and A. Nishida, Anal. Chim. Acta, 214 (1988) 229.
312 S. Hinkamp and G. Schwedt, Anal. Chim. Acta, 236 (1990) 345.
313 R.L. Benson, I.D. McKelvie, B.T. Hart and I.C. Hamilton, Anal. Chim. Acta, in press.
314 K.E. Williams, S.J. Haswell, D.A. Barclay and G. Preston, Analyst, 118 (1983) 245.
315 Y. Hirai, N. Yoza and S. Ohashi, Anal. Chim. Acta, 115 (1980) 269.
316 R. Kanai, S. Aoki and S. Miyachi, Pl. Cell Physiol., 6 (1965) 467.
317 B. Bostrom, O.S. Jacobsen and K. Peterson, Hydrobiologia, 170 (1988) 91.
318 R.J. Stevens and B.M. Stewart, Water Res., 16 (1982) 1591.
319 J.D.H. Williams, J.-M. Jaquet and R.L. Thomas, J. Fish Res. Bd. Can., 33 (1976) 413.
320 A.H.M. Hieltjes and L. Lijklema, J. Environ Qual., 9 (1980) 405.
321 R.J. Stevens and B.M. Stewart, Water Res., 16 (1982) 1507.
322 J.B. Cotner and R.G. Wetzel, Limnol. Oceanogr., 37 (1992) 232.
323 E. Bentzen, W.D. Taylor and E.S. Millard, Limnol. Oceanogr., 37 (1992) 217.
324 P. Ekholm, M. Yli-Halla and P. Kylmala, Verh. Int. Verein. Theor. Angew. Limnol., 24 (1991) 2994.
325 O. Lovstad and T. Krogstad, Verh. Int. Verein. Theor. Angew. Limnol., 24 (1990) 592.
326 T. Mayer, K.W. Kuntz and A. Moller, J. Gt. Lakes Res., 17 (1991) 446.
327 A.N. Sharpley, W.W. Troeger and S.J. Smith, J. Environ. Qual., 20 (1991) 235.
328 S.J. Tarapchak, J. Environ. Qual., 12 (1983) 105.
329 W.A. Dick and M.A. Tabatai, J. Environ. Qual., 6 (1977) 82.
330 D.A. Francko and R.T. Heath, Limnol. Oceanogr., 24 (1979) 463.
331 E. White and G. Payne, Can. J. Fish. Aquat. Sci., 37 (1980) 664.
332 D.R.S. Lean and C. Nalewajko, J. Fish. Res. Bd. Can., 33 (1976) 1312.
333 I.D. McKelvie, B.T. Hart, T.J. Cardwell and R.W. Cattrall, Talanta, in press.

334 M.E. Bradford and R.H. Peters, Limnol. Oceanogr., 32 (1987) 1124.
335 M. Hanna and A. Dauta, Ann. Limnol., 19 (1983) 59.
336 H. Olsson and M. Jansson, Verh. Int. Verein. Limnol., 22 (1984) 200.
337 I.D. McKelvie, Flow Injection Analysis of Dissolved Phosphorus Species in Natural and Wastewaters, PhD Thesis, La Trobe University, 1992.
338 Y. Shan, I.D. McKelvie and B.T. Hart, Anal. Chem., 65 (1993) 3053.
339 L.E. Sommers, R.F. Harris, J.D.H. Williams, D.E. Armstrong and J.K. Syers, Soil Sci. Soc. Amer. Proc., 36 (1972) 51.
340 W.C. Weimar and D.E. Armstrong, Anal. Chim. Acta, 94 (1977) 35.
341 D.J. Cosgrove, Inositol Phosphates – Their Chemistry, Biochemistry and Physiology, Elsevier, Amsterdam, 1980.
342 S.J. Eisenreich and D.E. Armstrong, Environ. Sci. Technol., 11 (1977) 497.
343 S.E. Herbes, H.E. Allen and K.H. Mancy, Science, 187 (1975) 432.
344 J.H. Steward and M.E. Tate, J. Chromatogr., 60 (1971) 75.
345 R.A. Minear, J.E. Segars and J.W. Elwood, Analyst, 113 (1988) 645.
346 C.M. Clarkin, R.A. Minear, S. Kim and J.W. Elwood, Environ. Sci. Technol., 26 (1992) 199.
347 L. Solorzano, Limnol. Oceanogr., 14 (1969) 799.
348 H.A. Kramer, J.R. Moed and H. De Haan, Water Res., 24 (1990) 221.
349 D. Scheiner, Water Res., 10 (1979) 31.
350 G. Toscano, R. Donazzolo and C. Calvo, Ann. Chim. (Rome), 78 (1988) 567.
351 M.A. Brzezinski, Mar. Chem., 20 (1987) 277.
352 X. Qiu and Y. Zhu, Analusis, 15 (1987) 254.
353 K. Nagashima, T. Ishimatsu, S. Suzuki and T. Hobo, Bunseki Kagaku, 37 (1988) 207.
354 M.M. Krunchak, T.P. Pershina and S.S. Stroev, Burn. Prom-st., 10 (1986) 28; C.A., 105 (1986) 232108f.
355 W. Merz and J. Oldeweme, Wasser, 69 (1987) 95.
356 G. Zhang and P.K. Dasgupta, Anal. Chem., 61 (1989) 408.
357 J.R.L. Smith, A.U. Smart, F.E. Hancock and M.V. Twigg, Chem. Ind. (London), 11 (1989) 353.
358 E. Strauss, J.-P. Favier, D. Bicanic, K. van Asselt and M. Lubbers, Analyst, 116 (1991) 77.
359 L. Ebdon, J. Braven and N.C. Frampton, Analyst, 116 (1991) 1005.
360 S. Motomizu, H. Mikasa and K. Toei, Anal. Chim. Acta, 193 (1987) 343.
361 M. Noufi, C. Yarnitzky and M. Ariel, Anal. Chim. Acta, 234 (1990) 475.
362 A.G. Fogg, S.P. Scullion and T.E. Edwards, Analyst, 113 (1988) 979.
363 C.M.G. van den Berg and H. Li, Anal. Chim. Acta, 212 (1988) 31.
364 H.-J. Kim and Y.-K. Kim, Anal. Chem., 61 (1989) 1485.
365 M. Jiang, F. Jiang, J. Duan, X. Tang and Z. Zhao, Anal. Chim. Acta, 234 (1990) 403.
366 C. Sanchez-Pedreno, M.T. Sierra, M.I. Sierra and A. Sanz, Analyst, 112 (1987) 837.
367 R. Liu and D. Liu, Analyst, 116 (1991) 497.
368 T. Perez-Ruiz, C. Martinez-Lozano and V. Tomas, Anal. Chim. Acta, 265 (1992) 103.
369 K. Markusova and M. Fedurco, Anal. Chim. Acta, 248 (1991) 109.
370 K.S. Johnson and R.L. Petty, Limnol. Oceanogr., 28 (1983) 1260.
371 C. Oudot and Y. Montel, Mar. Chem., 24 (1988) 239.
372 P. Raimbault, G. Slawyk, B. Coste and J. Fry, Mar. Biol., 104 (1990) 347.
373 J.R. Clinch, P.J. Worsfold and H. Casey, Anal. Chim. Acta, 200 (1987) 523.
374 H.P.S. Rathore and S.K. Tiwari, Anal. Chim. Acta, 242 (1991) 225.
375 R. Kaveeshwar, L. Cherian and V.K. Gupta, Analyst, 116 (1991) 667.
376 W. Holak and J.J. Specchio, Anal. Chem., 64 (1992) 1313.
377 A.G. Fogg, S.P. Scullion, T.E. Edmonds and B.J. Birch, Analyst, 116 (1991) 573.
378 Z.Q. Gao, G.Q. Wang and Z.F. Zhao, Anal. Chim. Acta, 230 (1990) 105.
379 S. Sabharwal, Analyst, 115 (1990) 1305.
380 G.H. Lu and S.L. Yao, Anal. Lett., 22 (1989) 1743.
381 K. Markusova, Anal. Chim. Acta, 221 (1989) 131.
382 A.G. Fogg and R.M. Alonso, Analyst, 113 (1988) 1337.
383 S.S. Nair, Int. J. Environ. Anal. Chem., 44 (1991) 153.
384 P.K. Tarafder and H.P.S. Rathore, Analyst, 113 (1988) 1073.
385 A.P. Doherty, R.J. Forster, M.R. Smyth and J.G. Vos, Anal. Chim. Acta, 255 (1991) 45.
386 J.N. Barisci and G.G. Wallace, Anal. Lett., 24 (1991) 2059.
387 X.H. Cai, J.H. Pei, X.Y. Zhou and Z.F. Zhao, Anal. Sci., 7 (1991) 109.
388 G. Zhiqiang and Z. Zaofan, Anal. Chim. Acta, 241 (1990) 161.
389 M.J. Dunphy, D.D. Goble and D.J. Smith, Anal. Biochem., 184 (1990) 381.
390 X. Yang and S. Deng, Lihua Jianyan, Huaxue Fence, 25 (1989) 287; C.A., 112 (1990) 83711n.
391 C. Diaz, J.C. Vidal, J. Galban, M.A. Navas and J. Lanaja, Fresenius' Z. Anal. Chem., 333 (1989) 619.
392 F.D. Snell, Photometric and Fluorimetric Methods of Analysis, Nonmetals, Wiley Interscience, New York, 1981, pp. 544–576.
393 H. Ciesielski, G. Sorgnet, M. Catone and P. Vancayzeele, Analusis, 6 (1978) 38.
394 G. Norwitz, J. Farino and P.N. Keliher, Anal. Chim. Acta, 105 (1979) 335.
395 K. Himeno, H. Matuura, K. Takeda, K. Yamamoto and K. Ichimura, Nara-ken Eisei Kenkyusho Nenpo, 23 (1989) 82; C.A., 113 (1990) 138193y

396 S. DeFulvio and L. Olori, Metodi Anal. Acque, 7 (1987) 15; C.A., 108 (1988) 173254n.
397 O. Thomas, S. Gallot and N. Mazas, Fresenius' Z. Anal. Chem., 338 (1990) 238.
398 D. Huiru, G. Meiyu and Z. Qing, Anal. Lett., 24 (1991) 305.
399 N. Suzuki and R. Kuroda, Analyst, 112 (1987) 1077.
400 H. Wang, X. Yu and J. Sun, Shanghai Huanjing Kexue, 8 (1989) 28; C.A., 113 (1990) 197441a.
401 G. Shimizu, T. Osada, T. Takahashi and M. Tsutsumi, Yamanashi-ken Eisei Kogai Kenkyusho Nenpo, 32 (1988) 35; C.A., 113 (1990) 125587e.
402 K. Nagashima, X.X. Qian and S. Suzuki, Analyst, 111 (1986) 771.
403 J. Simal, M.A. Lage and I. Iglesias, J. Assoc. Off. Anal. Chem., 68 (1985) 962.
404 K. Nagashima, M. Matsumoto and S. Suzuki, Anal. Chem., 57 (1985) 2065.
405 B.C. Madsen, Anal. Chim. Acta, 124 (1981) 437.
406 A. Al-Wehaid and A. Townshend, Anal. Chim. Acta, 186 (1986) 289.
407 L. Cherian and V.K. Gupta, J. Indian Chem. Soc., 66 (1989) 897.
408 S.J. Bajic and B. Jaselskis, Talanta, 32 (1985) 115.
409 J.I. Skicko and A. Tawfik, Analyst, 113 (1988) 297.
410 J.H. Margeson, J.C. Suggs and M.R. Midgett, Anal. Chem., 52 (1980) 1955.
411 J.F. Van Staden, Anal. Chim. Acta, 138 (1982) 403.
412 R.B. Willis, Anal. Chem., 52 (1980) 1376.
413 M.A. Koupparis, K.M. Walczak and H.V. Malmstadt, Anal. Chim. Acta, 142 (1982) 119.
414 H. Mori and J. Imai, Gifu-ken Eisei Kenkyushoho, 34 (1989) 7; C.A., 113 (1990) 158304p.
415 S. Devi and A. Townshend, Anal. Chim. Acta, 225 (1989) 331.
416 I.E. Kalinchenko, N.F. Kushchevskaya and A.T. Pilipenko, Zh. Anal. Khim., 43 (1988) 1051.
417 Z. Iskandarani and D.J. Pietrzyk, Anal. Chem., 54 (1982) 2601.
418 P.E. Jackson, P.R. Haddad and S. Dilli, J. Chromatogr., 295 (1984) 471.
419 K. Ito, Y. Ariyoshi, F. Tanabiki and H. Sunahara, Anal. Chem., 63 (1991) 273.
420 S.T. Sulaiman and I.J. Al-Nuri, Microchem. J., 33 (1986) 112.
421 S.T. Sulaiman, Anal. Chem., 56 (1984) 2405.
422 K. Kalcher, Talanta, 33 (1986) 489.
423 R.D. Cox, Anal. Chem., 52 (1980) 332.
424 R.S. Braman and S.A. Hendrix, Anal. Chem., 61 (1989) 2715.
425 H. Mottola, Kinetic Aspects of Analytical Chemistry, Wiley, New York, 1988.
426 R. Montes and J.J. Lasema, Talanta, 34 (1987) 1021.
427 M.A. Koupparis, K.M. Walczak and H.V. Malmstadt, Analyst, 107 (1982) 1309.
428 T. Okutani, A. Sakuragawa, S. Kamikura, M. Shimura and S.J.N. Azuchi, Anal. Sci., 7 (1991) 793.
429 J. Yuan, Q. Tian and X. Cai, Fenxi Huaxue, 16 (1988) 788; C.A., 110 (1989) 204752w.
430 R. Montes and J.J. Laserna, Anal. Sci., 7 (1991) 467.
431 Y.K. Agrawal and P.N. Bhatt, Anal. Lett., 21 (1988) 2323.
432 G. Norwitz and P.N. Keliher, Analyst, 112 (1987) 903.
433 D.P.S. Rathore and P.K. Taraider, J. Indian Chem. Soc., 66 (1989) 185.
434 S.-C. Pai, C.-C. Yang and J.P. Riley, Anal. Chim. Acta, 232 (1990) 345.
435 E. Szekely, Comm. Soil Sci., Plant Anal., 22 (1991) 1295.
436 A.A. Alhatim, Int. J. Environ. Anal. Chem., 38 (1990) 617.
437 B.B. Ibraheem and W.A. Bashir, Int. J. Environ. Anal. Chem., 30 (1987) 159.
438 R.B. Willis and C.E. Gentry, Commun. Soil Plant Anal., 18 (1987) 625.
439 J.J. Pauer, H.R. van Vliet and J.F. Staden, Water SA, 16 (1990) 105.
440 H. Casey, S. Smith and G. Williams, Proc. 5th Int. Env. and Safety Conf., London, 1985.
441 J. Maimo, A. Cladera, F. Mas, R. Forteza, J.M. Estela and V. Cerda, Int. J. Environ. Anal. Chem., 35 (1989) 161.
442 A.R. Thornton, J. Pfab and R.C. Massey, Analyst, 114 (1989) 747.
443 R. Nakata, M. Terashita, A. Nitta and K. Ishikawa, Analyst, 115 (1990) 425.
444 M. Trojanowicz, W. Matuszewski, B. Szostek and J. Michalowski, Anal. Chim. Acta, 261 (1992) 391.
445 M.M. Malone, A.P. Doherty, M.R. Smyth and J.G. Vos, Analyst, 117 (1992) 1259.
446 S. Wilke, H. Franzke and H. Muller, Anal. Chim. Acta, 268 (1992) 285.
447 M. Yaqoob, M.A. Siddiqui and M. Masoom, J. Chem. Soc. Pakistan, 13 (1991) 248.
448 R.L. Benson, P.J. Worsfold and F.W. Sweeting, Anal. Proc. (London), 26 (1989) 385.
449 J.F. van Staden, A.E. Joubert and H.R. Van Vliet, Fresenius' Z. Anal. Chem., 325 (1986) 150.
450 J.A. Cox and K.R. Kulkami, Analyst, 111 (1986) 1219.
451 P.R. Kraus and S.R. Crouch, Anal. Lett., 20 (1987) 183.
452 T. Aoki, J. Flow Injection Anal., 5 (1988) 95.
453 S. Alegret, J. Alonzo, J. Bartroli and E. Martinez-Fabregas, Analyst, 114 (1989) 1443.
454 S. Alegret, J. Alonzo, J. Bartroli, M. DeiValle, N. Jaffrezic-Renault and Y. Duvault-Herrera, Anal. Chim. Acta, 231 (1990) 53.
455 J.J.R. Rohwedder and C. Pasquini, Analyst, 116 (1991) 841.
456 D. Chen, M.D.L. de Castro and M. Valcarcel, Analyst, 116 (1991) 1095.
457 J.F. van Staden, Water SA, 13 (1987) 197.
458 J.R. Clinch, P.J. Worsfold and F.W. Sweeting, Anal. Chim. Acta, 214 (1988) 401.
459 V. Blet, M.-N. Pons and J.L. Greffe, Anal. Chim. Acta, 219 (1989) 309.
460 L. Cardoso de Faria and C. Pasquini, Anal. Chim. Acta, 245 (1991) 183.
461 N.E. Skelly, Anal. Chem., 54 (1982) 712.
462 R.J. Williams, Anal. Chem., 55 (1983) 851.
463 B.B. Wheals, J. Chromatogr., 262 (1983) 61.

464 A. Mangia and M.T. Lugari, Anal. Chim. Acta, 159 (1984) 349.
465 W.E. Barber and P.W. Carr, J. Chromatogr., 301 (1984) 25.
466 W.E. Barber and P.W. Carr, J. Chromatogr., 316 (1984) 211.
467 J. Osterloh and D. Goldfield, J. Liq. Chromatogr., 7 (1984) 753.
468 B.B. Wheals, J. Chromatogr., 402 (1987) 115.
469 M.C. Gennaro, J. Chromatogr., 449 (1988) 103.
470 R. Golombek and G. Schwedt, J. Chromatogr., 452 (1988) 283.
471 N. Chauret and J. Hubert, J. Chromatogr., 469 (1989) 329.
472 P. Pastore, I. Lavagnini, A. Boaretto and F. Magno, J. Chromatogr., 475 (1989) 331.
473 K.K. Verma and A. Verma, Anal. Lett., 25 (1992) 2083.
474 M.C. Gennaro, P.L. Bertolo and A. Cordero, Anal. Chim. Acta, 239 (1990) 203.
475 E. Hoffmann, G. Markovarga, I. Csiky and J.A. Jonsoon, Int. J. Environ. Anal. Chem., 25 (1986) 161.
476 S. Rokushika, K. Kihara, P.F. Subosa and W. Leng, J. Chromatogr., 514 (1990) 355.
477 United States EPA Method 300.D. Determination of Inorganic Anions in Water by Ion Chromatography.
478 E.M. Burke, F.X. Suarez, D.C. Hillman and E.M. Helthmer, Water Res., 23 (1989) 519.
479 M.D. Stewart, Ultrapure Water, 5 (1988) 24.
480 M.D. Stewart, Adv. Instrum. Control, 44(Pt. 1) (1989) 287.
481 G. Randon, Water Supply, 6 (3) (1988) 25.
482 C.L. Elliott, G.H. Snyder and J.L. Cisar, Commun. Soil Sci. Plant Anal., 20 (1989) 1873; C.A., 111 (1989) 219007b.
483 C. Yucesoy, F. Onur and S. Ozkan, FABAD Farm. Bilimler Derg., 14 (1989) 216; C.A., 113 (1990) 84482w.
484 P. Raimbault and G.A. Slawyk, Limnol. Oceanogr., 36 (1991) 405.
485 J.H. Lowry and K.H. Mancy, Water Res., 12 (1978) 471.
486 L. Solorzano, Limnol. Oceanogr., 25 (1980) 751.
487 P. MacCarthy, R.W. Klusman and J.A. Rice, Anal. Chem. 61 (1989) 269R.
488 J.I. Hedges, B.A. Bergamaschi and R. Benner, Mar. Chem., 41 (1993) 121.
489 J. Qian and L. Fu, Huanjing Kexue, 8 (1978) 81; C.A., 106 (1987) 219257e.
490 K. Dai, S. Fang, W. Mao, D. Xia and L. Jiang, Shanghai Huanjing Kexue, 6 (1987) 24; C.A., 107 (1987) 222880d.
491 E. Nakamura and H. Namiki, Kogyo Yosui, 341 (1987) 12; C.A., 107 (1987) 6445j.
492 A. Suzuki, M. Satoh, M. Kamiya and S. Ogawa, Mizu Shori Gijutsu, 26 (1985) 921; C.A., 106 (1987) 38122m.
493 M. Hosomi and R. Sudo, Int. J. Environ. Stud., 27 (1986) 267.
494 M.M. Smart, F.A. Reid and J.R. Jones, Water Res., 15 (1981) 919.
495 S. Hinkamp and G. Schwedt, Z. Wasser-Abwasser-Forsch., 24 (1991) 60.
496 K. Grasshof, Deep-Sea Res., 11 (1964) 597.
497 J. David Smith and P.J. Milne, Anal. Chim. Acta, 123 (1981) 263.
498 K. Kato, Anal. Chim. Acta, 82 (1976) 401.
499 V.W. Truesdale and C.J. Smith, Analyst, 100 (1975) 203.
500 F. Koroleff, in K. Grasshoff, M. Ehrhardt and K. Kremling, (Eds), Methods of Seawater Analysis, Verlag Chemie, Weinheim, 1983, pp. 174–187.
501 R. Ramachandran and P.K. Gupta, Anal. Chim. Acta, 172 (1985) 307.
502 Q. Zini, P.L. Baldini and L. Morettini, Microchem. J., 32 (1985) 148.
503 K.A. Fanning and M.E. Pilson, Anal. Chem., 45 (1973) 136.
504 R.A. Chalmers and A.G. Sinclair, Anal. Chim. Acta, 34 (1966) 412.
505 A. Jarabin, M. Vajda and P. Szarvas, Acta Phys. Chim. Debrecina, 15/16 (1970) 201.
506 A.G. Fogg and G.C. Cripps, Analyst, 108 (1983) 1485.
507 Y. Hirai, T. Yokoma, N. Yoza, T. Tarutani, and S. Ohashi, Bunseki Kagaku, 30 (1981) 350.
508 P. Linares, M.D. Luque de Castro and M. Valcarcel, Anal. Chim. Acta, 177 (1985) 263.
509 J.R. Ferreira, E.A.M. Kronka and A.M. Jacintho, Quim. Nova, 10 (1987) 270.
510 J. Thomsen, K.S. Johnson and R.L. Petty, Anal. Chem., 55 (1983) 2378.
511 T. Hori, T. Itoh, S. Okazaki and T. Fujinaga, Bunseki Kagaku, 30 (1981) 582.
512 G.M. Varshal, L.V. Dracheva and N.S. Zamokina, Khim. Anal. Morsk. Osadkov., 3 (1980) 156; C.A., 95 (1981) 67699q.
513 E. Kiss, Anal. Chim. Acta, 140 (1982) 197.
514 B. Sansoni, W. Brunner, G. Wolff, H. Ruppert and R. Dittrich, Fresenius' Z. Anal. Chem., 331 (1988) 154.
515 Y. Baba, N. Yoza and S. Ohashi, J. Chromatogr., 318 (1985) 319.
516 P. Nkedikizza and J. Owusuyaw, J. Environ. Sci. Health A, Environ. Sci. Eng., (1992) 245.
517 G. Bondoux, P. Jandik and W.R. Jones, J. Chromatogr., 602 (1992) 79.
518 A.O. Jacintho, E.A.M. Kronka, E.A.G. Zagatto, M.A.Z. Arruda and J.R. Ferreira, J. Flow Injection Anal., 6 (1989) 19.
519 L.K. Shpigun, I. Ya Kolotyrkina and Y.A. Zolotov, Anal. Chim. Acta, 261 (1992) 307.
520 Y. Narusawa and T. Hashimoto, Chem. Lett., (1987) 1367.
521 Y. Narusawa, Anal. Chim. Acta, 204 (1988) 53.
522 E.A. Maier, Trends Anal. Chem., 10 (1991) 340.

Analytica Chimica Acta, 287 (1994) 191–199
Elsevier Science B.V., Amsterdam

Development of a liposome immunosorbent assay for human interferon-γ

H.A.H. Rongen, H.M. van der Horst, G.W.K. Hugenholtz, A. Bult and W.P. van Bennekom

Department of Pharmaceutical Analysis, Faculty of Pharmacy, Utrecht University, P.O. Box 80082, 3508 TB Utrecht (Netherlands)

P.H. van der Meide

TNO Medical Biological Laboratory, P.O. Box 5815, 2280 HV Rijswijk (Netherlands)

(Received 27th August 1993; revised manuscript received 11th October 1993)

Abstract

A novel and sensitive liposome immunosorbent assay (LISA) for IFN-γ is described. Biotinylated liposomes with encapsulated carboxyfluorescein comprise a universal label for immunoassays. Stability of the liposomes is proven to be adequate for long-term storage, without loss of encapsulated marker. Sensitivity of the LISA of 6×10^{-12} M is comparable to the best colorimetric immunoassays for IFN-γ, and the linear detection range ($6–2400 \times 10^{-12}$ M) exceeds the colorimetric range. Analysis of biological samples with the LISA showed no interference on the liposomes from potential disturbing factors in either plasma or blood cell culture supernatants.

Keywords: Immunoassay; Fluorimetry; ELISA; Liposome immunosorbent assay (LISA); Interferon-γ

For low-level determination of exogenous and endogenous substances in biological materials highly selective and sensitive methods are required. Hyphenated instrumental methods, including chromatography with a suitable detection method, provide in many cases the selectivity and sensitivity for successful application in bioanalysis. However, also immunoassays meet these requirements. Both low-molecular-weight and high-molecular-weight analytes (haptens and antigens, respectively) can be assayed directly e.g. in plasma or serum with immunochemical methods.

In an immunoassay an antibody – raised against the antigen to be detected – recognizes an epitope on the antigen and binds it with high affinity. Either the antibody or the antigen is labelled allowing detection of the extent of interaction. If the antigen is large enough to contain at least two independent epitopes, the antigen can be sandwiched between two different but specific antibodies. The most powerful immunoassays are the sandwich ELISA methods, in which the second antibody is enzyme-labelled (Fig. 1a). The resulting amplification is dependent on the incubation time, the activity of the enzyme and the reaction conditions. Usually the measurement is performed in a 96-well microtitre plate with UV–visible detection. Lower detection limits can be achieved with fluorescence [1] or chemiluminescence [2] methods. In all cases, however, the limit of detection is largely determined by a non-enzymatic conversion of the substrate. This competing reaction is becoming increasingly pronounced at very low levels when prolonged incubation times are required to generate an appropriate amount of product for detection. Such a competing reaction, however, is

Correspondence to: H.A.H. Rongen, Department of Pharmaceutical Analysis, Faculty of Pharmacy, Utrecht University, P.O. Box 80082, 3508 TB Utrecht (Netherlands).

SSDI 0003-2670(93)E0592-U

absent in a liposome immunoassay (Fig. 1b and c).

Liposomes are artificial lipid vesicles (100–1000 nm) with an aqueous interior in which up to 2×10^5 molecules of a suitable marker can be entrapped. This amount is directly available when lysing or disintegrating the liposomes. The liposomes can be coupled directly to the second antibody (Fig. 1b) [3] or indirectly via a secondary antibody or the (strept)avidin–biotin complex (Fig. 1c) [4,5]. Biotin has the advantage of being a generic non-protein ligand.

Several analytical applications of liposomes in immunoassays have been reported [6]: (a) liposome immunolysis assays (LILAs): using the liposome lysing capability of free ouabain-melittin conjugate [7,8] or complement [9,10]; (b) liposome flow-injection immunoassays (FIIA) in which the liposomes are competitively bound to antibodies, immobilized on a column. Subsequent lysis is performed by means of detergent [11,12]; (c) a homogeneous assay with a single-liquid reagent containing liposomes [13] and (d) heterogeneous liposome immunoassays performed in microtitre plates [14], antibody-coated cuvettes [4] or tubes [15].

To be useful in a LISA liposomes should encapsulate as much as possible marker molecules, and release these molecules only on external triggering. Leakage should approach zero (or at least be constant) and the size and polydispersity (size distribution) should be fully controlled.

Various types of liposomes can be used. Multilamellar vesicles (MLVs) are stable, show relatively little leakage but only 4–5% of the interior volume is effectively filled with marker. In large unilamellar vesicles (LUVs) about 30% of the volume is available but LUVs are less stable and show more leakage. Leakage can be decreased by using saturated instead of unsaturated phospholipids in the lipid membrane. The resulting gel-state liposomes have a higher transition-state temperature. Increasing the cholesterol content also decreases leakage [16].

The encapsulated marker should be highly water-soluble and easily detectable. Carboxyfluorescein [17] and sulforhodamine B [15] are commonly used in liposome studies, including drug-targeting and model-membrane investigations [18,19].

In this paper we describe the development of a LISA using microtitre plates for the immunoregulatory cytokine interferon-γ (IFN-γ). IFN-γ is used in our studies as a model antigen. The IFN-γ LISA using biotinylated liposomes with entrapped carboxyfluorescein, will be applied to biological samples and the results will be compared with the colorimetric ELISA. The func-

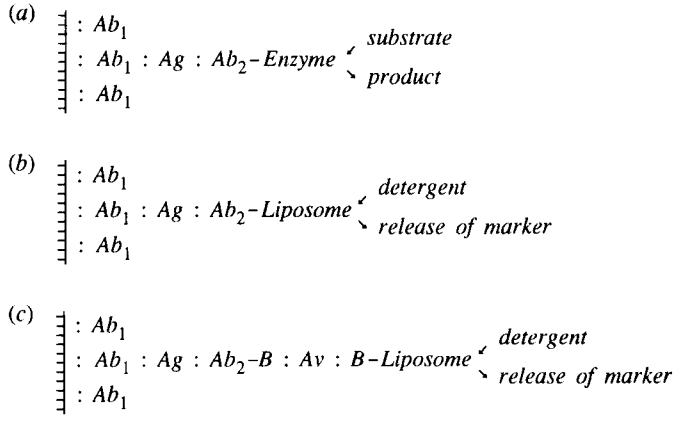

Fig. 1. Assay formats of (a) a sandwich ELISA, (b) a sandwich liposome immunosorbent assay (LISA) and (c) a LISA with (strept)avidin as bridging agent between the detecting antibody and the biotinylated liposome. Carboxyfluorescein (CF) as marker is entrapped in the liposomes. ⫶ = well wall, $Ab_{1\text{-}2}$ = antibody, Ag = antigen, B = biotin, Av = (strept)avidin; non-covalent bindings are indicated by : .

tional LISA should easily be transferable to other sandwich immunoassays.

EXPERIMENTAL

Materials

Dipalmitoylphosphatidylcholine (DPPC) and dipalmitoylphosphatidylglycerol (DPPG) were obtained from Nattermann (Cologne). Cholesterol and bovine serum albumin (BSA, RIA grade) were obtained from Sigma (St. Louis, MO). *N*-(biotinoyl)-1,2-dihexadecanoyl-*sn*-glycero-phosphoethanolamine, triethyl ammonium salt (B-DHPE) and *N*-{[6-(biotinoyl)amino]hexanoyl}-1,2-dihexadecanoyl-*sn*-glycero-phosphoethanolamine, triethyl ammonium salt (B-X-DHPE: X represents a long chain) were purchased from Molecular Probes (Eugene, OR). Avidin was bought from Pierce (Rockford, IL). 5(6)-Carboxyfluorescein (CF) was acquired from Eastman-Kodak (Rochester, NY) and purified before use [17]. Sephadex G–50 (medium) was obtained from Pharmacia (Uppsala) and Triton X-100 from Merck (Darmstadt). The polycarbonate filters and the high-binding EIA microtitre plates used for the ELISA and LISA were from Costar (Cambridge, MA). All other chemicals were of analytical grade and used as received. All aqueous solutions and buffers were made using water purified with the Milli-Q system (Millipore, Bedford, MA). Biological materials consisted of IFN-γ produced by chimpanzee blood cell cultures or of human plasma (Blood Bank, Utrecht) spiked with recombinant human-IFN-γ.

Preparation of liposomes

Gel-state liposomes containing 100 mM CF were prepared by the extrusion method [16]. A chloroform solution with 60 μmol DPPC, 6 μmol DPPG, 24 μmol cholesterol and 90 nmol B-X-DHPE (0.1 mol%) was dried to a lipid film in a Rotavapor. The film was hydrated at 50°C in 3 ml 100 mM CF in 10 mM Tris–HCl pH 7.4. This resulted in a liposome dispersion of 30 μM total lipid, which was extruded successively through 600, 200, 100 and/or 50-nm polycarbonate filters, depending on the liposome size required. The average size and the polydispersity of the resulting MLVs were measured with dynamic light scattering (DLS) with a Malvern 4600 particle sizer (Malvern, UK). The liposomes were stored under N_2 at 4°C.

Unencapsulated CF was removed directly before use by the minicolumn centrifugation method [20,21]. In short: 10 g of Sephadex G-50 (medium) was allowed to swell in 120 ml of 0.9% (w/v) NaCl for at least 5 h at room temperature. A 2.5-ml syringe barrel was filled with 2 ml of this gel and spun for 3 min at 2000 rpm in a bench centrifuge. On top of the dried gel bed 100 μl of undiluted liposome solution was applied. This was spun again for 10 min at 500 rpm and then for 3 min at 2000 rpm. The eluate contained the liposomes, while free CF remained on the column.

The accessibility of biotin was examined by incubating liposomes with free avidin until aggregation and measuring light scattering spectrophotometrically [4], and by performing a LISA (see below). Leakage was determined by measuring the amount of CF released through the intact membrane of the liposomes at regular time intervals at 37°C. Adding subsequently Triton X-100 resulted in release of the encapsulated marker and enabled the calculation of the encapsulation efficiency, which is defined as the ratio of the encapsulated amount of marker to total amount of marker [20].

Procedures

The coating antibody MD-2, the detecting antibody MD-1, IFN-γ, ELISA and the biotinylation procedure have been described previously [22]. The LISA procedure, also performed in a microtitre plate, was essentially the same up to the anti-biotin step. Then avidin (2.0 μg/ml in PBS–1% BSA–0.05% Tween 20) was incubated for 1 h at 37°C, while gently shaking on a vortex, and washed five times with iso-osmotic 10 mM Tris–HCl, pH 7.4 (containing 8.69 g/l NaCl) to remove Tween. Next 100 μl of liposomes (at various concentrations and of various sizes) were incubated for 2 h at 37°C, while shaking, and subsequently washed ten times with iso-osmotic Tris buffer. All washing steps were performed

with an SLT 96 PW microplate washer (SLT, Grödig/Salzburg). The LISA format is given in Fig. 1c.

The entrapped CF was released with 150 μl of 0.5% Triton X-100 in 10 mM Tris–HCl pH 7.4 (70°C). The microtitre plate was placed in a flow-injection system consisting of a pump (Kratos Spectroflow 400 solvent delivery system, Applied Biosystems, Foster City, CA), an autosampler (Model 232, Gilson, Middleton, WI) and a fluorescence detector (HP 1046A, Hewlett Packard, Palo Alto, CA) and 20 μl were injected. Fluorescence was measured with $\lambda_{ex} = 486$ nm and $\lambda_{em} = 525$ nm. Fluorescence is expressed for all experiments in the same arbitrary units, which can be related to the CF concentration: 1 μM CF = 22320 arbitrary fluorescence units.

RESULTS AND DISCUSSION

Preparation and characterization of liposomes

For biotin to be incorporated in the liposome membrane it has to be covalently coupled to a lipid. Liposomes containing the commercially available B-X-DHPE (with a long chain) or B-DHPE (without a long chain) were used. B-DHPE gave positive results with aggregation experiments [4], but the LISA itself showed satisfying results only at high IFN-γ concentrations. This suggests that the biotin moiety of the conjugate is hardly accessible for avidin, maybe because of its proximity to the hydrophilic outer layer of the liposome. The long-chain biotin derivative B-X-DHPE improved both results. Aggregation was more pronounced at lower avidin concentrations, and the LISA performed showed higher fluorescence signals at lower IFN-γ concentrations (discussed below). Therefore this derivative was used for the succeeding experiments.

With the extrusion method liposomes with different diameters were prepared (Table 1). Both size and polydispersity remained stable for over 6 weeks, when stored at 4°C and under N_2, indicating long-term storage possibilities of these labels. Also LISAs performed during that period of time showed no loss of fluorescence signal or sensitivity.

Leakage, cleaning and encapsulation efficiency

Leakage can only occur during and after separation of the non-trapped CF. This separation (or cleaning) can be performed by e.g. centrifugation and dialysis, but these are time-consuming processes, which still leave a substantial amount of CF outside the liposomes. The best results were obtained with the minicolumn centrifugation method. During centrifugation too high gravitational fields applied to the liposomes, might result in less and/or less-loaded liposomes [20].

This cleaning takes place directly before performing a LISA. From then on the liposomes are kept in a 10 mM Tris–HCl buffer pH 7.4, which is iso-osmotic with 100 mM CF, to keep leakage

TABLE 1

Preparation and stability of gel-state liposomes [a]

Size (nm)	262		155		125	
Extrusion	3 * 600 nm 3 * 200 nm		3 * 600 nm 3 * 200 nm 3 * 100 nm		3 * 600 nm 3 * 200 nm 3 * 100 nm 3 * 50 nm	
DLS	∅ (nm)	Polydisp.	∅ (nm)	Polydisp.	∅ (nm)	Polydisp.
Day 1	262	0.10	155	0.05	125	0.13
Day 25	261	0.09	155	0.08	126	0.16
Day 45	264	0.09	154	0.10	124	0.13

[a] After hydration the liposomes are extruded consecutively through a series of polycarbonate membranes with decreasing pore size. The first DLS measurements of size and polydispersity were performed directly after the last extrusion. The liposomes were kept at 4°C and under N_2 until the next measurement.

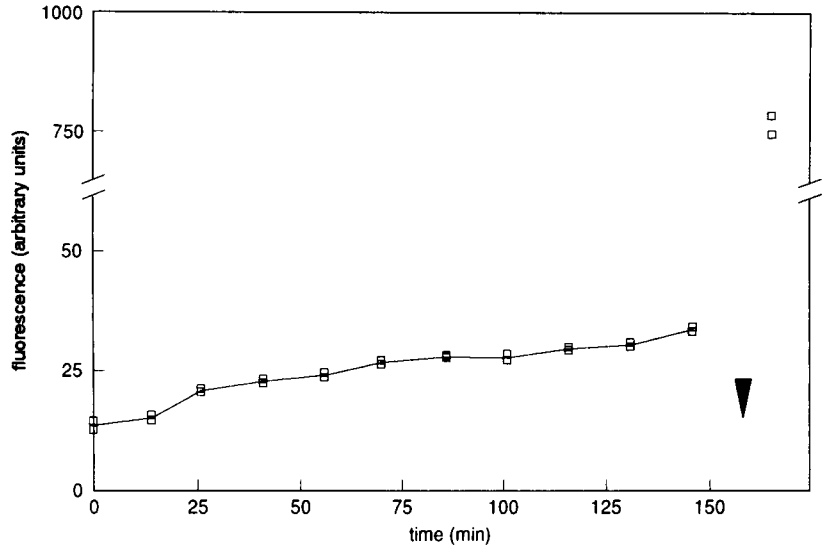

Fig. 2. Leakage of 'minicolumn centrifugated' liposomes. Liposomes (diameter 155 nm, concentration 30 nM) were kept in iso-osmotic 10 mM Tris–HCl pH 7.4 buffer at 37°C. At regular times a sample was taken and fluorescence measured ($n = 2$). For percentage release and encapsulation efficiency measurements Triton X-100 was added (indicated by ▼).

as low as possible. However, still some leakage occurs as can be seen in Fig. 2. Leakage is 1.1% per h, independent of liposome size, so during a 2-h incubation period a constant but tolerable amount is released. Further leakage could occur during the last washing step: this amount, however, is uncontrollable. Leakage was kept as low as possible by applying an iso-osmotic wash buffer, without the detergent Tween 20, which is normally used for washing.

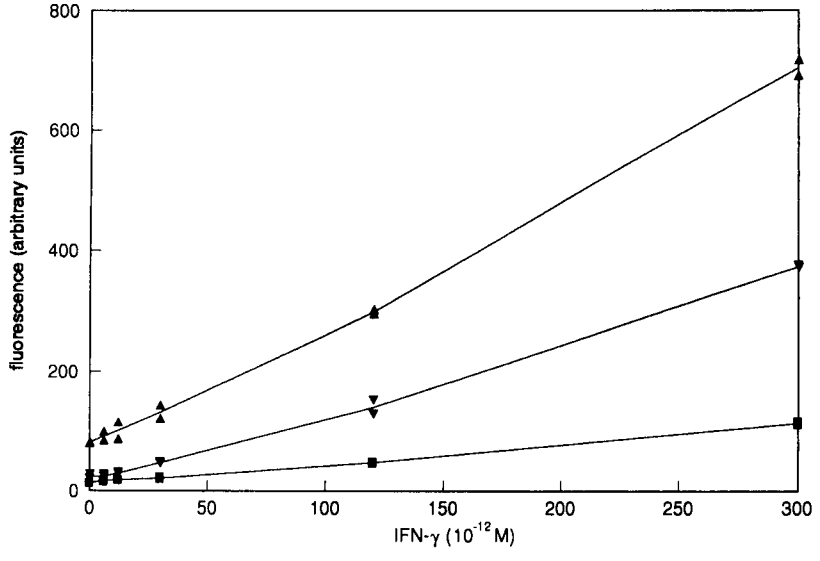

Fig. 3. Concentration vs. fluorescence intensity (CF, $\lambda_{ex} = 486$ nm, $\lambda_{em} = 525$ nm) for the IFN-γ sandwich LISA with 155-nm gel-state liposomes ($n = 2$). Liposome concentrations: 6 (■), 30 (▼) and 300 nM (▲).

Encapsulation efficiency was found to be 4–5%, independent of liposome size. This number correlates well with values normally found for MLVs [6,16].

LISA

The working concentration of liposomes was investigated in a first series of experiments (Fig. 3). Concentrations of 6 and 30 nM gave a low and similar blank signal; the slope increased, and accordingly the detection limit (defined as blank $+ 2 \cdot sd_{bl}$) improved with the liposome concentration. A concentration of 300 nM gave an increased blank signal without improving LISA performance.

Incubation time of the liposomes, which could be of importance because of the relatively large size of the label, was set at 2 h. Longer incubation times had no positive effect on the LISA, and an incubation period below 1 h decreased fluorescence and increased detection limits.

Experiments with non-cleaned liposomes gave an overall decrease in fluorescence, however not the blank signal. This suggests that the high CF concentration present in the wells (100 mM) during incubation interferes with the avidin-biotin binding.

TABLE 2

Statistical analysis of the data in Figs. 3 and 4. Liposomes: diameter and concentration, respectively

Liposomes	r	Intercept ± S.D.	Slope ± S.D
155 nm, 6 nM	0.997	12.58 ± 1.05	0.33 ± 0.008
155 nm, 30 nM	0.997	14.38 ± 3.70	1.18 ± 0.028
155 nm, 300 nM	0.998	72.51 ± 5.73	2.09 ± 0.043
125 nm, 300 nM	0.995	34.39 ± 6.25	1.42 ± 0.047
262 nm, 300 nM	0.996	50.57 ± 13.67	3.75 ± 0.10

An increased diameter of the liposomes raised the overall signal, approximately with liposome volume, but the detection limit for all sizes remained about 6×10^{-12} M (Fig. 4). A statistical evaluation of the results shown in Figs. 3 and 4 is given in Table 2. Clearly visible is the increasing slope with increasing liposome diameter and concentration. Also the blank signal increases with size and diameter, apart from the 262-nm liposomes, which can be explained by the larger standard deviation.

An interesting fact concerns the upper detection limit. When e.g. 125-nm liposomes are used, 6.4×10^9 liposomes will cover the whole well surface (i.e. 1 cm^2 at 100 μl and assuming liposomes cover a square surface area and one IFN-γ

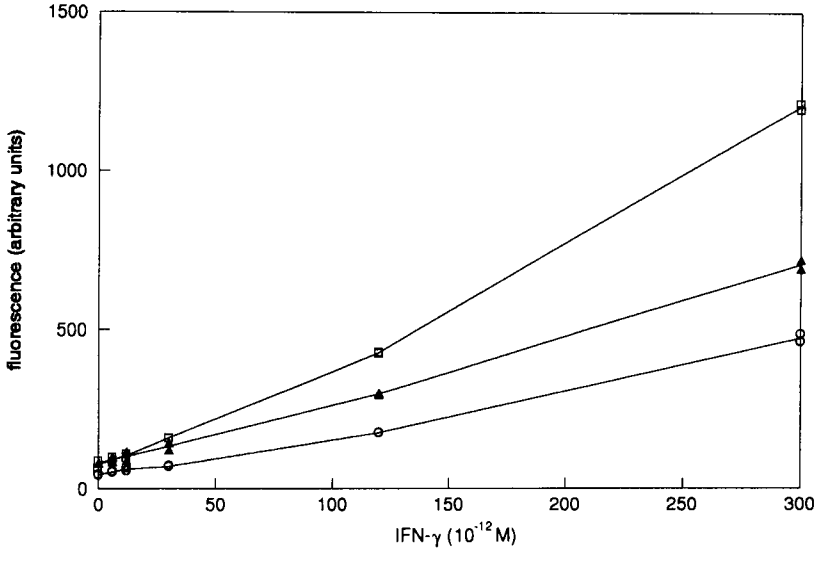

Fig. 4. Concentration vs. fluorescence intensity (CF, λ_{ex} = 486 nm, λ_{em} = 525 nm) for the IFN-γ sandwich LISA with 125- (□), 155- (▲) and 262-nm (■) liposomes, all at 300 nM (n = 2).

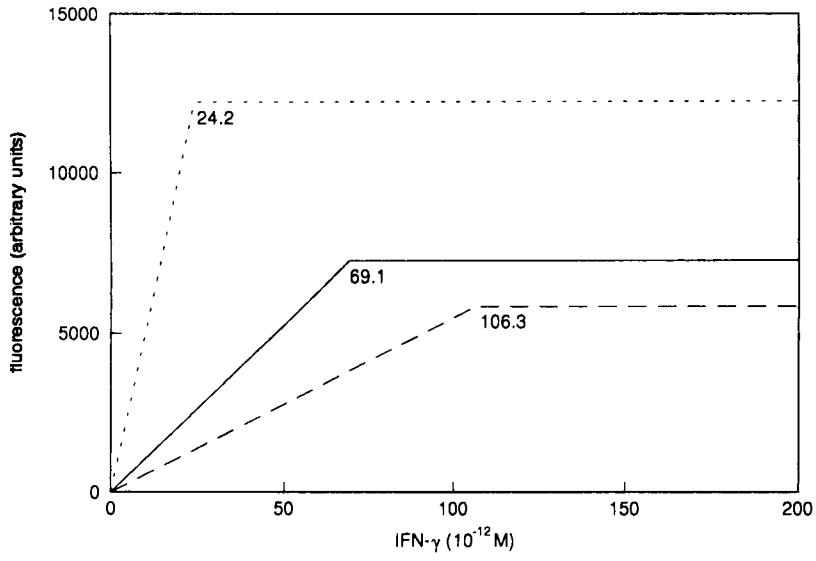

Fig. 5. Theoretically derived graphs for LISA. The numbers inside the figure indicate the calculated upper detection limits in 10^{-12} M for 125- (— — —), 155- (———) and 262-nm (· · · · · ·) liposomes. Fluorescence is calculated with an encapsulation efficiency of 4%, and assuming a yield of 100% in each step. See text for an explanation.

molecule binds one liposome). This number corresponds with 106.3×10^{-12} M IFN-γ. Higher IFN-γ concentrations will have no net result, because the maximum number of liposomes already covers the well wall. With larger liposomes even less IFN-γ can be quantified. This is graphically explained in Fig. 5. Experimentally we found these upper limits at IFN-γ concentrations about 200 times as high (Fig. 6). An explanation could be the fact that a(n) (E)LISA is a method with

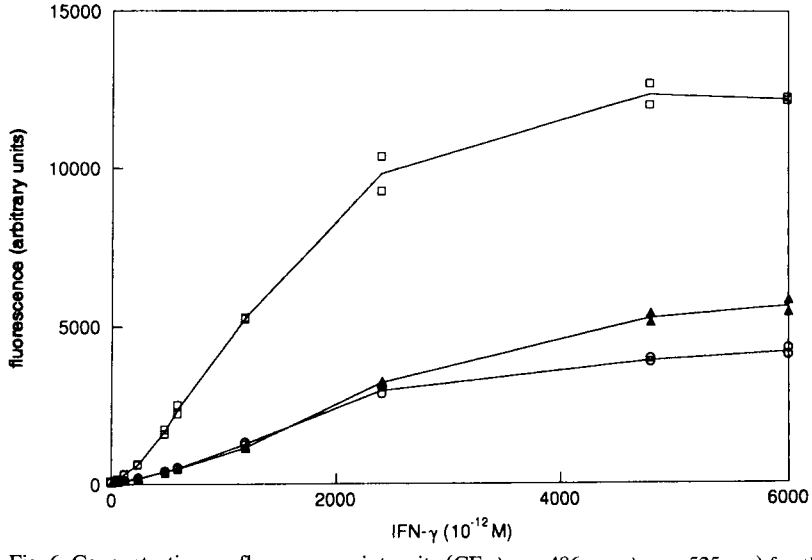

Fig. 6. Concentration vs. fluorescence intensity (CF, λ_{ex} = 486 nm, λ_{em} = 525 nm) for the IFN-γ sandwich LISA with 125- (○), 155- (▲) and 262-nm (□) liposomes, all at 300-nM total lipid concentration (n = 2). IFN-γ range has been extended to 0–6000×10^{-12} M for LDR determination.

(reproducible) efficiencies in each step of about 25% (assuming all steps have the same efficiency). The maximum fluorescence signals of Figs. 5 and 6 are comparable, which indicates that indeed the maximum number of liposomes has been attached to the LISA, however, at much higher IFN-γ concentrations.

From these experiments the Linear Dynamic Range (LDR) could be established as $6–2400 \times 10^{-12}$ M.

The LISA was tested on buffer (PBS–1% BSA–0.05% Tween 20), and on biological samples: chimpanzee cell culture supernatants containing natural IFN-γ (diluted with buffer) and human plasma spiked with recombinant IFN-γ (diluted with plasma), and compared with the colorimetric ELISA. The LISA showed a high correlation with the ELISA especially for the lower IFN-γ concentrations (Fig. 7) for all samples. Negative concentrations can be accounted for by variation in the triplicate blank samples.

Conclusions

In this study it has been proven that a liposome immunosorbent assay is a feasible and promising method. The detection limit of 6×10^{-12} M is comparable with the colorimetric ELISA for IFN-γ. The LDR of $6–2400 \times 10^{-12}$ M extends the colorimetric LDR, which ends at about 600×10^{-12} M.

The sigmoidal trend in Fig. 6 and the bend visible in Figs. 3 and 4 can be explained at higher IFN-γ concentrations by the specific nature of the liposomes, especially their size. At lower concentrations the statistical evaluation gives highly correlated linear calibration curves (Table 2).

This LISA has been tested on biological samples and potential disturbing factors in plasma or supernatants have clearly no effect on its performance, which makes it possible to apply this format for routine use.

The advantages of liposomes in immunoassays are clear from these experiments. The absence of enzymes in the label greatly improves the stability and storage possibilities. Biotin-conjugated liposomes are a universal label which can be used in any immunoassay. An important aspect is the fact that CF can be replaced by any other water-soluble marker. Chemiluminescent or electrochemical markers or even enzymes can be entrapped in the liposomes, with the latter creating a second amplifying cascade. The enzyme and its substrate of

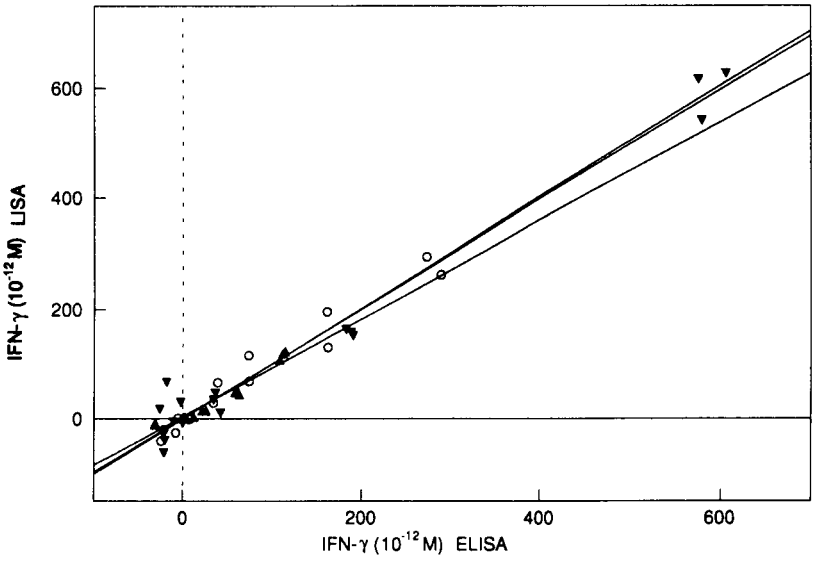

Fig. 7. Comparison of the LISA with the colorimetric ELISA, performed with the same antibodies, alkaline phosphatase and *p*-nitrophenylphosphate as substrate. Absorption is measured at 405 nm. For both assay formats IFN-γ is measured in buffer (○), plasma (▲) and supernatants (▼). Correlation coefficients r are 0.979 ($n = 14$), 0.965 ($n = 15$) and 0.988 ($n = 17$), respectively.

course can suit commonly available detection methods.

Instrumentally the 96-well microtitre plate in which multiple samples simultaneously can be processed, is retained and coupled through a sample injector to commonly available detectors, thus avoiding the use of expensive (fluorescence, chemiluminescence) or non-existent (electrochemistry) plate readers. The process can further be automated by applying an immunoassay column format instead of a microtitre plate. Some assays using this format have already been reported [11,12].

Immunoliposomes, liposomes covalently coupled to (fragments of) antibodies, could be used to eliminate the avidin step. This decreases assay time, and probably improves the overall signal, but for each antigen/analyte especially prepared liposomes will be necessary.

We thank Dr. D.J.A. Crommelin for introducing us to liposomes. M.J. van Steenbergen showed us the simplicity of preparing liposomes. We are also indebted to Dr. Y. Barenholz who encouraged us to continue in spite of experimental obstacles.

REFERENCES

1 I. Hemmilä, Clin. Chem., 31 (1985) 359.
2 H.A.H. Rongen, R.M.W. Hoetelmans, A. Bult and W.P. van Bennekom, J. Pharm. Biomed. Anal., in press.
3 H.C. Loughrey, L.S. Choi, P.R. Cullis and M.B. Bally, J. Immunol. Methods, 132 (1990) 25.
4 A.L. Plant, M.V. Brizgys, L. Locasio-Brown and R.A. Durst, Anal. Biochem., 176 (1989) 420.
5 H. Kitano, N. Kato and N. Ise, Biotechn. Appl. Biochem., 14 (1991) 192.
6 D. Monroe, J. Liposome Res., 1 (1989-90) 339.
7 M. Haga, S. Hoshino, H. Okada, N. Hazemoto, Y. Kato and Y. Suzuki, Chem. Pharm. Bull., 38 (1990) 252.
8 W.J. Litchfield, J.W. Freytag and M. Adamich, Clin. Chem., 30 (1984) 1441.
9 K. Hosada and T. Yasuda, J. Immunol. Methods, 121 (1989) 121.
10 B.S. Yu, Y.K. Choi and H. Chung, Biotech. Appl. Biochem., 9 (1987) 209.
11 A.L. Plant, L. Locascio-Brown, M.V. Brizgys and R.A. Durst, Bio/Techn., 6 (1988) 266.
12 L. Locascio-Brown, A.L. Plant, V. Horvath and R.A. Durst, Anal. Chem., 62 (1990) 2587.
13 E.F. Ullman, T. Tarnowski, P. Felgner and I. Gibbons, Clin. Chem., 33 (1987) 1579.
14 G.P. Vonk and D.B. Wagner, Clin. Chem., 37 (1991) 1519.
15 J.P. O'Connell, R.L. Campbell, B.M. Fleming, T.J. Mercolino, M.D. Johnson and D.A. McLaurin, Clin. Chem., 31 (1985) 1424.
16 R.R.C. New, in R.R.C. New (Ed.), Liposomes: A Practical Approach, Oxford University Press, Oxford, 1989, Chap. 2.
17 E. Ralston, L.M. Hjelmeland, R.D. Klausner, J.N. Weinstein and R. Blumenthal, Biochim. Biophys. Acta, 649 (1981) 133.
18 C.R. Alving, Biochim. Biophys. Acta, 1113 (1992) 307.
19 E. Claassen, Res. Immunol., 143 (1992) 235.
20 R.R.C. New, in R.R.C. New (Ed.), Liposomes: A Practical Approach, Oxford University Press, Oxford, 1989, Chap. 3.
21 D.W. Fry, J.C. White and I.D. Goldman, Anal. Biochem., 90 (1978) 809.
22 P.H. van der Meide, M. Dubbeld and H. Schellekens, J. Immunol. Methods, 79 (1985) 293.

Analytica Chimica Acta, 287 (1994) 201–210
Elsevier Science B.V., Amsterdam

Chromatographic monitoring of diuretics in urine samples using a sodium dodecyl sulphate–propanol micellar eluent

E. Bonet-Domingo, J.R. Torres-Lapasió, M.J. Medina-Hernández and M.C. García-Alvarez-Coque

Departamento de Química Analítica, Facultad de Química, Universidad de Valencia, 46100-Burjassot, Valencia (Spain)

(Received 14th June 1993; revised manuscript received 22nd October 1993)

Abstract

The effect of a varying pH, in the range 3–7, on the retention of several diuretics eluted with a sodium dodecyl sulphate (SDS) micellar mobile phase and with UV detection was studied. Significant changes in the capacity factors (k') of the diuretics bumetanide, ethacrynic acid, furosemide, probenecid and xipamide were observed. The protonation constants of these compounds were calculated from the k'–pH data. A study was also performed to select the optimum composition of the mobile phase (pH, concentration of SDS and nature and concentration of alcohol) for the separation of the above diuretics and the diuretics amiloride, bendroflumethiazide, chlorthalidone, hydrochlorothiazide, spironolactone and triamterene. Maximum resolution was achieved with a 0.042 M SDS + 4.0% propanol eluent. Limits of detection (at 254 nm) ranged between 0.082 μg ml^{-1} for xipamide and 0.76 μg ml^{-1} for ethacrynic acid. The method was applied to the study of the urinary excretion of several diuretics.

Keywords: Liquid chromatography; Diuretics; Micellar solutions; Pharmaceuticals; Urine

There is a need to develop methods of analysis to monitor diuretics in physiological fluids. These drugs are used therapeutically to enhance the renal excretion of water and electrolytes to lower the blood pressure. Diuretics are also misused in sports where weight categories are involved, to reduce weight prior to a competition or deliberately to dilute a urine specimen in an attempt to nullify a drug test.

Cooper et al. [1] indicated that the most greatest analytical problems in the detection and identification of diuretics are basically their wide variety of chemical structures, functional groups and protonation constants and their low volatility. Most of the procedures reported for the determination of diuretics in urine required solid–liquid or liquid–liquid extraction of the compounds prior to reversed-phase liquid chromatography (LC). A C_{18} stationary phase was usually used, the mobile phase being a mixture of methanol–water or acetonitrile–water with acetate and phosphate buffers, and UV detection was applied [2–6].

In recent years, interest in the use of micellar mobile phases in reversed-phase LC (micellar liquid chromatography, MLC) has grown. In such a system, complex interactions (electrostatic, hydrophobic and steric) between the solute and both the stationary and mobile phases exist [7]. The retention of the solutes is modified with the composition of the eluent: concentration of surfactant, pH, ionic strength and addition of modifiers, such as short-chain alcohols, which produce increased efficiencies [8] and decreased capacity factors [9,10]. The optimum combination of these

Correspondence to: M.C. García-Alvarez-Coque, Departamento de Química Analítica, Facultad de Química, Universidad de Valencia, 46100-Burjassot, Valencia (Spain)

SSDI 0003-2670(93)E0598-2

parameters leads to the effective separation of complex mixtures of compounds of different nature. Other advantages of MLC are the low cost, non-flammability, low toxicity and biodegradability.

One of the main appeals of MLC is the possibility of determining drugs in physiological fluids without the need for a previous separation of the proteins present in the samples [11]. This greatly accelerates the performance of the analyses. Micellar liquid chromatography has previously been applied to the determination of some diuretics in physiological samples and pharmaceutical preparations. Sentell et al. [12] reported a procedure for the determination of bumetanide in urine and serum using a C_{18} column and a 0.02 M sodium dodecyl sulphate (SDS)–10% propanol mobile phase at pH 3.5. Dadgar and Kelly [13] used a C_8 column and a 0.05 M SDS–5% propanol mobile phase at pH 4.5 to determine chlorthalidone in humane plasma. Cline Love and Fett [14] found an adequate retention for furosemide and hydrochlorothiazide using a C_{18} column and a 0.02 M Brij 35 eluent at pH 3 and a mixed 0.02 M Brij 35–0.004 M SDS eluent at pH 6.5, respectively.

In previous work, a procedure was developed for the evaluation of nine diuretics in twelve pharmaceutical preparations using a 0.05 M SDS–3% propanol eluent at pH 6.9 [15]. Later a 0.07 M SDS–0.5% pentanol mobile phase at pH 6.9 was proposed for the determination of the most retained diuretics, amiloride, bendroflumethiazide, chlorthalidone, spironolactone and triamterene, in eight pharmaceutical preparations [16]. In another paper a direct injection procedure was proposed for the determination of bendroflumethiazide and chlorthalidone in urine samples with a 0.05 M SDS–5% methanol mobile phase at pH 6.9 and 50°C [17]. Under these conditions other diuretics could not be assayed as their peaks were overlapped by the high background of the matrix at the beginning of the chromatogram, and the retentions of amiloride, spironolactone and triamterene were too long.

In this work, a study of the effect of pH on the retention of several diuretics eluted with an SDS micellar mobile phase was performed. The use of an optimized micellar mobile phase that allows the determination of diuretics of different character (high, intermediate and low efficacy diuretics) in a urine sample is proposed.

EXPERIMENTAL

Reagents

Mobile phases were prepared by mixing aqueous solutions of sodium dodecyl sulphate (99%) (Merck, Darmstadt) and a small amount of organic modifier (analytical-reagent grade, Merck). The pH was adjusted to be in the range 3–7 with 0.01 M phosphate buffer. The mobile phases were vacuum filtered through 0.47-μm nylon membranes (Micron-Scharlau, Barcelona). Nanopure deionized water (Barnstead Sybron, MA) was used to prepare the mobile phases.

Stock solutions of 100 $\mu g\ ml^{-1}$ of the diuretics were prepared. Most of the compounds were soluble in 0.1 M SDS, but it was necessary to dissolve some of them in a small volume of methanol prior to the addition of the SDS solution. Most of the compounds were kindly donated by several Spanish pharmaceutical laboratories: acetazolamide (Lederle, Madrid), amiloride (ICI Farma, Madrid), bendroflumethiazide (Davur, Madrid), bumetanide (Boehringer Ingelheim, Barcelona), chlorthalidone (Ciba-Geigy, Barcelona), ethacrynic acid (Merck, Sharp and Dohme, Madrid), furosemide (Lasa, Barcelona), hydrochlorothiazide (Gayoso Wellcome, Madrid), spironolactone (Searle, Madrid) and xipamide (Lacer, Barcelona). Probenecid and triamterene were purchased from Sigma (Buchs, Switzerland).

Apparatus

A Hewlett-Packard (Palo Alto, CA) HP 1050 chromatograph with an isocratic pump, a UV–visible detector and an HP 3396A integrator was used. Data acquisition was effected with Peak-96 software from Hewlett-Packard (Avondale, PA). The sample was injected through a Rheodyne (Cotati, CA) valve with a 20-μl loop. A Spherisorb octadecylsilane ODS-2 C_{18} (5 μm) column (120 × 4.6 mm i.d.) and a guard column of similar characteristics (35 × 4.6 mm i.d.) were used (Sharlau,

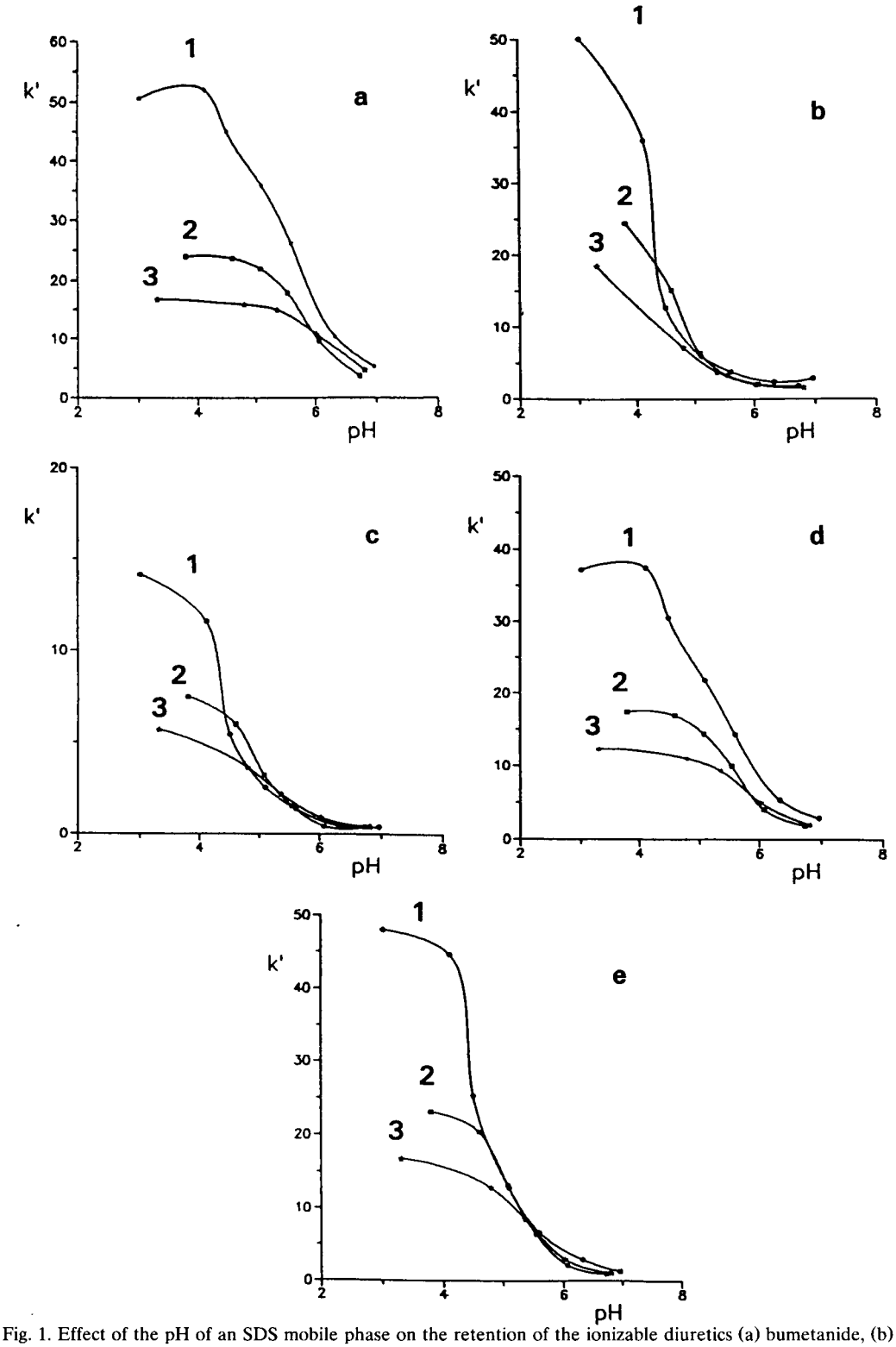

Fig. 1. Effect of the pH of an SDS mobile phase on the retention of the ionizable diuretics (a) bumetanide, (b) ethacrynic acid, (c) furosemide, (d) probenecid and (e) xipamide at three concentrations of SDS: (1) 0.05, (2) 0.1 and (3) 0.15 M.

Barcelona). The flow-rate was 1 ml min^{-1} and detection was performed at 254 nm.

RESULTS AND DISCUSSION

Effect of pH

The pH of the mobile phase is an important factor in the elution of ionizable solutes with non-polar stationary phases. The effect of a varying pH on the retention of several diuretics at different concentrations of SDS was studied in the pH range 3–7. Significant changes in retention were observed for ethacrynic acid, bumetanide, furosemide, probenecid and xipamide as the pH was modified (Fig. 1). The dependence of k' on pH at a given concentration of SDS was sigmoidal. A longer retention was observed in acidic media where the diuretics were protonated. The retention was very low at pH > 6 where the anionic form of the solutes predominated. This behaviour revealed that in acidic media the attraction of the solutes towards the surface of the stationary phase (modified by the adsorption of surfactant monomers) was greater than that towards the micelles. With increasing pH the retention decreased owing to the repulsion between the anionic deprotonated compounds and the negatively charged heads of the monomeric surfactant adsorbed on the stationary phase. It seems, therefore, that the interactions with the stationary phase were predominant. Other diuretics, with log $K > 6$–7 (acetazolamide, amiloride, bendroflumethiazide, chlorthalidone, hydrochlorothiazide, triamterene and spironolactone), did not experience changes in retention with pH.

The retention of the acid–base forms of an ionizable solute is different. At pH $\ll$ log K, the protonated species, HA, predominates and its retention will be given by

$$k'_1 = \frac{\phi(P_{SW})_{HA}}{1 + K_{HAM}[M]} \quad (1)$$

where [M] is the micelle concentration, K_{HAM} the solute–micelle association constant of the protonated species and $\phi(P_{SW})_{HA}$ its stationary phase–water partition coefficient multiplied by the phase ratio, where ϕ is the ratio of the volume of stationary phase to the volume of the mobile phase in the column [7]. Conversely, at pH $\gg$ log K, the basic species, A^-, predominates, with a retention given by

$$k'_0 = \frac{\phi(P_{SW})_{A^-}}{1 + K_{AM^-}[M]} \quad (2)$$

where K_{AM} and $\phi(P_{SW})_{A^-}$ are the corresponding parameters for the basic species. At any pH,

$$k' = k'_0\delta_0 + k'_1\delta_1 \quad (3)$$

where δ_0 and δ_1 are the molar fractions of A^- and HA, respectively. Finally,

$$k' = \frac{1}{1 + K_1 h} \cdot \frac{\phi(P_{SW})_{A^-}}{1 + K_{AM^-}[M]} + \frac{K_1 h}{1 + K_1 h} \cdot \frac{\phi(P_{SW})_{HA}}{1 + K_{AHM}[M]} \quad (4)$$

For ethacrynic acid, bumetanide, furosemide, probenecid and xipamide, k'_1 and k'_0 were estimated as the capacity factors at pH 3 and 6.9, respectively. The plot of the inverse of the capacity factors vs. the micelle concentration at these pH values gave the solute–micelle association constants and stationary phase–water partition coefficients for the protonated and basic species of these diuretics. Table 1 gives these values together with the $K_{AM}/\phi P_{SW}$ ratio. In all instances K_{AM} and ϕP_{SW} were larger at pH 3 than at pH 6.9. The change in capacity factors with variation in the concentration of SDS depends on

TABLE 1

Values of K_{AM} and ϕP_{SW} in SDS mobile phases containing 0.01 M phosphate buffer

Compound	pH 3.0			pH 6.9		
	ϕP_{SW}	K_{AM}	$K_{AM}/\phi P_{SW}$	ϕP_{SW}	K_{AM}	$K_{AM}/\phi P_{SW}$
Bumetanide	193	105	0.5	–	–	1.6
Ethacrynic acid	145	49	0.3	2.4	3.4	1.4
Furosemide	33	35	1.05	–	–	–
Probenecid	188	74	0.4	1.3	2.3	1.7
Xipamide	272	108	0.4	5.0	1.2	0.2

TABLE 2

Protonation constants (log K) of several diuretics [a]

Compound	SDS (M)	Log K
Acetazolamide	No surfactant	7.1 and 9.1
Amiloride	No surfactant	8.7
Bendroflumethiazide	No surfactant	8.5
Bumetanide	No surfactant	4.4 and 10.0
	0.05	5.22 ± 0.08
	0.10	5.64 ± 0.32
	0.15	5.68 ± 0.07
Chlorthalidone	No surfactant	9.4
Ethacrynic acid	No surfactant	3.5
	0.05	4.19 ± 0.20
	0.10	4.44 ± 0.25
	0.15	4.48 ± 0.06
Furosemide	No surfactant	3.9
	0.05	4.42 ± 0.14
	0.10	4.86 ± 0.06
	0.15	4.81 ± 0.25
Hydrochlorothiazide	No surfactant	7.0 and 9.2
Probenecid	No surfactant	3.4
	0.05	4.65 ± 0.11
	0.10	5.22 ± 0.20
	0.15	5.25 ± 0.08
Triamterene	No surfactant	6.2
Xipamide	No surfactant	4.8 and 10.0
	0.05	5.47 ± 0.10
	0.10	6.01 ± 0.31
	0.15	6.01 ± 0.11

[a] The data in a non-micellar aqueous media were taken from 12, 18 and 19.

the $K_{AM}/\phi P_{SW}$ ratio. This ratio was larger at pH 6.9 than at pH 3 for bumetanide, ethacrynic acid and probenecid, whereas for xipamide the behaviour was the reverse.

The logarithms of the protonation constants, log K, of several diuretics in a non-micellar aqueous solution are given in Table 2. The presence of micelles can modify the acid–base equilibria [20–22]. Khaledi and Rodgers [23] calculated the ionization constants of several solutes in micellar media using an expression which considered the dissociation constant in a non-micellar aqueous medium, together with the association constants to the micelle of the acid form and its conjugated base, and the micelle concentration. This calculation suffered from the disadvantage of using data at only two values of pH, where either of the acid–base species predominates, and for some solutes obtaining the acid–base constant in a non-micellar aqueous media and the association constants to the micelle of both acid–base species is not easy.

The calculation of the protonation constants may be much easier by the direct treatment of the k'–pH data in the micellar eluent. For a monoprotic acid–base system:

$$\log K = \mathrm{pH} + \log\left(\frac{k'_0 - k'}{k' - k'_1}\right) \quad (5)$$

The protonation constants of the diuretics obtained at three concentrations of SDS are given in Table 2. When the concentration of SDS was increased from 0.05 to 0.1 M, log K increased, but no further significant increase occured for 0.15 M SDS. The sign of the shift of log K depends on the values of the solute–micelle association constants of both acid–base forms. For the five diuretics considered, the shift was positive as $K_{AHM} > K_{AM}$.

Selection of the optimum mobile phase for the separation of diuretics in urine

The use of SDS micellar mobile phases, prepared without an alcohol at different pH values in the range 3–6.9, and in the presence of an alcohol at pH 6.9, did not give an adequate separation of a mixture of diuretics of high efficacy (bumetanide, ethacrynic acid, furosemide), intermediate efficacy (bendroflumethiazide, chlorthalidone, hydrochlorothiazide, xipamide) and low efficacy (amiloride, acetazolamide, spironolactone, triamterene) and the uricosuric agent probenecid, in a urine sample. A study was performed to select a suitable composition of the mobile phase (pH, concentration of SDS and nature and concentration of modifier) for the separation of these diuretics.

The profile of the background of the urine matrix depends on the composition of the mobile phase and is due to the presence of proteins and endogenous compounds. The chromatogram of the urine matrix shows a broad band due to the presence of the proteins at the solvent front and a prominent peak, together with other smaller peaks, all of them corresponding to endogenous compounds (Fig. 2a). The broad band and the

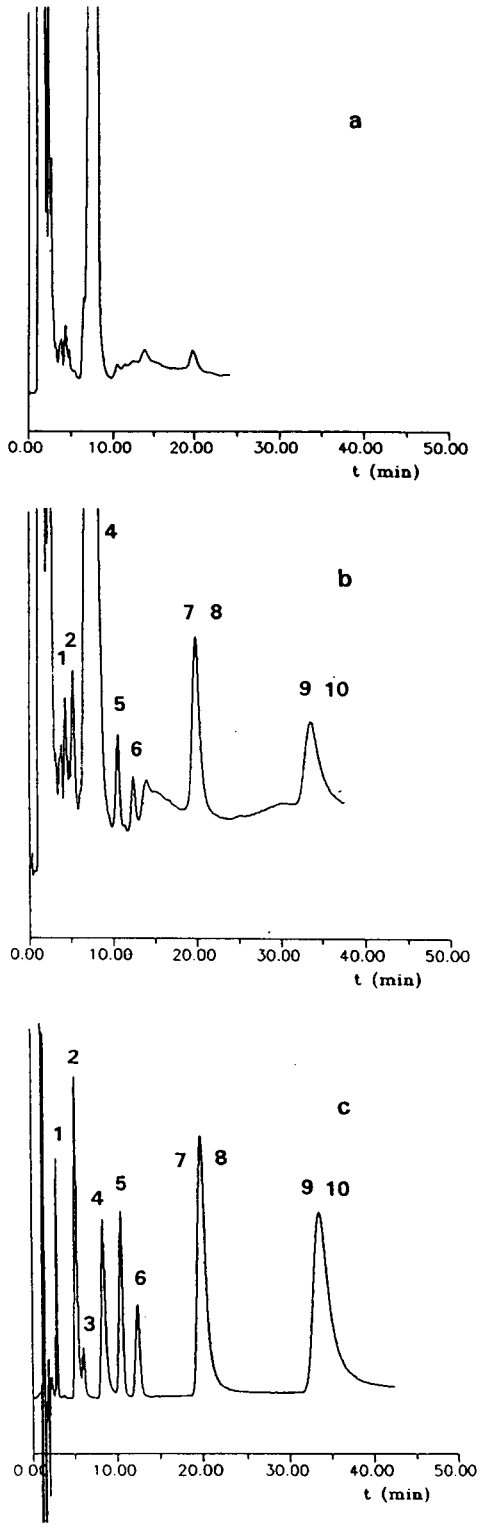

prominent peak may avoid the determination of the overlapped drugs.

In a previous paper [24] it was shown that, in a purely micellar medium of SDS, the retention of the prominent peak observed in urine samples was not large at pH 6–7 ($k' = 3$–5) and was scarcely affected by the concentration of SDS. The retention of the prominent peak in the urine matrix increased at decreasing pH, with $k' > 20$ for 0.05 M SDS at pH 3. As noted above, a similar behaviour was observed for those diuretics showing an acid–base behaviour in this pH range. Bumetanide, ethacrynic acid, furosemide, probenecid and xipamide were overlapped at pH 6–7 by the broad band of urine near the solvent front and were increasingly retained in more acidic media. Maximum separation of the peaks of these diuretics was achieved at pH 4.5. At this pH, the retention of the prominent peak of urine was $k' = 17$ for 0.05 M and $k' = 7$ for 0.15 M SDS.

The capacity factor of the most retained diuretic, spironolactone, at a relatively high concentration of SDS (0.15 M), was too high ($k' = 29$). Achievement of lower capacity factors required the presence of an organic modifier. Methanol scarcely modified the retention of the diuretics and of the urine matrix. In contrast, pentanol noticeably decreased the retention and some of the diuretics were overlapped by the background of urine. Finally, propanol was found to be appropriate as it had an intermediate behaviour [15,24]. However, acetazolamide and hydrochlorothiazide appeared at the solvent front together with the broad band of urine for all the mobile phases considered.

Optimization of the composition of the mobile phase (SDS and propanol concentration) required an adequate description of the retention

Fig. 2. Experimental chromatograms of (a) urine matrix, (b) a urine sample spiked with a mixture of ten diuretics (1 μg ml^{-1}) and (c) an aqueous solution of the same diuretics, eluted with the optimized mobile phase (0.042 M SDS–4% propanol at pH 4.5). Peaks: 1 = furosemide; 2 = chlorthalidone; 3 = ethacrynic acid; 4 = bendroflumethiazide; 5 = probenecid; 6 = bumetanide; 7 = amiloride; 8 = xipamide; 9 = spironolactone; 10 = triamterene.

behaviour of the drugs. It has been reported [25] that the retention in a hybrid mobile phase may be described by the equation

$$1/k' = A\mu + B\varphi + C\mu\varphi + D \quad (6)$$

where μ is the total concentration of surfactant and φ is the volume fraction of alcohol. The retention equations were obtained for each diuretic using the capacity factors obtained in the six mobile phases shown in Table 3.

The normalized product of the resolution was taken as the optimization criterion [26]:

$$r = \prod_{i=1}^{n=1} \frac{S_{i,i+1}}{\left(\Sigma \frac{S_{i,i+1}}{n-1}\right)^{n-1}} \quad (7)$$

TABLE 3

Capacity factors (k') obtained in mobile phases of SDS and propanol at pH 4.5

Compound	SDS (M)					
	0.05	0.05	0.07	0.03	0.03	0.05
	Propanol (%)					
	2	4	2	1	2	0
Acetazolamide	1.07	0.84	1.04	1.33	1.13	1.52
Amiloride	19.00	16.61	16.36	38.60	32.89	26.48
Bendroflumethiazide	10.19	8.56	7.51	19.27	16.28	14.32
Bumetanide	17.96	13.13	13.68	37.00	29.23	30.50
Chlorthalidone	5.36	4.71	4.92	11.77	9.22	9.88
Ethacrynic acid	8.17	6.14	7.14	14.55	12.29	12.69
Furosemide	3.90	2.93	3.35	6.66	5.67	5.45
Hydrochlorothiazide	1.18	0.97	1.04	1.63	1.40	1.53
Probenecid	14.80	16.63	12.64	28.0	22.25	25.30
Spironolactone	32.25	26.23	29.31	94.38	61.21	45.02
Triamterene	35.47	28.83	24.34	74.16	59.48	58.35
Xipamide	26.72	19.72	20.34	52.90	41.86	45.02

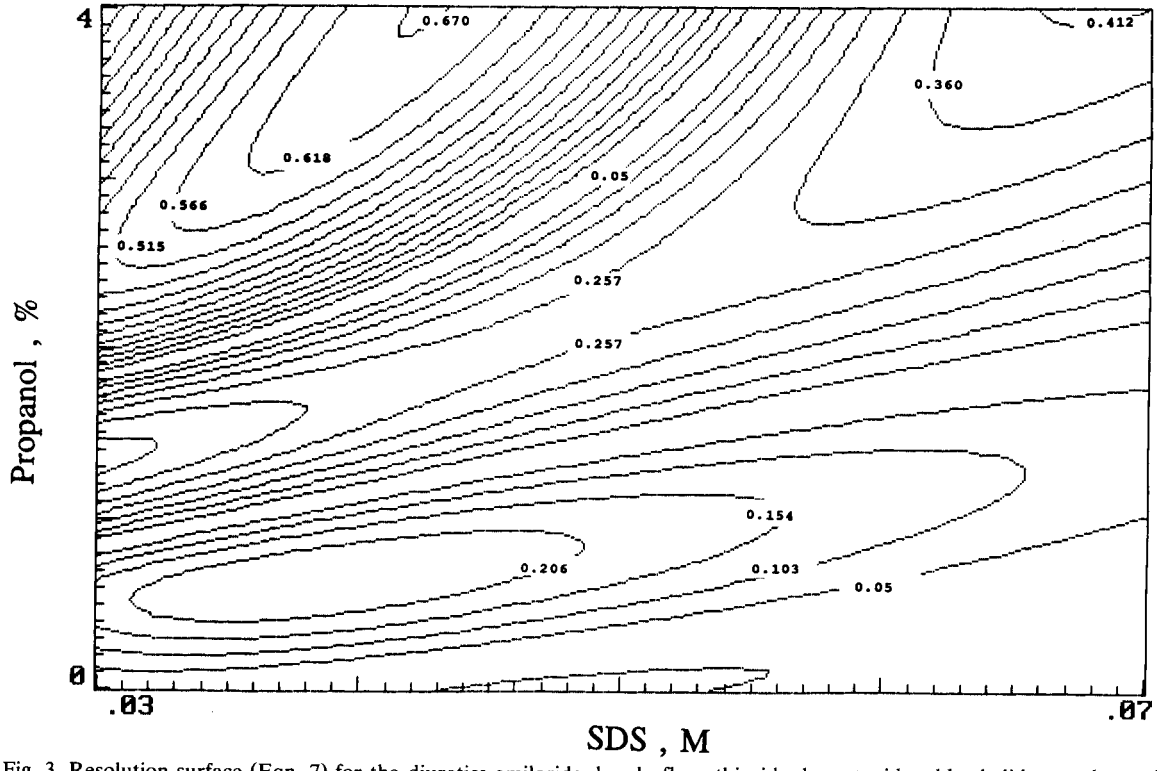

Fig. 3. Resolution surface (Eqn. 7) for the diuretics amiloride, bendroflumethiazide, bumetanide, chlorthalidone, ethacrynic acid, furosemide, probenecid, spironolactone, triamterene and xipamide as a function of the concentration of surfactant and modifier in the mobile phase (pH = 4.5).

where $S_{i,i+1}$ is the separation factor for two solutes:

$$S_{i,i+1} = \frac{t_{i+1} - t_i}{t_{i+1} + t_i} \quad (8)$$

The resolution surface was drawn for acetazolamide, amiloride, bendroflumethiazide, bumetanide, chlorthalidone, ethacrynic acid, hydrochlorothiazide, probenecid, spironolactone, triamterene and xipamide as a function of the concentration of surfactant and modifier (Fig. 3). The maximum resolution corresponded to a 0.042 M SDS–4.0% propanol eluent. Figure 2 shows the experimental chromatogram of a urine sample spiked with a mixture of the ten diuretics together with a similar chromatogram obtained in an aqueous solution with the optimized mobile phase. The retention times for both chromatograms were similar. The peaks of amiloride and xipamide on the one hand, and triamterene and spironolactone on the other, appeared overlapped in the chromatograms. The peak of bendroflumethiazide was overlapped with the prominent peak of urine.

Figures of merit

The calibration graphs of each diuretic were obtained by triplicate injection of spiked samples with various concentrations of the analyte. The concentration range was 2–15 μg/ml. The regression coefficients were always > 0.99.

The limits of detection (LODs) were calculated from the standard deviation of fivefold injections of 1 μg ml^{-1} solutions of the diuretics (Table 4). The LODs ranged between 0.082 μg ml^{-1} for xipamide and 0.76 μg ml^{-1} for ethacrynic acid. Amiloride, bendroflumethiazide, bumetanide, furosemide and triamterene are fluorescent and measurement of fluorescence at se-

TABLE 4

Limits of detection of the diuretics in a urine sample [a]

Compound	LOD (μg ml^{-1})	Compound	LOD (μg ml^{-1})
Amiloride	0.76	Probenecid	0.21
Bumetanide	0.39	Spironolactone	0.39
Chlorthalidone	0.29	Triamterene	0.21
Ethacrynic acid	0.76	Xipamide	0.082
Furosemide	0.35		

[a] Mobile phase: 0.042 M SDS–4% propanol at pH 4.5.

TABLE 5

Reproducibility and accuracy in intra- and inter-day assays

Compound	Taken (μg ml^{-1})	Found [a] (μg ml^{-1})	Mean (μg ml^{-1})	R.S.D. (%)
Amiloride	5.22	5.18 ± 0.03		
		5.21 ± 0.03		
		5.28 ± 0.07	5.23 ± 0.05	1.0
		5.27 ± 0.03		
		5.19 ± 0.04		
Bumetanide	5.32	5.19 ± 0.09		
		5.21 ± 0.03		
		5.62 ± 0.07	5.2 ± 0.3	5.8
		4.98 ± 0.11		
		4.91 ± 0.14		
Clorthalidone	5.32	5.54 ± 0.07		
		5.07 ± 0.11		
		5.20 ± 0.11	5.2 ± 0.2	3.8
		5.16 ± 0.06		
		5.02 ± 0.06		
Ethacrynic acid	5.05	5.30 ± 0.02		
		5.06 ± 0.02	5.1 ± 0.3	5.9
		4.77 ± 0.03		
		5.42 ± 0.01		
Furosemide	5.80	6.47 ± 0.19		
		6.45 ± 0.15		
		6.88 ± 0.21	6.6 ± 0.2	3.0
		6.40 ± 0.10		
		6.55 ± 0.08		
Probenecid	5.80	4.79 ± 0.13		
		4.67 ± 0.05		
		4.89 ± 0.10	4.7 ± 0.2	4.2
		4.59 ± 0.09		
		4.40 ± 0.15		
Spironolactone	5.22	5.34 ± 0.01		
		5.91 ± 0.02		
		6.02 ± 0.03	5.9 ± 0.3	5.1
		6.04 ± 0.02		
		5.95 ± 0.01		
Triamterene	5.37	4.93 ± 0.03		
		6.07 ± 0.08		
		5.81 ± 0.02	5.6 ± 0.4	7.1
		5.74 ± 0.05		
		5.64 ± 0.05		
Xipamide	5.17	5.10 ± 0.08		
		5.40 ± 0.04		
		5.51 ± 0.04	5.3 ± 0.2	3.8
		4.97 ± 0.07		
		5.40 ± 0.06		

[a] Each mean and standard deviation correspond to five injections of the samples performed on the same day (intra-day assay).

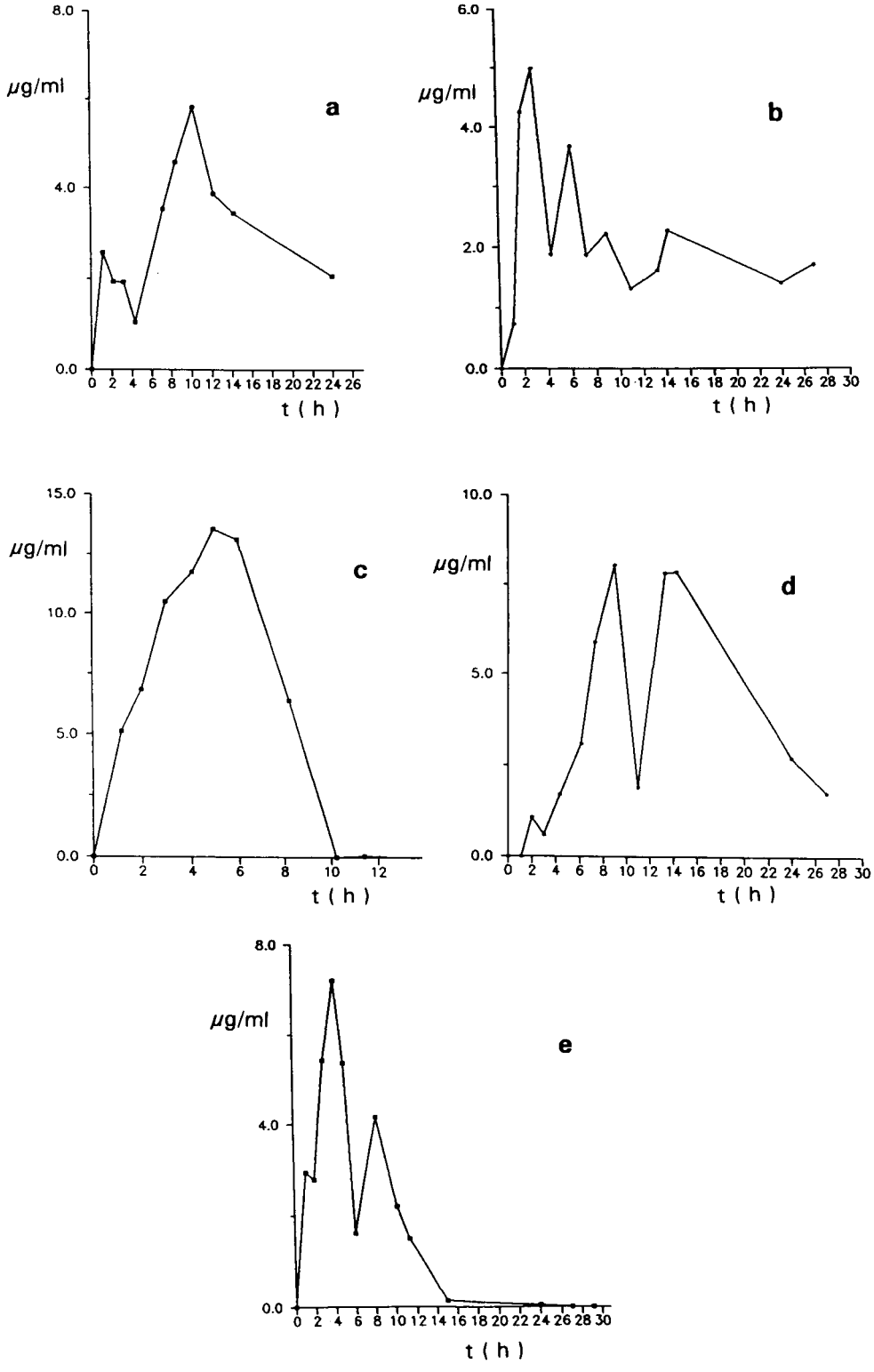

Fig. 4. Study of the urinary excretion of some diuretics after oral administration (oral dose given in parentheses): (a) amiloride (5 mg); (b) chlorthalidone (50 mg); (c) spironolactone (50 mg); (d) furosemide (77.6 mg); (e) triamterene (25 mg). Mobile phase: 0.042 M SDS–4% propanol at pH 4.5.

lected wavelengths can decrease the limits of detection of these diuretics.

The intra- and inter-day assay precision and accuracy for the determination of the diuretics are given in Table 5. For the intra-day assay five spiked samples of urine containing 5 μg ml^{-1} of a diuretic were analysed. For the inter-day assay, the same determination was performed during four or five days.

Application of the method to the study of the urinary excretion of diuretics

Urinary excretion studies were performed with normal healthy volunteers, who were given single oral doses of amiloride (5 mg), chlorthalidone (50 mg), furosemide (77.6 mg), hydrochlorothiazide (50 mg), spironolactone (50 mg) and triamterene (25 mg). A sample was collected just before the administration of the medicaments, to be used as the blank. Other urine samples were collected at appropriate time intervals post-dose and were refrigerated at 4°C until analysed.

Figure 4 shows the concentrations of amiloride, chlorthalidone, spironolactone, furosemide and triamterene during urinary excretion. The maximum excreted concentration, c_{max}, and the time at which this maximum value was reached, t_{max}, were $c_{max} = 5.8$ μg ml^{-1}, $t_{max} = 10.25$ h for amiloride, $c_{max} = 5.0$ μg ml^{-1}, $t_{max} = 3.0$ h for chlorthalidone, $c_{max} = 8.5$ μg ml^{-1}, $t_{max} = 8.0$ h for spironolactone, $c_{max} = 13.5$ μg ml^{-1}, $t_{max} = 5.25$ h for furosemide and $c_{max} = 7.2$ μg ml^{-1}, $t_{max} = 4.2$ h for triamterene. These data are similar to those obtained by Cooper et al. [1] using a reversed-phase LC procedure with an acetonitrile–water (0.05 M phosphate buffer) solvent gradient and previous extraction of the diuretics with ethyl acetate in acidic or basic media.

This work was supported by the DGICYT, Project PB91/629.

REFERENCES

1 S.F Cooper, R. Massé and R. Dugal, J. Chromatogr., 489 (1989) 65.
2 P.J.M. Guelen, A.M. Baars, T.B. Vree, A.J. Nijkerk and J.M. Vermeer, J. Chromatogr., 181 (1980) 497.
3 M.S. Yip, P.E. Coates and J.J. Thiessen, J. Chromatogr., 307 (1984) 343.
4 K.B. Alton, D. Desrivieres and J.E. Patrick, J. Chromatogr., 374 (1986) 103.
5 B. Ameer and M.B. Burlingame, Anal. Lett., 21 (1988) 1589.
6 F.G.M. Russel, Y. Tan, J.J.M. Van Meijel, F.W.J. Gribnau and C.A.M. Van Ginneken, J. Chromatogr., 496 (1989) 234.
7 M.J. Medina Hernández and M.C. García Alvarez-Coque, Analyst, 117 (1992) 831.
8 M.F. Borgerding, F.H. Quina, W.L. Hinze, J. Bowermaster and H.M. McNair, Anal. Chem., 60 (1988) 2520.
9 M.G. Khaledi, Anal. Chem., 60 (1988) 876.
10 M.G. Khaledi, J.K. Strasters, A.H. Rodgers and E.D. Breyer, Anal. Chem., 62 (1990) 130.
11 M.J. Koenigbauer, J. Chromatogr., 531 (1990) 79.
12 K.B. Sentell, J.F. Clos and J.G Dorsey, Biochromatography, 4 (1989) 35.
13 D. Dadgar and M.T. Kelly, Analyst, 113 (1988) 1223.
14 L.J. Cline Love and J. Fett, J. Pharm. Biomed. Anal., 9 (1991) 323.
15 E. Bonet Domingo, M.J. Medina Hernández, G. Ramis Ramos and M.C. García Alvarez-Coque, Analyst, 117 (1992) 843.
16 E. Bonet Domingo, M.J. Medina Hernández, and M.C. García Alvarez-Coque, J. Pharm. Biomed. Anal., 11 (1993) 711.
17 E. Bonet Domingo, M.J. Medina Hernández, G. Ramis Ramos and M.C. García Alvarez-Coque, J. Chromatogr., 582 (1992) 189.
18 M. Windholz (Ed.), The Index Merck, Merck, New York; 10th ed. 1983.
19 C. Hansch, in P.G. Sammes and J.B. Taylor (Eds.), Comprehensive Medicinal Chemistry, Vol. 6, Pergamon Press, Oxford, 1990.
20 E. Pelizzetti and E. Pramauro, Anal. Chim. Acta, 169 (1985) 1.
21 M.J. Rosen, Surfactants and Interfacial Phenomena, Wiley, New York, 1978.
22 K.L. Mittal (Ed.), Micellization, Solubilization and Microemulsions, Plenum, New York, 1977.
23 M.G. Khaledi and A. Rodgers, Anal. Chim. Acta, 239 (1990) 121.
24 E. Bonet Domingo, M.J. Medina Hernández and M.C. García Alvarez-Coque, Quim. Anal., in press.
25 J.R. Torres Lapasió, R.M. Villanueva Camañas, J.M. Sanchis Mallols, M.J. Medina Hernández and M.C. García Alvarez-Coque, J. Chromatogr., 639 (1993) 87.
26 A.C.J.H. Drouen, H.A.H. Billiet, P.J. Schoenmakers and L. de Galan, Chromatographia, 16 (1982) 48.

Analytica Chimica Acta, 287 (1994) 211–214
Elsevier Science B.V., Amsterdam

Coulometric detection of peptides by reversed-phase liquid chromatography with a solid-phase reactor containing copper metal

Hiroaki Kubo

School of Pharmaceutical Sciences, Kitasato University, 5-9-1, Shirokane, Minato-ku, Tokyo 108 (Japan)

(Received 26th July 1993; revised manuscript received 19th October 1993)

Abstract

A general reversed-phase liquid chromatographic method with coulometric detection for the determination of peptides has been established using a solid-phase reactor containing copper metal. The method is based on the formation of electrochemically oxidizable copper(II)–peptide complexes by the reaction of peptides with copper(II) ions in an alkaline mobile phase through the solid-phase reactor. Di- and tripeptides used as model compounds (6 species) are separated on a column contained C_{18}-bonded vinyl alcohol copolymer gel (Asahipak ODP-50, 5μm, 250 mm × 6.0 mm i.d.) and an alkaline mobile phase (pH 11.0, 40 mM borate buffer). A detection limit of 5 ng was obtained for alanylalanylalanine.

Keywords: Coulometry; Liquid chromatography; Copper; Peptides; Solid-phase reactor

The determination of peptides in biological matrices is of great interest in medicine, biology and the pharmaceutical industry. Liquid chromatography (LC) has become the analytical method of choice for the determination of peptides. The determination of peptides has been developed by both reversed-phase and ion-exchange chromatography [1–3]. Eluting peptides can be determined by UV detection commonly at 210 nm, pre- or post-column fluorescence detection and mass spectrometry. UV detection is not specific for peptides. Fluorescence detection is highly sensitive but original peptides have to be converted to fluorescing derivatives. Mass spectrometry is also highly sensitive, but also more expensive.

Correspondence to: H. Kubo, School of Pharmaceutical Sciences, Kitasato University, 5-9-1, Shirokane, Minato-ku, Tokyo 108 (Japan).

Recently, electrochemical detection of peptides using the classical biuret reaction has been reported [4–6]. The system is based on the reaction of peptides with copper(II) ions to form copper(II)–peptide complexes [7], which are then detected either amperometrically or coulometrically. These methods require an additional pump or a device for delivering the biuret reagent.

This paper reports the determination of peptides using an alkaline mobile phase, a solid-phase reactor containing copper metal and a coulometric detector, which does not require the biuret reagent and an additional pump or a delivering device. The method is based on the formation of the copper(II)–peptide complexes by the reaction of peptides with copper(II) ions dissolved in the alkaline mobile phase through the solid-phase reactor. Alanylalanylalanine and glycylleucine were used as the model compound for the reaction.

SSDI 0003-2670(93)E0595-X

EXPERIMENTAL

Apparatus

The chromatographic system (Fig. 1) consisted of a Model 576 LC pump (GL Sciences, Tokyo), a Rheodyne 9125 injector with a 5-μl sample loop, and an Asahipak ODP-50 column (5 μm, 250 mm × 6 mm i.d., Asahi Chemical, Kawasaki). The solid-phase reactor was inserted between the Asahipak ODP-50 column and a detector. The detector was an ESA Model 5100A (Environmental Sciences Assoc., Bedford, MA) dual-electrode coulometric detector. The guard cell was an ESA Model 5020 and the detector cell an ESA Model 5010. The guard cell voltage was set at +0.85 V, detector 1 of the dual-electrode analytical cell was set at +0.40 V to indicate interfering peaks, and detector 2 at +0.80 V to detect the complexes. The signal from detector 2 was recorded with an Unicorder U-228 chart recorder (Nihon Denshi Kagaku, Kyoto).

For the solid-phase reactor high-purity 100–200-mesh copper particles (Kanto Chemical, Tokyo) were dry-packed into 10 mm × 4 mm i.d. stainless-steel tube, using 3-μm stainless-steel frits.

Reagents

Prolylglycine (PG), glycylproline (GP), glycylleucine (GL), methionylglycine (MG), glycylglycylglycine (GGG), alanylalanylalanine (AAA) and prolylglycylglycine (PGG) were obtained from Sigma (St. Louis, MO). Water used was of liquid chromatographic grade. All chemicals were of reagent grade.

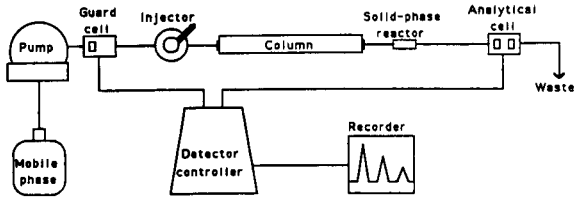

Fig. 1. Schematic diagram of the apparatus. Mobile phase: 40 mM borate buffer (pH 11.0, flow-rate: 1 ml min^{-1}); column: Asashipak ODP-50 (5 mm, 250 mm×6 mm i.d.); solid-phase reactor: stainless steel tube (10 mm×4 mm i.d.) containing copper particles (100–200 mesh); guard cell: potential of +0.85 V; analytical cell: detector 1 (+0.40 V), detector 2 (+0.80 V).

The mobile phase was 40 mM borate buffer adjusted to pH 11.0 with 6 M sodium hydroxide. The mobile phase was filtered through a 0.22-μm filter (Fuji Photo Film, Tokyo).

Optimization of the reaction

The optimum reaction conditions for electrochemical detection were examined by injecting 5 μl of the standard solution of AAA (50 ng) or GL (100 ng) into the chromatograph, with a mobile phase flow rate of 1.0 ml min^{-1}.

The pH of the borate buffer was adjusted with 6 M sodium hydroxide.

RESULTS

Applied potential

A hydrodynamic voltammogram of the copper(II)–peptide complexes is shown in Fig. 2. The peak current for AAA was obtained at +0.75 V and that for GL at +0.80 V. When the applied potential was larger than +0.80 V, the background current response increased. Therefore, the detection was performed with electrode 1 at +0.40 V to screen out interfering peaks, and electrode 2 at +0.80 V to detect the complexes. The guard cell was set at +0.85 V to oxidize the reducible components in the mobile phase.

Concentration of supporting electrolyte in mobile phase

Figure 3 shows the effect of sodium tetraborate at a concentration of 10–100 mM. The peak current responses for AAA and GL were maximum at 40 mM sodium tetraborate concentration. Therefore, the optimal final concentration of sodium tetraborate was chosen as 40 mM.

pH of mobile phase

Figure 4 shows the effect of pH in the range of 9.0 to 13.0 on the peak current response. Optimum pH occurred at 11.0 for GL and 11.5 for AAA. A pH of more than 11.5 increased the background current response. Therefore, a mobile phase of pH 11.0 was used.

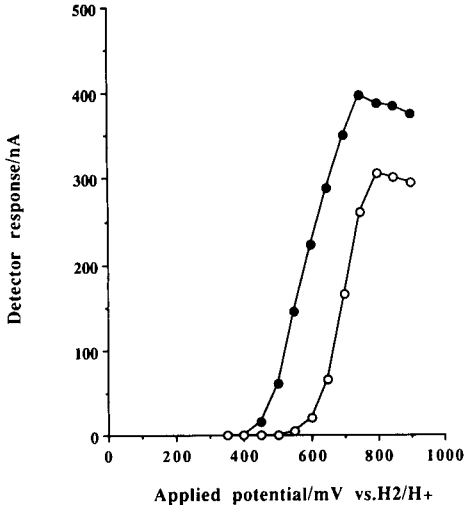

Fig. 2. Hydrodynamic voltammogram of copper(II)–peptide complexes formed by copper(II) ions and alanylalanylalanine (●) and glycylleucine (○).

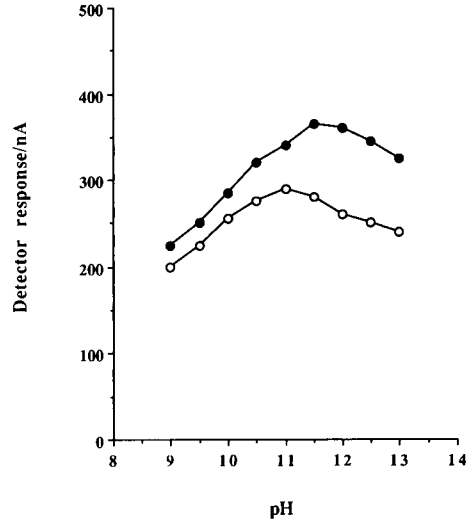

Fig. 4. Effect of pH on the peak current response of alanylalanylalanine (●) and glycylleucine (○).

Chromatographic separation and quantitative response

Figure 5 shows a chromatogram obtained from an authentic mixture of 100 ng of GGG, AAA, PG, PGG, MG and GL. Complete separation of the peptides was achieved within 15 min. GP did not appear in the chromatogram at the retention time that had been found with UV detection.

A linear regression analysis of the calibration curve yielded the equation $Y = 1.92X - 1.30$ ($r = 0.999$) for AAA and $Y = 0.619X - 3.05$ ($r = 0.999$) for GL. The peak current responses, nA, (Y)

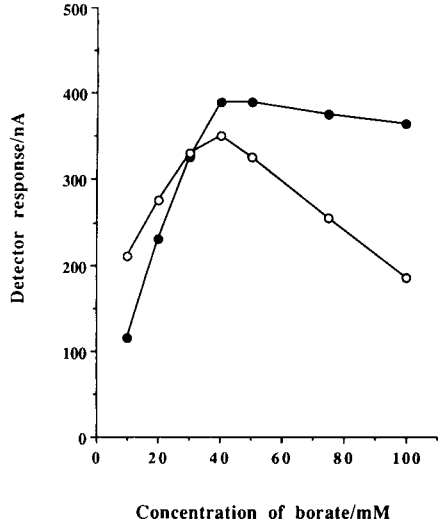

Fig. 3. Effect of sodium tetraborate concentration on the peak current response of alanylalanylalanine (●) and glycylleucine (○).

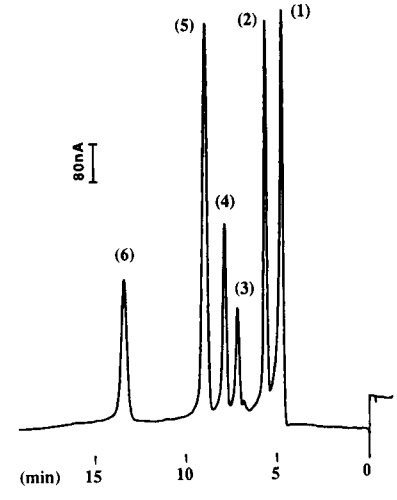

Fig. 5. Chromatogram obtained with a mixture of glycylglycylglycine (1), alanylalanylalanine (2) prolylglycine (3), prolylglycylglycine (4) methionylglycine (5) and glycylleucine (6), each 100 ng.

were related to the absolute quantities, 10 to 100 ng, (X) with high linearity.

The limits of detection for AAA and GL were 5 ng ($S/N = 3$) and 10 ng ($S/N = 3$), respectively.

Ten injections of the peptide mixture gave the following coefficients of variation for peak heights of 30 ng: GGG (1.90%), AAA(1.95%), PG (1.98%), PGG (2.01%), MG (2.32%) and GL (2.48).

DISCUSSION

The method described here was based on the in-line reaction of peptides with copper(II) ions to yield oxidizable copper(II)–peptides complexes. The copper(II) ions were formed in the alkaline mobile phase when passing through the solid-phase reactor containing fine-particle metallic copper. The complexes were then detected electrochemically. The difference in peak currents for GL and AAA is explained by the number of deprotonated-peptide nitrogen bondings in the copper(II)–peptides complexes [8]. GP does not form complexes because it is unable to form a hydrogen bridge with the peptide nitrogen. Therefore, GP was not detected electrochemically.

The limit of detection for the peptides may be improved when non-pulsating pumps are used. The use of phosphate or carbonate buffers may also increase the detection limit, because these buffers increase the sensitivity for amperometric detection with a copper electrode [9–11].

When the solid-phase reactor was removed from the system, the response of the detector for the peptides gradually decreased, because the copper(II) deposited onto the porous graphite electrode in the detector dissolves in the alkaline mobile phase.

Besides peptides, amino acids containing a phenol, indole or sulfur group were detected when a high potential is applied, but other amino acids were not detected. Since these amino acids are separated from peptides, the detection of peptides on a reversed-phase column is not a problem. As shown in Fig. 5, the peptide (MG) containing oxidizable sulfur exhibits a high sensitivity.

This method should aid the research of peptide and protein chemistry.

REFERENCES

1 M. Hermodson and W.C. Mahoney, Methods Enzymol., 91 (1983) 352. D.K. Aromatorio, J. Parker and W.E. Brown, Methods Enzymol., 91 (1983) 384.
2 K. Stulik, V. Pacakova and G. Jokuszies, J. Chromatogr., 436 (1988) 334.
3 S.-C. Chou and A. Goldstein, Biochem. J., 75 (1960) 109.
4 A.M. Warner and S.G. Weber, Anal. Chem., 61 (1989) 2664.
5 H. Tsai and S.G. Weber, J. Chromatogr., 515 (1990) 451.
6 H. Kubo, Y. Huang and T. Kinoshita, Anal. Sci., 6 (1990) 265.
7 D.W. Margerum, Pure Appl. Chem., 55 (1983) 23.
8 F.P. Bossu, K.L. Chellappa and D.W. Margerum, J. Am. Chem. Soc., 99. (1977) 2195.
9 W.Th. Kok, H.B. Hanekamp, P. Bos and R.W. Frei, Anal. Chim. Acta, 142 (1982) 31.
10 W.Th. Kok, U.A.Th. Brinkman and R.W. Frei, J. Chromatogr., 256 (1983) 17.
11 K. Stulik, V. Pacakova, K. Le and B. Hennissen, Talanta, 35 (1988) 455.

Analytica Chimica Acta, 287 (1994) 215–221
Elsevier Science B.V., Amsterdam

Alkoxyphenylglyoxals as fluorogenic reagents selective for guanine and its nucleosides and nucleotides in liquid chromatography

Yoshihito Ohba, Masaaki Kai, Hitoshi Nohta and Yosuke Ohkura

Faculty of Pharmaceutical Sciences, Kyushu University 62, Maidashi, Higashi-ku, Fukuoka 812 (Japan)

(Received 11th August 1993; revised manuscript received 19th October 1993)

Abstract

Glyoxal analogues which have a phenyl moiety substituted with electron-donating methoxyl group(s) or a methylenedioxyl group, react selectively with guanine and its nucleosides and nucleotides in phosphate buffer (pH 7.0) at 37°C for 5–7 min to give the corresponding fluorescent derivatives. The derivatives can be separated by reversed-phase liquid chromatography. 3,4-Dimethoxyphenylglyoxal is most sensitive; the detection limits ($S/N = 3$) for guanine and its nucleosides and nucleotides vary in the range 40–400 fmol per injection volume depending on the guanine-related compounds.

Keywords: Liquid chromatography; Fluorimetry; Alkoxyphenylglyoxals; Guanine; Nucleosides; Nucleotides; Phenylglyoxal; Pre-column derivatization

Nucleic acid bases and nucleos(t)ides have been generally measured by liquid chromatography (LC) with spectrophotometric, electrochemical or fluorometric detection. The spectrophotometric methods [1–5] are based on non-specific ultraviolet absorption of nucleic acid bases. The electrochemical methods [6–8] were studied for the chromatographic determination of guanine and its nucleotides which are susceptible to electrochemical oxidation at a high applied potential (+0.95 V vs. Ag/AgCl). Although the methods can detect the nucleotides at picomole level, there are several problems owing to the disturbance with detectable biogenic compounds and the unstable noise level depending on composition of the mobile phase for LC. Most of the fluorometric methods [9,10] are based on weak native fluorescence from nucleic acid bases. However, the bases fluoresce under strongly acidic or basic conditions only.

On the other hand, fluorogenic reagents which show a high molecular recognition specificity to one of the nucleic acid bases and/or nucleos(t)ides may be available for the selective and sensitive determination of nucleic acid constituents. Hitherto, a few fluorogenic reagents (e.g., glyoxal hydrate trimer [11], chloroacetaldehyde [12–14] and bromoacetaldehyde [15,16]) have been used for the selective determination of adenine and its nucleos(t)ides. We already reported that phenylglyoxal (PGO) can be a selective fluorogenic reagent for guanine and its nucleos(t)ides in LC, which reacts under mild conditions [17,18].

In the present study, glyoxal (GO) and methylglyoxal (MGO) as aliphatic glyoxals, and 3,4-dimethoxyphenylglyoxal (DMPG) and 3,4-methylenedioxyphenylglyoxal (MDPG) and 4-methoxyphenylglyoxal (MPG) and 3,4,5-trimethoxyphenylglyoxal (TMPG) as PGO analogues substituted

Correspondence to: Y. Ohkura, Faculty of Pharmaceutical Sciences, Kyushu University 62, Maidashi, Higashi-ku, Fukuoka 812 (Japan).

SSDI 0003-2670(93)E0596-Y

with electron-donating alkoxyl group(s) were subjected to the screening of fluorogenic reagents for the guanine and its nucleos(t)ides, in the hope that more sensitive pre-column fluorescence derivatization reagents in LC might be developed. All the PGO analogues were found to be reactive to the guanine-related compounds, and DMPG, MDPG and MPG appeared to be more sensitive than PGO. Guanosine 5′-monophosphate (GMP), guanosine 3′,5′-cyclic monophosphate (cGMP), guanine and deoxyguanosine were used as model compounds to establish the optimum reaction conditions. DMPG, selected as the most sensitive reagent, was further studied for the chromatographic determination of guanine and its nucleos(t)ides.

EXPERIMENTAL

Reagents and solutions

Nucleic acid bases, nucleosides and nucleotides such as guanosine 5′-triphosphate (GTP), guanosine 5′-diphosphate (GDP), 2′-deoxyGTP (dGTP), 2′-deoxyGDP (dGDP), 2′-deoxyGMP (dGMP), adenosine 5′-triphosphate (ATP), adenosine 5′-diphosphate (ADP), adenosine 5′-monophosphate (AMP), cytidine 5′-triphosphate (CTP), cytidine 5′-diphosphate (CDP), cytidine 5′-monophosphate (CMP), 2′-deoxyATP (dATP), 2′-deoxyADP (dADP) and 2′-deoxyAMP (dAMP) were purchased from Seikagaku Kogyo (Tokyo). Aqueous solutions of GO and MGO were obtained from Sigma (St. Louis, MO). PGO monohydrate was a product of Aldrich (Milwaukee, WI). DMPG, MDPG, MPG and TMPG were prepared as described previously [19]. Other chemicals were of analytical reagent grade. For the screening experiment, GO and MGO (0.1 M each) solutions were diluted with water, and the alkoxyphenylglyoxals (0.1 M each) were dissolved in dimethyl sulfoxide (DMSO). For the other experiments, DMPG, MDPG and MPG (0.1 M each) were dissolved in DMSO–water (2:3, 3:2 and 2:3, v/v, respectively). The standard solutions (2.0 μmol ml^{-1} each) of guanine and its

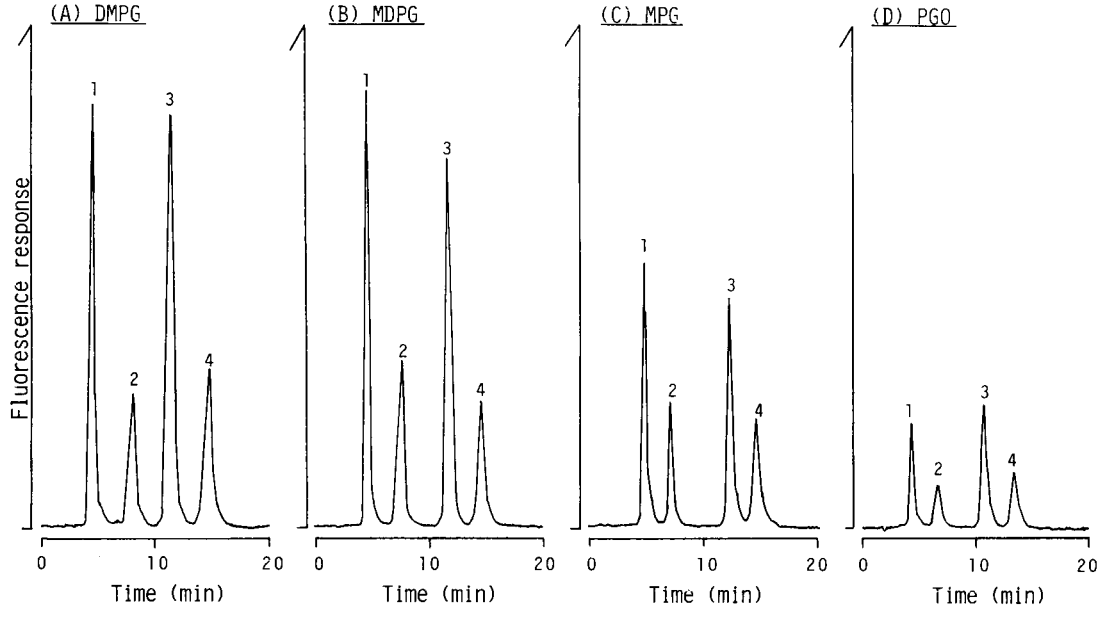

Fig. 1. Chromatograms of a standard mixture of GMP, cGMP, guanine and deoxyguanosine obtained with isocratic elution. A mixture (50 μl) of the compounds (10 nmol ml^{-1} each) was treated according to the derivatization procedure, followed by LC. Ratios (v/v) of acetonitrile, tetrahydrofuran, 50 mM phosphate buffer (pH 6.0) and water in the mobile phases: A = 4:5:25:66; B = 5:5:25:65; C = 7:5:25:63; D = 5:5:25:65. Peaks: 1 = GMP; 2 = cGMP; 3 = guanine; 4 = deoxyguanosine.

nucleos(t)ides were prepared in methylcellosolve–water (7 : 3, v/v) and then stored at −20°C. The solutions were diluted to appropriate concentrations with water and used within a day.

Procedure for screening of glyoxal analogues

A 100-μl portion of GMP, cGMP, guanine or deoxyguanosine (50 nmol ml^{-1} each) (or water for blank) was mixed with 100 μl of 0.1 M glyoxal reagent and 200 μl of 25 mM phosphate buffer (pH 6.0). The mixture was warmed at 37°C for 15 min. Uncorrected fluorescence spectra and intensities of the reaction mixtures were measured with a Hitachi MPF-4 spectrofluorometer using semimicro quartz cells (10 mm length parallel to the excitation beam, 3 mm width parallel to the emission beam, 1 ml); spectral bandwidths of 10 nm were used in both the excitation and emission monochromators.

Derivatization procedure (LC sample preparation)

A 50-μl portion of sample solution was mixed with 50 μl each of 0.1 M DMPG, MDPG or MPG, 30 mM phosphate buffer (pH 7.0) and water. The mixture was warmed at 37°C for 5 min for DMPG and MPG reagents, and for 7 min for MDPG reagent. A 20-μl portion of the final reaction mixture was used for LC. When PGO was used as a reagent for comparison, the sample solution was treated in the same way as that for the procedure for screening of glyoxal analogues.

LC system and operating conditions

The LC system consisted of a Yokogawa LC100P high-performance LC pump (for isocratic elution) or two of the same pumps (for stepwise and gradient elution) equipped with a Rheodyne Model 7125 syringe-loading sample injection valve (20-μl loop) and a Hitachi F-1000 spectrofluorometer fitted with a 12-μl flow cell. The column was TSK-gel ODS-120T (150 × 4.6 mm i.d., particle size 5 μm) (Tosoh; Tokyo). The column was kept at ambient temperature (24 ± 4°C). The mobile phase was a mixture of acetonitrile, tetrahydrofuran, 50 mM phosphate buffer (pH 6.0) and water (for the ratios of the solvents in isocratic and gradient elutions, see Figs. 1 and 5, respectively) and the flow-rate was 1.0 ml min^{-1}. The fluorescence intensity of the column eluate was monitored at 510 nm emission and 400 nm excitation for the DMPG, MDPG and MPG derivatives, and at 510 nm emission and 365 nm excitation for the PGO derivatives. Peak areas were obtained by a Hitachi D-2500 integrator.

RESULTS AND DISCUSSION

Screening of glyoxal analogues

Alkoxyphenylglyoxals of DMPG, MDPG, MPG and TMPG made GMP, cGMP, guanine and deoxyguanosine fluoresce (Table 1) under the reaction conditions established previously for the PGO reagent [18], i.e., warming in 12.5 mM phosphate buffer (pH 6.0) at 37°C for 15 min. DMPG, MDPG and MPG afforded generally more intense fluorescence than PGO. Therefore, these

TABLE 1

Excitation and emission maxima of the fluorescence produced by the reactions with alkoxyphenylglyoxals and PGO, and their relative fluorescence intensities (RFI) [a]

Reagent (0.1 M)	Compound (50 nmol ml^{-1})	Excitation maximum (nm)	Emission maximum (nm)	RFI
DMPG	GMP	397	510	108
	cGMP	397	508	80
	Guanine	395	505	123
	Deoxyguanosine	398	510	42
MDPG	GMP	398	512	108
	cGMP	398	508	49
	Guanine	395	505	125
	Deoxyguanosine	400	510	43
MPG	GMP	385	520	106
	cGMP	390	520	36
	Guanine	388	510	139
	Deoxyguanosine	392	520	57
TMPG	GMP	395	520	52
	cGMP	395	520	26
	Guanine	393	515	102
	Deoxyguanosine	398	520	17
PGO	GMP	365	515	47
	cGMP	365	515	35
	Guanine	360	505	100
	Deoxyguanosine	365	515	51

[a] The fluorescence intensity obtained by the reaction of guanine with PGO was taken as 100.

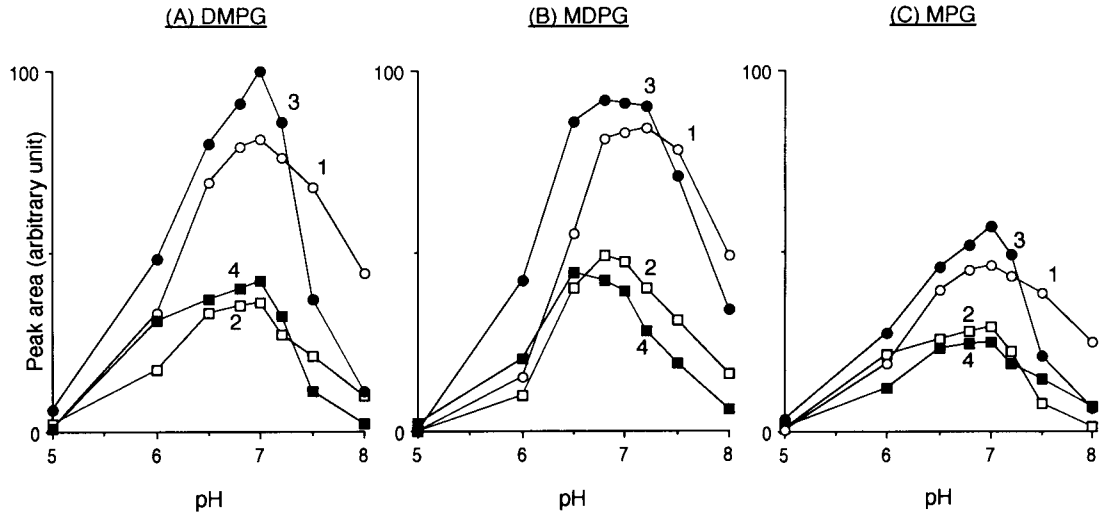

Fig. 2. Effect of pH of the phosphate buffer in the reaction mixture on the formation of fluorescent derivatives. A mixture (50 μl) of the compounds (10 nmol ml^{-1} each) was treated according to the derivatization procedure at various pH values of 30 mM phosphate buffer. For the LC conditions and curves, see Fig. 1.

three glyoxals were subjected to further investigations. On the other hand, aliphatic glyoxals of GO and MGO did not produce any fluorescence.

Derivatization conditions

Figure 1 depicts chromatograms of GMP, cGMP, guanine and deoxyguanosine (50 pmol on column each) obtained by reactions with DMPG, MDPG and MPG. The reaction with PGO was also carried out for comparison. The fluorescent derivatives gave the respective single peaks when separated on a reversed-phase column (TSK gel ODS-120T) with isocratic elution; this suggests that these glyoxal reagents yield the correspond-

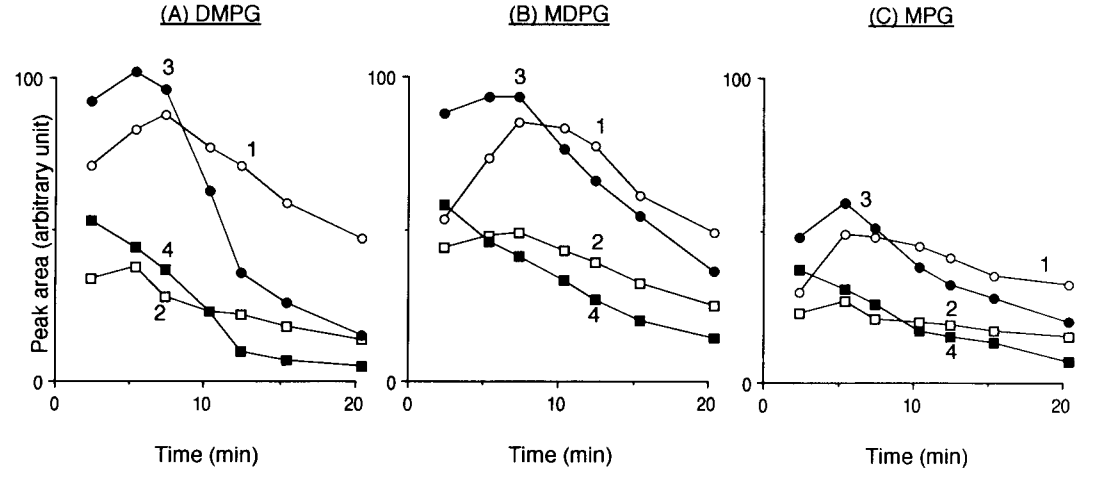

Fig. 3. Effect of reaction time at 37°C on the formation of fluorescent derivatives. A mixture (50 μl) of the compounds (10 nmol ml^{-1} each) was treated according to the derivatization procedure for various reaction times. For the LC conditions and curves, see Fig. 1.

ing derivatives to the guanine-related compounds. This LC separation was utilized to establish the following derivatization conditions.

The pH of 30 mM phosphate buffer used for the reaction affected the fluorescence production (Fig. 2). Maximum peak areas produced with the three reagents were attained at pH 6.8–7.2 of the buffer. For the three reagents, the concentration of the phosphate buffer (pH 7.0) did not have a great effect on peak areas in the range 10–30 mM, but 30 mM phosphate buffer (pH 7.0) afforded the maximum peak areas. When 30 mM borate buffer (pH 7.0) or 30 mM citrate buffer (pH 7.0) was used instead of the phosphate buffer, only 50–70% peak areas were obtained for the three reagents.

The reaction period influenced the production of the fluorescent derivatives (Fig. 3). At 37°C, which was employed for the procedure, the maximum peak areas from the tested compounds except for deoxyguanosine were achieved by warming for 5 min for the DMPG and MPG reactions, and for 7 min for the MDPG reactions. The production of the fluorescent derivatives from deoxyguanosine occurred rapidly in the reactions with the three reagents; the peak areas decreased with prolonging reaction periods after 2 min. At 60°C, the maximum peak areas were achieved by heating for approximately 1 min. However, the peak areas were approximately 70–90% of those given at 37°C. At 20°C with the three reagents, the maximum peak areas were obtained by the reactions after 5 min for deoxyguanosine and 30 min for the other compounds; the areas were almost the same as those given at 37°C.

Organic solvents such as DMSO, *N*,*N*-dimethylformamide, acetonitrile and methanol used for dissolving the glyoxal reagents influenced the fluorescence derivatization. Of the mixtures with a concentration of 25% (v/v) of organic solvent, DMSO gave the maximum peak areas for the tested compounds; the peak areas obtained by the other solvents were 20–90% of those given by DMSO in each of the three reagent reactions. Therefore, the effect of DMSO concentration in the reaction mixture was examined (Fig. 4). Although, lower concentrations of DMSO in the reaction mixture allowed the derivatization to proceed effectively, a DMSO concentration of 10% for DMPG and MPG, and 15% for MDPG in the reaction mixture were employed for the derivatization because these concentrations were necessary for dissolving the respective reagents.

The results shown in Figs. 2–4 indicate that

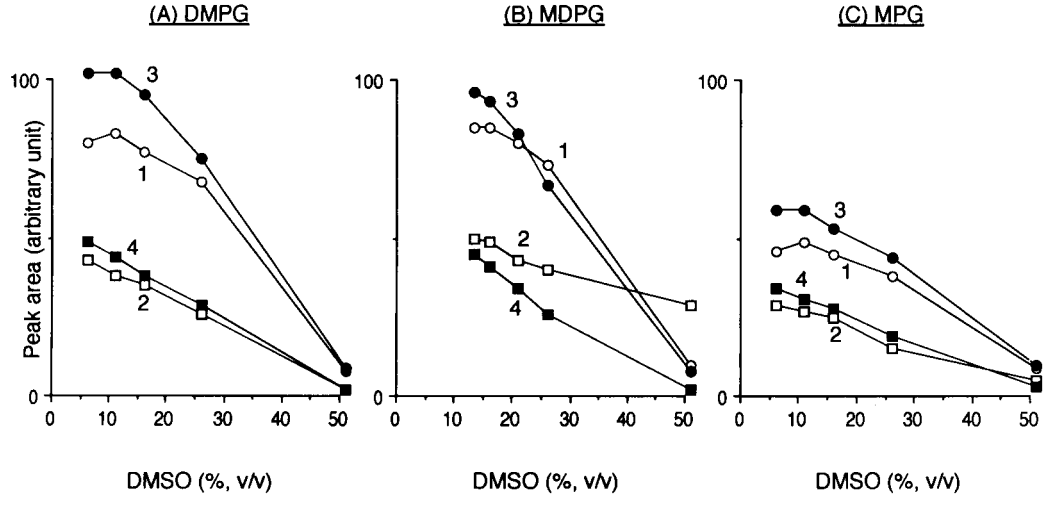

Fig. 4. Effect of DMSO concentration in the reaction mixture on the formation of fluorescent derivatives. A mixture (50 μl) of the compounds (10 nmol ml^{-1} each) was treated according to the derivatization procedure at various DMSO concentrations. For the LC conditions and curves, see Fig. 1.

DMPG is the most favourable pre-column derivatization reagent for the LC determination of guanine and its nucleos(t)ides.

LC determination with DMPG

A standard mixture of GTP, GDP, GMP, dGTP, dGDP, dGMP, cGMP, guanine, guanosine, deoxyguanosine and 9-ethylguanine (11 species in all) was subjected to the reaction with DMPG, and the resulting fluorescent derivatives were separated by reversed-phase LC with stepwise and gradient elution of acetonitrile (Fig. 5). The fluorescent derivatives were eluted within 30 min. THF in the mobile phase served to sharpen the fluorescent peaks.

The stability of the fluorescent products of guanine and its nucleos(t)ides was examined. When the reaction mixture, the result of which is shown in Fig. 5, was allowed to stand in an ice-water bath (0°C) for 3 h after the reaction, the peak areas from guanine, 9-ethylguanine and the nucleosides (25–35%) and from the nucleotides (72-87%) decreased. Therefore, the final reaction mixtures should be injected into the chromatograph immediately after the reaction.

The precision of the method was established by repeated determinations ($n = 8$). The standard deviations of the peak areas for guanine and its 10 nucleos(t)ides (5 nmol ml^{-1} each) were 3.5–6.0%. The calibration graphs for the compounds were all linear over the concentration range of 0–400 nmol ml^{-1} with correlation coefficients of 0.9987–0.9996. The limits of detection at a signal-to-noise ratio of 3 for the compounds were in the range 40–400 fmol per 100-μl injection volume; the present method is 2.0–5.0 times more sensitive than the previous method using PGO [18].

The following substances (100 nmol ml^{-1} each) did not provide any fluorescent peaks when treated under the present derivatization conditions and LC conditions; adenine, cytosine, thymine, uracil, hypoxanthine, xanthine, adenosine, cytidine, thymidine, uridine, ATP, ADP, AMP, CTP, CDP, CMP, dATP, dADP, dAMP, galactose, glucose, galactosamine, nicotinamide, nicotinic acid, ascorbic acid and 19 L-α-amino acids including tryptophan which reacts with PGO in the acidic medium [20]. The selectivity of the present methods was the same as described before [17,18].

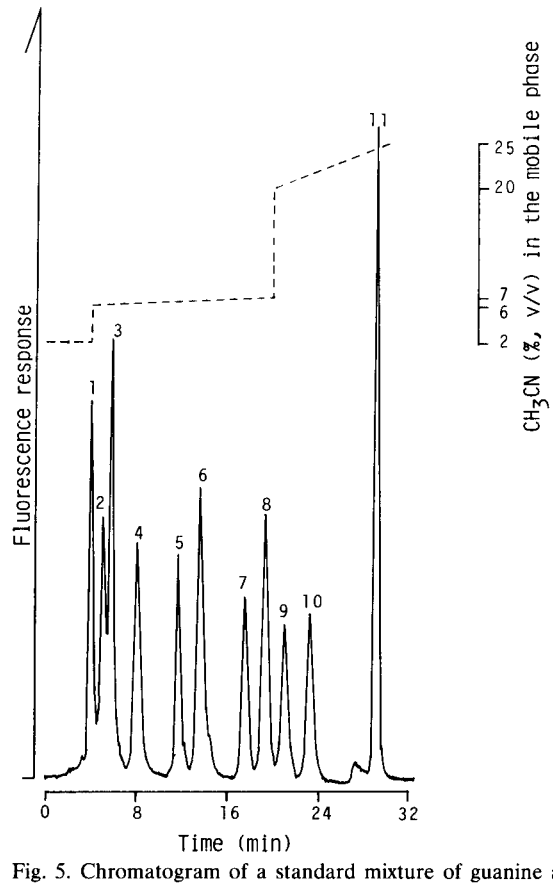

Fig. 5. Chromatogram of a standard mixture of guanine and its nucleos(t)ides obtained with stepwise and gradient elution. A mixture (50 μl) of the compounds (5 nmol ml^{-1} each) was treated according to the derivatization procedure using the DMPG reagent, followed by LC. The stepwise and gradient elution of acetonitrile (2–25%, v/v) in an aqueous mobile phase containing THF (3%, v/v), 50 mM phosphate buffer (pH 6.0) (25%, v/v) and water (70–47%, v/v) was carried out during 30 min. Peaks: 1 = GTP; 2 = dGTP; 3 = GDP; 4 = dGDP; 5 = GMP; 6 = dGMP; 7 = cGMP; 8 = guanine; 9 = guanosine; 10 = deoxyguanosine; 11 = 9-ethylguanine.

In conclusion, DMPG, MDPG and MPG were more sensitive than PGO, and DMPG was most sensitive and could be used as a pre-column fluorescence derivatization reagent for the determination of subpicomole amounts of guanine and its nucleos(t)ides. The reagent may be applied to the fluorescence labeling of high molecular nucleic acids. The elucidation of the structure of the fluorescent derivatives is in progress.

REFERENCES

1 R. Boulieu, C. Bory and C. Gonnet, J. Chromatogr., 339 (1985) 380.
2 A. Werner, W. Siems, H. Schmidt, I. Rapoport, G. Gerber, R. Toguzov, Y. Tikhonov and A. Pimenov, J. Chromatogr., 421 (1987) 257.
3 F. Arezzo, Anal. Biochem., 160 (1987) 57.
4 K.K. Tekkanat and I.H. Fox, Clin. Chem., 34 (1988) 925.
5 R.T. Smolenski, D.R. Lachno, S.J.M. Ledingham and M.H. Yacoub, J. Chromatogr., 527 (1990) 414.
6 T. Yamamoto, H. Shimizu, T. Kato and T. Nagatsu, Anal. Biochem., 142 (1984) 395.
7 J.B. Kafil, H.-Y. Cheng and T.A. Last, Anal. Chem., 58 (1986) 285.
8 T. Nakahara, A. Shiraishi, M. Hirano, T. Matsumoto, T. Kuroki, Y. Tatebayashi, T. Tsutsumi, K. Nishiyama, H. Ooboshi, K. Nakamura, H. Yao, M. Waki and H. Uchimura, Anal. Biochem., 180 (1989) 38.
9 S.P. Assenza and P.R. Brown, J. Chromatogr., 289 (1984) 355.
10 T.A. Ratko and J.M. Pezzuto, J. Chromatogr., 324 (1985) 484.
11 H. Yuki, C. Sempuku, M. Park and K. Takiura, Anal. Biochem., 46 (1972) 123.
12 M.R. Preston, J. Chromatogr., 275 (1983) 178.
13 S. Sonoki, Y. Tanaka, S. Hisamatsu and T. Kobayashi, J. Chromatogr., 475 (1989) 311.
14 J.-O. Svensson and B. Jonzon, J. Chromatogr., 529 (1990) 437.
15 M. Yoshioka, Z. Tamura, M. Senda and T. Miyazaki, J. Chromatogr., 344 (1985) 345.
16 H. Fujimori, T. Sasaki, K. Hibi, M. Senda and M. Yoshioka, J. Chromatogr., 515 (1990) 363.
17 M. Kai, Y. Ohkura, S. Yonekura and M. Iwasaki, Anal. Chim. Acta, 207 (1988) 243.
18 S. Yonekura, M. Iwasaki, M. Kai and Y. Ohkura, J. Chromatogr., 641 (1993) 235.
19 E. Kojima, Y. Ohba, M. Kai and Y. Ohkura, Anal. Chim. Acta, 280 (1993) 157.
20 E. Kojima, M. Kai and Y. Ohkura, Anal. Chim. Acta, 248 (1991) 213

Analytica Chimica Acta, 287 (1994) 223–227
Elsevier Science B.V., Amsterdam

2-Amino-4,5-ethylenedioxyphenol as fluorescence derivatization reagent for aromatic aldehydes in liquid chromatography

Hitoshi Nohta, Fumie Sakai, Masaaki Kai and Yosuke Ohkura

Faculty of Pharmaceutical Sciences, Kyushu University 62, Maidashi, Higashi-ku, Fukuoka 812 (Japan)

Mikihiko Saito

Dojindo Laboratories, Mashiki, Kumamoto 861-22 (Japan)

(Received 27th July 1993; revised manuscript received 26th October 1993)

Abstract

2-Amino-4,5-ethylenedioxyphenol was found to be useful as a precolumn fluorescence derivatization reagent for aromatic aldehydes in liquid chromatography. The reagent reacts selectively with the aldehydes in two steps: first, heating (100°C) for 45 min in methanol solution in the presence of dicyclohexylcarbodiimide; secondly, standing for more than 1 min at room temperature after acidification. The fluorescent product from 4-hydroxybenzaldehyde is shown to be 2-(4-hydroxyphenyl)-5,6-ethylenedioxybenzoxazole. The fluorescent derivatives of aromatic aldehydes can be separated by reversed-phase chromatography and their detection limits ($S/N = 3$) are 5–10 pmol on column.

Keywords: Liquid chromatography; Fluorimetry; 2-Amino-4,5-ethylenedioxyphenol; Aromatic compound; Pre-column derivatization

Dansyl hydrazine [1], 7-hydrazino-4-nitrobenzo-2-oxa-1,3-diazole [2], and some other hydrazino reagents [3] have been utilized for the fluorescence derivatization of a wide variety of aldehydes. These reagents also react with other carbonyl compounds, and the reagents and their degradation products are fluorescent; a clean-up procedure (chromatography or extraction) is required for the preparation of samples for liquid chromatography (LC). Aromatic 1,2-diamino and 1-amino-2-sulfhydryl compounds (all nonfluorescent) have been developed as highly selective fluorogenic reagents for aromatic aldehydes. The derivatizations are based on the cyclization reactions between 1,2-diamino moiety and 1-amino-2-sulfhydryl moiety in the reagents, and formyl moiety in the aldehydes, to form the corresponding fluorescent imidazole and thiazole derivatives, respectively; the former derivatives are 1,2-diaminonaphthalene [4], 1,2-diamino-4,5-dimethoxybenzene (DDB) [5], 1,2-diamino-4,5-dimethylbenzene [6], 1,2-diamino-4,5-ethylenedioxybenzene (DEB) [7] and 1,2-diamino-4,5-methylenedioxybenzene (DMB) [7], and the latter derivatives are 2-aminothiophenol [8], 2,2′-dithiobis(1-aminonaphthalene) (DTAN) [9], 2-amino-5-methoxythiophenol (MAT) [10], 2-amino-4,5-methylenedioxythiophenol (MDAT) [10] and some other alkoxyl 2-aminothiophenols [10]. In both types of reagents, alkoxyl groups were

Correspondence to: Y. Ohkura, Faculty of Pharmaceutical Sciences, Kyushu University 62, Maidashi, Higashi-ku, Fukuoka 812 (Japan).

SSDI 0003-2670(93)E0600-C

demonstrated to provide the aldehydes with higher sensitivity in their detection [7,10], and DDB, DEB, DMB, MAT and MDAT were applied to the precolumn derivatization of the aldehydes in LC.

The above-mentioned observations suggested that 1-amino-2-hydroxyphenyl compounds (2-aminophenols) could also react with aromatic aldehydes to yield the corresponding fluorescent oxazole derivatives. Although 2-aminophenols usually fluoresce more or less in organic solvents and in aqueous solutions at any pH, they were considered to be suitable as fluorogenic reagents for the precolumn derivatization of aromatic aldehydes in LC. In the present study, 2-aminophenol, 2-amino-4,5-methylenedioxyphenol (MDAP), 2-amino-4,5-ethylenedioxyphenol (EDAP), 2-amino-*tert.*-butylphenol, 2-amino-4-methylphenol, 2-amino-5-methylphenol and 2-amino-4-chlorophenol (seven species in all) were subjected to the investigation. EDAP selected as the best reagent was further investigated to establish the optimum conditions for the precolumn derivatization of aromatic aldehydes and LC separations of the derivatives.

EXPERIMENTAL

Reagents and solutions

The hydrochlorides of EDAP and MDAP were synthesized according to the literature [11]. 2-Amino-4-*tert.*-butylphenol and the other 2-aminophenols were purchased from Aldrich (St. Louis, MO) and Wako (Osaka), respectively, and their hydrochlorides were prepared in the usual way. The hydrochlorides were stable at −20°C for at least three months. The hydrochloride solutions (1.5 mM) were separately prepared in methanol before use. The standard solutions of aromatic aldehydes were prepared in methanol and the solutions were usable for at least 1 month when stored at −20°C. Dicyclohexylcarbodiimide (DCC) was obtained from Wako.

LC system and its operation conditions

The LC system was essentially the same as that used for the separation of MAT and MDAT derivatives of aromatic aldehydes [10]. The LC column was TSKgel ODS-80T$_M$ (150 × 4.6 mm i.d., particle size, 5 μm, Tosoh, Tokyo) and column temperature was 20–25°C. The mobile phase was an aqueous 70% (v/v) methanol, which was delivered at a flow rate of 0.8 ml min^{-1}. The fluorescence spectrometer was operated at the following excitation and emission wavelengths; 330 nm and 390 nm for EDAP and 340 nm and 390 nm for MDAP, respectively.

Isolation of the reaction product of 4-hydroxybenzaldehyde with EDAP

To a methanol solution of 4-hydroxybenzaldehyde (0.6 mmol in 20 ml) were added 10 ml each of EDAP solution (0.5 mmol in methanol) and DCC solution (0.12 mmol in methanol), and the mixture was refluxed for 2 h. After the addition of 20 ml of 6 M perchloric acid, the mixture was allowed to stand at room temperature (25°C) for 10 min with stirring. The mixture was neutralized with 6 M sodium hydroxide, then the fluorescent product was extracted with chloroform (40 ml, twice). After removal of the solvent, the residue was subjected to chromatography on a silica gel (60 g, Wako Gel C-200) column (20 × 1.5 cm i.d.) with chloroform; the main fluorescent fraction was collected and the solvent was removed in vacuo to give a colourless crystalline powder; yield 2 mg (0.7% calculated from EDAP). Elemental analysis (%), calculated for $C_{15}H_{11}NO_4$, C 66.91, H 4.12, N 5.20%; found C 66.87, H 4.14, N 5.19%. With electron-impact mass spectrometry (recorded with a JEOL JMS-01-SG mass spectrometer), a peak at $m/z = 269$ (M^+, base peak) was found.

Procedure for the determination with EDAP

To 0.5 ml of a methanol solution of aromatic aldehydes in a screw-capped 3.5-ml vial, 0.5 ml each of 1.5 mM EDAP solution and 5 mM DCC (in methanol) were added. The vial was tightly closed and heated at 100°C for 45 min. After cooling, 0.5 ml of 6 M perchloric acid was added, then the mixture was allowed to stand at room temperature for more than 1 min. After neutralization with approximately 0.5 ml of 6 M sodium hydroxide to pH 6–7.5, an aliquot (20 μl) of the resulting mixture was subjected to LC.

RESULTS AND DISCUSSION

Of the tested 2-aminophenols, only EDAP and MDAP yielded fluorescence derivatives towards the tested aromatic aldehydes (six species; see Fig. 1). The alkoxyl groups introduced to the reagents were indispensable for the production of the fluorescent derivatives. Figure 1 depicts typical chromatograms obtained with a standard mixture of the aldehydes with EDAP and MDAP, and Table 1 shows the retention times, fluorescence excitation and emission maxima, and relative peak heights of the derivatives. Both reagents afforded the corresponding single peaks to the aldehydes: EDAP gave higher peaks for most of the aldehydes. The derivatives of vanillin and isovanillin were unsatisfactorily separated: the resolution values estimated from the heights of the valley between the peaks [12], were 1.03 for EDAP and 0.92 for MDAP. The excitation and emission maxima of the fluorescent derivatives in the mobile phase were at 330–340 nm and 390–410 nm for EDAP, and at 340–345 nm and 340–410 nm for MDAP, respectively: the Stokes shifts of the EDAP derivatives were higher than those of the MDAP derivatives. EDAP seems to be preferable for the sensitive measurement of all the aromatic aldehydes tested.

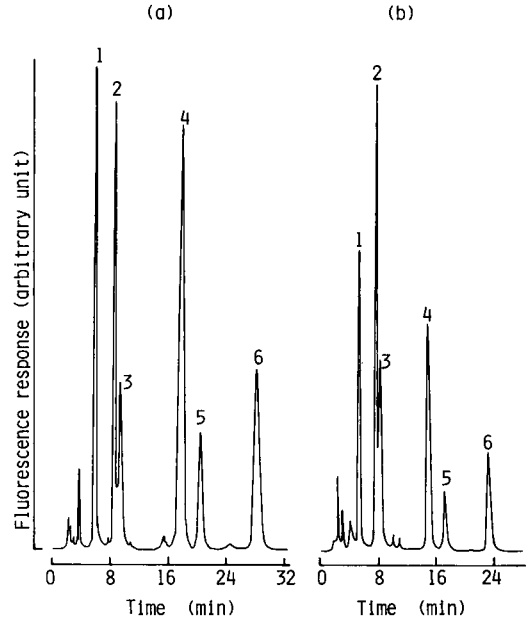

Fig. 1. Chromatograms of (a) EDAP and (b) MDAP derivatives of aromatic aldehydes. A portion (0.5 ml) of a standard mixture of six aldehydes (50 nmol ml^{-1} each) was treated as described in the Experimental section, and the resulting mixture was subjected to LC. Peaks: 1 = 3,4-dihydroxybenzaldehyde; 2 = isovanillin; 3 = vanillin; 4 = benzaldehyde; 5 = 4-methoxybenzaldehyde; 6 = 4-methylbenzaldehyde; others = reagent blank.

Aromatic 1,2-diamino and 1-amino-2-sulfhydryl compounds react with aromatic aldehydes in acidic media (hydrochloric acid, sulphuric acid or perchloric acid) [4–10], but EDAP did not react in the acidic conditions. The EDAP reaction was found to proceed by the following two steps: (i) heating (100°C) for 45 min in methanol solution in the presence of DCC, (ii) standing for more than 1 min at room temperature after acidifica-

TABLE 1

Retention times (t_R), excitation and emission maxima (λex, λem) and relative peak heights (RPH) of the EDAP and MDAP derivatives of aromatic aldehydes [a]

Aromatic aldehyde	EDAP				MDAP			
	t_R (min)	λex (nm)	λem (nm)	RPH [b]	t_R (min)	λex (nm)	λem (nm)	RPH
Benzaldehyde	17.3	330	405	100	15.1	345	395	55
Isovanillin	8.3	330	390	100	7.7	345	390	98
Vanillin	9.2	335	390	32	8.5	340	385	32
4-Methoxybenzaldehyde	20.0	330	390	28	17.2	340	390	14
4-Methylbenzaldehyde	27.9	340	410	42	23.2	340	410	24
3,4-Dihydroxybenzaldehyde	5.9	330	390	114	5.4	340	380	71

[a] Portions (0.5 ml) of a mixture of the six aldehydes (50 nmol ml^{-1} each) were treated according to the procedure using EDAP or MDAP, followed by LC. [b] The peak height of the EDAP derivative of benzaldehyde was taken as 100.

tion. In spite of the difference in reaction conditions, the fluorescence excitation and emission spectra of the EDAP derivatives in neutral media were almost the same in shapes and maxima as those of the derivatives of the 1,2-diamino- and 1-amino-2-sulfhydryl-type reagents (DEB and DMB, and MAT and MDAT, respectively) [7,10]. The LC conditions and separation pattern of the EDAP derivatives were also closely similar to those of the MAT and MDAT derivatives [10]. Therefore, it is expected that EDAP reacts with aromatic aldehydes to form the corresponding 2-aryl-5,6-ethylenedioxybenzoxazoles. This was supported by the mass spectrum and elemental analysis data of the isolated fluorescent product from 4-hydroxybenzaldehyde; the data corresponded to 2-(4-hydroxyphenyl)-5,6-ethylenedioxybenzoxazole. The retention time and fluorescence excitation and emission maxima of the product in the LC coincided with those for the corresponding reaction mixture. However, the mechanism of the reactions through the first and second steps remained unknown.

The optimum conditions of the reaction was established using the six aromatic aldehydes. EDAP gave almost maximum peak heights for all the aldehydes at around 1.5 mM; 1.5 mM was recommended. DCC accelerated the first step of the derivatization reaction most effectively at concentrations of 4–6 mM for each aldehyde, and in its absence the peak heights lowered to 10% or less compared to those given in the presence of 5 mM DCC; 5 mM was selected as optimum. The first step proceeded in water-miscible organic solvents (methanol, ethanol, 2-propanol, acetonitrile, dimethylsulfoxide and 2-methoxyethanol); methanol gave the best result. Addition of water strongly interfered with the reaction.

The second step proceeded under strongly acidic conditions (perchloric acid or sulphuric acid). The maximum reaction rate was attained at concentrations of 5–9 M perchloric acid and 7–10 M sulphuric acid, but sulphuric acid could not afford reproducible results; 6 M perchloric acid was recommended in the procedure.

The first step of the EDAP reaction occurred at a temperature higher than 90°C. The reaction was complete within 60 min at 90°C or within 45 min at 100–120°C; heating at 100°C for 45 min was selected as optimum. The second step proceeded rapidly and was not affected by reaction temperature (20–100°C) and time (1–100 min); standing for more than 1 min at room temperature (20–25°C) was used for convenience.

Aliphatic aldehydes (formaldehyde, acetaldehyde, propionaldehyde and *n*-butyraldehyde), aromatic carboxylic acid (benzoic acid and salicylic acid) and the following compounds of biological importance did not gave any fluorescent peak in the LC at a concentration of 100 nmol ml^{-1}; the compounds tested were seventeen different L-α-amino acid, biogenic amines (dopamine, norepinephrine, epinephrine, serotonin and histamine), their metabolites (homovanillic acid, vanillylmandelic acid, 5-hydroxyindoleacetic acid and imidazoleacetic acid), α-keto acids (α-ketoglutaric acid and phenylpyruvic acid), oxalic acid, acetic acid, uric acid, L-ascorbic acid, creatine, creatinine, sugars (D-glucose, D-fructose, D-galactose, D-ribose, D-glucosamine, maltose and sucrose), nucleic acid bases (adenine, guanine, thymine, cytosine and uracil) and their nucleosides and nucleotides, and cholesterol. This suggests that the EDAP reaction has sufficient selectivity for aromatic aldehydes.

The derivatization yield of 4-hydroxybenzaldehyde was obtained as 9% by comparing the values of the peak area for the reaction mixture with that of the isolated fluorescent derivative. The EDAP derivatives in the reaction mixture were stable for at least 72 h in daylight; the derivatives were more stable than the benzimidazole derivatives (with DDB, DEB and DMB) and benzothiazole derivatives (with MAT and MDAT) against light.

The calibration graphs for the tested aldehydes (Table 1) were linear in the range 2–500 nmol ml^{-1}; the linear regression correlation coefficients were 0.997 for 4-methyl- and 4-methoxybenzaldehydes, 0.996 for vanillin and benzaldehyde, 0.992 for isovanillin, and 0.987 for 3,4-dihydroxybenzaldehyde. The detection limits ($S/N = 3$) were 5–10 pmol on column. This sensitivity was 10–100 times lower than those with the highly sensitive reagents (DEB, DMB, MAT and MDAT). The precision was established by re-

peated determinations ($n = 10$) of a standard mixture of the six aldehydes (20 nmol ml^{-1}); the relative standard deviations were 2.1% for vanillin and 4-methoxybenzaldehyde, 2.2% for 4-methylbenzaldehyde, 2.4% for benzaldehyde, and 2.6% for 3,4-dihydroxybenzaldehyde and isovanillin.

In conclusion, EDAP requires two step reactions for the derivatization of aromatic aldehydes, and its sensitivity was not so high as the previously reported sensitive reagents due to the lower derivatization yield of the present method. However, EDAP reaction requires only 1 min standing time under the acidic conditions, and the EDAP derivatives were stable. Thus, EDAP may be useful as a derivatization reagent especially for acid-labile aldehydes. The comparative study between EDAP and the previously reported reagents (MAT and MDAT) in application to the assay of catechol-*O*-methyltransferase in human erythrocytes, which is based on the determination of vanillin and isovanillin formed enzymatically from a substrate (3,4-dihydroxybenzaldehyde), is now in progress.

REFERENCES

1 R.W. Frei and J.F. Lawrence, J. Chromatogr., 83 (1973) 321.
2 G. Gubitz, R. Wintersteiger and R.W. Frei, J. Liq. Chromatogr., 7 (1984) 839.
3 J.M. Anderson, Anal. Biochem., 152 (1986) 146.
4 Y. Ohkura and K. Zaitsu, Talanta, 21 (1974) 547.
5 M. Nakamura, M. Toda, H. Saito and Y. Ohkura, Anal. Chim. Acta, 134 (1982) 39.
6 M. Katayama, Y. Mukai and H. Taniguchi, Anal. Sci., 3 (1987) 369.
7 W.-F. Chao, M. Kai, J. Ishida and Y. Ohkura, Anal. Chim. Acta, 215 (1988) 259.
8 T. Uno and H. Taniguchi, Bunseki Kagaku, 21 (1972) 76.
9 Y. Ohkura, K. Ohtsubo, K. Zaitsu and K. Kohashi, Anal. Chim. Acta, 99 (1978) 317.
10 H. Nohta, F. Sakai, M. Kai, Y. Ohkura, S. Hara and M. Yamaguchi, Anal. Chim. Acta, 282 (1993) 625.
11 D.G. Orphanos and A. Taurins, Can. J. Chem., 44 (1966) 1875.
12 L.R. Snyder, J.L. Glajch and J.J. Kirkland, Practical HPLC Method Development, Wiley Interscience, New York, 1988, p. 15.

Analytica Chimica Acta, 287 (1994) 229–234
Elsevier Science B.V., Amsterdam

Determination of tungsten in low-grade tungsten ores by dual-column ion chromatography

D.N. Wagh, Sangita D. Kumar and C.S.P. Iyer

Analytical Chemistry Division, Bhabha Atomic Research Centre, Trombay, Bombay-400 085 (India)

(Received 19th July 1993)

Abstract

A simple and rapid method was developed for the determination of tungsten in low-grade tungsten ores by dual-column ion chromatography using a conductivity detector. The chromatographic parameters based on ion selectivity, retention time and signal response were optimized for tungstate ion. Chloride, fluoride, sulphate, nitrate, chromate, molybdate and vanadate anions did not interfere in the determination. The reliability of the method was tested by analysing two CANMET (Canadian reference) standards. The detection limit for tungstate was 1.35 mg l^{-1}. The relative standard deviation ($n = 10$) for the sample was 4.3% at 0.71% WO_3. The method was validitated by analysing the ore samples by spectrophotometry using thiocyanate, neutron activation analysis and energy-dispersive x-ray fluorescence spectrometry.

Keywords: Ion chromatography; Ores; Tungsten

The use of tungsten in the defence and aerospace industries, in addition to its various other important applications [1,2], has made tungsten strategically important. Several methods such as classical wet chemical methods, spectrophotometry, atomic absorption and emission methods, x-ray fluorescence (XRF) spectrometry and neutron activation analysis for the determination of tungsten in low-grade ores have been reported [3,4]. Spectrophotometry and atomic absorption spectrometry are the two most commonly used methods. The two classical spectrophotometric methods generally used are based on the formation of complexes with thiocyanate [5–7] or dithiol [8,9]. However, these methods suffer from interference by molybdenum and also from instability of the reagents. The atomic absorption method is also subject to interferences by various ions and the sensitivity for tungsten is decreased if the metal in solution is in a form in which it is bonded to oxygen. The presence of sulphuric or phosphoric acid decreases the absorbance signal. If iron is present the absorbance signal is decreased owing to the formation of a metal tungstate anion having limited reactivity [10]. In XRF, matrix absorption and enhancement problems are severe and require complicated mathematical processing of the data to obtain meaningful results, and also sample preparation is critical [4,11]. Neutron activation analysis, though very sensitive, requires a neutron source for sample irradiation.

In recent years, ion chromatography has become increasingly popular for the determination of ionic species in solutions, but few papers on the determination of tungsten using this technique have been published. Zolotov et al. [12] studied the determination of tungsten by convert-

Correspondence to: D.N. Wagh, Analytical Chemistry Division, Bhabha Atomic Research Centre, Trombay, Bombay-400 085 (India).

SSDI 0003-2670(93)E0599-3

ing it into tungstate form using H_2O_2 and eluting with 5 mM Na_2CO_3 solution. The method was applied to pure solutions only. Weiss et al. [13] used 1 mM Na_2CO_3 as eluent in 2 mM tetrabutylammonium hydroxide–acetonitrile and tungstate was determined in a mixture of thio- and selenometallates using spectrophotometric detection. Mehra and Frankenbergen [14] have used single-column ion chromatography (SCIC) for the determination of soluble tungsten in soils and sludges.

No attempt has been made so far to determine tungsten in ores using ion chromatography. In this investigation, a dual-column ion chromatographic (DCIC) technique was used for the determination of tungsten in low-grade ores. DCIC has the advantage over SCIC that the background due to the eluent is completely suppressed, thereby enhancing the sensitivities of the ions detected. The operating conditions were optimized.

EXPERIMENTAL

Reagents and materials

All reagents and chemicals were of analytical-reagent grade.

A four-module Nanopure Barnsted Cartridge system was used to purify deionized water having a conductivity of 2–3 μS. The system consisted of an organic removal cartridge followed by two mixed-bed deionization cartridges to remove dissolved inorganics and a 0.2-μm filter to remove microorganisms and particulates. The conductivity of the purified water was 0.05 μs.

The mobile phases used were 3 mM sodium hydrogencarbonate–2.4 mM sodium carbonate (standard eluent) and sodium carbonate of different concentrations ranging from 5 to 12 mM.

A stock standard tungstate solution (1 mg ml^{-1}) was prepared using sodium tungstate ($Na_2WO_4 \cdot 2H_2O$). This stock standard solution was diluted to prepare working standard solutions.

Low-grade tungsten ores Two CANMET standard low-grade tungsten ores, BH-1 (wolframite) and TLG-1 (Sheelite), were obtained from the Canada Centre For Minerology and Technology. Low-grade ore samples (wolframite and sheelite) were supplied by the Geological Survey of India. About 0.5 g of accurately weighed tungsten ore sample (300 mesh) was mixed with 2 g of Na_2CO_3 and the mixture was fused in a platinum crucible over a Maker burner. The advantage of using Na_2CO_3 for the fusion of samples was that it could also be used in the eluent. The fusion product was cooled, digested with the minimum volume of water, filtered through a Whatman No. 2 filter-paper and the filtrate was diluted to 25 ml with water. An aliquot of this solution was analysed for its tungsten content.

TABLE 1

Experimental conditions for DCIC measurements

Eluent	8 mM Na_2CO_3 solution
Flow-rate	120 ml h^{-1}
Analytical column	AS-1 anion separation column (250×3 mm i.d.)
Suppressor column	ASC-1 anion suppressor column (60×6 mm i.d.)
Column inlet pressure	500 psi
Detection sensitivity	3 and 10 μS full-scale
Injection volume	100 μl

Ion chromatography.

For DCIC, a Dionex Model 16 ion chromatograph employing a conductivity detector was used throughout. An AS-1 anion separation column (250 × 3 mm i.d.) and an ASC-1 anion suppressor column (60 × 6 mm i.d.) from Dionex were used.

All ion chromatographic measurements were carried out using the conditions given in Table 1. Sample and calibration standards containing tungstate at concentration between 5 and 200 mg l^{-1} were injected into the ion chromatograph and the results were calculated on a peak-area ratio basis. A typical ion chromatogram of the sample is shown in Fig. 1.

Spectrophotometry

The determination of tungsten content in low-grade ore samples was carried out using the modified thiocyanate method [11]. The ore sample was fused with potassium pyrosulphate and the melt was dissolved in 0.5 M tartaric acid. Tung-

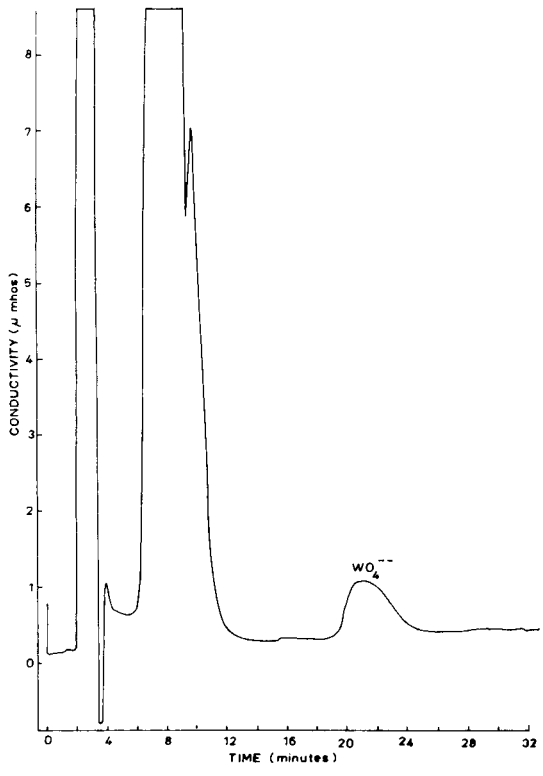

Fig. 1. Chromatogram of a sample of tungsten ore (KB-1/24) using Na_2CO_3 eluent. For conditions, see Table 1.

sten(VI) was reduced to tungsten(V) with tin(II) chloride in 9 M HCl. The yellow thiocyanate complex formed by addition of potassium thiocyanate was extracted with *n*-butyl acetate and the absorbance was measured at 400 nm using a Shimadzu UV-210 A double-beam spectrophotometer.

Neutron activation analysis (NAA) [15]

About 100 mg of accurately weighed tungsten ore sample and 0.05 mg of tungsten standard were irradiated in the Apsara swimming pool-type reactor at a flux of 3×10^{11} n cm^{-2} s^{-1} for 8 h and allowed to cool for 2 days before the activities were measured on a Canberra Series 35 multi-channel analyser. The photopeak activity at 680 keV of ^{187}W was measured using a Ge(Li) detector and used for calculations.

Energy-dispersive x-ray fluorescence (EDXRF) spectrometry [16]

The standards and sample pellets were prepared using microcrystalline cellulose as binder and excited with a ^{109}Cd radioisotope source of annular geometry. An Si(Li) x-ray detector with a resolution of 170 eV at 5.9 keV and a Canberra 2 K multi-channel analyser was used for measuring the x-ray intensities. The transmission method was used to compute individually the mass absorption coefficients of each pellet for both the primary and the emitted tungsten Lα x-rays. Using these mass absorption coefficients, the intensities of the W Lα peaks, obtained experimentally, were corrected and the concentration of tungsten was determined for each sample.

RESULTS AND DISCUSSION

Elution study

A 50 mg l^{-1} tungstate solution was chromatographed using the standard eluent. The elution of tungstate anions by the standard eluent from the pellicular anion-exchange resin was not satisfactory owing to its long retention time (50 min) and very broad elution peak. An elution study was therefore made using 5, 6, 8, 10 and 12 mM Na_2CO_3 solutions as eluent; the results are given in Table 2. Although an increasing concentration of the eluent caused a progressive decrease of the retention time and the peak area, it

TABLE 2

Effect of different eluents on retention time and peak area

Eluent	Concentration of eluent (mM)	Retention time (min)	Peak area (mm^2) [a]
Standard eluent ($NaHCO_3$–Na_2CO_3)	3+2.4	50	87
Na_2CO_3	5	46	91
Na_2CO_3	6	27	85
Na_2CO_3	8	20	70
Na_2CO_3	10	18	66
Na_2CO_3	12	14	60

[a] The average of ten determinations was used for calculating peak area.

also correspondingly increased the rate of exhaustion of the suppressor column balance was achieved by selecting 8 mM Na_2CO_3 as eluent where the suppressor column could be used for six samples compared to only two and one in the case of 10 and 12 mM Na_2CO_3, respectively.

Precision, detection limit and linearity

A calibration graph (5–200 mg tungstate l^{-1}) at a sensitivity of 10 μS full-scale was prepared to verify the linear response of the integrated peak areas (y) of the chromatograms against tungstate concentration (x). The calibration graph was linear ($y = 1.46x - 0.121$) within the range studied, as judged from the correlation coefficient ($r^2 = 0.998$) ($n = 10$). This calibration curve was used to determine the concentration of tungsten in the samples.

The precision of the method was determined by repeated injections ($n = 10$) of the standard (50 mg tungstate l^{-1}) and the sample (ten different fusions of sample KB-1/24 were made) solution. Relative standard deviations (RSD) of 3.3 and 4.3% were obtained for the standard and sample, respectively. The detection limit for tungstate calculated as three times the signal-to-noise ratio at the baseline was 1.35 mg tungstate l^{-1} using 3 μS as the full-scale sensitivity.

Interference studies

In order to check the potential interferences of anions and also anions that are chemically similar to tungstate, a chromatogram of tungstate was measured in the presence of anions such as chloride, fluoride, nitrate, sulphate, chromate, vanadate and molybdate. It was found that the retention times for fluoride (3.6), chloride (4.8), nitrate (9.4) and sulphate (10.4 min) were shorter than that for tungstate (19.8 min). Phosphate is usually not present in tungsten ores; it is eluted between nitrate and sulphate. For molybdate (29.4) and chromate (42.6 min) anions, the retention times were longer than for tungstate, chromate being maximally retained. Vanadate anions were not eluted under the experimental conditions used. Niobate and tantalate anions were not used owing to the difficulty in keeping them in solution without hydrolysis. Figure 2 shows a typical ion chromatogram for a simulated standard solution of anions containing fluoride (2), chloride (3), sulphate (15), nitrate (10), tungstate (50), molyb-

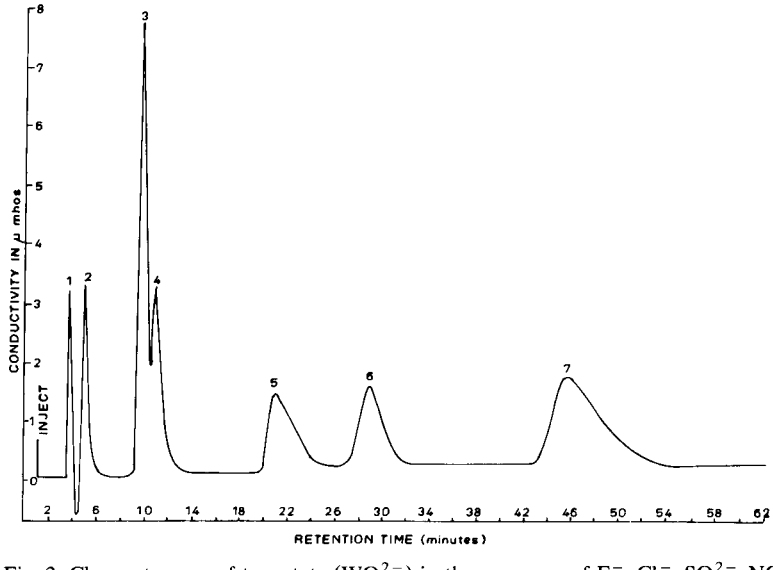

Fig. 2. Chromatogram of tungstate (WO_4^{2-}) in the presence of F^-, Cl^-, SO_4^{2-} NO_3^-, CrO_4^{2-}, MoO_4^{2-} and VO_3^-.

TABLE 3

Analytical results for low-grade tungsten ores and CANMET standards using different techniques

Sample	WO_3 (%)				
	Certified value	DCIC	Spectrophotometry	NAA	EDXRF
BH-1 (standard)	0.532 ± 0.010	0.52	0.52	0.49	0.54
TLG-1 (standard)	0.105 ± 0.005	0.10	0.11	0.10	0.08
KB-1/24	–	0.71	0.71	0.65	0.65
GROW-F	–	0.05	0.04	0.04	0.03
H-1234	–	0.46	0.48	0.51	0.47
NML-1	–	0.23	0.25	0.29	0.22
NML-2	–	0.85	0.87	0.83	0.87

date (5), chromate (55) and vanadate (50 mg l^{-1}). None of these anions interfered. It was noteworthy that molybdenum, which is a serious interferent in most other methods, did not interfere.

Recovery studies

The method of standard additions was followed to study the interference due to the sample matrix. For this purpose additions of standard tungsten solution of 20, 30 and 40 mg tungstate l^{-1} were made to a solution of the standard tungsten ore sample BH-1 (0.53% WO_3) and were analysed by the above method. The recoveries were in the range 97–109%.

Sample analysis

The results of the analysis of five low-grade ore samples for tungsten by the DCIC method are reported (as % WO_3) in Table 3; the values varied from 0.05 to 0.85%. The reliability of the method was tested by analysing two CANMET standards, BH-1 and TLG-1, having certified contents of 0.53 and 0.11% WO_3, respectively. Using the present method, values of 0.52 and 0.10%, respectively, were found (Table 3), showing very good agreement with the certified values.

The validity of the method was further verified by analysing the ore and standard samples by three different techniques, spectrophotometry, NAA and EDXRF, and the results are also given in Table 3. The relative standard deviations obtained ($n = 10$) for DCIC, spectrophotometry and NAA were 4.3, 3.7 and 5.2%, respectively, at 0.71% WO_3 and for EDXRF 7.0% at 0.5% WO_3. The spectrophotometric analysis results agreed well (within ±0.02%) with those given by the DCIC method. However, the agreement between the % WO_3 values determined by the NAA and EDXRF methods and that by the DCIC method was not so good (within ±0.06%), owing to the use of solid samples for measurements in the former methods.

In conclusion, ion chromatography offers a precise method for the analysis of ores with negligible matrix or intermolecular interferences. The major advantage of the method is that molybdenum, which is a serious interferent in many analytical methods for tungsten, does not interfere. Simultaneous analysis of other metals is possible. The method is precise, accurate and sensitive. Compared with other methods for the determination of tungsten, the present method is simple, faster and inexpensive.

The authors thank Dr. S. Gangadharan, Head of the Analytical Chemistry Division, and Shri. S.N. Revanker for their keen interest in this work.

REFERENCES

1 W.T. Elwel and D.F. Wood, Analytical Chemistry of Molybdenum and Tungsten, (International Series of Monographs in Analytical Chemistry, Vol. 47), Pergamon, Oxford, 1971, pp. 9–10.
2 C.L. Rollinson, J.C. Bailar, H.J. Elemeus, R. Nyholm and A.F. Trotman Dickenson (Eds.), Comprehensive Inorganic Chemistry, Vol. 3, Pergamon, Oxford, 1974, pp. 742–767.
3 J.J. Topping, Talanta, 25 (1978) 61.
4 Rajeev, J. Mines Metals Fuels, (1986) 411.
5 N. Cogger, Anal. Chim. Acta, 84 (1976) 143.

6 V. Yatirajam and S. Dhamija, Talanta, 22 (1975) 760.
7 Z. Marczenko, Separation and Spectrophotometric Determination of Elements, Wiley, New York, 1986.
8 B.F. Quinn and R.R. Brooks, Anal. Chim. Acta, 58 (1972) 299.
9 E.P. Welsch, Talanta, 30 (1983) 876.
10 P.E. Thomas and W.F. Pickering, Talanta, 18 (1971) 197.
11 D.N. Wagh, MSc Thesis, University of Bombay, Bombay, 1990.
12 Yu.A. Zolotov, O.A. Shpigun and L.A. Bubchikova, Fresenius' Z. Anal. Chem., 316 (1983) 8.
13 J. Weiss, H.J. Moeckel, A.J. Muller, E. Diemann and H.J. Walberg, J. Chromatogr., 439 (1988) 93.
14 H.C. Mehra and W.T. Frankenberger, Jr., Anal. Chim. Acta, 217 (1989) 383.
15 C.S.P. Iyer and R. Parthsarathy, Radiochem. Radioanal. Lett., 12 (1972) 210.
16 D.N. Wagh, C.S.P. Iyer, D. Joseph and M. Lal, Preprint Volume of ISAS Eighth National Symposium, 9–11 December 1991, pp. 25–27.

Analytica Chimica Acta, 287 (1994) 235–246
Elsevier Science B.V., Amsterdam

On-line monitoring of intracellular enzyme activities with flow-injection analysis

K. Steube and U. Spohn

Institute of Biotechnology, University of Halle-Wittenberg, Weinbergweg 16a, 06120 Halle (Germany)

(Received 3rd September 1993; revised manuscript received 26th October 1993)

Abstract

Micromethods for rapid and reproducible cell disintegration were combined with flow-injection analysis (FIA) to determine intracellular enzyme activities. Flow through chambers were developed for cell disintegration by the action of ultrasonic, ultraturrax and glass microball-mixer mills. A membrane device was incorporated into the FIA set-up to separate the cell debris and the released enzyme from the disintegrated sample solution. After mixing with the corresponding enzyme substrate the assay reaction takes place. The reaction product is transferred into the inlet tube of a fluorescence detector. Dehydrogenase activities were determined in the range of 0.001–2 U/ml with relative standard deviations $< 1\%$ ($n = 4$, $\alpha = 0.05$). The measuring set-up was completed by a chemically sterilized on-line sampling device connected to a bioreactor. Intracellular formate dehydrogenase and malate dehydrogenase were on-line determined to monitor yeast cultivation processes.

Keywords: Enzymatic methods; Flow injection; Cell disintegration micromethods; Intracellular enzymes; On-line sampling; Process monitoring; Yeast cultivation

For optimal control of biotechnological processes their essential biochemical parameters have to be monitored on-line. To control the microbial enzyme production the intracellular activity of the interesting enzymes should be measured [1]. The monoseptic on-line sampling of whole cells and their rapid and reproducible disintegration are the main problems to be solved [2].

Blankenstein and Kula [3] circumvented the cell disintegration step by chemical permeabilization of the cell wall. A selected substrate diffuses into the permeabilized cells and the enzymatically generated products diffuse back into the donor solution of a dialysis cell and from there into the detector flow channel. In this way the removal of solids is accomplished which is necessary for enzyme assays by optical methods. The method is restricted, however to lower molecular weight substrates and products.

Kracke-Helm et al. [4] used a flow-injection method to determine cytoplasmatic β-galactosidase on-line during the cultivation of recombinant *E. coli* in an airlift tower loop reactor. The microorganisms were disrupted ultrasonically. Essential problems such as the limited long term stability of the sonotrodes and the reproducibility of the cell disintegration were not addressed.

Flow-injection analysis (FIA) procedures were developed for the determination of enzyme activities in clinical samples [5–8] and in the media of downstream processing operations, e.g. after large scale cell disruption [9,10]. An important application is the use of fast responding FIA set-ups as postcolumn detectors in chromatographic systems for enzyme separation and purification [8,13–16].

No simple FIA procedures for the fast sequential determination of more than one enzyme ac-

Correspondence to: Dr. U. Spohn, Institute of Biotechnology, University of Halle-Wittenberg, Weinbergweg 16a, 06120 Halle (Germany).

SSDI 0003-2670(93)E0601-3

tivity in the same sample solution has been described previously.

Okuma et al. [17] described a system with two enzyme electrodes for the simultaneous detection of two different enzyme activities. But the peak widths (> 8 min) would not allow a fast enzyme determination under process conditions. The main objective of our work was to develop a robust and fully automated on-line FIA procedure for the determination of different enzyme activities in yeast cells during their fermentation. A miniaturized flow through mixer mill needed to be developed and applied. This disintegration procedure was compared with the ultraturrax and the ultrasonic disintegration on the micro scale.

EXPERIMENTAL

Reagents

Formate dehydrogenase, FDH (EC 1.2.1.2, Sigma, Deisenhofen), formaldehyde dehydrogenase, FAD (EC 1.2.1.46, Boehringer Mannheim) and malate dehydrogenase, MDH (EC 1.1.1.37, Merck, Darmstadt) were used for calibration after standardization. All other chemicals were p.a. grade from Merck.

FIA measuring set-up

Figure 1 shows the fully automated FIA measuring system. The system consists of the on-line sampling device for whole fermentation media with automated chemical sterilization, the cell disintegration chamber CDC and the FIA set-up with the enzyme membrane reactor DZ and the fluorescence detector D (RF 535, Shimadzu, Kyoto).

The sample solution is sucked out of the fermenter or from off-line obtained samples and propelled into the cryostated chamber CDC by pump P1. The sample solution is diluted and conditioned with the optimum pH buffer after switching the 3/2 way magnetic valves MV1 and MV2. After filling the chamber CDC the sample loop SL is automatically and periodically sterilized with 0.5 M NaOH solution. The chamber filling is controlled by the switching periods of the pumps P1, P2 and P3. During the sterilization the disintegration chamber is disconnected by the magnetic valves MV3 and MV4.

Thereafter, and after switching over the valves MV3 and MV4, the disintegrated sample solution flows to the injection valve IV1. After the injection the complete channel from MV1 to IV1 including the chamber CDC is rinsed with 0.025

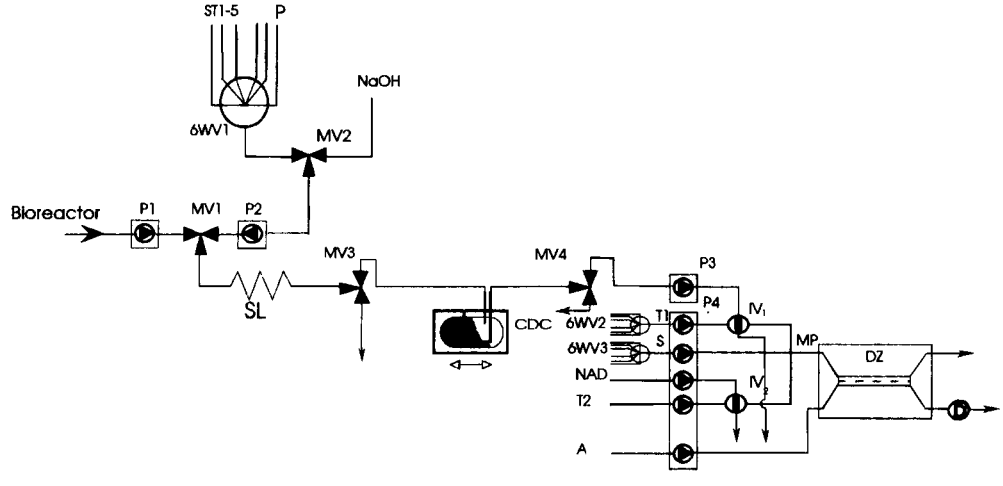

Fig. 1. Automatic FIA set-up for the determination of intracellular enzymes; ST1 = 5 standard solutions, T1 and T2 = carrier buffer solutions, A = acceptor solution, P = rinsing and conditioning buffer, see text for explanation.

M or 0.1 M NaOH for stronger demands to maintain the sterility and to clean the sample conditioning system. Thereafter the system is rinsed with buffer solution P selected by the six-way valve 6WV1. In a timesharing procedure, the FIA determination of the enzyme activity of interest is performed whilst the next sampling procedure takes place.

The automated periodic chemical sterilization of the sampling channel between MV1 and IV1 allows the on-line coupling to sterile cultivation processes.

In the FIA set-up the prepared sample solution is injected simultaneously with the NAD^+ cofactor solution. The cofactor solution NAD^+ is circulated through a sterile 25-ml bottle and the second injection valve IV2.

The six-way valves 6WV2 and 6WV3 select different buffer and substrate solutions. For up to six different enzymes the optimum pH and the corresponding specific substrates could be automatically selected.

Up to six standard solutions including the buffer as zero standard can be selected automatically by means of 6WV1 to calibrate the whole arrangement.

Between the injection valves and the detector D a thin-layer dialysis membrane device DZ is inserted to separate the enzymatically produced NADH from the cell debris and the higher molecular substances injected. A part of the NADH and other lower molecular substances diffuse into the acceptor solution that flows to the detector. The membrane device has a total volume of 50 μl on both sides (channel depth 0.5 mm, width 1.5 mm). Different separation membranes are placed between the two mirror symmetrical plexiglass plates held together only by screws and without additional sealings.

Apart from the sample solution all FIA solutions are propelled by pump P4. The pumps P1–4 are peristaltic pumps (Gilson Minipuls 3, Abimed, Langenfeld).

All sampling steps, the cell disintegration and the FIA system are controlled by a personal computer (IBM/PC 386). The magnetic valves, the six-way valves and the injection valves, the pumps, the corresponding cell disintegration device and the fluorescence detector are connected to a specially designed interface (Institut für Bioprozess- und Analysenmesstechnik, Mytron Heiligenstadt) communicating with the computer.

The FIA peak signals are evaluated by the program FIACCO (Flow Injection Analysis Control and Configuration). The automation of the FIA system and the computer program were described earlier by Spohn et al. [18,19]. The peak heights are measured in mV. Autoscaling and autozero are essential precautions for automatic on-line monitoring of intracellular enzyme activities.

Cell disintegration devices

For reference measurements an MM2 mixer mill with a 1.5-ml standard cell (Retsch, Nr. 22.008.0001, Haan) was used for cell disintegration with glass beads (diameter: 0.5–0.75 mm). The apparatus works with two vibrating arms to which two grinding vessels are screwed. The grinding time can be adjusted by an internal timer in the range 0–60 min. The mixing frequency can be steplessly adjusted from 150 to 1800 min^{-1}. The mixer mill was computer controlled with respect to the on/off switching times.

A flow cell (Fig. 2) was designed to enable on-line disintegrations to be performed. The disintegration chamber is made from stainless steel (V4A, Thyssen). The steel capillaries (inner diameter: 1 mm) S_e and S_o serve as sample inlet and outlet. A thin hole at the head (diameter: 0.3 mm) enables the cell to be deaerated. In earlier experiments the aeration hole was connected with a 30-cm long PTFE tube with an inner diameter

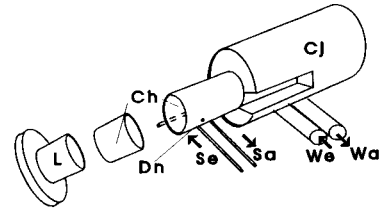

Fig. 2. Experimental through-flow chamber for the microball mixer mill; L = screwing lid, Ch = disintegration chamber, Dn = degassing hole, S_e and S_a = inlet and outlet for the sample solution, W_e and W_a = inlet and outlet for the cooling water, C_j = cooling jacket.

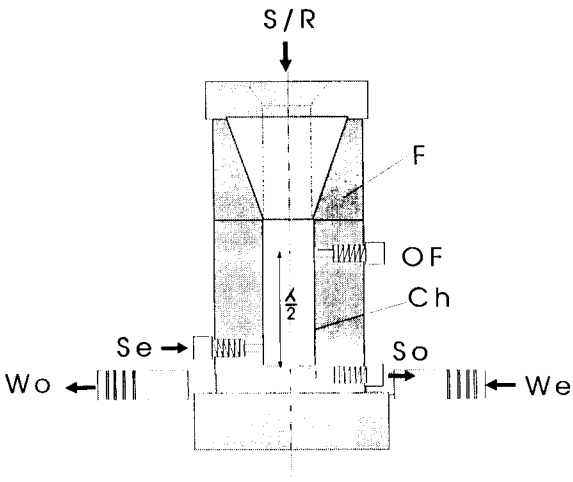

Fig. 3. Experimental through-flow chamber for the ultrasonic and ultraturrax cell disintegration; S/R mounting bore for the sontrode or the ultraturrax rotator, F = funnel lid, OF = overflow, S_e, S_o, W_e, W_o and Ch as in Fig. 2.

of 0.5 mm, which was closed automatically with a magnetic valve after the filling of the disintegration cell. Later this automatic closing set-up was omitted because also without the closing set-up no spillage of enzyme or cleaning solution took place during operation. The disintegration chamber is filled up to 90% with glass beads. The chamber is placed into the cooled jacket CJ connected to the cryostat (HAAKE, D1-G, Karlsruhe).

Another micro-flowthrough chamber had to be developed for ultrasonic and ultraturrax cell disintegration (Fig. 3). The effective chamber volume is 500 μl. The cryostated chamber is made from stainless steel. The upper part is made from plexiglass. Both the rotor of the ultraturrax device (outer diameter 4 mm) and sonotrodes (tip diameter 2 or 4 mm) can be placed axially into the chamber.

The ultrasonic generator HD 20 (Bandelin, Berlin) was used with a titanium sonotrode. The diameter of the diamond apex was 2 mm. The filling level in the disintegration chamber should be half the ultrasonic wavelength. The diameter of the chamber is adapted to the tip diameter of the sonotrode (diameter 4 mm).

The ultraturrax device T5 FU and the disperser S5N-5G (both IKA, Staufen) were used also. The outside diameter of the disperser was 3.8 mm.

Procedures

Cultivation of microorganism. To achieve more universally applicable disintegration procedures the yeast *Hansenula polymorpha* (HD 30, regular collection of the Institut für Biotechnologie Leipzig) was selected because the cell disintegration of the yeast is more difficult compared with other yeasts, e.g. *Saccharomyces* [20]. The mean cell wall thickness lies between 0.2 and 0.12 μm depending on the cell age [21]. The yeast cells were cultivated aerobically in a Biolab fermentor (Braun, Melsungen) at 30°C on a mineral medium (pH 5.0) containing 2% (v/v) methanol [22].

The CO_2 content in the exhaust gas was measured continuously by the on-line gas analyzer URAS 10E (Hartmann and Braun, Mannheim).

Off-line disintegration. The yeast cells were suspended in 0.1 M phosphate buffer (pH 7.5) and disrupted ultrasonically or with the ultraturrax mill. Mechanical disintegration in the microball mixer mill was performed with glass beads for 12 min according to Hummel and Kula [23]. The maximum oscillation frequency was used. Their method was used as the reference method to determine the efficiencies of the ultrasonic and ultraturrax disintegration and the on-line mixer mill procedure.

The disrupted cell samples were centrifuged for 5 min at 12 000 rev. min^{-1} (5200 *g*). The cell free supernatant was used to determine the enzyme activity.

Off-line enzyme assays. The enzyme activities were determined photometrically by measuring the increased concentration of NADH at 340 nm in a 1-cm cuvette with a computer controlled spectrophotometer (UV 2100, Shimadzu, Kyoto).

FDH and FAD activities were determined as described by Schütte et al. [24]. The MDH activity was determined as described by Bergmeyer et al. [25]. The assay was started by the injection of 20 μl disintegrated cell suspension into the corresponding assay mixtures filled into the photome-

ter cuvette (optical pathlength 10 mm, $\lambda_{abs} = 340$ nm) held at 30°C. The assay mixtures were:

(i) FDH: 3 mM NAD^+ and 2 M sodium formate in 0.1 M potassium phosphate buffer with pH 7.5,

(ii) FAD: 3 mM formaldehyde, 6 mM glutathione, 0.1 M sodium phosphate buffer with pH 8.0 and

(iii) MDH: 3 mM NAD^+ and 10 mM L-malate in 0.1 M glycine buffer with pH 10.

The following reactions were used:

$$\text{formate} + NAD^+ \rightarrow CO_2 + NADH + H^+ \quad (1)$$

$$\text{formaldehyde} + NAD^+ + H_2O \rightarrow \text{formate} + NADH + 2H^+ \quad (2)$$

$$\text{L-malate} + NAD^+ \rightleftharpoons \text{oxaloacetate} + NADH + H^+ \quad (3)$$

To determine the degree of disintegration independently of the enzyme deactivation the total protein content was determined by the method of Lowry et al. [26].

RESULTS AND DISCUSSION

FIA determination of enzyme activities

The FIA set-up shown in Fig. 1 can be used to determine up to six different enzyme activities. Without the sampling and the membrane device fast determinations of dehydrogenase activities can be performed (60 injections/h) in model solutions in the determination range between 0.001 and 2 U/ml with relative standard deviations $< 1\%$ ($n = 4$, the statistical significance level $\alpha = 0.05$). The corresponding calibration lines were stable for more than 5 days, thus enabling fast validation of enzyme standard solutions. The enzyme activities were linearly correlated with measured peak heights. In all cases, 20 μl sample or standard solution and 100 μl 30 mM NAD^+ solution were injected simultaneously. The reaction conditions described above are used also in the FIA set-up. The FIA enzyme assays were sequentially performed under their optimum reaction conditions. Both the corresponding enzyme substrate solution and the optimum carrier buffer were automatically selected by the 6-way valves 6WV2 and 6WV3, respectively, at the beginning of the determination of the next enzyme. Up to 20 complete determination cycles including MDH and FDH can be implemented per hour.

After insertion of the membrane device the same enzyme solutions were again analyzed to evaluate the performance of the dialysis cell, which was maintained at 30°C. Two different membrane materials were tested: a regenerated cellulose membrane (cut off 70 000 D, Reichelt, Heidelberg) and a polysulfon membrane (Sartorius, SM 14 659, 30 000 D). Reproducible results were obtained with both membranes. Table 1 summarizes the corresponding regression equations obtained with the polysulfon membrane. The regression lines were also stable for more than 2 days. The long term signal drift was smaller than 1% per day. Similar results were obtained with the cellulose membrane. The enzymes were completely retained by the separation membrane. 75% of the NADH were passing from the donor into the acceptor solution. Both solutions flowed with the rate 0.8 ml min^{-1}. The effective dispersion factors were $D = 19.5$ with and $D = 13.3$ without the membrane device. The FIA set-up provided highly reproducible results with relative standard deviation $< 1\%$ ($n = 4$, $\alpha = 0.05$) for more than 4 weeks.

To enhance the sensitivity, especially to detect small enzyme activities in cell suspensions, the stopped-flow technique was used. The reaction

TABLE 1

Enzyme	Regression line ($\alpha = 0.05$, $n = 5$)
FDH	$y = (2.196 \pm 0.018)$V ml $U^{-1}x - (0.528 \pm 0.011)$mV, $r = 0.998$
FAD	$y = (1.732 \pm 0.012)$V ml $U^{-1}x - (0.179 \pm 0.012)$mV, $r = 0.999$
MDH	$y = (0.540 \pm 0.007)$V ml $U^{-1}x - (0.152 \pm 0.011)$mV, $r = 0.999$

zone formed by the simultaneous injected sample and cofactor solutions was stopped in the dialysis cell. The sensitivity increased almost linearly with stop times up to 180 s. With stop times greater than 30 s the signal stability was significantly deteriorated.

In all cases the FIA determination of the enzyme activities provided a considerably improved precision compared with the classical photometric assay. A simple recalibration with NADH standards, in combination with a linear calibration line for the NADH detection and constant residence times in the FIA channel system, fulfilled the conditions for a reliable enzyme determination procedure. Such procedures may be adapted also for other enzyme assays.

The membrane device (cut off 30 000 D, Sartorius) avoided interferences either by cell debris or by larger molecular substances with the fluorescence detection. The automatic control of the whole system produced high reproducibility under all operating conditions, improving the precision of the enzyme activity determination.

FIA enzyme determinations in cell debris suspensions

Some preliminary investigations showed that the periodic rinsing of the FIA channel system and the separation of the cell debris from the sample solution by dialysis, are essential precautions for precise enzyme activity measurements. Again several membranes were tested for sensitivity, to protein adsorption, clogging and signal stability. The polysulphone membrane showed the best signal stability and the lowest protein adsorption in the presence of cell wall and cytoplasmic debris. This membrane material allows the use of more concentrated NaOH (up to 1 M) for cleaning the FIA channel from the injection valve to the waste outlet.

Up to 15 enzyme determinations could be performed per hour with incorporation of the dialysis cell. The disintegrated cell suspension of *Hansenula anomala* could be analysed over more than 3 days, giving precise and reliable results. After standard additions of known enzyme amounts to the cell suspensions, recoveries between 95 and 102% ($n = 5$, $\alpha = 0.05$) were

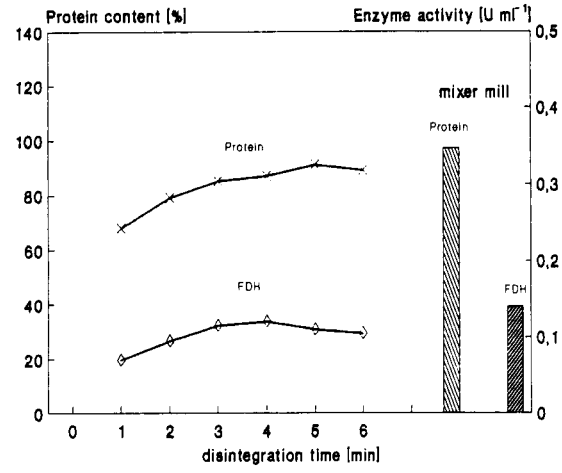

Fig. 4. Dependence of the measured protein content and FDH activity on the ultrasonic disintegration time by an ultrasonic power of 260 W/cm^2 compared to the reference mixer mill disruption.

achieved for FDH, demonstrating a relatively high accuracy.

Determination of intracellular enzyme activities

To find the most appropriate cell disintegration procedure the flow cells for the ultrasonic, the ultraturrax and the ball mixer mill disintegration, described above, were investigated and compared. The released FDH was measured with the FIA set-up shown in Fig. 1.

Ultrasonic disintegration

500 μl of the cell suspension are sonicated in the disintegration cell (Fig. 3). The optimum filling height of the disruption chamber is half the wavelength of the ultrasound. To minimize enzyme deactivation the cell was cooled to 4°C. The optimal sonication time was 3 min for a pulse intensity of 260 W cm^{-2}. The released FDH activity increased with the ultrasonic power density.

Figure 4 shows the dependence of the measured FDH activity and the protein concentration on the disintegration time. Both graphs reach a plateau. The protein plateau corresponds to around 93% of the protein content measured after 6 min disintegration in the mixer mill cell. The results are promising, especially with respect

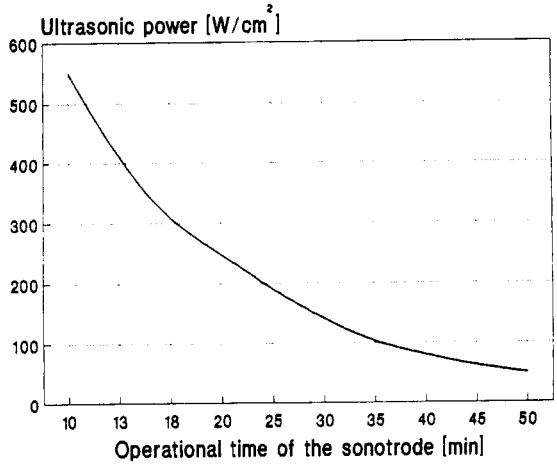

Fig. 5. Dependence of the ultrasonic power input on the operational time.

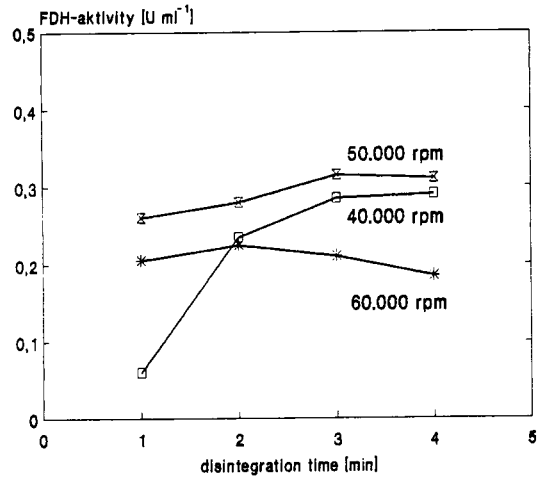

Fig. 6. Dependence of measured FDH activity on the rotation speed of the ultraturrax rotor.

to the recovery of enzyme activity. However the time course of the released protein concentration shows a significant enzyme deactivation.

The main disadvantage of the ultrasonic disintegration is the limited stability of the sonotrodes. The rate of decrease in the power input increases with decreasing tip diameters of the sonotrodes. For a sampling rate of 6 h^{-1} and a disintegration time of 3 min the sonotrode has to be changed after 6 h. Figure 5 shows the dependence of the ultrasonic power input on the time of operation.

Ultraturrax

Figure 6 shows the dependence of the released enzyme activity on the rotation speed of the ultraturrax rotor, which was immersed in the disintegration cell (Fig. 3). The maximum enzyme release was measured after 3 min for a rotational speed of around 50 000 rev. min^{-1}. The enzyme deactivation dominated at higher rotational speeds.

Figure 7 shows the dependence of the released protein concentration and the enzyme activity on the disintegration time. The measured protein concentration were considerably lower than those measured after the mixer mill procedure. Only 60% of the FDH activity could be obtained in comparison with the mixer mill disintegration.

However the reproducibility of both the ultrasonic and the ultraturrax procedure was improved considerably by the automatic control of all procedure steps including the sampling, filling, disintegration, and emptying of the disintegration cell. Also incomplete disintegration procedures worked with an acceptable reproducibility ($< 3\%$, $n = 5$, $\alpha = 0.05$). A constant biomass concentration and the absence of significant changes in the chemical composition (e.g. pH, ionic strength,

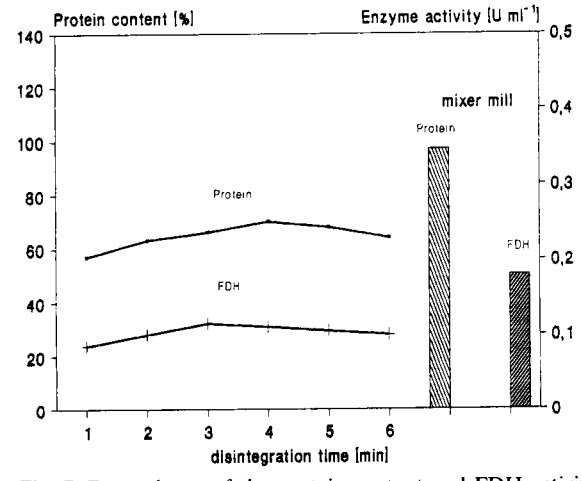

Fig. 7. Dependence of the protein content and FDH activity on the ultraturrax disintegration time for a rotation speed of 5000 U/min compared to the mixer mill disintegration.

surfactants) of the cell suspension medium are necessary precautions. To improve the reliability, the complete release of the intracellular enzyme activities without enzyme deactivation remains the preferred aim. Both the disintegration degree and the enzyme deactivation depend on the cell concentration with changes during the cultivation process.

With respect to the longterm stability and reliability, the ultraturrax procedure is preferred in comparison with the ultrasonic disintegration.

Mixer mill

The effectiveness of wet milling in the mixer mill was influenced by the types of organisms, the mixing frequency, the operation time, the size and the loading volume of the microballs [23,27].

The flow cell (Fig. 2) provided almost the same degree and time of disintegration as the commercially available 1.5-ml cell. The reproducibility of our flow mixer mill was found to be better, because all operational parameters could be exactly defined. An additional advantage is that no external cooling was necessary [24].

The optimal glass beads diameter for the *Hansenula polymorpha* was found to be between 0.5 and 0.75 mm. The working level of the glass beads should lie between 60 and 85% of the disintegration chamber volume. The maximum degree of disruption and the maximum protein concentration were achieved after 9 min.

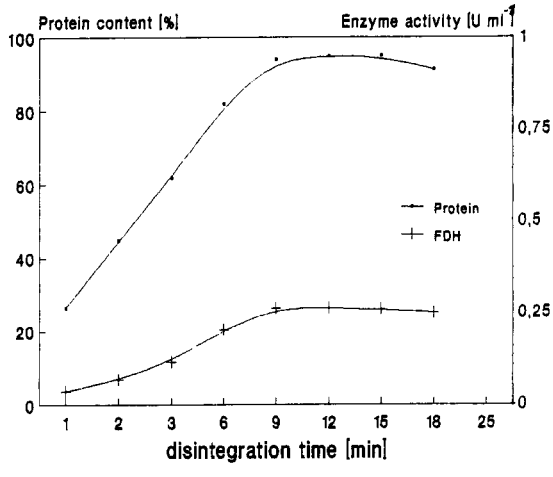

Fig. 8. Dependence of protein content and FDH activity on the mixer mill disintegration time.

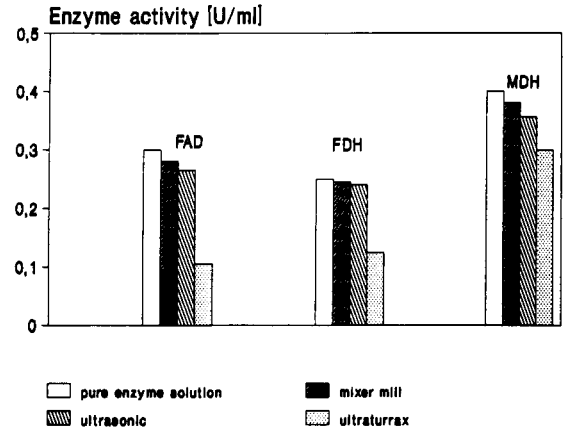

Fig. 9. Dependence of the enzyme desactivation on various methods of disintegration.

Figure 8 shows the time dependence of protein and enzyme activity release. Following a disintegration time of 9 min the enzyme activity remains almost constant for the next 8 min. The deactivation of the FDH was much smaller than during the ultrasonic and ultraturrax disintegration procedures. Figure 9 confirms this on the basis of a comparison of the influence of the three disintegration procedures on the activity of pure FAD, FDH and MDH solutions in 0.1 M potassium phosphate buffer (pH 8). In all three cases the mixer mill procedure caused the lowest degree of deactivation.

Particularly because of this result together with the best long term stability of the mixer mill disintegration, this method is recommended for the on-line coupling to a fermentation process for monitoring.

Figure 10 shows the results for a sequential FIA determination of MDH and FDH in a yeast cell suspension with constant biomass concentration demonstrating the relative small signal drift of the method.

On-line FIA monitoring of FDH during a yeast fermentation process

The flow through mixer mill was inserted between the magnetic valves MV3 and MV4 of the FIA set-up (Fig. 1). The FIA set-up was con-

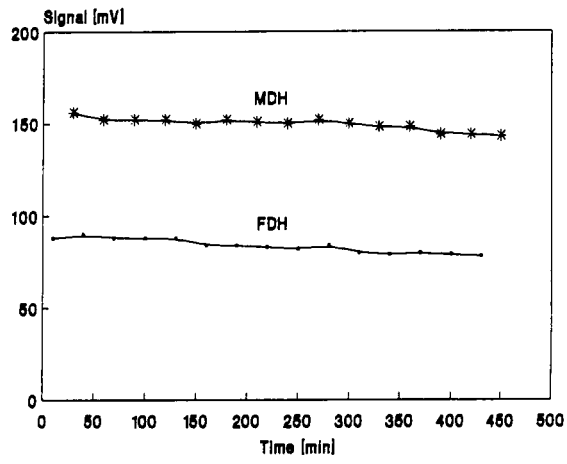

Fig. 10. Sequential FIA determination of MDH and FDH in a yeast cell suspension with constant biomass.

nected by a PTFE tube (0.8 mm i.d.) to the fermentation vessel. The tip of this sampling tube is placed in the vicinity of the stirrer around 5 cm above the bottom of the vessel. The stirrer had 650 rev. min^{-1}. Figure 11 shows the optimized time table for the on-line FIA procedure.

During the sampling process the pump P1 propels the process media with 1.8 ml min^{-1} through the sampling loop. The sampling tube is completely rinsed with fresh sample solution up to the valve MV3 before each determination. The response time T^{90} of the primary sampling system was 30 s up to the valve MV3, which was measured by a conductometric flow detector (flow cell volume 5 μl) after the fast injection of 10 ml 1 M HCl solution into the reactor vessel, which was filled with 2 l distilled water.

P1 pumped 500 μl of the complete fermentation broth into the mixer mill. Thereafter MV3 and MV4 were closed. After the disintegration step the valves were opened. The cell suspension was propelled with P3 to the injection valve. During the stopped-flow FIA determination of the enzyme activity, the disintegration chamber was washed three times with 0.5 M NaOH and then with the conditioning buffer. The mixer mill was also switched on at the moment the cleaning and the buffer solutions flowed into the disintegration cell. Table 2 summarizes the optimized FIA parameters used for the on-line monitoring.

Figure 12 shows the on-line measured intracellular FDH activity dependence on the fermentation time. The measured FDH activities agree with the off-line determined enzyme activities in an interval of $\pm 5\%$. The off-line values were measured by the initial rate method. The enzyme formation correlated with the CO_2 production. When the methanol feed was stopped enzyme

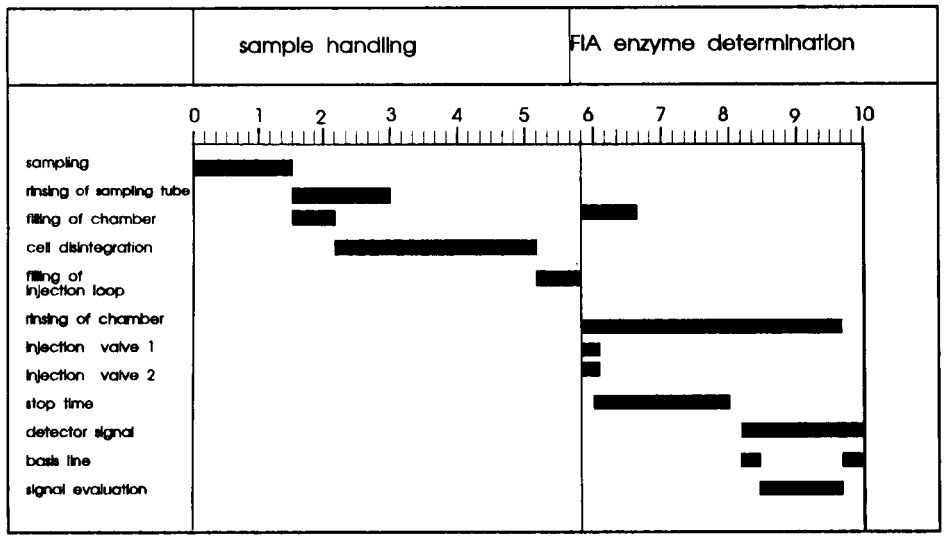

Fig. 11. Time table of sampling, disintegration and FIA system, see text for explanation.

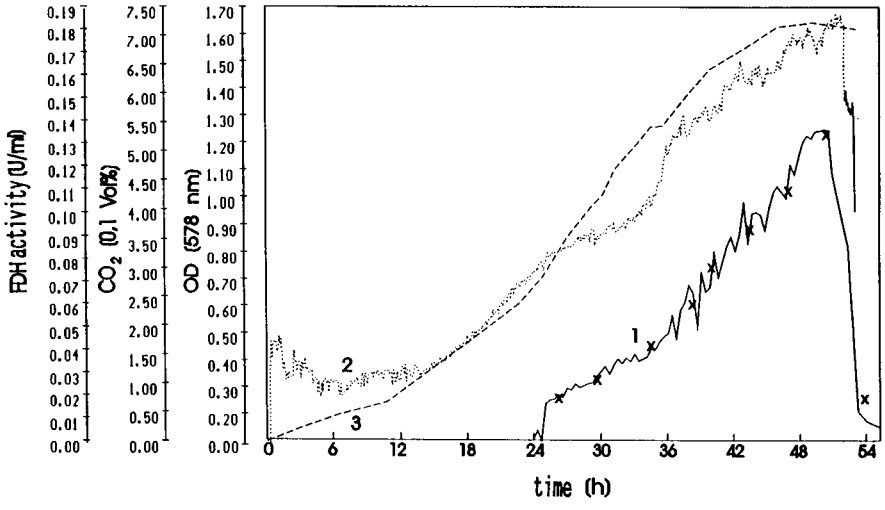

Fig. 12. Plot of the on-line (solid line) and the off-line (×) determined FDH activity (1), the CO_2 content in the exhaust gas (2) and the optical density of the fermentation medium (3) biomass during the fermentation of *Hansenula polymorpha* during the exponential growth phase.

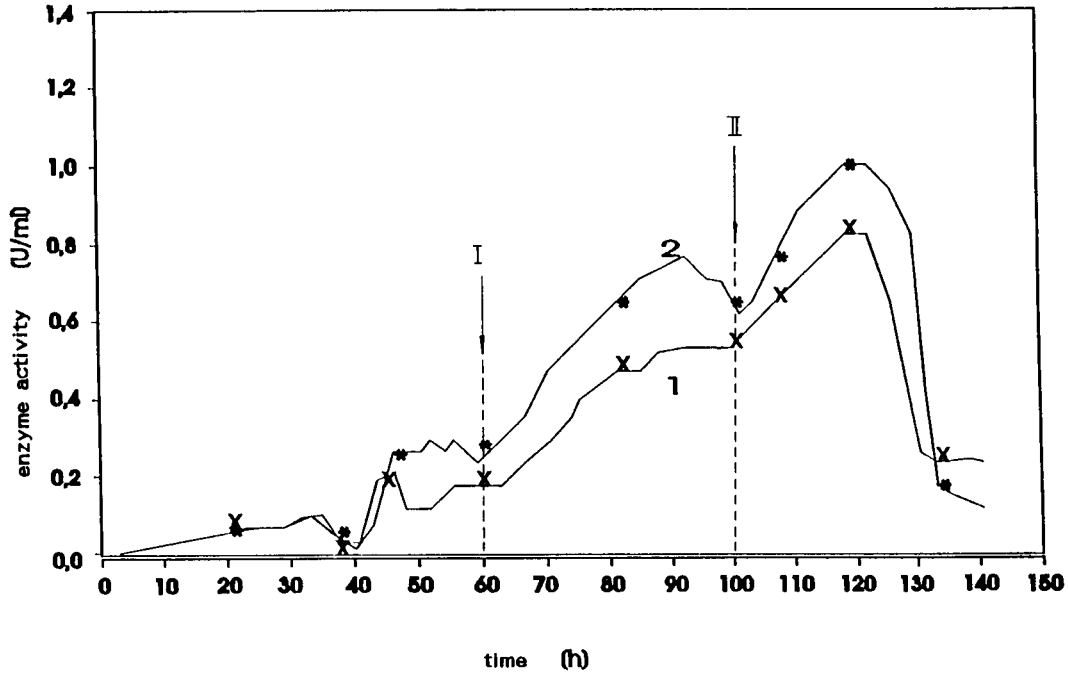

Fig. 13. Plot of the on-line (solid line) and off-line (*, ×) recorded FDH (1) and MDH (2) activity during a 2-l fed-batch fermentation of *Hansenula polymorpha*; I = addition of 75 ml methanol, II = addition of 25 ml methanol.

TABLE 2

Technical data for the FIA system designed to determine FDH in *Hansenula polymorpha* cells after mixer mill disintegration

Disintegration time	9 min
Injection volumes	sample: 20 μl
	NAD^+: 100 μl
Dispersion *D* between IV and D	19,5
Temperature	30°C
Stopped flow time	30 s
Flow rates of carrier, reagent and acceptor solution	0.8 ml min^{-1}
Peak maximum time	12 s
Baseline return	35 s
Measuring frequency	4 cycles h^{-1}

activity and CO_2 production decreased during 4 h to values < 20% of their maximum values. During growth the enzyme activity correlated also with the biomass concentration, which was off-line measured turbidimetrically at 578 nm.

Figure 13 shows the courses of the on-line measured activities of the intracellular FDH and MDH, which show a high degree of similarity. The biosynthesis of both enzymes is coupled with the microbial growth, which is accelerated after the addition of the main substrate methanol.

No significant cell growth or attachment in the sampling tube could be indicated during these cultivations.

Conclusions

Three different intracellular dehydrogenases can be determined by the proposed combination of miniaturized disintegration procedures and FIA. The most reliable results can be obtained using the mixer mill and a flow disintegration cell described here. FDH and MDH can be sequentially determined both in enzyme mixtures and after cell disintegration in yeast homogenate as well as on-line in the process media during batch fermentations of the yeast *Hansenula anomala*. Because yeasts are difficult to disintegrate, the proposed method should be applicable to determine intracellular enzymes in other microorganisms as well.

The authors thank Mr. R. Eberhardt, Institut für Biotechnologie II, Forschungszentrum, Jülich for the software package FIACCO and Mr. B. Fuhrmann for his excellent technical assistance.

REFERENCES

1 K. Schügerl, A. Lübbert and T. Scheper, Chem. Tech., 59 (1987) 701.
2 N. Ahlmann, A. Niehoff, U. Rinas, T. Scheper and K. Schügerl, Anal. Chim. Acta, 190 (1986) 221.
3 G. Blankenstein and M.-R. Kula, Anal. Chim. Acta, 248 (1991) 371.
4 H.-A. Kracke-Helm, L. Brandes, B. Hitzmann, U. Rinas and K. Schügerl, J. Biotechnol., 20 (1991) 95.
5 J.M. Fernandez-Romero, M.D. Luque de Castro and M. Valcarcel, J. Biotechnol., 14 (1990) 43.
6 J.M. Fernandez-Romero and M.D. Luque de Castro, Analyst, 116 (1991) 167.
7 J.M. Fernandez-Romero, M.D. Luque de Castro and M. Valcarcel, Anal. Chim. Acta, 219 (1989) 191.
8 M.D. Luque de Castro and J.M. Fernandez-Romero, Anal. Chim. Acta, 263 (1992) 43.
9 A. Recktenwald, K.-H. Kroner and M.-R. Kula, Enzyme Microb. Technol., 7 (1985) 607.
10 K.-H. Kroner, Fresenius' Z. Anal. Chem., 329 (1988) 718.
11 K.-H. Kroner and M.-R. Kula, Anal. Chim. Acta, 163 (1984) 3.
12 U.E. Giesecke, G. Bierbaum, H. Rudde, U. Spohn and Ch. Wandrey, Appl. Microbiol. Biotechnol., 35 (1991) 720.
13 W.W. Stamm and M.-R. Kula, J. Biotechnology, 14 (1990) 99.
14 K. Takahashi, S. Taniguchi, T. Kurioski, K. Yasuda and T. Sano, Anal. Chim. Acta, 220 (1989) 13.
15 W. Künnecke, H.M. Kalisz and R.D. Schmid, Anal. Lett., 22 (1989) 1471.
16 W.W. Stamm and M.-R. Kula, in G. Durand, L. Bobichon and J. Florent (Eds.), 8th Int. Biotechnology Symp., Soc. Francaise de Microbiologie, Paris, 1988, Abstract Book, S. 178.
17 H. Okuma, H. Takahashi, S. Sekimukai and E. Watanabe, Enzyme Microb. Technol., 13 (1991) 134.
18 U. Spohn, R. Eberhardt, B. Joksch, Ch. Wandrey, R. Wichmann and H. Voss, in R.D. Schmid (Ed.), Flow Injection Analysis (FIA) Based on Enzymes or Antibodies (GBF Monographs, Vol. 14), VCH, Weinheim, 1990, p. 51
19 U. Spohn, R. Eberhardt, J. van der Pol, B. Joksch and Ch. Wandrey, Anal. Chim. Acta, in press.
20 G.H. Petersen, Enzyme Microbiol. Technol., 7 (1985) 339.
21 M.L.F. Giuseppin, H.M.J. van Eijk, M. Hellendoorn and J.W. van Almkerk, Appl. Microbiol Biotechnol., 27 (1987) 31.
22 H. Sahm and F. Wagner, Arch. Microbiol., 84 (1973) 29.

23 W. Hummel and M.-R. Kula, J. Microbiol. Methods, 9 (1989) 201.
24 H. Schütte, J. Flossdorf, H. Sahm and M.-R. Kula, Eur. J. Biochem., 62 (1976) 151.
25 H.U. Bergmeyer, J. Bergmeyer and M. Grassl, Methods of Enzymatic Analysis, Vol. II, VCH, Weinheim, 2nd edn., 1987, pp. 168–171.
26 D.H. Lowry, N.J. Rosenbrough, A.L. Farr and R.J. Randall, Biol. Chem., 193 (1951) 265.
27 H. Schütte and M.-R. Kula, Enzyme Microb. Technol., 10 (1988) 552.
28 B. Bernhardsson, E. Martins and G. Johansson, Anal. Chim. Acta, 167 (1986) 111.

Analytica Chimica Acta, 287 (1994) 247–252
Elsevier Science B.V., Amsterdam

Flow-injection preconcentration of Co(II) on 1-nitroso-2-naphthol-3,6-disulphonate-modified alumina for flame atomic absorption spectrometry

Marek Trojanowicz and Krystyna Pyrzyńska

Department of Chemistry, University of Warsaw, Pasteura 1, 02-093 Warsaw (Poland)

(Received 24th March 1993; revised manuscript received 22nd October 1993)

Abstract

The possibility of using alumina loaded with 1-nitroso-2-naphthol-3,6-disulphonate for the on-line preconcentration of cobalt(II) was investigated. The relatively high capacities of this simply and reproducibly prepared material and the absence of swelling complications allow for its effective use in a flow-injection analysis–atomic absorption spectrometric system. In the time-based system with a 20-min preconcentration time a detection limit of 0.44 $\mu g\ l^{-1}$ was obtained with a precision of 2.3% (R.S.D.) at the 10 $\mu g\ l^{-1}$ level. A 97% recovery was obtained for artificial ocean water spiked with 1 $\mu g\ l^{-1}$ of Co(II). The method was applied to the determination of cobalt in oriental tobacco leaves certified standard material.

Keywords: Atomic absorption spectrometry; Flow injection; Cobalt; Preconcentration; Tobacco; Waters

The growing interest in the use of flow-injection (FI) techniques in atomic spectrometry has been demonstrated in several reviews [1–4] and a book [5]. Flow-injection sample processing coupled with flame atomic absorption spectrometry (FI–FAAS) offers improvements in detectability and selectivity. This sample pretreatment mode also allows the elimination of chemical matrix interferences and rivals the sensitivity and speed of AAS with electrothermal atomization (ETA-AAS). Moreover, in ETA-AAS the matrix components often cause interferences in practical analytical procedures. As has been reported, the excess of chlorine is responsible for losses of cobalt as chloride and also for the formation of a compound with graphite [6]. Perchloric and sulphuric acid, used for mineralization of biological material, significantly change the mechanism of cobalt atomization [6]. Volland et al. [7] stated that, in addition to other factors, the graphite surface and gas impurities influence the results of cobalt determination by ETA-AAS.

Flow-injection systems for Co(II) preconcentration can be classified into two groups with respect to the method of sample delivery. In the systems with volume-based loading a defined volume of the sample solution is introduced using the injection valve [8–12], whereas in the systems with time-based loading the sample solution is pumped at a constant flow-rate in an appropriate time interval through the microcolumn [10,13–16]. In FI measurement for preconcentration of cobalt, commercial chelating resins such as Chelex 100 or Muromac A-1 are mostly used. Other sorbents include quinolin-8-ol immobilized on controlled-porosity glass (CPG) [10,14,15] or on silica [11,20,21] and also non-polar sorbents such as Amberlite XAD modified with chelating ligands [16]. The efficiency of a Chelex 100 microcolumn for Co(II) was only 45–60%, so this sys-

Correspondence to: M. Trojanowicz, Department of Chemistry, University of Warsaw, Pasteura 1, 02-093 Warsaw (Poland).

SSDI 0003-2670(93)E0597-Z

tem has limited application to relatively clean samples [17]. Difficulties created by the swelling and shrinking properties of Chelex 100 when acids were used in the mobile phase have been reported [8]. CPG-immobilized quinolin-8-ol has sufficient mechanical and kinetic properties for FI systems. However, it has a relatively low exchange capacity, which apparently is the reason for its low tolerance to interferences [1]. For example, a strong influence of the presence of excess of Zn was observed in Co(II) preconcentration [10]. Amberlite XAD polymer adsorbents required a minimum of two successive elutions to release the preconcentrated metal [16].

In this study, alumina was used for the on-line preconcentration of cobalt. Depending on the solution pH, activated alumina can function as either a cation or an anion exchanger. The effectiveness and versatility of activated alumina have been demonstrated for the preconcentration of lead [12,22], cadmium [23], sulphates [24] and chromium [25,26]. Acidic activated alumina has also been used for the speciation determination of Cr(III) and Cr(VI) in water samples [27,28]. The possibility of the immobilization of several complexing reagents (sulphoderivatives of aromatic ligands) on alumina for the separation of cations has been investigated by Brajter and Dabek-Złotorzyńska [29].

The aim of this work was to examine the possibility of using alumina modified with nitroso-R-salt (NRS) for the on-line preconcentration of cobalt in system with FAAS detection. It is based on the formation of a very stable Co(III)–NRS complex in acidic medium that prevents the retention of the complexes of other cations. NRS has been used in the spectrophotometric determination of cobalt [30]. The effect of different experimental parameters (e.g., flow-rates during preconcentration and the elution step and column dimensions) were studied in detail.

EXPERIMENTAL

Apparatus

A Zeiss Jena Model AAS-30 atomic absorption spectrometer was used. The hollow-cathode lamp for cobalt was operated at 6 mA and the spectrometer was set to 240.7 nm with a slitwidth of 1.0 nm. A standard air–acetylene nebulizer–burner system was operated at the gas flow-rates recommended by the manufacturer. The nebulizer uptake rate was adjusted to give the optimum response for conventional sample aspiration. Time-resolved absorbance signals of the elution peak for cobalt were displayed on the monitor and printed together with integrated absorbance values.

Reagents

The alumina used was acid alumina for column chromatography with Brockmann activity I, a specific surface area of 186 $m^2\ g^{-1}$ and an average pore diameter of 41 Å. It was repeatedly washed with hot water and finally air-dried.

Analytical-reagent grade chemicals were used for the preparation of all solutions with deionized water obtained from a Milli-Q system (Millipore, Bedford, MA).

Solution of disodium 1-nitroso-2-naphthol-3,6-disulphonate (nitroso-R-salt, NRS) was prepared by dissolving the commercial reagent (POCh, Gliwice, Poland) in deionized water.

Working standard cobalt solutions were prepared by appropriate dilution of a 1000 mg l^{-1} stock standard solution from Merck.

Procedure

The FI systems used, shown schematically in Fig. 1, consisted of an MS/4 Reglo peristaltic pump from Ismatec (Zurich, Switzerland) and a

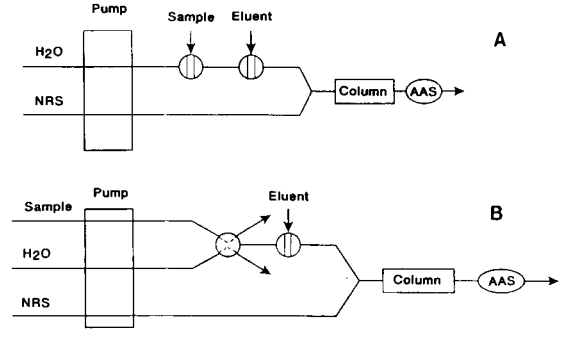

Fig. 1. Schematic diagrams of the flow-injection systems used: (A) volume-based system; (B) time-based system.

laboratory-made rotary injection valve with exchangeable sample loops. The connecting PTFE tubings were of 0.8 mm i.d. The flow systems used were operated in the volume-based (Fig. 1A) or time-based mode (Fig. 1B). A microcolumn was prepared from a glass tube of 2.5 mm i.d. The length of the alumina bed was 20 or 50 mm. Deionized water served as the carrier stream. NRS solution (5 mM) was pumped continuously through the microcolumn at a flow-rate of 3 ml min^{-1} in order to modify the alumina surface. After preconcentration of the analyte on the column, elution was done by injection of sodium hydroxide solution. An interval of 40 s was necessary before commencement of the next sorption–elution cycle to immobilize a new portion of ligand.

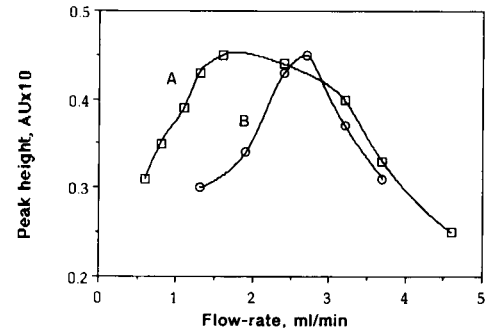

Fig. 2. Effect of flow-rate during (A) preconcentration and (B) elution in the volume-based system on the magnitude of the flow-injection response. A 1-ml volume of 3 mg l^{-1} Co(II) solution was used for preconcentration and 0.2 ml of 0.1 M NaOH for elution. Column length, 20 mm.

RESULTS AND DISCUSSION

Optimization of sorption and elution of cobalt

It has already been observed that the column dimensions and sample loading flow-rate are critical factors for the complete retention of trace metal ions [10]. Under conditions of complete retention, the performance of a system is less likely to be affected by small variations in microcolumn packing and flow-rates or by the presence of other metal ions that compete for the ion-exchange sites. Retention is increased with lower sample loading flow-rates and longer columns. However, lower flow-rates for sorption of the analyte decrease the sample throughput and longer column bed volumes worsen the detection limit owing to increased dispersion.

Studies of the effect of the flow-rate during preconcentration and elution on the magnitude of the cobalt flow-injection response were conducted with the volume-based system. Optimum flow-rates of 1.6 ml min^{-1} for Co(II) preconcentration and 2.7 ml min^{-1} for elution were assumed (Fig. 2). The decrease in the elution efficiency at higher flow-rates suggests that the contact time between the eluent and the modified alumina is of great importance.

Optimization of the volume and concentration of sodium hydroxide used as the eluent was also carried out. The smallest volume of eluent sufficient for complete recovery of retained cobalt was 0.1 ml of 0.3 M or 0.2 ml of 0.1 M NaOH.

The effect of the sample pH on the cobalt response was investigated over the range 2–10. As expected, the maximum retention of cobalt occurs in acidic media. The adjustment of the sample solution pH to the optimum value for the complete retention of cobalt can be achieved by mixing the aspirated sample solution with 0.01 M HCl or using nitroso-R-salt solution at pH 2.0. The latter approach is more convenient and was used in further studies.

Analytical performance of optimized flow-injection system

Regarding the possibility of an improvement in the analytical detectability of cobalt by the flow sample processing with preconcentration on a alumina microcolumn, the time-based system shown in Fig. 1B is much more convenient. The volume of sample introduced into the system at a constant flow-rate is determined by the time interval of sampling.

In the time-based system, a relationship between absorbance and preconcentration times from 2 to 20 min was examined for 20 and 100 μg l^{-1} cobalt solutions. Preconcentration was performed using a 20 × 2.5 mm i.d. microcolumn at a flow-rate of 1.6 ml min^{-1}, whereas elution was done with 0.2 ml of 0.1 M NaOH at 2.7 ml min^{-1}.

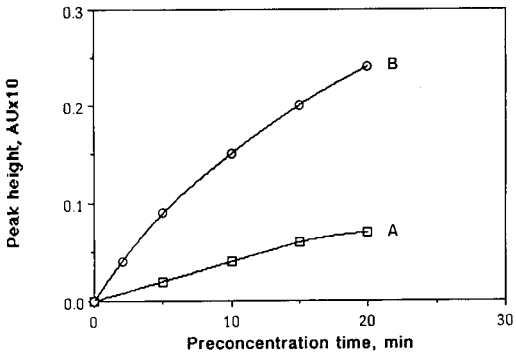

Fig. 3. Effect of preconcentration time on FI–AAS cobalt determination with an NRS-modified alumina microcolumn at a flow-rate of 1.6 ml min^{-1} in the preconcentration phase. Concentration of Co(II) solutions: (A) 20 and (B) 100 $\mu g\ l^{-1}$.

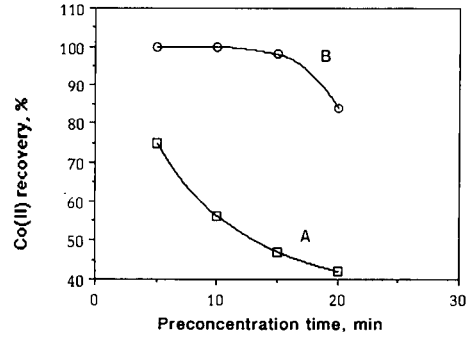

Fig. 4. Effect of length of microcolumn with NRS-modified alumina on sorption efficiency during preconcentration of a 50 $\mu g\ l^{-1}$ solution of Co(II) at a flow-rate of 2.4 ml min^{-1}. Column length: (A) 20 and (B) 50 mm (i.d. 2.5 mm).

The extent of linearity of response versus time depends on the concentration of Co(II) in the sample (Fig. 3). With increase in cobalt concentration the fraction of metal retained on the microcolumn decreases. Sorption efficiencies of 93% and 39% were achieved when 20 and 100 $\mu g\ l^{-1}$ solutions of Co(II), respectively, were pumped through the column at a flow-rate of 1.6 ml min^{-1} for 20 min. The loss of analyte does not result, however, in a serious decrease in the enrichment factor or precision, as the losses may be reproducible for both sample and standard in the FI system. However, under such conditions, the results are more likely to be affected by the sample matrix and interferences from competing species.

The effect of column length on the preconcentration of cobalt was also examined. Two columns, 20 and 50 mm long, were prepared, both with the same i.d. of 2.5 mm. An increase in the length of the column enhances the observed signal and increases the effectiveness of sorption (Fig. 4, Table 1).

In order to determine the breakthrough of retention of the microcolumn for cobalt preconcentration, 0.70 g of alumina was used for packing. A 50 $\mu g\ l^{-1}$ Co(II) solution was preconcentrated for 10 min. The recovery of cobalt at a flow-rate of 2.4 ml min^{-1} was $101 \pm 4\%$, which corresponds to 1.71 mg per gram of alumina. The breakthrough capacity for Co sorbed on the NRS–Al_2O_3 evaluated with the manual column preconcentration technique was 1.0 mg g^{-1} [29]. A much smaller retention capacity of the Chelex 100 microcolumn towards cobalt, 0.006 mg g^{-1} dry resin, was shown earlier [9].

For the alumina microcolumn modified with NRS, the effect of alkali, alkaline earth and heavy metal ions on the sorption of Co(II) was examined. Solutions of 50 $\mu g\ l^{-1}$ Co(II) containing a given level of the other metal ions were pumped through the preconcentration column at a flow-rate 2.4 ml min^{-1}. This was followed by elution with 0.2 ml of 0.1 M NaOH. The signal obtained was compared with that observed for a Co(II) solution in the absence of other metal ions (Table 2). No significant changes in the monitored signals were observed. These results suggest a preferred uptake of cobalt also in the presence of Fe(III), Cu(II) or Ni(II), which form stable complexes with NRS. A strong influence of of Fe(III)

TABLE 1

Effect of length of microcolumn with NRS-modified alumina on sorption efficiency during preconcentration of a 50 $\mu g\ l^{-1}$ solution of Co(II) at a flow-rate of 2.4 ml min^{-1}

Column length (mm)	Co recovery (%)		
	5 min [a]	10 min [a]	20 min [a]
20	75	56	42
50	100	100	84

[a] Preconcentration time.

TABLE 2

Effect of the presence of other metal ions on the recovery of Co(II) preconcentrated from a 50 $\mu g\ l^{-1}$ solution on NRS-modified alumina with a preconcentration time of 10 min at a flow-rate of 2.4 ml min^{-1}

Metal added	Concentration ($mg\ l^{-1}$)	Co(II) recovery (%)
Na	500	102
K	500	100
Ca	100	105
Mg	50	101
Pb(II)	1	103
Mn(II)	1	100
Cu(II)	1	98
Zn(II)	1	102
Cd(II)	0.5	101
Ni(II)	1	97
Al(III)	0.5	99
Fe(III)	5	106
Cr(III)	0.5	99
Cr(VI)	0.5	103

and Al on the cobalt recovery was observed for immobilized quinolin-8-ol on porous glass [14]. A longer column with a sufficient resin capacity or the addition of citrate to the carrier solution was necessary to avoid this problem. Citrate solution was also used for removing the interferences from Fe(III) during preconcentration of Co(II) on a Chelex 100 microcolumn [9]. Insufficient effectiveness of Co(II) sorption on the chelating resin Muromac A-1 in the presence of Ni, Cu and Al has been reported [19], whereas the presence of excess of Mg results in an increase in the recovery of cobalt.

An important aspect of the developed method was to demonstrate the preconcentration capability of the FI system for the determination of Co(II) at trace levels. Calibration graphs with a 20-min preconcentration at various sampling flow-rates using a 50 × 2.5 mm i.d. microcolumn are presented in Fig. 5. Satisfactory linearity of response was observed up to 20 $\mu g\ l^{-1}$ of cobalt for preconcentration carried out at 2.4 ml min^{-1} with a correlation coefficient of 0.9956. The detection limit, calculated as three times the standard deviation of the blank signal for deionized water, with a 20-min sampling time was 0.44 $\mu g\ l^{-1}$. The relative standard deviation ($n = 6$) at the 10 $\mu g\ l^{-1}$ level was 2.3%. The sensitivity enhacement compared with conventional continuous nebulization was 300. Higher enrichment factors are impractical because of the long sampling times.

In previously published papers on FI–AAS using microcolumn preconcentration, the detection limit for Co with Chelex 100 was estimated as 20 $\mu g\ l^{-1}$ [9], with Muromac A-1 chelating resin 2.9 $\mu g\ l^{-1}$ [19], and with immobilized quinolin-8-ol 0.2 $\mu g\ l^{-1}$ [15]. However, in the last work the matrix effects on cobalt retention were not examined. The study with preconcentration of Cu on Pyrocatechol Violet (PV)-loaded XAD-2 resin indicated the significant role of experimental parameters such as preconcentration time, flow-rate and the size of the column on the detection limit for time-based FI–AAS measurements [31].

Determination of Co in natural samples

The proposed FI–AAS system with on-line preconcentration of cobalt on NRS-modified alumina was applied to the determination of Co(II) in oriental tobacco leaves certified reference material (CTA-OTL-1) (Institute of Nuclear Chemistry and Technology, Warsaw, Poland). For sample preparation microwave-assisted digestion with a mixture of nitric and perchloric acid was employed. The results of the analysis with different weights of CTA-OTL-1 sample are given in Table 3. The mean value of 0.85 $\mu g\ g^{-1}$ of cobalt is in

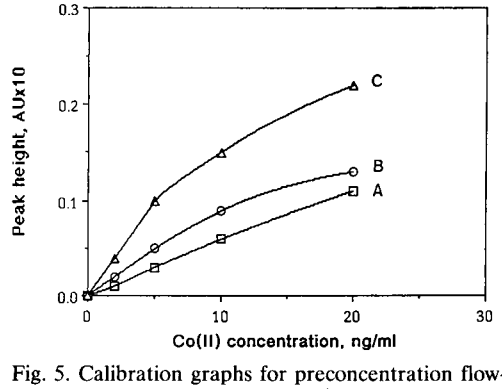

Fig. 5. Calibration graphs for preconcentration flow-rate: (A) 2.4, (B) 3.0 and (C) 6.0 ml min^{-1} using a 50-mm NRS-modified alumina microcolumn. Preconcentration time, 20 min. Elution with 0.2 ml of 0.1 M NaOH at 2.7 ml min^{-1}.

TABLE 3

Analysis of CTA-OTL-1 oriental tobacco leaves certified referenced material [a] by the proposed FIA method

Sample taken (g)	Co found ($\mu g\ g^{-1}$)
0.1489	0.82
0.1545	0.86
0.1627	0.84
0.1803	0.88
Mean	0.85 [b]

[a] Certified Co content, 0.88 ± 0.04 mg/l. [b] R.S.D. = 3.5%.

good agreement with the certified value of $0.88 \pm 0.04\ \mu g\ g^{-1}$.

In order to evaluate possible effects from a more complicated matrix, the recovery of cobalt added to artificial ocean water [32] was also studied. A 97% recovery was obtained for addition of $1\ \mu g\ l^{-1}$ of Co(II). The reproducibility was satisfactory, with a relative standard deviation of 3.3% ($n = 5$). These results indicate that the proposed method is essentially free from interferences when applied to the analysis of saline waters.

Conclusion

The proposed FI system with on-line preconcentration coupled with FAAS provides good selectivity and sensitivity for the determination of cobalt in natural samples. Preconcentration–separation using NRS-modified alumina proved to be an efficient and convenient way to overcome the interferences from matrix elements.

REFERENCES

1 Z. Fang, Spectrochim. Acta Rev., 14 (1991) 235.
2 V. Carbonell, A. Salvador and M. de la Guardia, Fresenius' J. Anal. Chem. 342 (1992) 529.
3 M. Trojanowicz and E. Olbrych-Sleszyńska, Chem. Anal. (Warsaw), 37 (1992) 111.
4 J. Alienza, M.H. Herrero, A. Maqueira and R. Puchades, CRC Crit. Rev. Anal. Chem., 23 (1992) 1.
5 J.L. Burguera (Ed.), Flow injection Atomic Spectroscopy, Dekker, New York, 1989.
6 A. Hulanicki, R. Karwowska and J. Sowiński, Talanta, 28 (1981) 455.
7 G. Volland, G. Kolblin, P. Tschopel and R. Tolg, Fresenius' Z. Anal. Chem., 284 (1977) 1.
8 S. Olsen, L.C.R. Pessedena, J. Ruzicka and E.H. Hansen, Analyst, 108 (1983) 905.
9 M.C. Valdes-Hevia y Temprano, J.P. Parajon and M.E.D. Garcia, Analyst, 116 (1991) 1141.
10 Z. Fang, S. Xu and S. Zhang, Anal. Chim. Acta, 200 (1987) 35.
11 M.A. Marshall and H.A. Mottola, Anal. Chem., 57 (1985) 729.
12 C.W. McLeod, J. Anal. At. Spectrom., 2 (1987) 549.
13 S.D. Hartenstein, G. Christian and J. Ruzicka, Can. J. Spectrosc., 30 (1985) 144.
14 F. Malamas, M. Bengtsson and G. Johansson, Anal. Chim. Acta, 160 (1984) 1.
15 Z. Fang, Z. Zhu, S. Zhang, S. Xu, L. Guo and L. Sun, Anal. Chim. Acta, 214 (1988) 41.
16 V. Porta, O. Abollino, E. Mentasi and C. Sarzanini, J. Anal. At. Spectrom., 6 (1991) 119.
17 S.D. Hartenstein, J.Ruzicka and G.D. Christian, Anal. Chem., 57 (1985) 21.
18 S. Carrolli, A. Alimonti and F. Petrucci, Anal. Chim. Acta, 248 (1991) 241.
19 S. Hirata, K. Honda and T. Kumamaru, Bunseki Kagaku, 36 (1987) 678.
20 C.M. Sakamoto-Arnold and K.S. Johnson, Anal. Chem., 59 (1987) 1789.
21 D. Beauchemin and S. S. Berman, Anal. Chem., 61 (1989) 1857.
22 Y. Zhang, P. Riby, A.G. Cox and C.W. McLeod, Analyst. 113 (1988) 125.
23 A. Karakaya and A. Taylor, J. Anal. At. Spectrom., 4 (1989) 261.
24 A.G. Cox, C.W. McLeod, D.L. Miles and I.G. Cook, J. Anal. At. Spectrom., 2 (1987) 553.
25 A.G. Cox, I.G. Cook and C.W. McLeod, Analyst, 110 (1985) 331.
26 A.G. Cox and C.W. McLeod, Anal. Chim. Acta, 179 (1986) 487.
27 S. Ahmad, R.C. Murthy and S. V. Chandra, Analyst, 115 (1990) 287.
28 M. Sperling, S. Xu and B. Weltz, Anal. Chem., 64 (1992) 3101.
29 K. Brajter and E. Dabek-Zlotorzyńska, Talanta, 37 (1990) 613.
30 D.W. Dewey and H.R. Marston, Anal. Chim. Acta, 57 (1971) 45.
31 A. M. Naghmush, M. Trojanowicz and E. Olbrych-Sleszyńska, J. Anal. At. Spectrom., 7 (1992) 323.
32 Annual Book of ASTM Standards, Vol. 11.02, ASTM, Philadelphia, PA, 1986, D 1141-75, pp. 550–551.

Analytica Chimica Acta, 287 (1994) 253–258
Elsevier Science B.V., Amsterdam

Electrochemical enzyme immunoassay using sequential saturation technique in a 20-μl capillary: digoxin as a model analyte

Noriaki Kaneki [1], Yan Xu [2], Anu Kumari, H. Brian Halsall and William R. Heineman
Department of Chemistry, University of Cincinnati, Cincinnati, OH 45221-0172 (USA)

Peter T. Kissinger
Department of Chemistry, Purdue University, West Lafayette, IN 47907 (USA)

(Received 25th February 1993; revised manuscript received 15th October 1993)

Abstract

Capillary enzyme immunoassay with flow-injection analysis for digoxin using the sequential saturation technique has been developed. Glass capillary tubes (10 cm × 0.53 mm i.d.) with immobilized digoxin antibody were used as the immunoassay reactor. The product of enzymatic reaction, 4-aminophenol, was detected amperometrically. The digoxin and the labeled digoxin binding reaction with the immobilized digoxin antibody were completed in 2 and 10 min, respectively. Digoxin was determined in a 20-μl sample with a detection limit of 10 pg ml^{-1} (200 fg or 260 attomoles) and a 3 orders of magnitude range.

Keywords: Amperometry; Enzymatic methods; Immunoassay; Digoxin; Sequential saturation technique

Electrochemical enzyme immunoassays have evolved dramatically during the past decade. These assays are a combination of an immunoassay procedure with an electrochemical determination of the product of the enzymatic reaction [1]. Electrochemical enzyme immunoassays have low detection limits and a wide range [1–7]. In the initial development of these immunoassays, plastic cuvettes were mainly used as the immunoassay reaction vessel [2,3]. However, the geometry of these cuvettes gives a relatively poor surface area to volume ratio. Since the antibody–antigen reaction for a heterogeneous assay occurs only at the surface, as does the enzyme catalysis, the design of the cuvette is inefficient with respect to mass transport of reactants to the surface and dilution of enzyme-generated product. Recently, the microcapillary immunoreactor, which has a relatively large surface area to volume ratio, has been adapted for immunoassay to improve assay sensitivity and speed [4–10]. Thus far, we have demonstrated this electrochemical capillary immunoassay for the determination of high-molecular-weight compounds (proteins) by sandwich immunoassay, with detection limits as low as 4 zeptomoles [4–6].

Correspondence to: W.R. Heineman, or H.B. Halsall, Department of Chemistry, University of Cincinnati, Cincinnati, OH 45221-0172, USA.
[1] Current address: Department of Computer Science and Systems Engineering, Muroran Institute of Technology, Mizumoto, Muroran 050 (Japan).
[2] Current address: Department of Chemistry, Cleveland State University, Cleveland, OH 44115 (USA).

SSDI 0003-2670(93)E0612-B

The objective of the present research was to develop sequential saturation capillary enzyme immunoassay as an analytical method having a low detection limit for low-molecular-weight compounds such as therapeutic drugs. The sandwich immunoassay that we previously demonstrated is not applicable to low-molecular-weight compounds. Digoxin was chosen as a model compound, alkaline phosphatase (EC 3.1.3.1) as the labeling enzyme, and fused silica capillary (10 cm × 0.53 mm i.d.) as the immunoreactor. Digoxin, a steroidal cardiac glycoside, has a relatively narrow therapeutic range from 0.5 to 2.0 ng ml^{-1} [11]. Alkaline phosphatase catalyzes the conversion of *p*-aminophenyl phosphate (PAPP) to *p*-aminophenol (PAP), which can be detected electrochemically by oxidation [3,12].

The increased surface area to volume ratio of the microcapillary reactor increases undesirable nonspecific interactions between the enzyme conjugate and components of the immunoreactor other than the antibody paratope. An effort was made therefore to limit access of the conjugate to the silica matrix of the capillary wall by using polyethylene glycol as both a coating and extender for the attachment of the capture antibody.

EXPERIMENTAL

Apparatus

The flow-injection amperometric detection system used for this work was a model BAS 400 LCEC system (Bioanalytical Systems, West Lafayette, IN) without a separation column. The thin-layer electrochemical cell had dual glassy carbon working electrodes (only one of which was used), a Ag/AgCl (3 mol l^{-1} NaCl) reference electrode, and a stainless-steel auxiliary electrode. The injection volume was 5 μl, and the flow rate was 1.0 ml min^{-1}.

Materials

Digoxin was purchased from Calbiochem-Behring (La Jolla, CA). Digoxin–alkaline phosphatase conjugate (EC3.1.3.1) was from Immunotech (Cambridge, MA). Digoxin antibody in goat serum was a gift from the Centers for Disease Control (Atlanta, GA). The goat antidigoxin antisera was partially purified using a Sephadex G-25-80 (1 × 48 cm) column with 0.02 M sodium acetate (pH 5.5). *p*-Aminophenyl phosphate was synthesized using reported procedures [13,14]. Sephadex G-25-80, polyethylene glycol (average mol.wt. 3350), adipic acid dihydrazide, boron trifluoride etherate, bovine serum albumin fraction V powder (BSA), and D-glucose were from Sigma (St. Louis, MO). 3-Glycidoxypropyltrimethoxysilane, sodium periodate, tris(hydroxymethyl) aminomethane and 1,1′-carbonyldiimidazole were from Aldrich (Milwaukee, WI). 1,4-Dioxane, sodium acetate, Tween 20, magnesium chloride, and sodium chloride were from Fisher Scientific (Cincinnati, OH). Sodium azide was obtained from Eastman (Rochester, NY). Undeactivated fused-silica capillary (10 cm × 0.53 mm i.d.) was from J&W Scientific (Folsom, CA).

Buffers and solutions

The following aqueous buffer solutions were used. Buffer A1: 0.1 M sodium acetate–acetic acid, pH 5.5. Buffer A2: 0.1 M sodium acetate–acetic acid and 0.15 M sodium chloride, pH 5.5. Buffer A3: 0.1 M sodium acetate–acetic acid, 0.15 M sodium chloride and 0.02% (w/v) sodium azide, pH 4.5. Buffer B: 1 M sodium bicarbonate–sodium hydroxide, pH 10. Buffer C: 0.1 M tris(hydroxymethyl)aminomethane, 1 mM magnesium chloride, and 0.02% (% w/v) sodium azide, pH adjusted to 9.0 by hydrochloric acid. Krebs-Ringer (K–R) solution: 138 mM sodium chloride, 11 mM sodium bicarbonate, 5 mM potassium chloride, 1 mM dihydrogen phosphate, 1 mM calcium chloride, 1 mM magnesium chloride, 11 mM glucose, 0.02% (w/v) sodium azide and 1% (w/v) BSA, pH 7.1. Glycidoxypropyltrimethoxysilane (GPTMS) solution: 375 μl GPTMS in 35 ml buffer A1. PEG solution: 35 ml of 5 mM PEG in dioxane with 800 μl boron trifluoride etherate. 1,1′-Carbonyldiimidazole (CDI) solution: 1 mM CDI in 6 ml of 1,4-dioxane. Adipic acid dihydrazide (AADH) solution: 4.5 mmol AADH and 8 ml of 1 M carbonate buffer, pH 10.

Preparation of microcapillary immunoreactor

Microcapillaries (10 cm × 0.53 mm i.d.) were used as immunoreactors after the inner surface was modified by covalent attachment of digoxin

antibody. The antibody was immobilized at the inner surface according to the procedure of Kumari [15], which involves covalent attachment via the IgG glycan chains using a polyethylene glycol linker:

(A) Antibody oxidation. The lyophilized antibody was dissolved in buffer A2 and the antibody solution oxidized with 0.4 M sodium periodate for 20 min. The oxidized antibody was desalted by passing through a Sephadex G-25-80 column in buffer A3.

(B) Immobilization. The microcapillaries were pretreated with 1 M sodium hydroxide and 1 M hydrochloric acid and were rinsed with buffer A1. The capillaries were filled with GPTMS solution and heated at 90°C for 5 h. After rinsing the capillaries with 1,4-dioxane, PEG solution was pipetted into the capillaries and incubated at 90°C for 0.5 h. After rinsing with 1,4-dioxane, the capillaries were filled with CDI solution and left at room temperature for 15 min. AADH solution was pipetted into the capillaries and incubated at 4°C overnight. The antibody was covalently attached to this surface by pipetting the oxidized antibody solution into the capillaries and incubating overnight.

Immunoassay procedure

The general assay protocol is outlined in Fig. 1. The microcapillary immunoreactor was used in a sequential saturation enzyme immunoassay. Krebs-Ringer solution was used to prepare samples and for blocking and rinsing because it is a suitable perfusion solution in microdialysis sampling, which is one of the intended applications of this assay. The microcapillary immunoreactor was rinsed with 1 M sodium chloride, deionized water and K–R solution. Twenty μl of a 1/1000 dilution of enzyme conjugate (digoxin–alkaline phosphatase conjugate) were incubated in the capillaries for various periods of time. The conjugate solution was removed and the capillaries were rinsed with buffer C. Finally, the capillaries were filled with 20 μl of substrate (4 mM PAPP) and incubated for 5 min. The contents of the capillary were then injected directly into the FIAEC. The oxidation peak currents of 4-aminophenol at an applied potential of +300 mV (versus Ag/AgCl) and the corresponding concentrations of digoxin standards were used to construct the calibration curve.

RESULTS AND DISCUSSION

In the development of an immunoassay method it is important to ascertain the optimum conditions for each stage of the procedure. The sequential saturation enzyme immunoassay required evaluation of the conditions for immobilization and the incubation times of digoxin and labeled digoxin.

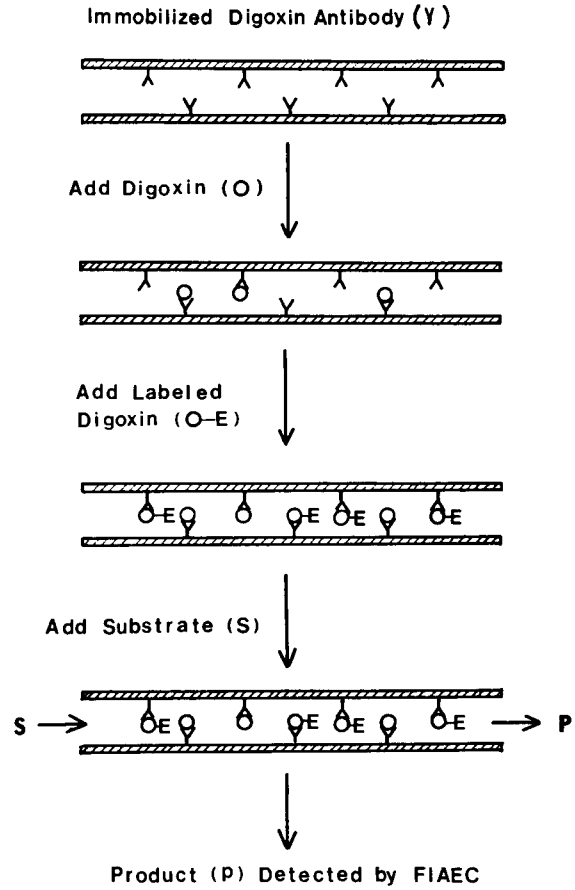

Fig. 1. General protocol for capillary sequential saturation immunoassay.

Immobilization

The immobilization of digoxin antibody was carried out by attaching the antibody oxidized with sodium periodate to PEG on the inner surface of the capillaries. Sodium periodate selectively oxidizes the vicinal hydroxyl groups of the oligosaccharide portions of immunoglobulins to aldehyde groups without destruction of the antigen-binding sites [16,17]. It has been reported (18–20) that the oxidation of carbohydrates with sodium periodate is dependent on a number of variables including the concentration of sodium periodate, pH, temperature and reaction time. In this work, the antidigoxin immunoglobulins were oxidized with sodium periodate at a concentration of 0.4 M for 20 min at room temperature at pH 5.5 (buffer A2). The oxidized antibody was immobilized on PEG by coupling the aldehyde groups of immunoglobulin to amino functional groups of PEG. The digoxin antibody was incubated in the capillary at pH 4.5 (buffer A3). The amount of attached antibody was then determined by reaction with labeled digoxin and then with the substrate solution. The result is shown in Fig. 2. There is a sharp increase in the amount of attached antibody in the first 2 days. For convenience, an incubation time of 1 day was chosen.

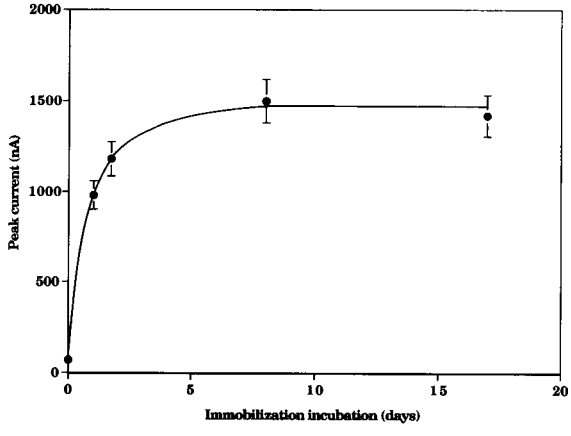

Fig. 2. Effect of incubation time on the immobilization of digoxin antibody. Assay conditions: 12 μg ml^{-1} digoxin antibody concentration, 1/1000 labeled digoxin conjugate dilution, 10 min labeled digoxin–digoxin antibody incubation time, and 5 min substrate (4 mM PAPP) reaction time.

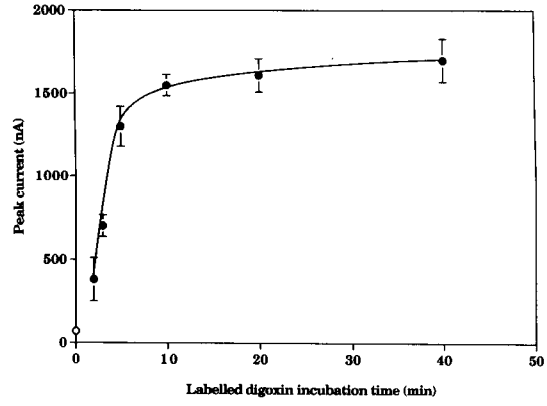

Fig. 3. Effect of incubation time on the binding of labeled digoxin. Assay conditions: 20 μg/ml digoxin antibody concentration, labeled digoxin diluted 1/1000, 5 min substrate (4 mM PAPP) reaction time.

Sequential saturation enzyme immunoassay

Competitive heterogeneous immunoassays are most sensitive when the antigen–antibody reaction is allowed to proceed to equilibrium [21]. Evaluation of the equilibrium incubation times for digoxin and labeled digoxin binding with digoxin antibody for the sequential saturation enzyme immunoassay was necessary to optimize assay sensitivity.

Incubation time of labeled digoxin. Alkaline phosphatase labeled digoxin was incubated in the immunoreactor for various periods of time. Then, enzyme substrate, 4-aminophenyl phosphate, was added and incubated for 5 min at room temperature. The oxidation peak current of enzyme product was measured by the FIAEC system. As shown in Fig. 3, the binding reaction was complete within 10 min (similar binding reaction times were obtained for tubes made with antibody concentrations of 6 and 12 μg ml^{-1}). This incubation time for labeled digoxin is much shorter than that (180 min) previously reported for a competitive enzyme immunoassay using conventional immunoplates with LCEC detection [22]. This dramatic reduction is mainly due to the shortened diffusional path from bulk solution to the inner surface of the capillary compared with that of cuvettes [6,11].

Incubation time of enzyme substrate. Alkaline phosphatase labeled digoxin was incubated in the

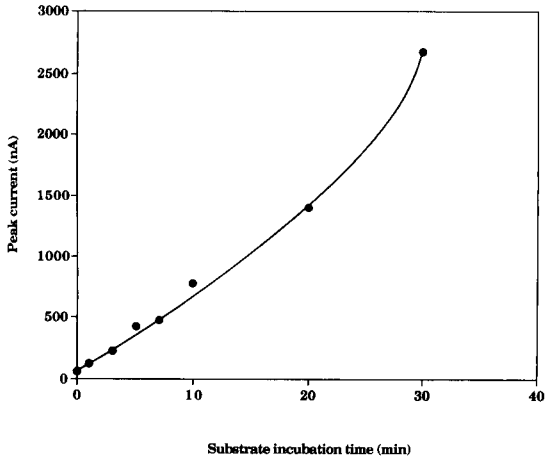

Fig. 4. Plot of peak current vs. substrate incubation time. Assay conditions: 6 μg ml^{-1} digoxin antibody concentration, labeled digoxin diluted 1/1000 and 10 min incubation time.

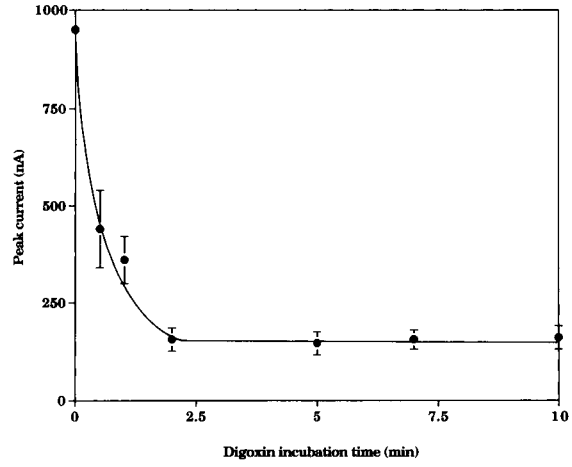

Fig. 5. Effect of incubation time on the binding of digoxin. Assay conditions: 12 μg ml^{-1} digoxin antibody concentration, labeled digoxin diluted 1/1000, 10 min incubation time, and 5 min substrate (4 mM PAPP) reaction time.

immunoreactor for 10 min at room temperature to allow formation of the antibody–antigen complex. After this step, the immunoreactor was rinsed with buffer C and then incubated with 4-aminophenyl phosphate at room temperature for various periods of time. The result is shown in Fig. 4. In the final assay a substrate incubation time of 5 min was used.

Incubation time of digoxin. The immunoreactor was incubated with 1 ng ml^{-1} digoxin solution for various periods of time. After rinsing with K–R solution, it was incubated with alkaline phosphatase labeled digoxin for 10 min at room temperature. After rinsing with buffer C, the extent of digoxin binding after different incubation times was assessed by the enzyme reaction. The result is shown in Fig. 5. The digoxin binding reaction was completed within 2 min. The time required for the digoxin reaction to reach equilibrium is short because digoxin has a low molecular weight (781). Labeled digoxin has a high molecular weight (70 000–120 000), so the time required for a labeled digoxin reaction to reach equilibrium is 5-fold longer than that for digoxin.

Assay for digoxin

The standard curve for a series of digoxin standard solutions is shown in Fig. 6. The assay requires 25 min for a 20-μl sample and has a detection limit of 10 pg ml^{-1} with a range spanning about 3 orders of magnitude. This detection limit is 5-fold lower than that reported for the competitive enzyme immunoassay for digoxin using a polystyrene cuvette reaction vessel [22]. This improvement was mainly due to the large surface area-to-volume ratio of the capillary as an immunoreactor. The main source of imprecision in

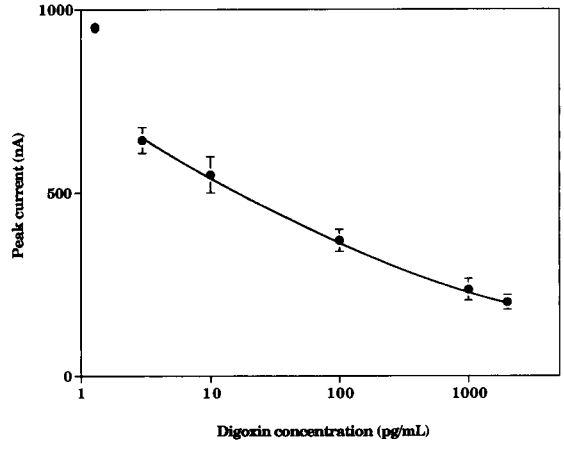

Fig. 6. Calibration curve for digoxin standard solutions. Assay conditions: 12 μg ml^{-1} digoxin antibody concentration, 1/1000 labeled digoxin conjugate dilution, 5 min digoxin–digoxin antibody incubation time, 10 min labeled digoxin–digoxin antibody incubation time, 5 min substrate (4 mM PAPP) reaction time, and sample solution at pH 7.1. The point in the upper left corner is the zero dose response.

the assay is reproducibility of the immunoreactor tubes with immobilized antibody, since a different tube is used for each measurement.

Nonspecific binding

Nonspecific binding of the conjugate to surfaces in the immunoreactor is the most important contributor to the magnitude of the detection limit in immunoassays [4,23]. The problem becomes more acute as the surface area to volume ratio of the immunoreactor increases. The present method was designed specifically to limit nonspecific binding by sterically limiting access of the conjugate to the silica surface of the capillary wall. In addition, although this was not used in the present work, Kumari [15] has shown that addition of PEG and AADH to the conjugate incubation solution further reduces nonspecific binding, presumably by competitive inhibition of interactions between the conjugate and these components of the attachment chemistry.

Although an increased surface area may result in greater nonspecific binding, the shortened diffusional distances dramatically reduce the necessary incubation times. Apart from the operational advantage of this, it serves also to limit the incidence of nonspecific interactions [25].

Conclusion

The sequential saturation capillary enzyme immunoassay for digoxin had a low detection limit (10 pg ml^{-1}), small sample volume (20 μl) and short incubation times (2 and 10 min for digoxin and labeled digoxin, respectively). The detection limit and incubation time for labeled digoxin were 3-fold lower and 6-fold shorter than those previously reported for the competitive enzyme immunoassay for digoxin in serum using a polystyrene cuvette. In terms of amount, the detection limit is 200 fg (260 amol), which is ca. 90 times lower than the detection limit of 19 pg (24 fmol) for the polystyrene cuvettes, which required 375 μl of sample.

The authors acknowledge Dr. James E. Myrick of the Centers for Disease Control (Atlanta, GA) for providing the digoxin antisera.

REFERENCES

1 W.R. Heineman and H.B. Halsall, Anal. Chem., 57 (1985) 1321A.
2 K.R. Wehmeyer, H.B. Halsall and W.R. Heineman, Clin. Chem., 31 (1985) 1546.
3 Y. Xu, H.B. Halsall and W.R. Heineman, J. Pharm. Biomed. Anal., 7 (1989) 1301.
4 S.H. Jenkins, H.B. Halsall and W.R. Heineman, J. Clin. Immunol., 13 (1990) 99.
5 H.B. Halsall, W.R. Heineman and S.H. Jenkins, Clin. Chem., 34 (1988) 1701.
6 H.B. Halsall, S.H. Jenkins, W.R. Heineman, M.J. Doyle, K.R. Wehmeyer and D.S. Wright, J. Res. Nat. Bur. Standards, 93 (1988) 491.
7 H.B. Halsall and W.R. Heineman, J. Int. Fed. Clin. Chem., 2 (1990) 179.
8 P.A. Nagainis, C.H. Nakagawa, S.L. Baron, S.A. Fuller, H.M. Chandler and J.G. Hurrell, Clin. Chim. Acta, 160 (1986) 273.
9 H.M. Chandler, S.A. Fuller, C.H. Nakagawa, P.A. Nagainis and J.G. Hurrell, Clin. Chem., 33 (1989) 498.
10 M.D. Frutos, S.K. Paliwal and F.E. Regnier, Anal. Chem., 65 (1993) 2159.
11 T.W. Smith and E.J. Haber, Clin. Invest., 49 (1970) 2377.
12 R.Q. Thompson, M. Porter, C. Stuver, H.B. Halsall, W.R. Heineman, E. Buckley and M. Smyth, Anal. Chim. Acta, 271 (1993) 223.
13 L.H. DeRiemer and C.F. Meares, Biochemistry, 20 (1981) 1606.
14 R.Q. Thompson, G.C. Barone, H.B. Halsall and W.R. Heineman, Anal. Biochem., 192 (1991) 90.
15 A. Kumari, M.S. Thesis, University of Cincinnati, 1991.
16 R.K. Yu and R. Ledeen, J. Biol. Chem., 244 (1969) 1306.
17 P.K. Nakane and A. Kawaoi, J. Histochem. Cytochem., 22 (1974) 1084.
18 L. VanLeten and G. Ashwell, J. Biol. Chem., 246 (1971) 1889.
19 E. Ishikawa, M. Imagawa, S. Hashida, S. Yoshitake, Y. Hamaguchi and T. Ueno, J. Immunoassay, 4 (1983) 209.
20 D.J. O'Shannessy and R.H. Quarles, J. Appl. Biochem., 7 (1985) 347.
21 J.C. Standefer and G.C. Saunders, Clin. Chem., 24 (1978) 1903.
22 K.R. Wehmeyer, H.B. Halsall, W.R. Heineman, C.P. Volle and I.-W. Chen, Anal. Chem., 58 (1986) 135.
23 S.H. Jenkins, W.R. Heineman and H.B. Halsall, Anal. Biochem., 168 (1988) 292.
24 R.P. Ekins, in A. Albertini and R.P. Ekins (Eds.), Monoclonal Antibodies and Developments in Immunoassay, New York, Elsevier, 1981.
25 C.H. Pollema, J. Ruzicka and G.D. Christian, Anal. Chem., 64 (1992) 1356.

Analytica Chimica Acta, 287 (1994) 259–266
Elsevier Science B.V., Amsterdam

Preconcentration of trace metals in sea water matrix for differential pulse anodic stripping voltammetry

Jun-Der Lee and Jem-Mau Lo

Institute of Nuclear Science, National Tsing Hua University, Hsinchu 30043 (Taiwan)

(Received 30th July 1993; revised manuscript received 19th October 1993)

Abstract

A preconcentration procedure with two-step extraction was proposed to be used in conjunction with differential pulse anodic stripping voltammetry (DPASV) for the determination of trace metals in sea water. The two-step extraction involved extraction of trace metals from sea water with dithiocarbamate into chloroform followed by backextraction with a Hg^{2+} solution at pH 3.5, as previously reported. The aqueous solution containing simply the enriched metals and the nonreacted Hg^{2+} was analysed by DPASV using a glassy carbon electrode. Anodic stripping voltammetry of the metals including Zn, Cd, Pb and Cu was conducted in the preconcentrated solution after adding 0.025 M KCl. The preconcentrated solution was observed not to cause any interference in the anodic stripping voltammetry. Besides, the Hg^{2+} could be in situ utilized as the source of the mercury film coated on the glassy carbon electrode, rendering it as an efficacious working electrode. The detection limits achieved were as low as 0.004 μg/l for Zn, 0.002 μg/l for Cd, 0.002 μg/l for Pb and 0.003 μg/l for Cu in sea water by DPASV coupled with the preconcentration procedure with an enrichment factor of 20. The analytical reliability was confirmed by checking with NASS-3 (NR-A4) open ocean sea water.

Keywords: Anodic stripping voltammetry; Metals; Preconcentration; Sea water; Trace metals; Waters

Differential pulse anodic stripping voltammetry (DPASV) is an important method for the simultaneous determination of heavy metals in water samples at μg/l or sub μg/l level. Direct analysis of sea water for Zn, Cd, Pb and Cu by DPASV using a hanging mercury drop electrode [1–7] and a film mercury electrode [8–12] were reported in the literature. The direct DPASV method has some disadvantages such as a highly sloping baseline, low resolution, unavoidable interference, and a hardly detectable zinc oxidation peak. Sea water is a challenging sample for trace metal analysis because of the very low concentrations of the metals of interest and the possible interference from the high salt matrices. A two-step preconcentration method for enriching trace metals from sea water prior to instrumental analysis was previously reported [13,14]. The preconcentration procedure serves the dual purposes of removing the major matrix material and of increasing the concentration of trace metals for the final instrumental detection. The method involved solvent extraction for enriching trace metals in sea water by dithiocarbamate–chloroform solution associated with subsequent backextraction using Hg^{2+} as the backextracting agent. The Hg^{2+} backextraction method was based on the fact that the extraction constant of the mercury(II)–dithiocarbamate complex was much higher than most of the other metal dithiocarbamates. The substitution of Hg^{2+} for the metals of interest in the form of the dithiocarbamate complex in the extracted solution was extremely fast. The efficiency of recovery was very high by the two-

Correspondence to: J.-M. Lo, Institute of Nuclear Science, National Tsing Hua University, Hsinchu 30043 (Taiwan).

SSDI 0003-2670(93)E0593-V

step preconcentration procedure for a number of metals including zinc, cadmium, lead, copper, etc. in sea water. The enrichment factor could become very high by technically enlarging the volume ratios both at the extraction step and at the backextraction step. In this study, the similar two-step preconcentration method was utilized in combination with DPASV for the determination of trace metals in sea water. Due to the very low concentration of these metals in sea water, interest has been focused on modification of the combination technique leading to a decrease in detection limit whereas interferences were excluded. It should be emphasized that the proposed preconcentration technique possessed the unique feature that the Hg^{2+} played a role both as the backextraction agent and as the in situ source for the mercury film coated on the glassy carbon electrode for the subsequent DPASV.

EXPERIMENTAL

Extracting agents

Two derivatives of dithiocarbamate (DTC), sodium diethyldithiocarbamate (NaDDC) and ammonium tetramethylene dithiocarbamate (APDC) were used. Both were analytical reagent grade (Merck). A mixture of NaDDC and APDC (1 g each) was dissolved in 100 ml of water, stirred well and shaken two times with 10 ml chloroform. The organic phase was discarded, removing any possible metal impurities present in the reagents. The aqueous phase was referred to as the purified extracting agent used in subsequent work.

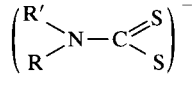

DTC (Dithiocarbamate)

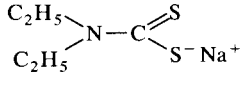

NaDDC (Sodium Diethyldithiocarbamate)

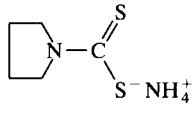

APDC (Ammonium Tetramethylene dithiocarbamate)

Reagents

The chemical compounds, $ZnCl_2$, $CdCl_2 \cdot H_2O$, $Pb(NO_3)_2$ and $CuCl_2 \cdot 2H_2O$ were purchased from Merck. The stock solutions (ca. 100 mg/l) of metal ions were prepared by dissolving 0.0521 g $ZnCl_2$, 0.0448 g $CdCl_2 \cdot H_2O$, 0.0401 g $Pb(NO_3)_2$ and 0.0671 g $CuCl_2 \cdot 2H_2O$, respectively in 0.1 M nitric acid and diluting to 250 ml with pure water which was then adjusted to pH 1.6 and stored in polyethylene (PE) bottles. Standard solutions of metals were prepared from the stock solutions by appropriate dilution with pure water. A Hg^{2+} backextracting solution was obtained by dissolving 1.0797 g mercury oxide in a minimum volume of 2.4% nitric acid and then adding 200 ml pure water to make a final Hg^{2+} concentration of 5000 mg/l with a pH at about 2.5. Pure water was obtained from a two-stage distillation by a quartz apparatus of deionized water which was produced via an ion exchange and reverse osmosis (Micropore, Hsinchu). All pyrex glassware and polyethylene bottles were washed sequentially by a detergent solution, soaked in 10% nitric acid for at least 24 h, and washed three times with pure water.

Sea water samples

A synthetic sea water sample was prepared by mixing 25.40 g of NaCl, 5.083 g of $MgCl_2$, 1.104 g of $CaCl_2$, 0.722 g of KCl, 0.026 g of H_3BO_3 and 0.203 g of $SrCl_2$ in a volumetric flask and made up to 1 l with pure water. The synthetic sea water was filtered through a 0.45-μm Millipore membrane filter before use.

A natural sea water sample was collected from the coast of Taiwan Strait near Hsinchu. The surface sea water was stored in a 20-l PE bottle. Subsequently, the sea water was filtered through a 0.45-μm Millipore membrane and stored after acidification to pH 1.5 with 1.0 M nitric acid. UV irradiation of sea water was carried out by exposing the treated sample to a 1200 W UV lamp for 1 h.

Apparatus

Voltammetric measurements were performed in an electrochemical cell consisting of a 20-ml covered beaker with the three electrodes (i.e.,

working, reference and auxiliary) being immersed in the electrolytic solution. A glassy carbon electrode was used as the working electrode, a silver/silver chloride electrode as the reference electrode, and a Pt wire as the auxiliary electrode. The three electrodes as well as the tube used for N_2 purging were inserted through the four holes with an O-ring on the cell cover. A multipurpose microprocessor-based voltammetric analyzer from Bioanalytical Systems (BAS-100 B) was used.

Two-step preconcentration procedure

Pyrex separatory funnels (250 ml) were filled with 200 ml of pure water, synthetic sea water or real sea water unspiked or spiked with certain amounts of trace metals, separately. The solutions were adjusted to pH 4.0 by adding 0.01 M nitric acid; then 4 ml of the purified extracting agent was added. Exactly 20 ml of chloroform was added into the funnels and the mixture was shaken up-and-down vigorously by a shaking machine for 20 min. After waiting for 5 min to allow the phases to separate, the organic phase was transferred into a flask, and 10 ml of a 400 mg/l Hg^{2+} solution was added for backextraction. The solution mixture was shaken for 5 min which was sufficient to complete the backextraction. The aqueous phase separated was adjusted to pH 3.5 with a few drops of 0.01 M ammonia, 0.5 ml of 0.5 M KCl was added, and finally made up to 10 ml with pure water. The solution was immediately transferred to the electrochemical cell for DPASV.

Differential pulse anodic stripping voltammetry

Voltammograms were recorded with a BAS-100 B system. Analysis of metal ions in the preconcentrated solution was started by electrochemical formation of a mercury film on the glassy carbon electrode by applying a deposition potential of −1300 mV for 150 s. Simultaneously, the metal ions were reduced and amalgamated in the mercury film during the deposition step. After the deposition step, the solution was equilibrated for 10 s (no stirring), and the metals were then stripped from the mercury film back into the solution. Differential pulse anodic stripping voltammetry was employed for the measurement of the metals under the following conditions: stripping potential from −1300 to 0 mV, scan rate 20 mV/s, pulse amplitude 50 mV, sample width 17 ms, pulse width 50 mV, pulse period 200 ms, and stirring rate 20 rpm. The solutions were purged with the nitrogen gas and stirred for at least 5 min before analysis. The glassy carbon electrode was polished with a very fine paper (wet and dry), alumina, and finally with diamond paste before use.

All of the analytical solutions including the blanks containing 0.025 M KCl and nonreacted Hg^{2+}, and trace metals in the preconcentrated solutions were brought in the medium of 0.025 M KCl and 300 mg/l Hg^{2+} with pH adjusted to 3.5. The metals of interest were identified by their stripping potentials at approximately −1.15 V for Zn, −0.72 V for Cd, −0.55 V for Pb and −0.18 V for Cu and quantified by the corresponding oxidation peak currents.

RESULTS AND DISCUSSION

The two-step extraction procedure (i.e., extraction by DTC and backextraction by Hg^{2+}) was previously described to be an efficacious preconcentration technique for enriching trace metals in sea water with simultaneous elimination of large amounts of matrix species such as Ca, S, Al, Na, Cl, K, Sr, Mg, Ba, etc. [13]. Combination of the preconcentration procedure with graphite furnace atomic absorption spectrometry was proven to be beneficial for the determination of trace metals in sea water [13]. By the same rationale, a similar two-step extraction procedure but Pd^{2+} in lieu of Hg^{2+} as the backextraction agent was also demonstrated to be efficacious in the determination of trace metals in sea water when conjugated with graphite atomic absorption spectrometry [15] or inductively coupled plasma atomic emission spectrometry [16]. In the present study, the two-step extraction procedure was used in conjunction with differential pulse anodic stripping voltammetry for the determination of Zn, Cd, Pb and Cu in sea water. Hg^{2+} was employed as the backextraction agent because it has the advantage that it can also be used as the source for the

mercury film coated on the glassy carbon electrode as the working electrode in the DPASV. The mercury film carbon electrode has the advantage over the classical hanging mercury drop electrode of better sensitivity and better resolution of the stripping currents [8–12]. The mercury film carbon electrode used in this work was similar to the "Florence type", where the mercury film was formed in situ on a glassy carbon electrode [17].

The conditions suitable for the DPASV following the preconcentration procedure were systematically investigated in this work. The concentration of Hg^{2+} in the electrolyte solution may be a special and important parameter in the DPASV using the in situ mercury film electrode but not in the general anodic stripping voltammetry by means of hanging mercury drop electrode [1–7] or pre-coated mercury film electrode [8–12]. Besides, other parameters such as pH, electrolyte, deposition time, etc. may be affected by the magnitude of the concentration of Hg^{2+}. Practically, a sufficient concentration of Hg^{2+} is needed for the formation of an integral mercury film on the glassy carbon electrode. This may be important especially for the measurement of Zn among the four metals investigated. The relationship between the stripping peak currents of the four metals investigated and the concentration of

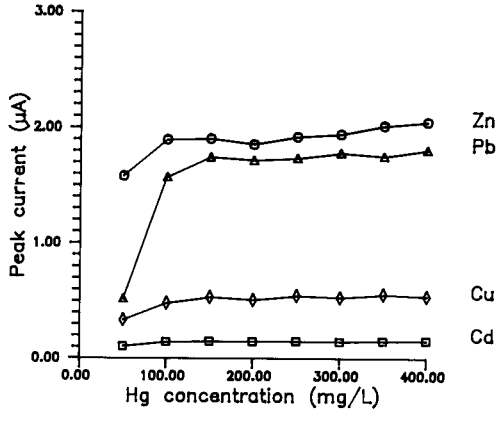

Fig. 1. Relationship between DPASV peak currents of the metals and Hg^{2+} concentration. 2.50 μg/l Zn^{2+}, 0.50 μg/l Cd^{2+}, 5.00 μg/l Pb^{2+} and 5.00 μg/l Cu^{2+} in electrolyte solution of 0.025 M KCl at pH 3.5 with a deposition time of 150 s.

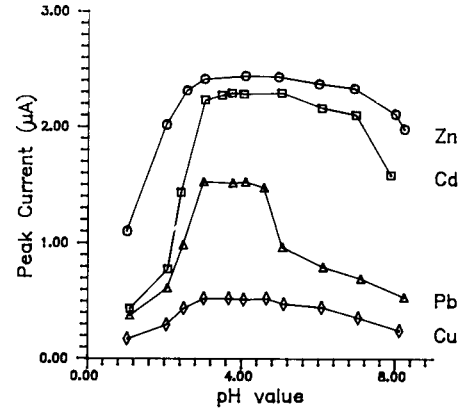

Fig. 2. Effect of pH on DPASV peak current. 3.75 μg/l Zn^{2+}, 6.00 μg/l Cd^{2+}, 5.00 μg/l Pb^{2+} and 5.00 μg/l Cu^{2+} in electrolyte solution of 0.025 M KCl containing 300 mg/l Hg^{2+} with a deposition time of 150 s.

Hg^{2+} in the electrolyte solution of 0.025 M KCl at pH 3.5 with deposition of 150 s is shown in Fig. 1. All peak currents of the metals reach a maximum and remain constant when the concentration of Hg^{2+} is higher than 150 mg/l up to at least 400 mg/l. The concentration of Hg^{2+} as the backextraction agent was thus chosen at 300 mg/l in the practical analytical work; a small portion of the mercury will be consumed in the preconcentration procedure but a large portion ($\geqslant$ 250 mg/l) will remain and is transferred to the electrolyte solution for DPASV.

The effect of pH on the stripping peak currents of the metals in the electrolyte solution of 0.025 M KCl containing 300 mg/l Hg^{2+} is demonstrated in Fig. 2. The peak currents of the four metals gradually decrease either in more acidic solutions with pH < 2 or in more alkaline solutions with pH > 7. A flat-plateau of peak current versus pH, however, can be reached for each metal in a certain pH range which is commonly the pH range from 3.0 to 4.6 (see Fig. 2). A pH of 3.5 was therefore used in the practical analytical procedure.

Stripping peaks of all four metals can be discerned in the case of 0.025 M KCl as the electrolyte. Figure 3 demonstrates high resolution and high stability of the DPASV voltammograms which can be obtained under the optimal conditions established in the study mentioned above. It

is noted that the half width values of the stripping peaks are better than 1 mV for each concentration of the metals above 0.2 μg/l.

It should be emphasized that the proposed DPASV procedure coupled with the two-step extraction procedure is practical for the determination of trace metals in sea water. Owing to the inherent sensitivity of DPASV, all four metals of interest are readily measured in the preconcentrated solution with the metals enriched by a factor of 20. Technically, the two-step extraction starting with 200 ml of sea water sample is convenient and fast. The backextraction by Hg^{2+} is a kind of metal-to-metal replacement reaction which is different from the classical backextraction involving the breakdown of the metal chelates by strong acids or oxidants. The final backextracted solution simply consists of the enriched metal ions and nonreacted Hg^{2+} and is well suited for DPASV with minimum interference. Labuda and Vanickova [18] used the hybrid technique of direct coupling of DTC extraction with anodic stripping voltammetry for the determination of trace metals in sea water. Stripping voltammetry was done in benzene–methanol or chloroform–ethanol–water medium with supporting electrolyte containing Hg^{2+}. In comparison, the hybrid technique appears to be very complicated and Zn and Cu are beyond detectability in the method.

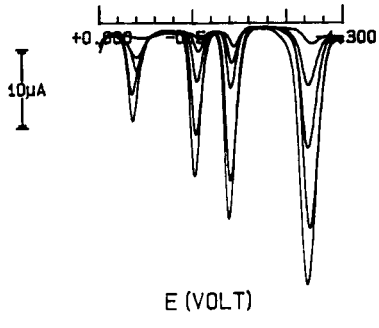

Fig. 3. DPASV of the increasing concentrations of Zn^{2+} (2.00, 10.00, 20.00, 30.00 and 40.00 μg/l), Cd^{2+} (5.00, 10.00, 20.00, 50.00 and 60.00 μg/l), Pb^{2+} (5.00, 10.00, 20.00, 40.00 and 60.00 μg/l) and Cu^{2+} (10.00, 30.00, 50.00, 80.00 and 100.00 μg/l) in electrolyte solution of 0.025 M KCl at pH 3.5 containing 300 mg/l Hg^{2+} with a deposition time of 150 s.

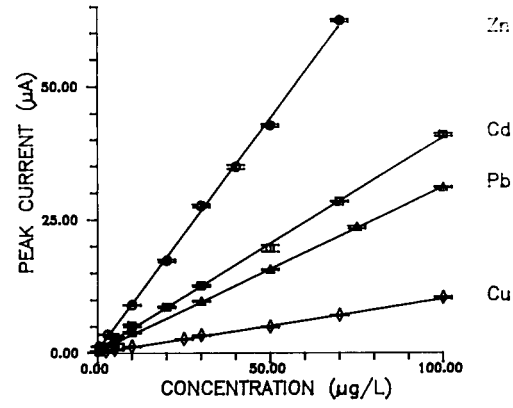

Fig. 4. Calibration curves for DPASV of Zn^{2+}, Cd^{2+}, Pb^{2+} and Cu^{2+} in electrolyte solution of 0.025 M KCl at pH 3.5 containing 300 mg/l Hg^{2+} with a deposition time of 150 s.

The calibration curves for simultaneous determination of Zn^{2+}, Cd^{2+}, Pb^{2+} and Cu^{2+} in the 0.025 M KCl electrolyte at pH 3.5 containing 300 mg/l Hg^{2+} with deposition of 150 s is shown in Fig. 4. All peak currents of the metals demonstrate a proportional increase with increasing the concentrations of the corresponding metal ions. The correlation coefficients of linearity for the straight lines are all higher than 0.996. The range of the concentrations of metals suited for the quantitative measurement by the calibration method is clearly indicated in Fig. 4. It should be emphasized that all the peak currents are produced from a fresh and sufficiently thick mercury film carbon electrode in every analysis, i.e., being fabricated by the in situ 150-s deposition of a high concentration of Hg^{2+} (i.e., 300 mg/l) onto a blank or polished glassy carbon electrode. The fresh mercury film carbon electrode is used not more than three runs in the same analysis. Otherwise, the copper peak current will gradually become sloped and reduced in the more runs, especially pronounced in the analyses of higher concentration of the metals (e.g., $\geqslant 100$ μg/l). This may be resulted from the generation of Zn–Cu intermetallic compound on the electrode as reported in several articles [3,4]. It is clear that the Zn–Cu intermetallic interference commonly found in DPASV can be avoided by the proposed procedure in this work.

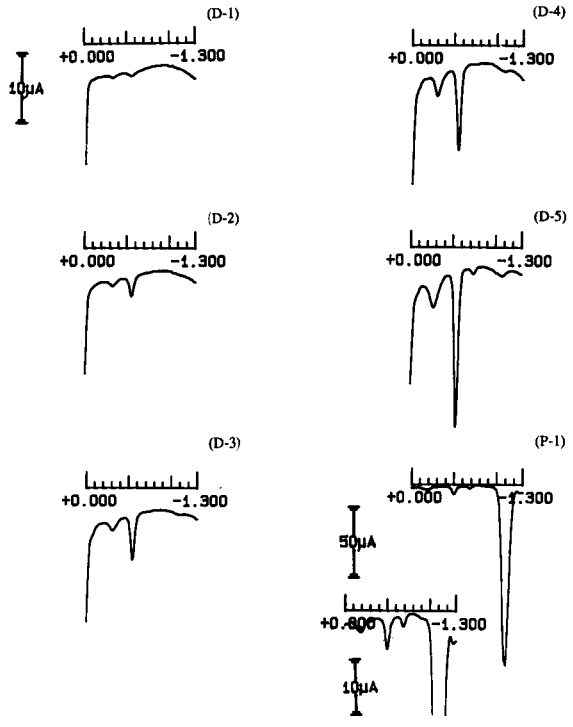

Fig. 5. DPASV of natural sea water post-UV-irradiated by direct measurement with varying deposition time (D-1, 150 s; D-2, 300 s; D-3, 600 s; D-4, 1200 s; D-5, 1800 s) and by the proposed procedure (P-1) (see Experimental section).

It is interesting to compare the proposed method with the direct method for the determination of trace metals in sea water. The natural sea water samples subjected to UV irradiation were divided into two parts for analysis by the two different methods. In the direct method, 10-ml portions of sea water were adjusted to pH 3.5, 300 mg/l Hg^{2+} was added and DPASV was performed with varying deposition times. The results are summarized in Fig. 5 (D-1 to D-5). No detectable peak current appears for deposition times of less than 150 s when traces of Pb and Cu peaks are observed. Increase in deposition time seems to produce corresponding increases in peak current for Pb and Cu. The peaks of Zn and Cd, however, are observed at a much longer period of time when the deposition time is as large as 1800 s. On the other hand, the same sea water was analyzed indirectly by the proposed method starting with 200 ml of sample along with the typical procedure (see Experimental). The result is also indicated in Fig. 5 (P-1). The stripping peaks for Zn, Cd, Pb and Cu are clearly discernible and the corresponding currents are prominent, indicating that the trace metals in sea water is readily determined by the proposed method. By comparison, Zn and Cd seems to be hardly determined by the direct method but easily determined by the proposed method. Seitz [19] and Bradford [20] reported that the absolute concentration of Zn in sea water may not be measurable by direct voltammetry because only a fraction of the total Zn present is reducible at the electrode, and the determination may be subject to interference from Ni, Cu and Co. It has been well-documented that dissolved organics in natural sea water can substantially influence the stripping voltammetric response [21]. The problems encountered in the direct analysis as mentioned can be solved by the proposed method. In essence, the four metals of interest are transferable with their total amount in sea water by DTC extraction and Hg^{2+} back-extraction into the final preconcentrated solution for DPASV. Comparing the observed results of both methods, it is clear that Zn and Cd are seriously suppressed in direct voltammetry and may not be suitably determined by the direct method.

The feasibility of the DPASV coupled with the two-step extraction in practical analysis of water samples for Zn, Cd, Pb and Cu was investigated as follows. Pure water, synthetic sea water and natural sea water, post UV-irradiated, were analyzed by the proposed procedure along with the optimal conditions previously established. In addition, all water samples were spiked with certain concentrations of the metal ions and the spiked samples were analyzed in parallel with the original ones. The results are summarized in Tables 1, 2 and 3 for the original and spiked pure waters, the original and spiked synthetic sea waters, and the original and spiked natural sea waters, respectively. The recovery of the spiked metals is observed to be very good for the different water samples. The results provide evidence of the feasibility of the proposed method for determining trace metals in natural sea water. The reliability and accuracy of the proposed method in sea

TABLE 1

Results of DPASV by the proposed procedure for the metals in the original and spiked pure waters (mean ± S.D., $n = 5$)

Metal investigated	Concentration of metals (μg/l)			Recovery (%)
	Original	Spiked	Found	
Zn	0.015 ± 0.004	0.010	0.024 ± 0.001	90 ± 10
		0.020	0.036 ± 0.001	105 ± 5
		0.030	0.045 ± 0.002	100 ± 7
		0.060	0.076 ± 0.004	102 ± 7
Cd	0.035 ± 0.003	0.030	0.063 ± 0.002	93 ± 7
		0.100	0.140 ± 0.003	105 ± 3
		0.135	0.173 ± 0.004	102 ± 3
		0.160	0.197 ± 0.007	101 ± 4
Pb	0.042 ± 0.005	0.050	0.095 ± 0.003	107 ± 6
		0.060	0.102 ± 0.004	102 ± 3
		0.150	0.190 ± 0.007	99 ± 5
		0.300	0.351 ± 0.008	103 ± 3
Cu	0.085 ± 0.008	0.120	0.207 ± 0.004	102 ± 3
		0.200	0.288 ± 0.008	104 ± 4
		0.250	0.333 ± 0.007	98 ± 3
		0.400	0.498 ± 0.008	103 ± 2

water was tested by analyzing NASS-3 (NR-A4) open ocean sea water. The result is indicated in Table 4. The concentrations of Zn, Cd, Pb and Cu found are in good agreement with the certified values (also indicated in Table 4). Limits of detections by the proposed method were estimated from a blank test by starting from 200 ml of the metal-depleted sea water from which the

TABLE 2

Results of DPASV by the proposed procedure for the metals in the original and spiked synthetic sea water samples (mean ± S.D., $n = 5$)

Metal investigated	Concentration of metals (μg/l)			Recovery (%)
	Original	Spiked	Found	
Zn	0.028 ± 0.002	0.018	0.045 ± 0.002	94 ± 11
		0.035	0.064 ± 0.003	103 ± 5
		0.060	0.089 ± 0.005	102 ± 6
Cd	0.211 ± 0.007	0.200	0.417 ± 0.007	103 ± 4
		0.300	0.509 ± 0.005	99 ± 2
		0.400	0.606 ± 0.009	99 ± 4
Pb	0.422 ± 0.008	0.250	0.674 ± 0.006	101 ± 2
		0.400	0.835 ± 0.011	103 ± 4
		0.800	1.214 ± 0.017	99 ± 1
Cu	0.577 ± 0.011	0.250	0.831 ± 0.005	102 ± 2
		0.500	1.047 ± 0.017	94 ± 3
		1.000	1.629 ± 0.012	105 ± 1

TABLE 3

Results of DPASV by the proposed procedure for the metals in the original and spiked post-UV-irradiated natural sea water samples (mean ± S.D.)

Metal investigated	Concentration of metals (μg/l)			Recovery (%)
	Original	Spiked	Found	
Zn	11.27 ± 0.07	2.00	13.23 ± 0.08	98 ± 4
		4.00	14.88 ± 0.07	90 ± 2
		9.00	19.87 ± 0.09	96 ± 1
Cd	0.21 ± 0.03	0.40	0.61 ± 0.03	105 ± 8
		0.60	0.79 ± 0.05	97 ± 8
		0.80	0.96 ± 0.07	94 ± 9
Pb	0.85 ± 0.06	1.00	1.91 ± 0.05	106 ± 5
		1.50	2.42 ± 0.07	105 ± 5
		2.50	3.27 ± 0.06	97 ± 3
Cu	0.91 ± 0.05	0.50	1.46 ± 0.04	110 ± 8
		1.00	1.98 ± 0.08	107 ± 8
		1.50	2.53 ± 0.09	108 ± 6

TABLE 4

Results of DPASV by the proposed procedure for Zn, Cd, Pb and Cu in the NASS-3 (NR-A4) standard reference open ocean sea water

Metal investigated	Concentration of metals (μg/l)				
	1st	2nd	3rd	Average and standard deviation	Certified
Zn	0.192	0.193	0.190	0.192 ± 0.002	0.178
Cd	0.026	0.031	0.024	0.027 ± 0.004	0.029
Pb	0.040	0.036	0.036	0.037 ± 0.002	0.039
Cu	0.115	0.121	0.108	0.115 ± 0.007	0.109

metals of Zn, Cd, Pb, Cu, etc. had been removed by DTC extraction and running through the proposed analytical procedure. The detection limits, which were estimated from three times the standard deviations of the blank values, were 0.004 μg/l for Zn, 0.002 μg/l for Cd, 0.002 μg/l for Pb and 0.003 μg/l for Cu in sea water, respectively.

REFERENCES

1 G.C. Whitnak and R. Sanelli, Anal. Chim. Acta, 47 (1969) 267.
2 W. Lund and D. Dshus, Anal. Chim. Acta, 86 (1976) 109.
3 E. Jacobsen and H. Lindseth, Anal. Chim. Acta, 86 (1976) 123.

4 A.M. Bond, I.D. Heritages and W. Thormann, Anal. Chem., 58 (1986) 1063.
5 D.R. Turner, S.G. Robinson and M. Whitfield, Anal. Chem., 56 (1984) 2387.
6 D. Jagner, Anal. Chem., 50 (1978) 1924.
7 G. Gillain and G. Duyckaerts, Anal. Chim. Acta, 106 (1979) 23.
8 W. Lund and M. Salberg, Anal. Chim. Acta, 76 (1975) 131.
9 M.I. Abdullah, B. Ressch Berg and R. Klimek, Anal. Chim. Acta, 76 (1975) 131.
10 G.E. Batley and J.P. Matousek, Anal. Chem., 49 (1977) 2031.
11 G.E. Batley and J. P. Matousek, Anal. Chem., 52 (1980) 1570.
12 G.E. Baltey, Anal. Chim. Acta, 124 (1981) 121.
13 J.M. Lo, J.C. Yu, F.I. Hutchison and C.M. Wai, Anal. Chem., 54 (1982) 2536.
14 J.M. Lo, H.J. Sun, Y.P. Lin and K.L. Wu, Anal. Chim. Acta, 224 (1989) 139.
15 S. Sachsenberg, Th. Klenke, W.E. Krumbein and E. Zeeck, Fresenius' J. Anal. Chem., 342 (1992) 163.
16 J.M. Lo, Y.P. Lin and K.S. Lin, Anal. Sci., 7 (1991) 455.
17 T.M. Florence, Analyst, 111 (1986) 489.
18 J. Labuda and M. Vanickova, Anal. Chim. Acta, 208 (1988) 219.
19 W.R. Seitz, Ph.D. Thesis, Massachusetts Institute of Technology, Cambridge, MA, 1970.
20 W.R. Bradford, Ph.D. Thesis, The Johns Hopkins University, Baltimore, MD, 1972.
21 G.E. Batley and T.M. Florence, J. Electroanal. Chem., 72 (1976) 121.

Analytica Chimica Acta, 287 (1994) 267–273
Elsevier Science B.V., Amsterdam

Fibre-optic sensor for the determination of carboxylic acids based on fluorescence enhancement of lipophilized fluorescein isologues

Hui-Hui Zeng, Ke-Min Wang, Xiao-Hai Yang and Ru-Qin Yu

Department of Chemistry and Chemical Engineering, Hunan University, 410082 Changsha (China)

(Received 15th July 1993; revised manuscript received 4th October 1993)

Abstract

A fibre-optic sensor for the determination of carboxylic acids based on fluorescence enhancement of lipophilized fluorescein isologues dissolved in a plasticized poly(vinyl chloride) membrane was developed. With the optimum conditions described, carboxylic acids in sample solutions from 1 to 9 M (formic acid), 0.5 to 10 M (acetic acid), 0.1 to 2.7 M (propionic acid) and 1×10^{-4} to 1×10^{-2} M (benzoic acid) can be determined. The response times of the sensor to carboxylic acid are less than 1.5 min. In addition to high reproducibility of the fluorescence signal, the sensor exhibits fair selectivity for carboxylic acids.

Keywords: Fluorimetry; Sensors; Carboxylic acids; Fibre-optic sensors; Fluorescein isologues

Optical chemical sensors (optrodes) have become a rapidly expanding area of analytical chemistry [1] and recent advances and trends have been reported in several reviews [2–6]. An important advantage over electrochemical sensors is that optrodes can directly sense many neutral species (e.g., ethanol [7], water [8], ammonia [9,10], organic solvent vapours [11–13], carbon dioxide [14] and polycyclic aromatic hydrocarbons [15]). In this paper, a new kind of organic neutral species–selective fibre-optic chemical sensor based on lipophilized fluorescein isologues for the determination of carboxylic acids is reported.

Fluorescein is a classical analytical reagent. Because of its hydrophilicity, fluorescein tend to leach from the the sensing membrane of the optrode into the aqueous analytical solutions. Tan et al. [16] first synthesized a series of lipophilized fluorescein isologues as chromoionophores and incorporated them with trioctyltin chloride as an ionophore in a plasticized poly(vinyl chloride) (PVC) matrix to construct an optrode for the determination of chloride in serum. Lipophilized fluorescein served as a pH indicator in the sensing membrane, showing different absorption properties when in contact with analytical solutions of different pH. In this work it was found that a plasticized PVC membrane containing only lipophilized fluorescein isologues shows interesting fluorescence analytical properties for many carboxylic acids. The response signals used by most fluorescent chemical sensors are usually fluorescence quenching signals. The optrode presented in this paper is based on reversible fluorescence enhancement of lipophilized fluorescein isologues.

Carboxylic acids such as formic, acetic, propionic and benzoic acids are very important organic

Correspondence to: R.-Q. Yu, Department of Chemistry and Chemical Engineering, Hunan University, 410082 Changsha (China).

SSDI 0003-2670(93)E0579-V

acids. Conventional methods for the determination of these carboxylic acids involve acid–base titration [17], liquid chromatography [18,19], spectrophotometry [20] and enzymatic methods [21]. These conventional methods are time consuming and hardly suitable for on-line measurement. The proposed fibre-optic sensor offers an alternative approach for the determination of carboxylic acids.

EXPERIMENTAL

Reagents

The lipophilized fluorescein isologues fluorescein octadecyl ester (FODE), fluorescein hexadecyl ester (FHDE), fluorescein dodecyl ester (FDDE), fluorescein decyl ester (FDE), 4′,5′-dichlorofluorescein octadecyl ester (DCFODE), 2′,4′,5′,7′-tetrabromofluorescein octadecyl ester (TBFODE) were synthesized according to the literature [16]. PVC (high molecular weight; Fluka Selectophore), bis(2-ethylhexyl) phthalate (C.P; Shanghai Chemical Reagents) and tetrahydrofuran (THF) (analytical-reagent grade; Shanghai Chemical Reagents) were used for membrane preparation. Aqueous solutions of carboxylic acids (formic, acetic, proponic and benzoic acid) were prepared from analytical-reagent grade reagents (Shanghai Chemical Reagents) and deionized water. The concentrations of the carboxylic acids were determined by titration with standard sodium hydroxide solution.

Preparation of the optrode

The following spin-on technique was used for preparing the optrode membrane. The optrode membrane solution was prepared by dissolving a mixture of 3 mg of lipophilized fluorescein isologue, 50 mg of PVC and 100 mg of bis(2-ethylhexyl) phthalate in 2 ml of freshly distilled THF. An aliquot of 0.1 ml of this solution was pipetted on to a circular 12-mm diameter quartz plate which was fixed in a rotating (ca. 600 rpm) aluminium alloy rod under a THF-saturated atmosphere. After about 5 s the quartz plate with a ca. 4-μm thick sensing membrane was removed and dried in ambient air for 5 min. The quartz plate covered with the sensing membrane was tightly connected through a screw-cap to the 5-mm diameter common end of a glass bifurcated fibre optic of length 1 m, 3.6 mm i.d. per single bundle and diameter 5 mm at the common end (Fig. 1).

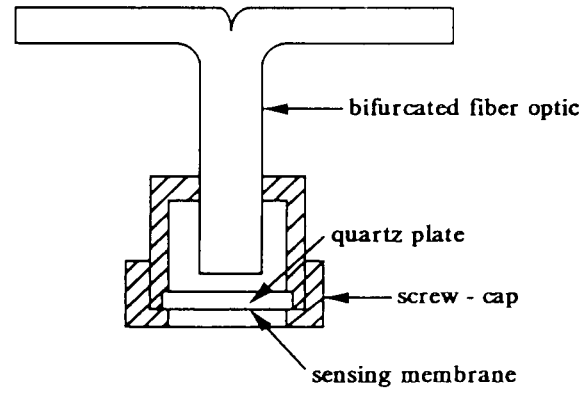

Fig. 1. Schematic diagram of carboxylic acid-selective fibre-optic sensor.

Procedure

The exciting radiation from a Hitachi M-850 spectrofluorimeter was guided through the input bundle of the bifurcated fibre optic into the sensing membrane. Emission fluorescence produced by the sensing membrane was collected and guided back to the detector of the spectrometer by the output bundle.

The common end of the bifurcated fibre optic was inserted into a vessel containing the analyte solution. The vessel was made of brown glass and was protected from natural light by wrapping it with black cloth. The top of the vessel was also covered with black cloth. Care must be taken not to shift the position of the light guide in the solution during experiments.

Before an experiment, the optrode must be kept in deionized water until a steady fluorescence signal is obtained. For initial optimization, the detected fluorescence signal is maximized while the optrode is immersed in a water blank. This optimization usually consists in simply repositioning the input fibre bundle with respect to exciting radiation or the output fiber bundle with respect to the detector.

TABLE 1

Spectral data for FODE in dichloromethane (2×10^{-5} M), ethyl acetate (2×10^{-5} M) and in PVC membrane (3.35×10^{-5} mol g^{-1})

Solvent	Fluorescence properties		Absorption properties	
	λ(ex)/λ(em) (nm)	Fluorescence intensity	λ(max) (nm)	Absorbance
Dichloromethane	465.9/524.9	103.7	486.5	0.116
	465.0/546.0	97.3	459.0	0.174
			438.0	0.153
Ethyl acetate	466.2/525.0	9.89	454.5	0.150
	466.4/546.1	10.36	431.0	0.141
PVC membrane	470.8/553.2	52.80	488.0	0.240
	470.8/528.7	50.10	459.5	0.374
			437.0	0.305

To determine the concentration of a carboxylic acid, the optrode is immersed in a series of standard solutions of the carboxylic acid, the fluorescence intensity is read and then a calibration graph of fluorescence intensity vs. logarithm of concentration is plotted. Unknown concentrations are read from the calibration graph.

The data in Tables 1 and 2 were measured using a flow-through cell described elsewhere [22].

RESULTS AND DISCUSSION

Properties of lipophilized fluorescein isologues

Unlike fluorescein, fluorescein isologues dissolve readily in many organic solvents (e.g., dichloromethane and ethyl acetate) but are very difficult to dissolve in water. The high hydrophobicity satisfies the basic condition for a compound acting as sensing membrane component. After

TABLE 2

Spectral data for lipophilized fluorescein isologues (3.35×10^{-5} mol g^{-1}) in PVC membrane

Fluorescein isologue	Fluorescence properties			Absorption properties		
	λ(ex)/λ(em)	Fluorescence intensity [a]		λ(max) (nm)	Absorbance [a]	
		A	B		A	B
FDE	464.2/544.8	43.25	70.28	486.5	0.122	0.145
	464.2/524.7	43.56	71.30	457.5	0.184	0.218
				431.5	0.171	0.201
FDDE	470.8/554.3	41.78	77.83	485.5	0.162	0.198
	470.8/528.0	40.92	73.52	459.5	0.250	0.278
				434.0	0.228	0.230
FHDE	471.5/555.0	42.05	99.75	488.5	0.234	0.285
	471.5/527.5	41.28	90.12	460.5	0.347	0.408
				436.0	0.301	0.315
FODE	470.8/553.2	52.80	103.4	488.0	0.240	0.342
	470.8/527.5	50.10	107.5	459.5	0.374	0.475
				437.0	0.305	0.314
DCFODE	472.2/548.5	80.53	81.74	468.0	0.385	0.394
				444.0	0.356	0.362
TBFODE	474.5/548.9	32.21	30.85	485.5	0.102	0.114
				472.5	0.125	0.138
				450.0	0.112	0.126

[a] (A) Before and (B) after contacting with 0.54 M propionic acid.

immobilization in a plasticized PVC membrane, the spectral properties of FODE in the membrane remain the same as those measured in organic solvents (e.g., dichloromethane, ethyl acetate). Table 1 summarizes the spectral data in dichloromethane, ethyl acetate and in the PVC membrane. It can be seen that the immobilization does not change the spectral properties of FODE. Table 2 summarizes the spectral data for the lipophilized fluorescein isologues in the PVC membrane before and after contacting with solutions of propionic acid. It can be seen that except for the chloro and bromo derivatives, all fluorescein alkyl derivatives show a fluorescence enhancement effect when the membrane contacts propionic acid solution. This fluorescence enhancement is thought to be related to hydrogen bonding between the carboxylic acid molecule and the hydroxyl group of the fluorescein alkyl ester. The probability of collision of fluorescein alkyl ester molecules with themselves would be decreased as a result of hydrogen bond formation. The fluorescence quenching due to this kind of collision would be weakened and the fluorescence quantum efficiency increased. Macroscopically, one would observe a fluorescence enhancement effect of carboxylic acid species. Chlorine or bromine atoms in the vicinity of the hydroxyl group would hinder the formation of hydrogen bonds, which might be the reason for the absence of fluorescence enhancement for DCFODE and TBFODE according to the above reasoning. Table 2 shows that the fluorescence enhancement effect increases with increase in the length of the alkyl chain. FODE, with an octadecyl group, shows the highest fluorescence enhancement effect. The carboxylic acid also causes the enhancement of light absorption, although to a much smaller extent than the fluorescence enhancement. FODE as the best sensing membrane component for carboxylic acids was chosen for further studies.

Characteristics of the fibre-optic sensor

Some representative carboxylic acids were used for investigating the characteristics of the fibre-optic sensor, including formic, acetic, propionic and benzoic acid. The extent of fluorescence increase of the sensor is related to the acid lipophilicity (Table 3). It can be seen from Table 3 that the concentration of carboxylic acid causing a 5% increase in the fluorescence signal of the sensor decreases when the acid lipophilicity increases. Propionic acid was chosen for further studies. Figure 2 shows the fluorescence spectra of the optrode exposed to different concentrations of propionic acid. Fluorescence intensity measurements of the optrode were made at an excitation wavelength of 470 nm and an emission wavelength from 530 to 620 nm. The fluorescence intensity of the optrode is enhanced when the

TABLE 3

Concentrations of carboxylic acids causing a 5% increase in fluorescence signal of the sensor

Acid	Concentration (M)
Formic acid	0.85
Acetic acid	0.38
Propionic acid	0.095
Isobutyric acid	4.0×10^{-3}
n-Hexanoic acid	2.5×10^{-3}
Benzoic acid	3.6×10^{-4}

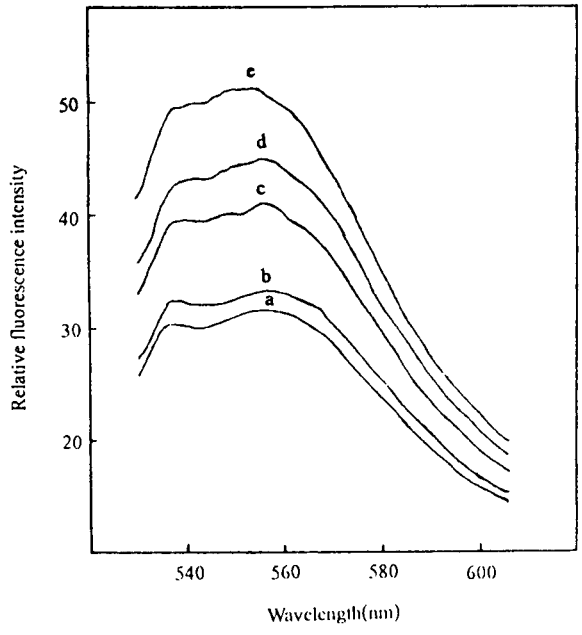

Fig. 2. Fluorescent emission spectra of optrode membrane when immersed in (a) 0.01, (b) 0.13, (c) 0.54, (d) 0.94 and (e) 2.68 M propionic acid. Excitation wavelength, 470 nm.

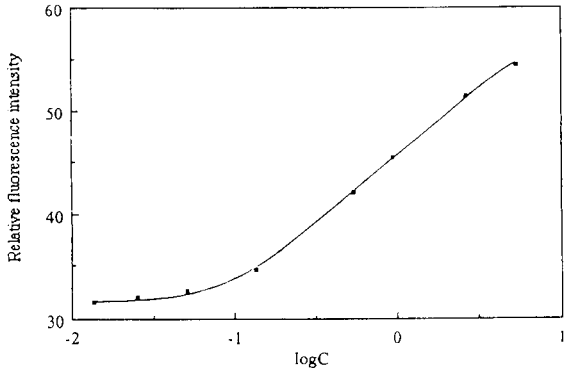

Fig. 3. Calibration graph for the determination of propionic acid.

concentration of propionic acid increases. This illustrates that the sensor can be used to determine the concentration of propionic acid in sample solutions.

Figure 3 shows the calibration graph for the determination of propionic acid. The linear range of the fluorescence intensity versus log C plot is from a concentration of 2.7 M down to 0.1 M. The measuring ranges were similarly obtained for other carboxylic acid as 1–9 M for formic acid, 0.5–10 M for acetic acid and 5×10^{-4}–1×10^{-2} M for benzoic acid.

The effect of pH was studied. For benzoic acid, which can be examined at low hydrogen ion concentrations, the fluorescence intensity is enhanced at low pH and decreases at high pH (Fig. 4). The results show that the response time of the

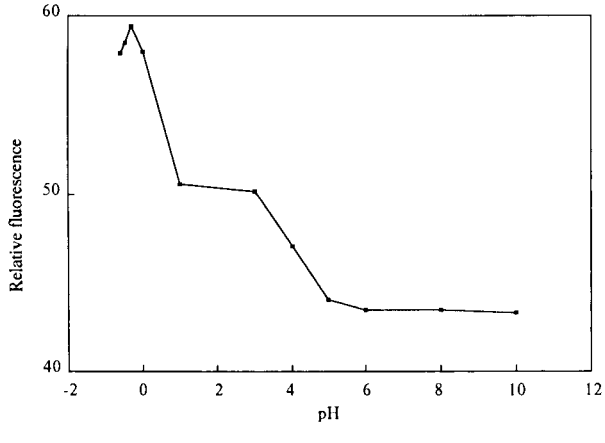

Fig. 4. Effect of pH on 1.0×10^{-3} M benzoic acid.

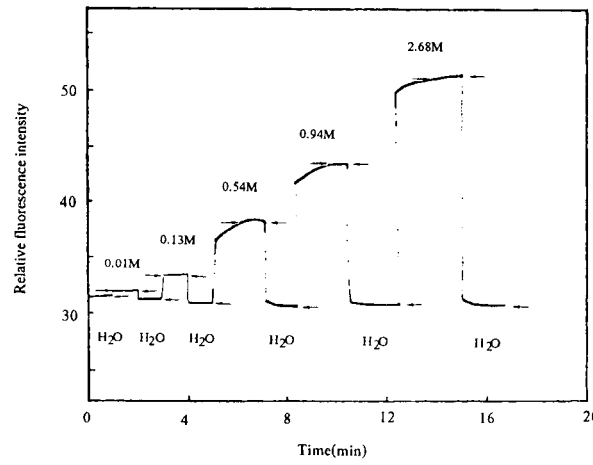

Fig. 5. Response curves for the sensor at different concentrations of propionic acid. ←, Adding acid or changing to pure water background; →, 90% response.

sensor depends on the thickness of the membrane. When the thickness of the membrane reaches the order of millimetres, the response time can reach 10 min. In order to prepare very thin membranes, the spin-on technique was used, which allow the production of very thin, homogeneous and reproducible PVC-based membranes. A typical time response of the sensor is shown in Fig. 5. The fluorescence signal reaches 90% of its final value within 20 s to 1.5 min. The response time also depends on the relative change in concentration. The time required to reach equilibrium increases with increasing proponic acid concentration. For formic, acetic and benzoic acid, the response times are 10 s–1 min, 15 s–1 min and 15 s–1.5 min, respectively.

The reproducibility of the fluorescence signal was evaluated by alternate measurements in two solutions of 0.13 and 0.94 M propionic acid. The mean fluorescence intensity values with standard deviations ($n = 5$) were found to be 33.9 ± 0.7 (0.13 M) and 44.6 ± 0.6 (0.94 M). The fluorescence intensity of the sensor in contact with 0.94 M propionic acid was recorded over a period of 8 h. From fluorescence intensity values taken every 30 min ($n = 16$) a mean value of 43.8 and a standard deviation of 1.5 were obtained.

After a series of 100 measurements of propionic acid, the fluorescence signal of the sensor

TABLE 4

Effect of different substances on the fluorescence signal of the optrode membrane

Substance	Concentration (M)	Fluorescence intensity	Fluorescence intensity change (%)
Blank solution	–	30.15	–
Propionic acid	0.54	42.10	+39.7
Formic acid	0.5	31.00	+2.8
Acetic acid	0.5	32.50	+4.5
Benzoic acid	5×10^{-4}	34.00	+12.8
Ethanedicarboxylic acid	5	32.45	+7.6
Propanedicarboxylic acid	5	29.00	−3.3
Citric acid	1	29.30	−2.8
Tartaric acid	1	31.35	+4.0
Hydrochloric acid	3	30.00	−0.5
	5	28.50	−5.5
Sulphuric acid	3	29.85	−1.0
	5	28.75	−4.6
Phosphoric acid	5	29.50	−2.2
Boric acid	1	30.50	+1.2
Phenol	1	12.00	−60.2
Methanol	5	31.00	+2.3
	10	34.00	+12.8
	15	40.00	+32.7
Ethanediol	5	29.00	−3.3
Acetaldehyde	10	28.80	−4.5
Acetone	5	29.00	−3.3
	8	28.50	−5.5
	10	26.38	−12.5
Ammonia solution	10	31.00	+2.8
Sodium hydroxide	5	28.50	−5.5
Sodium perchlorate	2	29.60	−1.8
Sodium thiocyanate	2	29.80	−1.2

had decreased by 4%. The decrease in sensitivity may be due to washing out of the dye. When the optrode was immersed in deionized water for 10 days, the fluorescence intensity of the sensor did not change significantly.

In addition to the four carboxylic acids above, the effects of different substances on the fluorescence signal of the optrode were examined and the results are summarized in Table 4. It is interesting that inorganic acids such as sulphuric, hydrochloric and phosphoric acid do not show the fluorescence enhancement effect. It seems that the postulate that the fluorescence enhancement is due to an increase in hydrogen ion concentration is not valid. Propanedicarboxylic, citric and tartaric acid also do not show a substantial fluorescence enhancement. The mechanism of the reaction involved requires further investigation. Acetone can dissolve the fluorescein species and leach them from the membrane. Phenol causes fluorescence quenching because of the strong interaction with the membrane phase, which turns from yellow to dark brown after contact with phenol solution. It is interesting that there is a significant response to methanol. The possibility of designing a sensor for methanol deserves further investigation.

Conclusions

The sensor described in this paper provides a simple means for the determination of carboxylic acids. It appears to be the first sensor to make use of a fluorescent dye to determine the concentration of carboxylic acids. As the sensor does not require excitation with ultraviolet radiation, it is compatible with standard fibre optics and also may be applied for remote process control. Potential fields of application include the the monitoring of product quality in chemical plants.

This work was supported by the National Science Fundation of China and the Chinese National Educational Committee Science Foundation for Excellent Young Teachers.

REFERENCES

1 J. Janata, Anal. Chem., 62 (1990) 33R.
2 O.S. Wolfbeis, Trends Anal. Chem., 4 (1985) 184.
3 R. Narayanaswamy, Anal. Proc., 22 (1985) 204.
4 W.R. Seitz, CRC Crit. Rev. Anal. Chem., 19 (1989) 135.
5 W.R. Seitz, Anal. Chem., 56 (1984) 16A.
6 J.O.W. Norris, Analyst, 114 (1989) 1359.
7 K. Seiler, K.M. Wang, M. Kuratli and W. Simon, Anal. Chim. Acta, 244 (1991) 151.
8 K.M. Wang, K. Seiler, J.P. Haug, B. Lehmann, S. West, K. Hartman and W. Simon, Anal. Chem., 63 (1991) 970.
9 S. Ozawa, P.C. Hauser, K. Seiler, S.S.S. Tan, W.E. Morf and W. Simon, Anal. Chem., 63 (1991) 640.
10 S.J. West, S. Ozawa, K. Seiler, S.S.S. Tan and W. Simon, Anal. Chem., 64 (1992) 533.
11 F.L. Dickert, S.K. Schreiner, G.R. Mages and H. Kimmel, Anal. Chem., 61 (1989) 2306.

12 F.L. Dickert, E.H. Lehmann, S.K. Schreiner, H. Kimmel and G.R. Mages, Anal. Chem., 60 (1988) 1377.
13 S.M. Barnard, D.R. Walt, Environ. Sci. Technol., 25 (1991) 130.
14 C. Munkholm, D.R. Walt and F.P. Milanovich, Talanta, 35 (1988) 109.
15 C. Zhu and G.M. Hieftje, Anal. Chem., 62 (1990) 2079.
16 S.S.S. Tan, P.C. Hauser, K.M. Wang, K. Fluri, K. Seiler, B. Rusterholz, G. Suter, M. Kuratli, U.E. Spichiger and W. Simon, Anal. Chim. Acta, 255 (1991) 35.
17 R.J.N. Harries, Talanta, 15 (1968) 1345.
18 R. Mogele, B. Pabel and R. Galensa, J. Chromatogr., 591 (1992) 165.
19 M. Calull, R.M. Marce, and F. Borrull, J. Chromatogr., 590 (1992) 215.
20 M. Pesez and J. Bartos, Talanta, 21 (1974) 1306.
21 G.G. Cuilbault, Handbook of Enzymatic Methods of Analysis, Dekker, New York, 1976, p. 248.
22 K.M. Wang, K. Seiler, B. Rusterholz and W. Simon, Analyst, 117 (1992) 57.

Analytica Chimica Acta, 287 (1994) 275–283
Elsevier Science B.V., Amsterdam

Derivative Fourier transform infrared spectrometric determination of ethanol in alcoholic beverages

Máximo Gallignani, Salvador Garrigues and Miguel de la Guardia

Department of Analytical Chemistry, University of Valencia, C / Dr. Moliner 50, 46100 Burjassot, Valencia (Spain)

(Received 5th August 1993; revised manuscript received 6th October 1993)

Abstract

A derivative Fourier transform infrared (FT-TR) spectrometric procedure was developed for the direct determination of ethanol in alcoholic beverages, from beers to spirit samples. The method is based on first-order derivative FT-IR measurements between the peak at 1052 cm^{-1} and the valley at 1040 cm^{-1}, which are present in aqueous solutions and alcoholic beverages, by using a micro flow transmittance cell with ZnSe windows and a spacer of 0.029 mm. The method involves the accumulation of ten scans and provides accurate results in the determination of ethanol in alcoholic beverages without requiring any previous chemical treatment of the sample or a previous separation or extraction step. The limit of detection corresponds to 0.025% (v/v) and results obtained in the analysis of real samples of beer, wine, vodka, gin and whisky agree with those found by different reference procedures. For the determination of ethanol in beverages containing high concentrations of sugars, it is necessary previously to determine the sugar content by measuring the derivative value between 1164 and 1147 cm^{-1} and subsequently to correct the negative interference of sugars on the determination of ethanol between 1052 and 1040 cm^{-1}.

Keywords: Infrared spectrometry; Alcoholic beverages; Ethanol

The determination of ethanol in alcoholic beverages can be carried out by physical measurements of the distilled samples [1,2] and also by a simple volumetric procedure [3]. In recent years, various instrumental methods have been proposed in order to provide a direct determination of ethanol based on chromatographic measurements, both by gas chromatography [4,5] and liquid chromatography [6,7], and also by electroanalytical techniques such as potentiometry [8] and differential-pulse polarography [9]. In addition, enzymatic procedures, based on the oxidation of ethanol to acetaldehyde, in the presence of aldehyde dehydrogenase, provide sensitive methods for the analysis of alcoholic beverages in the batch mode and also by flow-injection methods [10–13].

Infrared (IR) spectrometry is a powerful technique for the determination of ethanol and near IR procedures have been developed for the direct determination of ethanol in beers [14,15] and wines, by means of the use of optical fibres [16] and by reflectance measurements [17], and also in beers [18] and molasses [19] by using transmittance measurements. Recently a direct procedure was developed for the near-IR determination of ethanol in all types of alcoholic beverages, based on a first-order derivative measurement carried out between the 1680-nm peak and the 1703-nm valley, which provides a limit of detection of 0.1% (v/v) [20].

There are some precedents to the infrared spectrometric determination of ethanol in the mid-IR range but, in general, this kind of analysis

Correspondence to: M. de la Guardia, Department of Analytical Chemistry, University of Valencia, C/Dr. Moliner 50, 46100 Burjassot, Valencia, Spain.

SSDI 0003-2670(93)E0587-W

involves the use of orthogonal functions [21–23], and only a few methods have been published for the direct derivative FT-IR determination of ethanol in beverages using attenuated total reflectance cells [24] or transmittance cells [21]. However, in the latter instance the low sensitivity obtained by using the 1086 cm^{-1} band, makes the method of interest only for high-concentration alcoholic beverages, such as spirits and liqueurs.

The aim of this work was to develop a procedure for the on-line derivative FT-IR measurements of ethanol in all types of alcoholic beverages, without the need for any chemical pretreatment of the samples or any preconcentration or separation step.

EXPERIMENTAL

Apparatus and reagents

A Perkin-Elmer Model 1750 FT-IR spectrometer with a temperature-stabilized DTGS detector was employed to carry out the spectral measurements at a nominal resolution of 4 cm^{-1}, using a Specac (Orpington, UK) micro flow cell with ZnSe windows and with different lead spacers of 0.029, 0.058 and 0.1 mm. A Series 7700 data station was used to control the instrument.

The manifold employed for the derivative FT-IR measurement was a single-channel manifold with a Gilson P-2 Minipuls peristaltic pump, equipped with 0.15 mm i.d. diameter Viton (Iso-Versinic) tubing. All the connecting tubes were made of 0.8 mm i.d. PTFE. Alternatively, for the on-line dilution of spirit samples, a double-channel manifold with a Y-shaped merging zone was used.

A software package developed in-house was used to obtain and store the FT-IR spectra as a function of time to measure the corrected peak-height first-order derivative values. This various programs of the software were written in OBEY (a Perkin-Elmer computer language) and also in BASIC, and a brief description of these can be found in previous papers [25–27].

A Perkin-Elmer Sigma-3 gas chromatograph, with a flame ionization detector and equipped with a 2 m × 2 mm i.d. glass column containing 15% (w/w) Carbowax on Chromosorb (80–100 mesh) was employed for the analysis of spirit samples. For the determination of ethanol in wine samples by the pycnometric procedure, a Gibertini Hydromatic hydrostatic balance was employed. An Anton Parr FPR 09 automatic beer analyser (German Weber) was employed for the determination of ethanol in beer samples.

Analytical-reagent grade absolute ethanol (99.5%), glucose, fructose and sucrose were obtained from Panreac (Barcelona).

All standard solutions were prepared with distilled, deionized water with a measured resistivity of 18 $M\Omega\ cm^{-1}$.

General procedure

Derivative FT-IR determination of ethanol. Beer samples are degassed and then introduced directly into the flow cell and the corresponding interferogram is recorded by accumulating ten scans at a nominal resolution of 4 cm^{-1}, using a path length of 0.029 mm. The first-order derivative spectrum is then established with a derivative window of thirteen points and the concentration of ethanol in the sample is determined by measuring the derivative value between the peak at 1052 cm^{-1} and the valley at 1040 cm^{-1}, using aqueous solutions of ethanol as standards. Wine samples are analysed by the same procedure without the need for previous degassing. For the determination of ethanol in spirits a dilution of 5 ml of sample to a final volume of 25 ml with water must be carried out. This dilution can be carried out on-line, using a two-channel manifold.

Gas chromatographic determination of ethanol. For the determination of ethanol in samples of spirits a direct chromatographic procedure is used, which consists of diluting the sample 1 + 9 with distilled water and injecting 1 μl into the gas chromatograph using nitrogen as the carrier gas at a flow-rate of 25 ml min^{-1}, an oven temperature of 105°C and an injector and detector temperature of 250°C. In this procedure, a 3.85% (v/v) ethanol standard, prepared from analytical-reagent grade reagent 96% (v/v) ethanol, is used as a reference.

This analysis was carried out in the Customs Laboratory of Valencia, Spain (SOIVRE) and

these results were employed to check the accuracy of the developed procedure.

Pycnometric procedure for the determination of ethanol. A 250-ml volume of wine sample is distilled in an alkaline medium, obtained from CaO, and the density of the distillate is measured with a hydrostatic balance.

The analysis was carried out in the Laboratorio Agrario de la Consellería de Agricultura de Valencia (Burjassot) and the results were employed as a reference to check the accuracy of the developed procedure.

Analytical procedure for beer analysis

A 25-ml volume of previously filtered beer sample is directly analysed for ethanol using an Anton Parr FPR 09 instrument, using a characterized sample as a reference.

This analysis were carried out in the laboratory of Cervezas El Aguila and the same samples were analysed by the proposed procedure.

RESULTS AND DISCUSSION

IR spectra of ethanol and alcoholic beverages

Figure 1 shows the IR spectra of an ethanol standard, a wine sample, a beer sample and a vodka sample diluted 1 + 4 with distilled water and, as can be seen, the characteristic bands of ethanol at 1046 and 1086 cm^{-1} are well resolved in all types of samples without interferences. However, in the wavenumber range considered it seems difficult to establish an adequate baseline of the IR spectra for all the different samples considered.

The above spectra were obtained with a path length of 0.029 mm, because when higher spacer values are used water absorbs strongly, can be seen in Fig. 2.

Derivative FT-IR spectra of ethanol in alcoholic beverages

The use of derivative spectroscopy provides a convenient method for the resolution of mixtures of compounds and also for the compensation of matrix interferences [28–31]. In the IR range the use of derivative spectra also provide an excellent way to avoid problems related to the determination of the spectral baseline [27] and therefore, in this work, ethanol was determined in real samples by using first-order derivative measurements.

Figure 3 shows, as an example, the first-order derivative spectrum of a 10% (v/v) ethanol standard solution and those of samples of different alcoholic beverages and, as can be seen, in the wavenumber range between 1200 and 1000 cm^{-1} quantitative measurements can be carried out between the peak at 1052 cm^{-1} and the valley at 1040 cm^{-1}, and also between the peak at 1092 and the valley at 1080 cm^{-1}, but in the latter instance with lower sensitivity. In all instances derivative spectra were obtained with a derivative window of thirteen points.

Effect of the accumulated number of scans

In order to improve the limit of detection of the infrared measurements, the effect of the number of scans on the signal-to-noise ratio between the first-order derivative spectrum of a 1% (v/v) ethanol solution and that of pure water was studied and, as can be seen in Fig. 4, the background strongly decreases when the number of scans is increased from one to ten. However, for

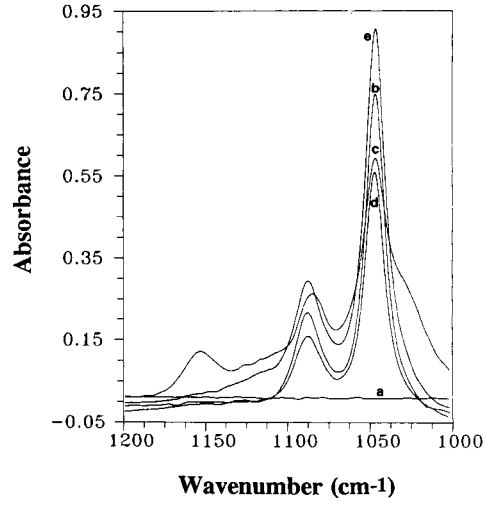

Fig. 1. FT-IR absorbance spectra of (a) pure water, (b) a 10% (v/v) ethanol standard solution, (c) a beer sample containing 5% (v/v) of ethanol, (d) a 1+4 dilution in water of a vodka sample containing 37.5% (v/v) of ethanol and (e) a red wine sample containing 11% (v/v) of ethanol.

TABLE 1

Analytical figures of merit of the derivative FT-IR spectrometric determination of ethanol [a]

Parameter	Band at 1046 cm^{-1}	Band at 1086 cm^{-1}
Calibration line	$(dA/d\bar{\nu}) = 0.000_2 + 0.108_7\ C$	$(dA/d\bar{\nu}) = 0.0001_6 + 0.025\ C$
Regression coefficient (R)	0.99998	0.99978
Dynamic range	Up to 15% (v/v)	Up to 25% (v/v)
Relative signal of a 10% (v/v) solution	1.085 ± 0.006	0.253 ± 0.002
Sensitivity (derivative units $cm^{-1}\ C^{-1}$)	37.48	8.62
Limit of detection (3σ)	0.025% (v/v)	0.12% (v/v)

[a] The calibration lines were obtained from nine standard solutions with increasing ethanol concentrations. The typical signal obtained for a standard solution of 10% (v/v) of ethanol corresponds to the average of five independent measurements ± standard deviation. C in % (v/v).

a larger number of accumulated scans the time required to obtain the analytical results increased without improving the limit of detection at the same level. Therefore, the use of ten accumulated scans is recommended in order to obtain good results in the analysis of different types of alcoholic beverages.

Analytical figures of merit of the derivative FT-IR determination of ethanol

Under the above-mentioned conditions, using a path length of 0.029 mm and ten accumulated scans, the analytical figures of merit of the FT-IR determination of ethanol indicated in Table 1 were obtained from a series of standards contain-

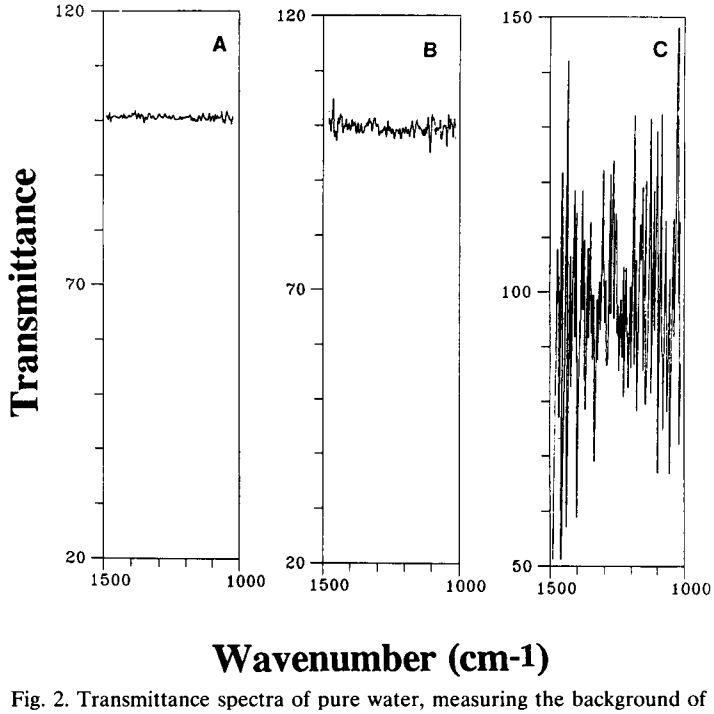

Fig. 2. Transmittance spectra of pure water, measuring the background of the cell with water by using different path lengths, (A) 0.029, (B) 0.058 and (C) 0.1 mm, and after accumulation of three scans at a nominal resolution of 4 cm^{-1}.

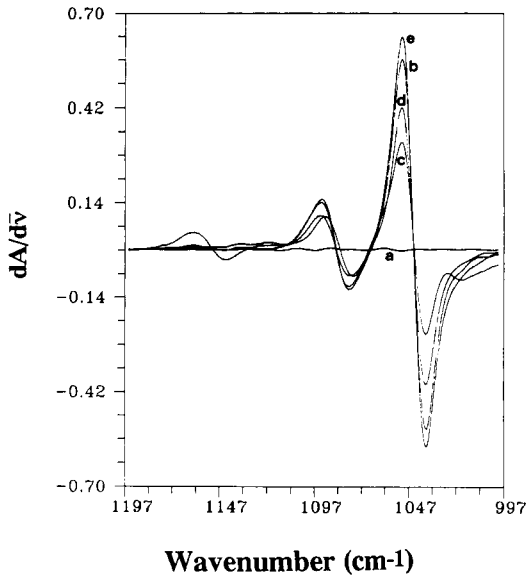

Fig. 3. First-order derivative spectra of (a) water, (b) an ethanol standard of 10% (v/v) and those of samples of (c) beer with 5% (v/v) ethanol, (d) a 1+4 dilution in distilled water of a vodka sample containing 37.5% (v/v) of ethanol and (e) a wine sample containing 11% (v/v) of ethanol. All the spectra were obtained from the accumulation of ten scans, with a nominal resolution of 4 cm^{-1} and a path length of 0.029 mm.

ing 0.2–15% (v/v) of ethanol. As can be seen, the use of the derivative values of the band at 1046 cm^{-1} provides an analytical sensitivity four times greater than that obtained by using the derivative values of the band at 1086 cm^{-1} and also a better repeatability and a four times lower limit of detection. Hence the use of derivative measurement from 1052 to 1040 cm^{-1} can be recommended for the analysis of alcoholic beverages with ethanol concentrations higher than 0.025% (v/v) and lower than 15% (v/v). For the analysis of more concentrated samples, the use of a double-channel manifold with a Y-shaped merging zone can be recommended for carrying out the on-line dilution of this kind of sample and, on the other hand, off-line dilution with water can be also employed to determine ethanol in spirits.

In all instances the experimental values were found for a derivative window of thirteen points. The use of lower window values provides a better sensitivity but a poorer repeatability, as can be seen from the data in Table 2, in which the derivative values found for an ethanol solution of 10% (v/v) and their corresponding standard deviations are summarized for four different derivative window values. In summary the use of a derivative window of thirteen points provides a 20% lower sensitivity, at the 1046 cm^{-1} band, but a three times better repeatability than the use of a window of five points, hence for the analysis of real samples the thirteen-point window is recommended.

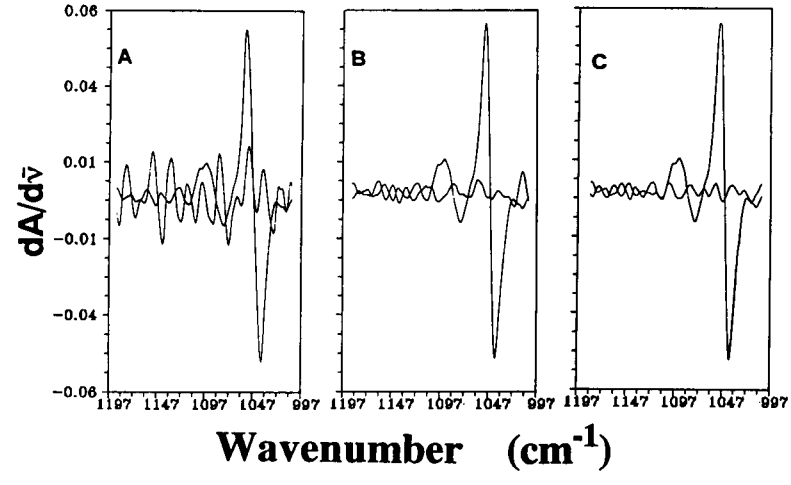

Fig. 4. Effect of the number of accumulated scans on the signal-to-noise ratio between ethanol solutions of 1% (v/v) and water blank for (A) 1, (B) 10 and (C) 25 scans.

TABLE 2

Effect of the derivative window on the sensitivity and repeatability of the derivative FT-IR measurements

Window	Derivative value for a 10% (v/v) ethanol solution			
	Band at 1046 cm^{-1}		Band at 1086 cm^{-1}	
	Value [a]	R.S.D. [b] (%)	Value [a]	R.S.D. [b] (%)
5 points	1.39 ±0.02	1.4	0.268±0.008	3.0
9 points	1.25 ±0.01	1.0	0.252±0.006	2.3
13 points	1.085±0.006	0.5	0.234±0.004	1.5
19 points	0.845±0.003	0.3	0.199±0.002	1.0

[a] Mean ± standard deviation of five independent measurements of a standard solution. [b] Relative standard deviation ($n = 5$).

Under the experimental conditions described previously, the developed procedure provides a sample throughput of 45 measurements per hour.

Analysis of real samples

A series of samples of beer, wine and spirits were analysed by the developed procedure and the results obtained were compared with those obtained by different reference procedures.

For the analysis of beers, the samples are previously degassed by using an ultrasonic waterbath and then directly measured by FT-IR spectrometry. Table 3 summarizes the results given by this procedure and also those obtained in the laboratory of Cervezas El Aguila by using a commercial automatic system. The results found by both procedures agree well.

The proposed derivative FT-IR procedure does not permit spirit samples with ethanol concentrations higher than 15% (v/v) to be measured directly. However, different approaches can be used to solve this problem. The use of the band at 1086 cm^{-1}, which provides a lower sensitivity than that found at 1046 cm^{-1}, has been proposed [21]. However, the dynamic range obtained at this wavenumber is not adequate for the direct analysis of spirits, so we preferred to make a previous dilution, which can be carried out off-line or on-line.

TABLE 3

Determination of ethanol in beer samples

Sample No.	Ethanol (%, v/v)		
	Reported value [a]	FT-IR [b]	Automatic procedure
1	5.0	5.17±0.07	4.98
2	5.0	5.10±0.06	5.05
3	7.2	7.25±0.09	7.30

[a] As indicated by the producer. [b] Mean ± standard deviation of five independent analyses.

TABLE 4

Determination of ethanol in spirits

Sample	Ethanol (%, v/v)		
	Reported	FT-IR [a]	GC
Vodka	37.5	37.3±0.2	37.3
Gin	40	39.8±0.2	39.6
Rum 1	40	40.3±0.2	40.3
Rum 2	40	40.0±0.1	39.8
Scotch whisky 1	40	40.3±0.2	40.36
Scotch whisky 2	40	39.4±0.2	39.22
Tennessee whiskey 1	43	42.6±0.2	42.6
Tennessee whiskey 2	43	42.2±0.2	42.0

[a] Mean ± standard deviation of five independent determinations.

Table 4 summarizes the results obtained by the proposed procedure and by a reference chromatographic method, and it can be see that they agreed well.

The reference procedure for the determination of ethanol in alcoholic beverages in most countries is based on the pycnometric analysis of previously distilled samples [1,2]. In order to check the accuracy of the developed procedure, fourteen samples of different types of wines were analysed by using the derivative FT-IR procedure and also, in an independent laboratory, by the pycnometric procedure and results obtained are given in Table 5. The regression between the values found by the developed procedure and those obtained by the reference method provides over the range 8–15% the equation $y = 0.090 + 0.995\ x$, with a regression coefficient (R) of 0.998, where y is the concentration obtained by FT-IR and x that by pycnometry (both in %, v/v) which indicates that the method does not require a blank correction and does not have constant relative errors (the slope is statistically equal to 1) [32].

Analysis of samples with a high concentration of sugars

An important problem in the determination of ethanol in beverages is the presence of sugars, which greatly affects the IR absorption bands in the near-IR range [20]. Therefore, a systematic study of the interference of sugars on the derivative FT-IR measurements of ethanol was carried out.

Figure 5 shows the effect of increasing concentrations of different sugars on the measurement between the peak at 1052 cm^{-1} and the valley at 1040 cm^{-1} and, as can be see, sucrose does not affect these measurements and glucose reduces the derivative measurement to only a small extent for concentrations higher than 180 g l^{-1}. In contrast, fructose strongly depresses the derivative measurement of ethanol in the selected wavenumber range and hence this effect must be considered in the analysis of samples with high fructose concentrations.

Natural sugars in wine correspond to a 1 + 1 mixture of fructose and glucose and, as can be seen in Fig. 5, the effect of this mixture on the derivative measurements of ethanol corresponds to the average behaviour of both pure compounds.

The first-order derivative spectra of different solutions containing a fixed concentration of 10% (v/v) of ethanol in the presence of increasing amounts of a glucose–fructose mixture (see Fig. 6) indicate that the derivative values found between 1052 and 1040 cm^{-1} decrease as a function of the sugar concentration. A typical regression line of

$$\Delta(dA/d\bar{\nu})_{(1052-1040)} = 0.000_1 - 8.35 \times 10^{-4} C_S \quad (1)$$

where C_S is the sugar concentration in g l^{-1}, with $r = 0.9998$ ($n = 4$), was found in the presence of 10% (v/v) of ethanol, and a slope of -8.39×10^{-4} in the presence of 5% (v/v) of ethanol, indicating that the depressant effect of sugars does not depend on the ethanol concentration.

On the other hand, the sugar content in real samples can be quantified by measuring the derivative values between 1164 and 1147 cm^{-1}. Under these conditions ethanol does not absorb and so a typical regression line,

$$(dA/d\bar{\nu})_{(1164-1147)} = 0.000_6 + 7.32 \times 10^{-4} C_S \quad (2)$$

with $r = 0.9997$ ($n = 4$), can be used to determine the sugar concentration independently of the presence of ethanol. From Eqn. 2, the sugar

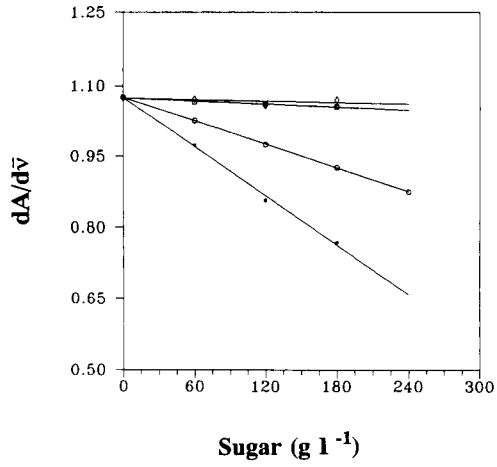

Fig. 5. Effect of sugars on the variation of the derivative FT-IR measurement of ethanol between 1052 and 1040 cm^{-1}. All the measurements were carried out on 10% (v/v) ethanol solutions containing increasing amounts of (◇) saccharose, (□) glucose, (*) fructose and (○) a mixture 1:1 of glucose and fructose.

TABLE 5

Determination of ethanol in wine samples

Sample	Ethanol (%, v/v)	
	FT-IR [a]	Pycnometric
White	10.95 ± 0.04	10.91
Red	11.95 ± 0.08	12.05
White	11.69 ± 0.05	11.71
Red	13.16 ± 0.07	13.26
Rose	10.30 ± 0.05	10.38
White	11.97 ± 0.05	12.00
Red	12.20 ± 0.09	12.30
White	10.6 ± 0.1	10.44
White	11.0 ± 0.1	11.05
White	9.25 ± 0.09	9.00
White	10.96 ± 0.09	11.00
Rose	12.20 ± 0.09	12.00
Red	12.1 ± 0.1	12.00
Red	15.00 ± 0.08	14.80

[a] Mean ± standard deviation of five independent analyses.

concentration can be determined and, taking into account this value, and also Eqn. 1 and the characteristic calibration line obtained for ethanol between 1052 and 1040 cm^{-1} (see Table 1), the following equation, which relates the experimental derivative values and the concentrations of both ethanol and sugar can be established:

$$(dA/d\bar{\nu})_{(1052-1040)} = 0.1087\ C_E - 8.35 \times 10^{-4}\ C_S \quad (3)$$

where C_E is the ethanol concentration expressed in % (v/v) and C_S is the sugar concentration in g l^{-1} in the glucose–fructose mixture.

The data in Table 6 shows that for wine samples with high sugar contents, the direct determination of ethanol by derivative FT-IR spectrometry provides defect errors, which can be corrected by means of the above-mentioned procedure in order to obtain results comparable to those found by pycnometric measurements carried out after sample distillation.

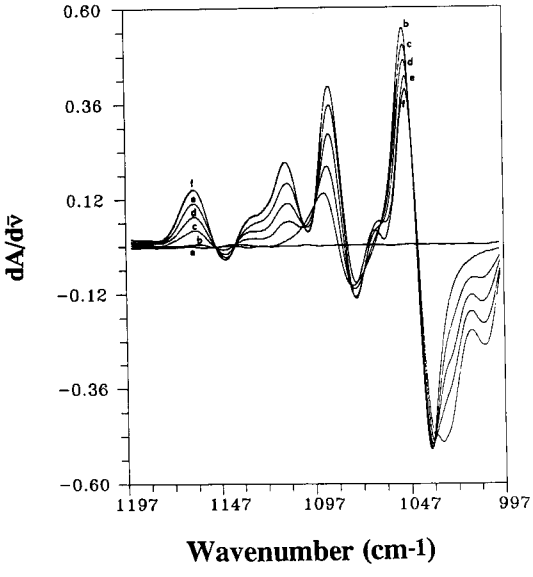

Fig. 6. First-order FT-IR spectra of 10% (v/v) ethanol solutions containing increasing amounts of a 1+1 glucose–fructose mixture. (a) Pure water; 10% (v/v) ethanol solution (b) in the absence of sugar, (c) 60 g l^{-1} of sugar, (d) with 120 g l^{-1} of sugar, (e) with 180 g l^{-1} of sugar and (f) with 240 g l^{-1} of sugar.

TABLE 6

Determination of ethanol in wine samples with high concentrations of sugars

Sample No.	Ethanol (%, v/v)		
	Direct FT-IR [a]	Corrected FT-IR [a]	Pycnometry
1	10.22±0.06	10.60±0.08	10.53
2	10.80±0.03	11.00±0.05	11.00
3	14.42±0.09	14.80±0.09	14.71
4	10.7 ±0.1	11.9 ±0.1	11.91
5	14.3 ±0.1	15.4 ±0.1	15.30
6	17.05±0.08	17.88±0.08	17.90
7	15.3 ±0.2	15.8 ±0.2	16.00
8	15.2 ±0.2	15.9 ±0.2	16.00

[a] Mean ± standard deviation for five independent analyses.

Conclusions

The developed procedure is the only method available for the FT-IR determination of ethanol in all types of alcoholic beverages, from beer samples to spirits. The method is very rapid and does not require any chemical pretreatment of samples. Added sugars (sucrose) do not affect the determination of ethanol, and the interference of natural sugars, present in alcoholic beverages, can be easily corrected for by determining the concentration level of sugar using a characteristic IR band that is not affected by the presence of ethanol and using this value to modify the ethanol concentration found by direct measurement of the derivative between 1052 and 1040 cm^{-1}.

Compared with published methods, based on FT-IR, the procedure developed here does not requires complex mathematical treatment, and the sensitivity obtained, by using the first-order derivative spectrum of the band at 1046 cm^{-1}, is four times higher than that obtained using the band at 1086 cm^{-1} proposed previously [21].

Compared with the near-IR derivative procedure developed previously [20] for the determination of ethanol in all types of alcoholic beverages, the derivative FT-IR procedure provides a better sensitivity and the limit of detection is four times lower. FT-IR measurements are less subject to interference by the presence of sugars and this kind of interference can be corrected more easily, very accurate results being obtained in both instances.

Máximo Gallignani acknowledges a grant from the Agencia Española de Cooperación Internacional for carrying out PhD studies in Spain and the financial support of Los Andes University and CONICIT (Venezuela). Salvador Garrigues acknowledges a grant from the Conselleria de Cultura, Educació i Ciència de la Generalitat Valenciana, for carrying out PhD studies. The authors acknowledge the financial support of the Spanish DGICYT, project PB-92-0870.

REFERENCES

1 Official Methods of Analysis of the Association of Official Analytical Chemists AOAC, Washington, DC, 1990.
2 M.A. Amerine and C.S. Ought, Methods of Analysis of Must and Wines, Wiley, New York, 1980.
3 G.J. Pilone, J. Assoc. Off. Anal. Chem., 68 (1985) 188.
4 A.J. Caputi and D.P. Mooney, J. Assoc. Off. Anal. Chem., 66 (1983) 1152.
5 A.J. Cutaia, J. Assoc. Off. Anal. Chem., 67 (1984) 192.
6 T. Iwachido, K. Ishimauruk and K. Toei, Anal. Sci., 2 (1986) 495.
7 J. Morawski, A.K. Dincer and K. Ivie, Food Technol., 37 (1983) 57.
8 G.J. Kakabadse, Lab. Pract., 39 (1990) 51.
9 W.H. Chan, A.W.M. Lee and P.X. Cai, Analyst, 117 (1992) 1509.
10 F. Lazaro, M.D. Luque de Castro and M. Valcarcel, Anal. Chim. Acta, 185 (1986) 57.
11 F. Lazaro, M.D. Luque de Castro and M. Valcarcel, Anal. Chem., 59 (1987) 1859.
12 C.J. Junge, J. Assoc. Off. Anal. Chem., 70 (1987) 1089.
13 P.J. Worsfold, J. Ruzicka and E.H. Hansen, Analyst, 106 (1981) 1309.
14 S.A. Hasley, J. Inst. Brew., 91 (1985) 306.
15 S.A. Hasley, Anal. Proc., 23 (1986) 126.
16 B.R. Buchanan, D.E. Honigs, C.J. Lee and W. Roth, Appl. Spectrosc., 42 (1988) 1106.
17 A. Gomez-Requejo, Tec. Lab., 8 (1983) 911.
18 A.G. Coventry and M.J. Hunston, Cereal Food World, 29 (1984) 715.
19 E.D. Dumoulin, B.P. Azain and J.T. Guerain, J. Food Sci., 52 (1987) 626.
20 M. Gallignani, S. Garrigues and M. de la Guardia, Analyst, 118 (1993) 1167.
21 P. Lopez-Mahia, J. Simal Gándara and P. Paseiro Losada, Vib. Spectrosc., 3 (1992) 133.
22 A.L. Glenn, J. Pharm. Pharmacol., 15, Suppl. (1963) 123T.
23 J.V. Agwu and A.L. Glenn, J. Pharm. Pharmacol., 19 (1967) 76s.
24 O. Heisz, Labor Praxis, 13 (1989) 402.
25 M. de la Guardia, S. Garrigues, M. Gallignani, J.L. Burguera and M. Burguera, Anal. Chim. Acta, 261 (1992) 53.
26 M. Gallignani, S. Garrigues and M. de la Guardia, Anal. Chim. Acta, 274 (1993) 267.
27 M. de la Guardia, M. Gallignani and S. Garrigues, Anal. Chem. Acta, 282 (1993) 543.
28 R.N. Hager, Anal. Chem., 45 (1973) 113A.
29 A.F. Fell, Anal. Proc., 15 (1978) 260.
30 J.N. Miller, T.A. Ahmad and A.F. Fell, Anal. Proc., 19 (1982) 37.
31 F. Sanchez Rojas, C. Bosch, Ojeda and J.M. Pavón Cano, Talanta, 35 (1989) 753.
32 J.C. Miller and J.N. Miller, Statistics for Analytical Chemistry, Wiley, New York, 1984.

Analytica Chimica Acta, 287 (1994) 285–291
Elsevier Science B.V., Amsterdam

Theoretical study of the redox and acid–base equilibria of 2,6-dichloroindophenol immobilised on Amberlite XAD-4

G. Goodlet, R. Narayanaswamy and A. Przybylko

Department of Instrumentation and Analytical Science, University of Manchester Institute of Science and Technology, P.O. Box 88, Manchester M60 1QD (UK)

(Received 5th July 1993; revised manuscript received 15th October 1993)

Abstract

By using three equations, viz., the Nernst equation, the acid–base dissociation constant equation and the equation for the Kubelka-Munk function for reflectance, an equation describing the redox behaviour of the immobilised indicator 2,6-dichloroindophenol has been formulated. After determination of the acid dissociation constant of the reduced form of the indicator, theoretical responses were calculated and compared to the experimental responses. The results indicate that the redox equilibrium involves a one-electron transfer in the pH range 2 to 5.

Keywords: Immobilised reagent; Mathematical modelling; Redox indicator

In order to characterise the response of a fibre optic chemical sensor, the chemistry of the immobilised reagent needs to be understood. A theoretical treatment of the chemistry of the immobilised indicator would enable its comparison to the experimental observations which can then lead to a better understanding of the processes occurring in the sensing mechanism.

Previously we have reported the effect of pH on the redox equilibria of 2,6-dichloroindophenol (DIP) both in solution and in the immobilised form [1]. In this paper a mathematical model is proposed to explain the experimental observations, and this is the first such theoretical model proposed for explaining the reactivity of an immobilised redox indicator.

The model is based on the use of three equations: (i) the Nernst equation, (ii) the acid dissociation constant equation for the indicator, and (iii) the equation for the Kubelka-Munk function relating the reflectance to concentration. By combining these equations, a single overall equation can be produced which models the sensor system. The model equation can be plotted on a three-dimensional surface producing a representation of the response of the immobilised indicator as a function of pH and the redox potential.

Correspondence to: R. Narayanaswamy, Department of Instrumentation and Analytical Science, University of Manchester Institute of Science and Technology, P.O. Box 88, Manchester M60 1QD (UK).

EXPERIMENTAL

Instrumentation

All redox measurements were performed using a platinum electrode (fabricated by the procedure recommended by Brennan and Tipper [2]), an EIL reference electrode and an EDT Research pH/ion meter (ECM 201). The solutions were not stirred due to the fact that equilibrium potentials were recorded. Reflectance measurements were obtained for the immobilised indicator using a system which featured a bifurcated optical fibre

0003-2670/94/$07.00
SSDI 0003-2670(93)E0602-4

and flow cell arrangement [3]. Normalised spectra of the immobilised indicator were obtained in this work. A normalised spectrum is a spectrum which is due to the interrogated material only, i.e., instrumental contributions are eliminated. A computer-based instrument developed previously in this laboratory was used to record the normalised spectra [4]. The reflectance measured in the instrument was calibrated using a barium sulphate reference (as recommended [5]). Barium sulphate was dispersed in distilled water, then was placed in the flow cell and allowed to settle. The reflectance spectrum of the barium sulphate was recorded between the wavelength range of 380 and 820 nm (at 5 nm intervals) by scanning automatically. The data was stored on a computer which could be imported to a graphics software package to obtain a printout of the spectrum. Normalised spectra could be obtained by scanning the spectrum of a sample in the flow cell and then dividing its reflectance signal obtained by the corresponding reflectance signal obtained for the barium sulphate. The resultant reflectance spectrum was also stored on the computer.

Reagents

2,6-Dichloroindophenol of analytical grade (99.9% pure) was obtained from Aldrich. Thin-layer chromatographic studies showed that only one isomer was present. All other reagents used were of analytical reagent grade.

Potentiopoised solutions (solutions of fixed redox potential) were prepared by taking 0.1 M potassium orthophosphate buffer solution and adjusting the pH using sodium hydroxide (5 M) or sulphuric acid (0.5 M) thus producing a pH buffer solution. The ionic strength of the solution was maintained at 0.2 M (NaOH/Cl) by adding sodium chloride. These pH buffer solutions were then used to prepare potentiopoised solutions by mixing different ratios of potassium hexacyanoferrate(III) and potassium hexacyanoferrate(II) from stock solutions of 0.002 M and 0.095 M respectively. When very low redox potentials were required the concentration of potassium hexacyanoferrate(II) used was 0.28 M. The buffer solution was deaerated (using nitrogen) prior to the preparation of potentiopoised solutions. The solutions were also deaerated continuously after preparation.

The indicator was immobilised on Amberlite XAD-4 resin (particle sizes 71–90 μm) by equilibrating 1.0 g of the resin with 25 ml of a 1 mg ml^{-1} aqueous solution of the indicator for 24 h. Before use, the resin was placed in methanol and then rinsed well with water. The resulting reagent phase was then washed thoroughly with distilled water until the washings were colourless. The immobilised indicator was stored at pH 6 due to a previous observation [6] that at pH > 7 the indicator was noted gradually to desorb from the resin.

Procedure

In order to use the theoretical model, the pK_a of the reduced form of the indicator had to be evaluated. This was achieved by recording the change in reflectance at a fixed potential (low potential in order to ensure 100% reduction) with varying pH. The redox equilibrium was observed by recording the change in reflectance of the immobilised indicator with corresponding changes in the redox potential at a fixed pH.

The reflectance changes in the indicator were obtained by loading the immobilised indicator into the flow cell and passing a solution of known pH or redox potential over the indicator until a constant reflectance value was recorded indicating the attainment of an equilibrium. This was repeated for a series of potentials or pH values. Equilibration time was typically 5–10 min depending on the degree of change in the redox potential. Preliminary studies indicated that the greatest reflectance change occurred at a wavelength of 545 nm on either oxidation or reduction. Thus, all measurements were recorded at this wavelength. Three sets of measurements were made at each of the pH values (2, 3, 4 and 5) to allow statistical analysis to be carried out. Each set of measurements involved the use of a fresh batch of immobilised indicator.

The results of the measurements were plotted as normalised reflectance values versus potential and as Kubelka-Munk function $F(R)$ vs. potential.

RESULTS AND DISCUSSION

Variation of reflectance with potential and pH

Figure 1 shows the variation of reflectance with pH. The sigmoid curve resembles a titration curve and can be correlated with changes in the relative amounts of the acid and base forms of the indicator. In the acidic form the indicator is red/purple ($\lambda_{max} \approx 515$ nm) whereas in the basic form the indicator is blue ($\lambda_{max} \approx 605$ nm). The variation of reflectance with potential was recorded as described previously [1].

Evaluation of the pK_a^{red}

The pK_a of an indicator HInd can be defined as the pH at which $[Ind^-] = [HInd]$ in the following equilibrium:

$$HInd \rightleftharpoons H^+ + Ind^-$$

When $[Ind^-]/[HInd] = 1$, $K_a = [H^+]$ or $pK_a =$ pH. The pK_a value was deduced for the reduced form of the indicator using Kubelka-Munk function F(R) vs. pH plots. This method was chosen due to the fact that the Kubelka-Munk function is linearly related to concentration [7]. The pK_a^{red} was taken as the pH at the F(R) value which was exactly half way between $F(R)_{max}$ and $F(R)_{min}$ (which are, respectively the maximum and minimum F(R) values in the plot) and this value correspond to $[Ind^-] = [HInd] = 50\%$.

Evaluation of the formal potential

The definition of the formal potential (E_m) used here was the same as that used previously [1]. However, the formal potential was evaluated from the F(R) vs. potential graphs for reasons already mentioned. The formal potential was taken as the potential at the F(R) value which was exactly half way between $F(R)_{max}$ and $F(R)_{min}$, this value corresponded to [Ox] = [Red] = 50%.

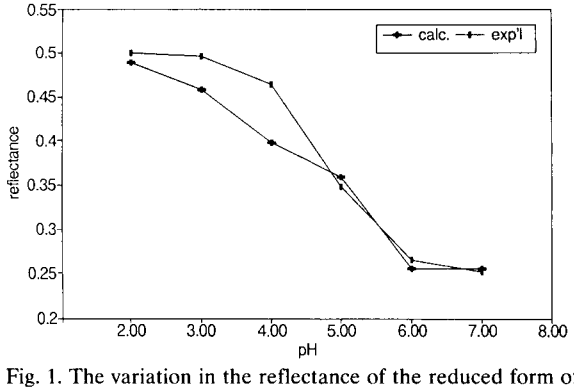

Fig. 1. The variation in the reflectance of the reduced form of the indicator with pH.

Evaluation of the redox equilibrium constants

K is a redox equilibrium constant for the general equilibrium:

$$Ind_{ox} + 2e^- \overset{K}{\rightleftharpoons} Ind_{red}$$

where

$$K = \frac{[Ind_{red}]}{[Ind_{ox}]} \tag{1}$$

From the Nernst equation,

$$E = E^\circ - \frac{RT}{nF} \ln K \tag{2}$$

thus

$$K = \exp[nF(E^\circ - E)/RT] \tag{3}$$

Derivation of the Model

The system under study involved the following set of equilibria:

$$\begin{array}{ccc} HOx + 2e^- & \overset{K_a}{\rightleftharpoons} & HRed \\ \Big\| K_a^{ox} & & \Big\| K_a^{red} \\ H^+ + Ox^- + 2e^- & \overset{K_b}{\rightleftharpoons} & Red^- + H^- \end{array}$$

where HOx and Ox^-, are respectively the oxidised forms of the indicator in acidic and basic media, and where HRed and Red^- are respectively the reduced forms in acidic and basic conditions. K_a^{ox} and K_a^{red} are the acid dissociation constants of the oxidised and reduced forms at high and low redox potential respectively and K_a and K_b are the redox equilibrium constants at low and high pH respectively. The equilibrium constants are defined as:

$$K_a^{red} = \frac{[H^+][Red^-]}{[HRed]} \tag{4}$$

$$K_a^{ox} = \frac{[H^+][Ox^-]}{[HOx]} \quad (5)$$

$$K_a = \frac{[HRed]}{[HOx]} \quad (6)$$

and

$$K_b = \frac{[Red^-]}{[Ox^-]} \quad (7)$$

Let $[Ind]_t$ be the total indicator concentration, then

$$[Ind]_t = [HOx] + [HRed] + [Ox^-] + [Red^-] \quad (8)$$

Substituting Eqns. 4, 6 and 7 into 8 gives

$$[Ox^-] = \frac{[Ind]_t K_a^{red} K_a}{K_b[H^+] + K_a K_b[H^+] + K_a^{red} K_a K_b + K_a^{red} K_a} \quad (9)$$

Let $Z = K_b[H^+] + K_a K_b[H^+] + K_a^{red} K_a K_b + K_a^{red} K_a$ then from Eqns. 7 and 9

$$[Red^-] = \frac{[Ind]_t K_a^{red} K_a K_b}{Z} \quad (10)$$

then from Eqns. 4 and 10

$$[HRed] = \frac{[Ind]_t K_b K_a [H^+]}{Z} \quad (11)$$

and from Eqns. 6 and 11

$$[HOx] = \frac{K_b[H^+][Ind]_t}{Z} \quad (12)$$

The Kubelka-Munk function states [7]:

$$F(R) = k_1'[Ox^-] + k_2'[Red^-] + k_3'[HRed] + k_4'[HOx] \quad (13)$$

Now at 100% oxidation and high pH let

$$F_b^{ox} = k_1'[Ox^-] = k_1'[Ind]_t \quad (14)$$

at 100% reduction and high pH let

$$F_b^{red} = k_2'[Red^-] = k_2'[Ind]_t \quad (15)$$

at 100% reduction and low pH let

$$F_a^{red} = k_3'[HRed] = k_3'[Ind]_t \quad (16)$$

and at 100% oxidation and low pH let

$$F_a^{ox} = k_4'[HOx] = k_4'[Ind]_t \quad (17)$$

Substituting Eqns. 9, 10, 11 and 12 into Eqn. 13 and substituting the limiting values from Eqns. 14, 15, 16 and 17, e.g. $F_b^{ox} = k_1'[Ind]_t$, gives

$$F(R) = \{(F_b^{ox} K_a^{red} K_a + F_b^{red} K_a^{red} K_a K_b + F_a^{red} K_a K_b [H^+] + F_a^{ox} K_b [H^+])\} / \{K_b[H^+](1 + K_a) + K_a^{red} K_a (1 + K_b)\} \quad (18)$$

By measuring the reflectance values at the limiting conditions, the values of limiting Kubelka-Munk functions can be deduced. Then by using deduced equilibrium constants for both the redox and acid–base equilibria, the overall Kubelka-Munk function can be calculated using this equation. The reflectance can then be calculated from the Kubelka-Munk function by evaluating R from the equation

$$F(R) = \frac{(1-R)^2}{2R} \quad (19)$$

This gives

$$R = [F(R) + 1] - \sqrt{[F(R) + 1]^2 - 1} \quad (20)$$

The negative root from Eqn. 20 was used because R can only take a value between 0 and 1.

Equation 18 has been verified by assuming the presence of only one equilibrium. By cancelling out the terms which then become zero, the resulting equation was, in each case, the same as that derived from first principles. In the model studied it was assumed that the redox reaction of the immobilised indicator was a single-step, 2-electron process.

Computer modelling

In order to model the system two software packages were utilised; Mathcad® to create a 3-dimensional surface of the response of the immobilised DIP, and Quatro® to calculate the theoretical values and compare them with the experimental values. The 3-D surface was created by the input of the relevant equations into the package, assigning values to the known values and by the input of measured values to the unknown values. The measured values were:

(i) the reflectances of the indicator under the limiting conditions (i.e., in the oxidised and

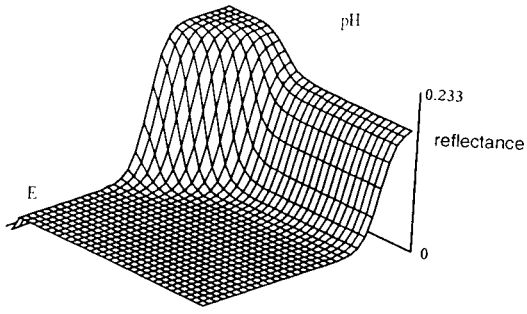

Fig. 2. A three-dimensional surface plot which represents the change in reflectance of immobilised DIP with pH and redox potential (E).

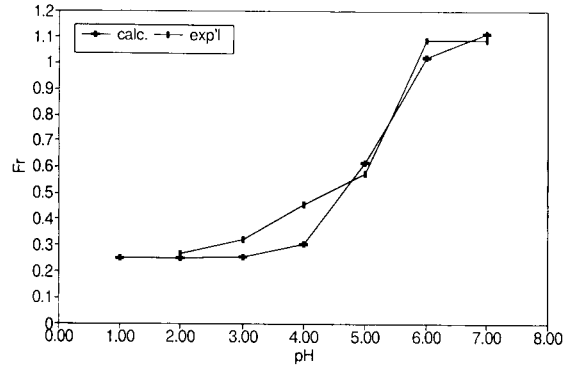

Fig. 3. A comparison of the theoretical and experimental Kubelka-Munk function versus pH plots where $pK_a^{red} = 5.15$.

reduced forms each at low and high pH values);

(ii) the formal potentials of the immobilised indicator at selected pH values (pH 2 and 5);

(iii) The pK_a of the reduced form of the indicator (at ≈ 230 mV).

Figure 2 shows the 3-dimensional surface of reflectance values as functions of E and pH. It can be seen that, though the reflectance of the oxidised form does not alter with pH (in the pH range 2 to 5), the reflectance of the reduced form does change with pH. Therefore, this model will be valid only in the pH range 2 to 5 and, in this work, the model's validity at higher pH values was not evaluated owing to limitations imposed by the potentiopoised solutions.

The theoretical plots were compared with the experimental plots using the spreadsheet package Quatro®. Here F(R) was calculated using Eqn. 18 as before by the input of the relevant known and measured parametric values. The data from experimental work was also input so that F(R) vs. potential and the reflectance vs. potential plots from the model and the experiment could be compared.

Application of the model

In order to utilise the model, a value for the dissociation of the reduced form of the indicator (pK_a^{red}) was required. It can be noted that the theoretical plots closely match the experimental plots when pK_a^{red} was 5.15 (see Fig. 3). This value was then used in all subsequent modelling work. From three assays pK_a^{red} was evaluated as 4.93 ± 0.35. The large error in the pK_a^{red} value is attributed to the method of deducing its value as small variations in the reflectance values cause large variations in the Kubelka-Munk function values.

The effect of pH on the redox equilibria of the indicator was observed by comparing reflectance vs. potential plots. Preliminary work saw variations between the experimental and calculated

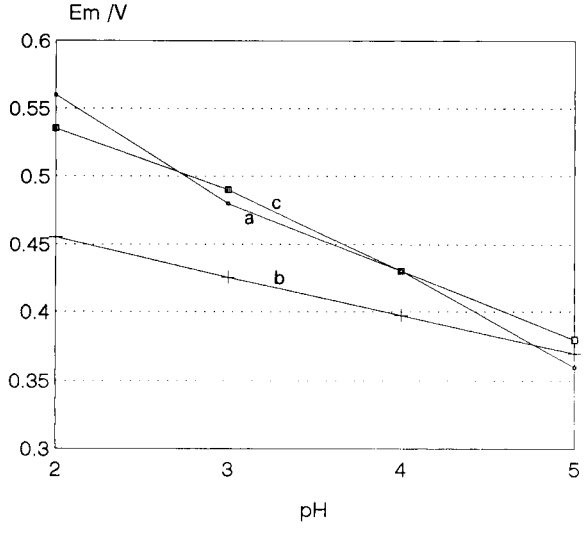

Fig. 4. A comparison of the experimentally and theoretically determined formal potential versus pH plots. a = Experimental; b = model, $n = 2$; c = model, $n = 1$.

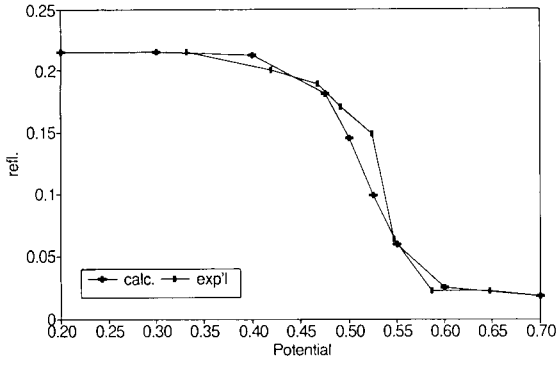

Fig. 5. A comparison of the experimental and theoretical reflectance versus redox potential plots at pH 2.

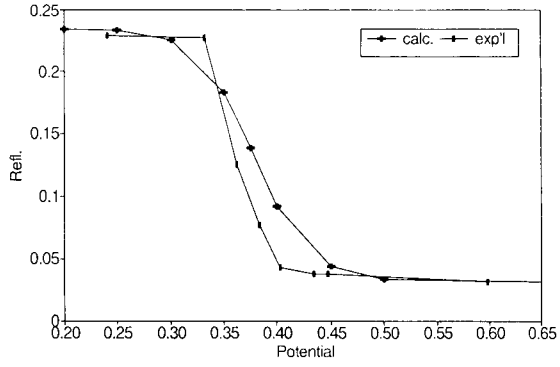

Fig. 7. A comparison of the experimental and theoretical reflectance versus redox potential plots at pH 4.

plots. A trend was also noted in these variations. At low pH (pH 2) the calculated plots occurred at significantly lower potentials than the experimental plots, and as the pH was increased, the theoretical plots approached the experimental plots until pH 4, above which the theoretical plots occurred at significantly higher potentials. A plot of formal potential (E_m) vs. pH for the theoretical and experimental data is shown in Fig. 4. The slope of the theoretical plot was ≈ 30 mV pH^{-1}, while that of the experimental plot was ≈ 60 mV pH^{-1}. Thus, according to the Nernst equation, the redox equilibrium (observed experimentally) would involve only a one-electron change. When $n = 1$ was used in the model, it showed excellent correlation with the experimental values (see Figs. 5–8). Bishop [8] studied the solution chemistry of DIP and deduced that below pH 5 the redox reaction involved only one electron. The excellent correlations and the agreement with previous work suggest that the model described here is valid for the description of both the redox and acid–base chemistry of immobilised DIP in the pH range 2 to 5. Table 1 shows the formal potentials deduced in this work.

These formal potential values were approximately 30–60 mV higher than those previously observed [1]. The standard deviations were also much higher. This was thought to be due to the different method used in the deduction of the formal potential. The method used here is subject to large variations in the Kubelka-Munk function value for small variations in the reflectance value. The plot of E_m vs. pH agreed well with published work [1].

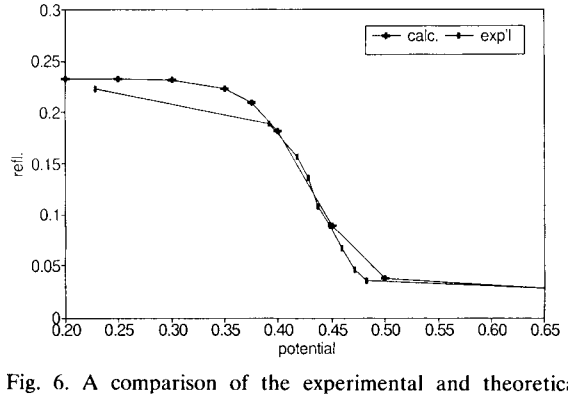

Fig. 6. A comparison of the experimental and theoretical reflectance versus redox potential plots at pH 3.

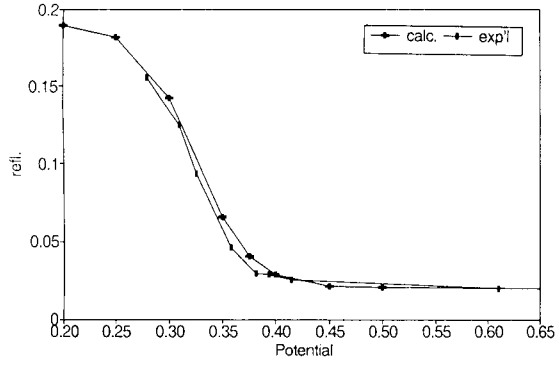

Fig. 8. A comparison of the experimental and theoretical reflectance versus redox potential plots at pH 5.

TABLE 1

Formal potentials of immobilised DIP between pH 2 and 5.

pH	E_m (V) [a]
2	0.560 ± 0.034
3	0.482 ± 0.016
4	0.405 ± 0.022
5	0.357 ± 0.012

[a] $x \pm \sigma(n = 3)$.

This model could be extended to pH > 5 if suitable potentiopoised solutions can be found. The model equations, however, would have to be modified for use above pH ≈ 10 in order to incorporate the second pK_a^{red} of DIP and the alteration in the reflectance of the oxidised form of DIP.

The authors wish to thank the Science and Engineering Council for the PhD studentship to G.G.

REFERENCES

1 G. Goodlet and R. Narayanaswamy, Anal. Chim. Acta, 279 (1993) 335.
2 D. Brennan and C.F.H. Tipper, A Laboratory Manual of Experiments in Physical Chemistry, McGraw-Hill, London, 14671 Expt. 35, pp. 128–129.
3 R. Narayanaswamy and F. Sevilla III, Mikrochim. Acta, 1 (1989) 293.
4 H.R. Guestrin, PhD thesis, University of Manchester, 1992.
5 G. Kortum, Reflectance Spectroscopy, Springer, Berlin, 1969.
6 R. Narayanaswamy and F. Sevilla III, J. Optical Sensors, 1 (1986) 403.
7 A.J. Guthrie, R. Narayanaswamy and D.A. Russell, Analyst, 113 (1988) 457.
8 E. Bishop (ed.), Indicators, Pergamon, Oxford, 1972, pp. 472–476.

ELSEVIER

Analytica Chimica Acta 287 (1994) 293–296

ANALYTICA CHIMICA ACTA

Book reviews

M. Richardson (Ed.), *Exotoxicology Monitoring*, VCH, Weinheim, 1993 (ISBN 3-527-28560-1 and 1-56081-736-4). xxv + 384 pp. Price DM192.00.

Ecotoxicology is a relatively new discipline that includes aspects of chemistry, ecology and toxicology and is defined in this book as that science concerned with the toxic effects of physical and chemical agents on living organisms, especially on populations and communities within defined ecosystems. It includes transfer pathways of these agents and their interactions with the environment.

Since there are almost 11 million documented chemicals, both natural and man-made, it is clearly desirable, for toxicity monitoring purposes, to have available tests that are fast, simple and cost effective. Analytical techniques such as GC–MS can be used but they are expensive and can produce data that are difficult to evaluate effectively. Tests utilising living organisms, particularly fish and invertebrates, are also widely used and in recent years bacterial systems have become increasingly popular. This book devotes considerable attention to the evaluation of one such system (Microtox®) based on lyophilized strain NRRL B-11177 of the marine bacterium *Photobacterium phosphoreum*.

Half of the contents of this book is based on presentations made at an RSC Toxicology Group international symposium held in Leeds, UK, in June 1992. There are additional contributions from other workers, most notably from Scandinavia.

The contents are divided into five major sections that cover introductory material, alternative biological tests, comparison of Microtox® with other systems, regulatory matters and case studies (based exclusively on the role of Microtox®). The tests considered in section two include the use of invertebrates for marine and estuarine monitoring, bacteria and fish cells for in vitro testing, micro-algae for the hazard assessment of aquatic contaminants, seaweed for marine toxicology, nucleic acid probes and other molecular tools for the functional analysis of microorganisms in soil and water and measurement of monooxygenase activity in chick embryo liver to monitor aromatic contaminants.

The main focus of the book is the Microtox® test but there is also good overall coverage of alternative approaches and background information relating to, e.g., legislation and public sources of data. In general the contributions are clearly written and well presented and have been edited into a standard format. There is a full glossary of terms that will assist readers who are unfamiliar with the subject matter and a reasonable index.

It is therefore a useful introduction to ecotoxicology monitoring that is relatively easy for the non-expert to read but also contains good quantitative details throughout.

P.J. Worsfold

Zhaolun Fang, *Flow Injection Separation and Preconcentration*, VCH, Weinheim, 1993 (ISBN 3-527-28308-0). xiv + 259 pp. Price DM148.00.

The author has aimed to produce a monograph on separation and preconcentration methods based on flow-injection analysis (FIA) principles and techniques. Following a brief introduction and discussion of basic FIA principles and

SSDI 0003-2670(94)00004-6

instrumentation the main text deals with five separation/concentration areas namely: liquid–liquid extraction, sorption, gas–liquid separation, dialysis and precipitation. The principles and practical aspects of these areas are illustrated within two applications chapters on "Environmental and Agricultural Analysis" and "Clinical and Pharmaceutical Analysis". Both of these chapters most usefully contain working details for selected procedures for the analysis of difficult samples.

It is the reviewer's opinion that the author has met his declared aim in what is a beautifully produced volume, well illustrated and in excellent format and English. This monograph provides a useful introduction to FIA per se and to the field of FIA separations/concentrations in particular.

D. Thorburn Burns

Karl Blau and John M. Halket, *Handbook of Derivatives for Chromatography*, Wiley, Chichester, 1993 (ISBN 0-471-92699-X). ix + 369 pp. Price US$95.00.

This handbook presents a variety of derivatization reagents for gas chromatography (GC) and liquid chromatography (LC), including the details of their chemistry, guidance of their use, examples of their applications to real samples and plenty of references. Non-volatile analytes would be easily derivatized and analyzed by GC with various detection methods including mass spectrometry referring to the suggestions described in the text. The less detectable analytes would also be converted to the derivatives separable by LC and sensitively detected with UV–visible or fluorescence detection. Thus, this book deserves to be an appropriate textbook, guidebook or handbook for graduate students and researchers in the fields of pharmaceutical chemistry, analytical biochemistry, clinical chemistry, food chemistry and environmental analytical chemistry.

K. Imai

Dominic M. Desiderio, *Mass Spectrometry. Clinical and Biomedical Applications*, Vol. 1, Plenum Press, London, 1993 (ISBN 0-306-44261-2). xiii + 353 pp. Price US$83.40.

This volume, part of the *Modern Analytical Chemistry* series, is a collection of self-contained articles describing recent developments in the use of mass spectrometry in clinical and medical research. A large proportion of the mass spectrometry content is devoted to the electrospray ionisation technique which is considered in some detail and merits a complete chapter detailing theoretical and practical considerations. Other mass spectral methods are dealt with in a less rigorous manner and are considered only as methods of analysis of the biomolecules under examination. The analytical procedures discussed involve the use of gas and liquid chromatography–mass spectrometry (GC–MS and LC–MS) metastable ion analysis, tandem mass spectrometry (MS–MS), chemical ionisation (CI), electron bombardment ionisation (EB) and fast atom bombardment (FAB).

Several broad areas of biomedical and clinical research are described in the fields of metabolism and physiology. Specifically the employment of mass spectrometry in the analysis of amino acids, proteins, platelet-activating factor, muscle relaxants, acylcarnitines, neurotransmitters, neuropeptides, cannabinoids and glycoproteins is presented. Alternative methods of analysis are also considered and their relative merits in comparison with mass spectrometry assessed. Each chapter is concluded with an extensive collection of literature references, review articles and suggestions for further reading.

This work will appeal most to clinicians and biochemists engaged in, or contemplating, mass spectral analysis of biochemical systems. There is no doubt that workers in the broad areas described will find a wealth of chemical and analytical information and practical direction within the text. Mass spectroscopists will find less to appeal, however. The coverage of electrospray ionisation is wide ranging but other techniques are described in considerably less detail and the analyst already possessing a basic knowledge of mass

spectral methods will probably only gain in biochemical understanding from a reading of this text.

A.D. Roberts

J.R. Chapman, *Practical Organic Mass Spectrometry* (2nd edn.) – *A Guide for Chemical and Biochemical Analysis*, Wiley, Chichester, 1993 (ISBN 0-471-92753-8). xiii + 330 pp. Price £34.00.

This volume extends the coverage of mass spectrometry to include techniques which have become readily available in the eight years since the first edition was published. Two new chapters are presented on the ionisation of labile materials including fast atom bombardment, secondary ion mass spectrometry, desorption chemical ionisation, electrospray, thermospray, plasma desorption, laser desorption and field desorption. The sections dealing with liquid chromatography–MS, tandem mass spectrometry and collision induced dissociation have been expanded and updated and time of flight and Fourier transform–MS introduced. The overall layout is retained, each technique being considered in respect of theory, instrumentation and practical details and applications. Extensive updating of the reference sections which follow each chapter has been conducted.

The main appeal of this work will once again be to readers with some initial understanding of mass spectrometry who wish to expand their breadth of knowledge of practical techniques and require direction to more specific reading. Students at both undergraduate and postgraduate level will also find this to be an excellent text book at, what is by present standards, a very modest cost.

A.D. Roberts

Vladimir Betina, *Chromatography of Mycotoxins* (*Journal of Chromatography Library*, Vol. 54), Elsevier, Amsterdam, 1993 (ISBN 0-444-81521-X). xiii + 436 pp. Price US$180.00/Dfl.350.00.

Mycotoxins (aflatoxins, tricothecenes, etc.) present a particular challenge to analytical scientists. The variety of compounds and matrices, their toxicity and the very low levels at which they often are found make their accurate analysis difficult. This book brings together many aspects of mycotoxins analysis, mainly covering chromatographic techniques, but also dealing with sample preparation, and with ELISA procedures. There are nine chapters, each written by experts, and grouped into *Techniques* (sampling, sample preparation, extraction and clean up, and TLC, LC, GC, immunoaffinity chromatography and ELISA) and *Applications* (the applications of TLC, LC and GC). The material is clearly presented, in camera ready copy, and, in addition to a considerable amount of descriptive and instructional material, includes a great deal of data. There is an extensive subject index.

Phyllis R. Brown and Eli Grushka (Eds.), *Advances in Chromatography*, Vol. 33, Marcel Dekker, New York, 1993 (ISBN 0-8247-9064-2). xviii + 283 pp. Price US$135.00.

This volume contains six articles on topical themes, viz. planar chips technology of separation systems (Harrison, Widmer et al.), liquid chromatographic determination of ligand–biopolymer interactions (Wainer and Noctor), expert systems in chromatography (Hamoir and Massart), information potential of chromatographic data for pharmacological classification and drug design (Kaliszan), fusion reaction chromatography (for polymers) (Haken), and enantioselective liquid chromatography using chiral stationary phases in pharmaceutical analysis (Levin and Abu-Lafi). All are well written, with a considerable amount of information, and supported by a good subject index.

M. Parkany, *Quality Assurance for Analytical Laboratories*, Royal Society of Chemistry, Cambridge, 1993 (ISBN 0-85186-705-7). xiii + 193 pp. Price £39.50.

This book contains, in camera-ready format, lectures and presentations at the *Fifth ISO / IUPAC / AOAC International Symposium on the Harmonization of International Quality Assurance Schemes for Analytical Laboratories*, held in Washington, DC, 22–23 July, 1993, and published in May 1993. There are 20 lectures, from speakers from many countries, and covering a range of situations, and there is a great deal of detailed information on the "nuts and bolts" aspects of QA schemes included. The subject of the Symposium is the "harmonization of existing QA schemes at an international level", and there is no doubt that the information presented in this book will provide a considerable impetus to achieving this goal. At the end of the text, there are compilations of general terms and their definitions and international standards, ISO/IEC guides related to QA and standardisations, and an extensive subject index.

Committee for Systematic Toxicological Analysis, *Thin-layer Chromatographic R_F Values of Toxicologically Relevant Substances on Standardized Systems*, 2nd edn., VCH, Weinheim, 1992 (ISBN 3-572-27361-1). 308 pp. Price DM138.00.

The Committee has coordinated the work of Dr. A.C. Moffatt and his colleagues in the UK and Prof. de Zeeuw in the Netherlands to provide standardized, optimized TLC systems for general screening procedures for identification of toxicologically relevant substances. Some more specialist systems are included, as are tests based on the Toxi-Lab colour development system (a removable colour chart is included for the latter). hR_F data for some 1600 compounds (compared to 1100 in the first edition) are given for ten general TLC systems, as well as more specialised data, in a format that eases correlation of an hR_F value for one system with that for other systems.

ANALYTICA CHIMICA ACTA, VOL. 287 (1994)

AUTHOR INDEX

PUBLICATION SCHEDULE FOR 1994

	S'93	O'93	N'93	D'93	J	F	M	A	M			
Analytica Chimica Acta	281/1 281/2 281/3	282/1 282/2 282/3	283/1 283/2	283/3 284/1 284/2	284/3 285/1–2 285/3	286/1 286/2 286/3	287/1–2 287/3 288/1–2	288/3 289/1 289/2	289/3 290/1–2 290/3			
Vibrational Spectroscopy		6/1			6/2		6/3		7/1			

INFORMATION FOR AUTHORS

Detailed "Instructions to Authors" for *Analytica Chimica Acta* was published in Volume 256, No. 2, pp. 373–376. Free reprints of the "Instructions to Authors" of *Analytica Chimica Acta* and *Vibrational Spectroscopy* are available from the Editors or from: Elsevier Science B.V., P.O. Box 330, 1000 AH Amsterdam, The Netherlands. Telefax: (+31-20) 5862459.

Manuscripts. The language of the journal is English. English linguistic improvement is provided as part of the normal editorial processing. Authors should submit three copies of the manuscript in clear double-spaced typing on one side of the paper only. *Vibrational Spectroscopy* also accepts papers in English only.

Rapid publication letters. *Letters* are short papers that describe innovative research. Criteria for letters are novelty, quality, significance, urgency and brevity. Submission data: max. of 2 printed pages (incl. Figs., Tables, Abstr., Refs.); short abstract (e.g., 3 lines); *no* proofs will be sent to the authors; submission on floppy disc; *no* revision will be possible.

Abstract. All papers and reviews begin with an Abstract (50–250 words) which should comprise a factual account of the contents of the paper, with emphasis on new information.

Figures. Figures should be prepared in black waterproof drawing ink on drawing or tracing paper of the same size as that on which the manuscript is typed. One original (or sharp glossy print) and two photostat (or other) copies are required. Attention should be given to line thickness, lettering (which should be kept to a minimum) and spacing on axes of graphs, to ensure suitability for reduction in size on printing. Axes of a graph should be clearly labelled, along the axes, outside the graph itself. All figures should be numbered with Arabic numerals, and require descriptive legends which should be typed on a separate sheet of paper. Simple straight-line graphs are not acceptable, because they can readily be described in the text by means of an equation or a sentence. Claims of linearity should be supported by regression data that include slope, intercept, standard deviations of the slope and intercept, standard error and the number of data points; correlation coefficients are optional.

Photographs should be glossy prints and be as rich in contrast as possible; colour photographs cannot be accepted. Line diagrams are generally preferred to photographs of equipment. Computer outputs for reproduction as figures must be good quality on blank paper, and should preferably be submitted as glossy prints.

Nomenclature, abbreviations and symbols. In general, the recommendations of IUPAC should be followed, and attention should be given to the recommendations of the Analytical Chemistry Division in the journal *Pure and Applied Chemistry* (see also *IUPAC Compendium of Analytical Nomenclature, Definitive Rules*, 1987).

References. The references should be collected at the end of the paper, numbered in the order of their appearance in the text (*not* alphabetically) and typed on a separate sheet.

Reprints. Fifty reprints will be supplied free of charge. Additional reprints (minimum 100) can be ordered. An order form containing price quotations will be sent to the authors together with the proofs of their article.

Papers dealing with vibrational spectroscopy should be sent to: Dr J.G. Grasselli, 150 Greentree Road, Chagrin Falls, OH 44022, U.S.A. Telefax: (+1-216) 2473360 (Americas, Canada, Australia and New Zealand) or Dr J.H. van der Maas, Department of Analytical Molecular Spectrometry, Faculty of Chemistry, University of Utrecht, P.O. Box 80083, 3508 TB Utrecht, The Netherlands. Telefax: (+31-30) 518219 (all other countries).

0003-2670/94/$07.00

This issue is printed on acid-free paper.

PRINTED IN THE NETHERLANDS

Intelligent Software for Chemical Analysis

Edited by **L.M.C. Buydens** and **P.J. Schoenmakers**

Data Handling in Science and Technology Volume 13

Various emerging techniques for automating intelligent functions in the laboratory are described in this book. Explanations on how systems work are given and possible application areas are suggested. The main part of the book is devoted to providing data which will enable the reader to develop and test his own systems. The emphasis is on expert systems; however, promising developments such as self-adaptive systems, neural networks and genetic algorithms are also described.

Contents:

1. Introduction. Automation and intelligent software. Expert systems. Neural networks and genetic algorithms. Reader's guide. Concepts. Conclusions. **2. Knowledge-based Systems in Chemical Analysis** (P. Schoenmakers). Computers in analytical chemistry. Sample preparation. Method selection. Method development. Instrument control and error diagnosis. Data handling and calibration. Data interpretation. Validation. Laboratory management. Concluding remarks. Concepts. Conclusions. Bibliography. **3. Developing Expert Systems** (H. van Leeuwen). Introduction. Prerequisites. Knowledge acquisition. Knowledge engineering. Inferencing. Explanation facilities. The integration of separate systems. Expert-system testing validation and evaluation. Concepts. Conclusions. Bibliography. **4. Expert-System-Development Tools** (L. Buydens, H. van Leeuwen, R. Wehrens). Tools for implementing expert systems. Tool selection. Knowledge-acquisition tools. Concepts. Conclusions. Bibliography. **5. Validation and Evaluation of Expert Systems for HPLC Method Development - Case Studies** (F. Maris, R. Hindriks). Introduction. Case study I: Expert systems for method selection and selectivity optimization. Case study II: System-optimization expert system. Case study III: Expert system for repeatability testing, applied for trouble-shooting in HPLC. Case study IV: Ruggedness-testing expert system. General comments on the evaluations. Concepts. Conclusions. Bibliography. **6. Self-adaptive Expert Systems** (R. Wehrens). Introduction - maintaining expert systems. Self-adaptive expert systems: Methods and approaches. The refinement approach of SEEK. Examples from analytical chemistry. Concluding remarks. Concepts. Conclusions. Bibliography. **7. Inductive Expert Systems** (R. Wehrens, L. Buydens). Introduction. Inductive classification by ID3. Applications of ID3 in analytical chemistry. Concluding remarks. Concepts. Conclusions. Bibliography. **8. Genetic Algorithms and Neural Networks** (G. Kateman). Introduction. Genetic algorithms. Artificial neural networks. Concepts. Conclusions. Bibliography. **9. Perspectives.** Limitations of Intelligent Software. Dealing with intelligent software. Potential of intelligent software. **Index.**

ELSEVIER SCIENCE B.V.

© 1993 366 pages Hardbound
Price: Dfl. 350.00 (US $ 200.00)
ISBN 0-444-89207-9

ORDER INFORMATION

For USA and Canada
ELSEVIER SCIENCE INC.
P.O. Box 945
Madison Square Station
New York, NY 10160-0757
Fax: (212) 633 3880

In all other countries
ELSEVIER SCIENCE B.V.
P.O. Box 330
1000 AH Amsterdam
The Netherlands
Fax: (+31-20) 5862 845

US$ prices are valid only for the USA & Canada and are subject to exchange rate fluctuations; in all other countries the Dutch guilder price (Dfl.) is definitive. Customers in the European Community should add the appropriate VAT rate applicable in their country to the price(s). Books are sent postfree if prepaid.

0003-2670(19940321)287:3;1-7